Modelling nasopharyngeal colonisation by *Streptococcus pyogenes*: Bioluminescence and other longitudinal techniques

---

A thesis submitted for the degree of
Doctor of Philosophy

Department of Infectious Diseases & Immunity

Imperial College London

Supervised by

Professor Shiranee Sriskandan &

Dr Siouxsie Wiles

2013

ABSTRACT

Streptococcus pyogenes causes an estimated 616 million pharyngitis cases per year and a variety of invasive diseases such as necrotising fasciitis and toxic shock syndrome. The human nasopharynx is the major reservoir for all *S. pyogenes* infection, including severe invasive disease. A combination of biophotonic imaging (BPI) and direct nasal sampling techniques were used to longitudinally measure the *in vivo* carriage of *S. pyogenes*, looking at the effects of virulence factor expression on carriage and transmission and to enable vaccine evaluation.

Direct nasal sampling demonstrated that the two component regulatory system, CovR/S, is required for infection and transmission from the nasopharynx. The fitness cost conferred by *covR/S* mutation in the nasopharynx may explain why *S. pyogenes* with altered *covR/S* have not become prevalent in community infections despite conferring a selective advantage in invasive infection.

Bioluminescent *S. pyogenes* strains expressing the *luxABCDE* operon demonstrated a growth deficit independent of the target site for integration *in vitro* that manifested as a fitness cost during infection *in vivo*. Notwithstanding this, bioluminescence expression permitted longitudinal quantitation of *S. pyogenes* within the nasopharynx using BPI. Intramuscular vaccination with heat killed streptococci or the streptococcal chemokine protease SpyCEP conferred protection against pharyngeal infection in this model.

These longitudinal techniques allow for *S. pyogenes* to be tracked in the nasopharynx non-invasively, and allow for new insights into the pathogenesis of this disease.

DECLARATION OF ORIGINALITY

The data, ideas and concepts presented in this document have been fully acknowledged and referenced, or are those of the author.

Faraz M. Alam

ACKNOWLEDGEMENTS

I am grateful to Dr Siouxsie Wiles, who brought me onto this amazing project. I learned a lot from her hands-on approach, and her boundless enthusiasm for doing good science and applying statistics. Because of her, I will forever associate cloning with cake days.

Professor Shiranee Sriskandan also deserves a great deal of credit for her supervision of this work. Her advice was essential for showing me how to turn some of my half formed ideas into actual experiments. I am amazed at how readily she indulged some of my crazy ideas, even though a lot of them didn't pan out.

I would also like to thank Dr Claire Turner for being the lab authority, always ready to help out and troubleshoot problems when they occurred, and for helping me out in my later experiments when my "n" numbers became somewhat unmanageable.

There are a number of other people who have been a part of the gram positive group over the years who I would like to thank. I am not sure that I understood what a "work ethic" was until I saw Dr Nuria Andreu in action. I still feel a little guilty for the time that Dr Frances Davies stayed in the lab well after nightfall showing me how to do FACS. I am glad that I had Major Dr Lucy Lamb around so that we could both share in the excitement of BPI, and in the frustration of its limitations. I should probably mention James Peacock, who sacrificed his soul to the electroporator, to no avail. I should probably thank the technician (who shall remain nameless) who got my initial mouse order wrong inadvertently introduced me to the FVB/n mouse strain. I should thank Dr Deborah Chong for introducing the world to Prof L.ion, and Dr Nicola Lynskey for being an awesome "PhD buddy". I would like to thank everybody for making this PhD more fun than it had any right to be.

TABLE OF CONTENTS

Abstract 1

Declaration of originality 2

Acknowledgements 3

Table of Contents 4

Figures List 13

Tables List 16

List of Abbreviations 17

Chapter 1. Introduction 18

1.1. *Streptococcus pyogenes* 18

1.2. The molecular basis of streptococcal adhesion and invasion. 19

1.3. Virulence factors enable *S. pyogenes* to evade the immune system. 21

1.4. Tissue tropism 25

1.4.1. The role of *emm* types in determining tissue tropism 25

1.4.2. Regulation of virulence 28

1.5. Transmission 32

1.6. Vaccination 33

1.7. Animal models for streptococcal infection and colonisation 38

1.7.1. Animal models of skin and soft tissue infections 39

1.7.2. Animal models of septicaemia and toxic shock syndrome 41

1.7.3 Models of respiratory infection 41

1.8. Biophotonic imaging 47
1.8.1. Fluorescence 47
1.8.2. Bioluminescence 48
1.9. Preliminary work to develop new methodology 53
1.10. Aims 57
1.10.1. Developing a mouse model of nasopharyngeal infection 57
1.10.2. Developing a bioluminescent strain of *S. pyogenes* 57
1.10.3. Applying a bioluminescent strain of *S. pyogenes* to a model of nasopharyngeal infection 57
1.10.4. Determining the effect of virulence regulator dysfunction in a model of nasopharyngeal infection 58
1.10.5. Utilising a model of nasopharyngeal infection to assess vaccine candidates 58
Chapter 2. Materials and Methods 59
2.1 Materials 59
2.1.1. Chemicals 59
2.1.2. Antibodies 60
2.1.3. Enzymes 60
2.1.3. Primers 60
2.1.4. Plasmids 61
2.1.5. Buffers and Standardised solutions 61
2.1.6. Bacterial Media 63

2.1.7. Kits 64

2.1.8. Bacterial strains 64

2.2. Methods 66

2.2.1. PCR to amplify the Kanamycin resistance gene Aph-a3. 66

2.2.2. PCR to amplify the Spy0535 Locus 66

2.2.3. PCR to confirm chromosomal insertion into the Spy0535 Locus 66

2.2.4. Plasmid construction of pICL18^{lux} and pICL18^{vlux} 67

2.2.5. Excising LuxABCDE from pICL18^{lux} 67

2.2.6. DNA extraction from *S. pyogenes* 70

2.2.7. Plasmid extraction from *E.coli* 70

2.2.8. Transformation of *E.coli* 71

2.2.9. Electrotransformation of *S. pyogenes* 71

2.2.10. CEP5 production from *E.coli* 72

2.2.11. Agarose gel electrophoresis 73

2.2.12. SDS gel electrophoresis 74

2.2.13. Western blot 74

2.2.14. Biofilm assay 74

2.2.15 Growth kinetics and light production kinetics 75

2.2.16. Light production of the bioluminescent strains 75

2.2.17. Stability of bioluminescence expression 76

2.2.18. Animal housing and enrichment 76

2.2.19. Intranasal infection 77

2.2.20 Intramuscular infection 78

2.2.21 *In vivo* Competition assay 78

2.2.22 Mouse immunisation 78

2.2.23. Saliva Collection 79

2.2.24. *In vivo* biophotonic imaging 79

2.2.25 Dissection 80

2.2.26. Broncho-alveolar lavage 82

2.2.27. Colony identification 83

2.2.28. Enzyme linked immunosorbent assay for immunoglobulin 84

2.2.29. Histopathology 85

2.2.30. Statistics 85

2.3. New Techniques 86

2.3.1. Direct nasal sampling 87

2.3.2. Settle plates in individually ventilated cages 87

Chapter 3: Characterising a model of infection in the murine nasopharynx 88

3.1. Introduction 88

3.2. Results 89

3.2.1. Colony counts of *S. pyogenes* shed by mice correlate with *s. pyogenes* colony counts from dissected nasal tissue. 89

3.2.2 FVB/n strain mice carry *S. pyogenes* in their nasopharynx better than other mouse strains. 90

3.2.3. Gender has an effect on the nasopharyngeal carriage of S. pyogenes that is dependent on the age of the mice. 94

3.2.4. Intranasal administration of *S. pyogenes* results in a suppurative upper respiratory tract infection that resolves over 21 days. 97

3.2.5. Transmission of *S. pyogenes* within a mouse cage is dependent on the proportion of donor mice present. 100

3.2.6. Transmission between mice and to the air is not dependant on passive transfer of *S. pyogenes* directly after inoculation..... 102

3.2.7. Infection of different *emm* types in the nasopharynx 104

3.3. Discussion 107

3.4. Appendix..... 111

Chapter 4: Characterisation of a bioluminescent strain of *S. pyogenes* 113

4.1. Introduction 113

4.2. Results..... 115

4.2.1. Expression of bioluminescence in *S. pyogenes* with a plasmid borne construct 115

4.2.2. Integration of a bioluminescent construct into *S. pyogenes*. 117

4.2.3. The growth and luminescence of the integrated constructs in *S. pyogenes* 120

4.2.4. Comparison of bioluminescence expression between *S. pyogenes* strains transformed with replicating plasmid or integrated constructs..... 123

4.2.5. The stability of the bioluminescent constructs in *S. pyogenes* 125

4.2.6. The effect of bioluminescence expression on streptococcal biofilm formation 127

4.3. Discussion 129

Chapter 5: *In vivo* characterisation of bioluminescent *S. pyogenes* 131

5.1 Introduction 131

5.2. Results 132

5.2.1. Characterisation of the background luminescent signal from the murine nasopharynx 132

5.2.2. *In vivo* instability of the multi-copy plasmid in *S. pyogenes* antibiotic application 134

5.2.3. Intranasal infection with stably bioluminescent *S. pyogenes* over a longitudinal time course 136

5.2.4. Correlation of bioluminescent *S. pyogenes* with the bioluminescent signal detected from the nasopharynx 138

5.2.5. The expression of bioluminescence *in vivo* confers a competitive disadvantage in the nasopharynx. 140

5.2.6. Bioluminescent *S. pyogenes* occasionally causes a suppurative upper respiratory tract infection 142

5.2.7. The effect of intranasal infection with stationary vs exponential phase *S. pyogenes* 144

5.3. Discussion 146

Chapter 6: Impact of *covR/S* mutation on nasopharyngeal *S. pyogenes* infection and transmission 149

6.1 Introduction 149

6.2. Results 150

6.2.1 The *in vitro* characterisation of a *covR/S* mutant 150

6.2.2 CovR/S mutation confers enhancement of virulence in an invasive model of *S. pyogenes* infection. 153

6.2.3. Mutation of *covR/S* is detrimental to long term *S. pyogenes* colonisation in the nasopharynx. 155

6.2.4. *S. pyogenes* with a *covR/S* mutation can cause an attenuated suppurative upper respiratory tract infection. 157

6.2.5. Investigation of *covR/S* mutation using bioluminescence: intensity of infection in nasopharynx and lungs 160

6.2.6. *CovR/S* mutation may partially compensate for growth defects conferred by bioluminescence during long term *S. pyogenes* colonisation in the nasopharynx 164

6.2.7. Bioluminescent Δ*covR/S S. pyogenes* causes a suppurative upper respiratory tract infection 166

6.2.8. *CovR/S* mutation is detrimental to the transmission of *S. pyogenes* in a mouse model 168

6.3. Discussion 171

6.4. Appendix 175

Chapter 7: The utility of biophotonic imaging in assessing vaccine efficacy 176

7.1. Introduction 176

7.2. Results 177

7.2.1 Intramuscular but not intranasal immunisation confers protection against intranasal challenge against *S. pyogenes* 177

7.2.2 Use of BPI to determine the protective efficacy of a heat killed *S. pyogenes* based vaccine 183

7.2.3. The use of BPI to determine the protective efficacy of a vaccine based on SpyCEP 185

7.3. Discussion 187

Chapter 8: General discussion 191

8.1. The susceptibility of mice to *S. pyogenes* infection in the nasopharynx is based on the host strain, gender and age 191

8.2 The characterisation of *S. pyogenes* infection in the mouse 194

8.3. The transmission of *S. pyogenes* between mice 196

8.4. Efficacy of different methods for determining the presence of *S. pyogenes* in the nasopharynx longitudinally 199

8.5. The utility of bioluminescence imaging for evaluating vaccines and imaging infection 201

8.6. *CovR/S* mutations impair *S. pyogenes* colonisation of the nasopharynx 202

8.7. Summary 205

8.8. Further Work. 206

8.8.1. Characterisation of the FVB/n mouse strain susceptibility to *S. pyogenes* 206

8.8.2. The study of the commensal bacteria within the murine nasopharynx before and during *S. pyogenes* infection 207

8.8.3. The characterisation of *S. pyogenes* infection of the urogenital tract after infection in the nasopharynx 208

8.8.4. Further studies on transmission, and the relative impact of mouse behaviour 209

References 211

Publication 238

FIGURES LIST

Figure 1.1. Diversity of circulating *emm* types associated with pharyngitis within the USA and the UK 27

Figure 1.2. The molecular basis of bioluminescence 51

Figure 1.3. Biophotonic imaging of bacterial distribution after intranasal inoculation with bioluminescent *C. rodentium* 54

Figure 1.4. Shedding intensity of different serotypes of *S. pyogenes* in BALB/c mice 56

Figure 2.1 Schematic diagrams of plasmids 69

Figure 2.2. SDS PAGE demonstrating production and purification of recombinant CEP5 73

Figure 2.3. ROI for analysing luminescence from the mouse nasopharynx 80

Figure 2.4. Dissection of the mouse nasopharynx 82

Figure 3.1. Quantitative correlation of *S. pyogenes* (H347) recovered from nasal shedding with *S. pyogenes* recovered from dissection of the nasopharynx 90

Figure 3.2. Comparison of commensal bacteria in different mouse strains 92

Figure 3.3. Comparison of nasopharyngeal shedding of *S. pyogenes* (H347) between different mouse strains 93

Figure 3.4. Comparison of duration of shedding for *S. pyogenes* (H347) between genders in two different age groups 96

Figure 3.5. Histopathological analysis of upper respiratory tract tissue from mice infected intranasally with *emm75 S.pyogenes* (H347) 100

Figure 3.6. Transmission of *S. pyogenes* (H347) occurs more frequently as the density of infected carriers within a cage is increased 101

Figure 3.7. Transmission of *S. pyogenes* (H347) between mice and to the air is not dependant on passive inoculum transfer 103
Figure 3.8. Invasive infection in the nasopharynx caused by *emm1* and *emm12* types 106
Figure 4.1. Growth kinetics and luminescence and production of H347^{pTHLK} 116
Figure 4.2. Confirmation of integration into the *S. pyogenes* H347 chromosome .. 119
Figure 4.3. Growth kinetics and luminescence production of H347^{vlux} and H347^{lux} 121
Figure 4.4. Bioluminescence expression confers *in vitro* growth defects 122
Figure 4.5. Characterisation of bioluminescent strains 124
Figure 4.6. Stability of bioluminescent plasmids 126
Figure 4.7. Biofilm forming capacity of bioluminescent strains 128
Figure 5.1. Background luminescence from mice 133
Figure 5.2. Instability of the pTHLK replicating plasmid *in vivo* 135
Figure 5.3. Imaging of *S. pyogenes* (H347) with a stably integrated *lux* operon over a time course 137
Figure 5.4. Correlation of bioluminescent signal to *S. pyogenes* numbers within the nasopharynx 139
Figure 5.5. Bioluminescence confers *in vivo* growth defects 141
Figure 5.6. Biophotonic imaging of mice inoculated with either exponential or stationary phase grown *S. pyogenes* 145
Figure 6.1. Inactivation of *CovR/S* results in loss of cysteine protease SpeB expression 151
Figure 6.2. Biofilm formation is affected by the loss of *CovR/S* regulation 152
Figure 6.3. The loss of virulence factor regulation aids bacterial dissemination in invasive infection 154

Figure 6.4. Nasopharyngeal infection is adversely affected by *covR/S* mutation ... 156
Figure 6.5. Histopathological analysis of the ethmoturbinates during nasal infection 158
Figure 6.6. Imaging of a bioluminescent *covR/S* mutant during nasopharyngeal infection 162
Figure 6.7. Imaging of a bioluminescent *covR/S* mutant during intrapulmonary infection 163
Figure 6.8. Expression of bioluminescence alters the impact of *covR/S* mutation . 165
Figure 6.9. Transmission of *S. pyogenes* is hampered by the loss of CovR/S regulation 169
Figure 6.10. Transmission of *S. pyogenes* is hampered by the loss of CovR/S regulation 170
Figure 7.1. Intranasal immunisation with heat killed *S. pyogenes* or *L. lactis* and the resultant immune response 178
Figure 7.2. Intramuscular immunisation with heat killed *S. pyogenes* or *L.lactis* and the resultant immune response 180
Figure 7.3. Salivary IgA and IgM responses following vaccination with heat killed *S. pyogenes* administered intramuscularly or intranasally 182
Figure 7.4. BPI revealed the protective efficacy of a vaccine based on heat-killed bacteria 184
Figure 7.5. BPI revealed the protective efficacy of a vaccine based on SpyCEP ... 186

TABLES LIST

Table 1.1. Virulence regulation 29

Table 1.2. Outcomes utilised to evaluate vaccine candidates 37

Table 1.3. Intranasal models of infection 46

Table 2.1. Primers and oligonucleotides 61

Table 2.2. Plasmids used in this study 61

Table 2.3. Strains of *S. pyogenes* used in this study 65

Table 3.1. Histopathological analysis of upper respiratory tract tissue from mice infected with *emm*75 *S. pyogenes* (H347) 98

Table 3.2. The carriage of different *S. pyogenes emm* types in the nasopharynx of a mouse over time 105

Table 4.1. Histopathological analysis of upper respiratory tract tissue from mice infected with bioluminescent *S. pyogenes* 143

Table 5.1. Histopathological analysis of upper respiratory tract tissue from mice infected with the *covR/S* mutant (H494) 159

Table 5.2. Histopathological analysis of upper respiratory tract tissue from mice infected with a bioluminescent Δ*covR/S S. pyogenes* ($H494^{lux}$) 167

LIST OF ABBREVIATIONS

AMP	Antimicrobial peptides
AUC	Area under the curve
BAL	Bronchoalveolar lavage
BPI	Biophotonic imaging
CBA	Columbia blood agar
CFU	Colony forming units
$FMNH_2$	Reduced flavin mononucleotide
GFP	Green fluorescent protein
HRP	Horseradish peroxidase
LB	Luria-bertani
MAC	Membrane attack complex
MHC	Major histocompatibility complex
NALT	Nasal associated lymphoid tissue
PAGE	Polyacrylamide gel electrophoresis
PBS	Phosphate buffered saline
PCR	Polymerase chain reaction
ROI	Region of interest
SCID	Severe combined immunodeficiency
SDS	Sodium dodecyl sulphate
SIC	Streptococcal inhibitor of complement
SmeZ	Streptococcal mitogenic exotoxin Z
SpeA/B/C	Streptococcal pyogenic exotoxin A/B/C
TH	Todd-hewitt
THA	Todd-hewitt agar
THY	Todd-hewitt yeast

CHAPTER 1. INTRODUCTION

1.1. *STREPTOCOCCUS PYOGENES*

Streptococcus pyogenes is a Gram positive bacterium that primarily afflicts the nasopharynx, and is responsible for an estimated 616 million new cases of pharyngitis worldwide every year [1]. It was first named in relation to pyogenic osteomyelitis and wound infections [2], and was later found to be the causative bacterium of septicaemia [3], erysipelas, puerperal sepsis [3], necrotising fasciitis [4] and scarlet fever [5]. The links between streptococcal infection and the onset of rheumatic heart disease [6], and glomerulonephritis were later understood to be immune sequelae triggered by an initial infection with *S. pyogenes* [7,8]. The worldwide mortality from these diseases, taken together, is estimated to be 517,000 deaths per year [1].

S. pyogenes is also the cause of contagious skin conditions such as impetigo, which is found mainly in populations where such disease is endemic and exposure is common [9]. Although *S. pyogenes* is associated with 30-40% of cases of paediatric pharyngitis, the bacterium can occur asymptomatically within the nasopharynx at a rate of 12% within children [10], and at much lower rates in adults [11]. *S. pyogenes* is an exclusively human pathogen and is known to utilise a number of strategies to survive in different niches within the human body.

Streptococci were first differentiated from other bacteria based on their shape and structure when observed under the microscope [3]. *S. pyogenes* in particular was notable for causing β-haemolysis on the surface of blood agar plates. Further work differentiated it from other β-haemolytic streptococci based on the surface expressed group A carbohydrate. Genetic tools have provided even more insight into the vast

diversity that exists within the *S. pyogenes* population. During the course of its evolution, *S. pyogenes* has acquired an array of accessory gene elements, such as phages and phage-like elements that allow it to colonise the human host, and the tissues within [12,13]. These often carry important virulence factors. The presence of these virulence factors and the regulation thereof form the basis for the diversity of different diseases encoded by *S. pyogenes*.

1.2. THE MOLECULAR BASIS OF STREPTOCOCCAL ADHESION AND INVASION.

S. pyogenes encodes a variety of different surface expressed factors which play important roles in the binding and invasion of host cells. In *S. pyogenes*, relevant surface proteins are exported across the cytoplasmic membrane via the Sec pathway. These are localised within a distinct region of the cell membrane known as the Exportal, which contains factors that enable the folding and maturation of secreted proteins [14]. Proteins to be expressed on the bacterial surface often demonstrate an LPXTG sequence motif within the C-terminal domain, which is recognised by bacterial sortases that anchor it to the peptidoglycan cell wall [15]. The M protein, identified by Rebecca Lancefield and colleagues in the late 1930's was one of the first such proteins to be described for *S. pyogenes* [16].

However, *S. pyogenes* also produces a number of polysaccharides on its surface that also play important roles in bacterial adhesion [17]. Lipoteichoic acid is one such example. This carbohydrate binds to host membrane phospholipids, fibronectin and the CD14 receptors, which enable *S. pyogenes* to bind weakly to a variety of human cell types [18,19]. This interaction brings the host cell membrane and streptococcal surface antigens into close proximity, allowing for a second more strongly adherent and more specific streptococcal surface protein receptor to bind,

such as M-protein. There are multiple variants of M-proteins, encoded by *emm* genes in different strains of *S. pyogenes,* that bind to host factors such as CD46, laminin and fibronectin [19]. *S. pyogenes* also possesses a number of different adhesins which bind to fibronectin, such as sfb1, Fbp54, Fbp29, serum opacity factor and glyceraldehyde-3-phosphate dehydrogenase. In addition to this, *S. pyogenes* produces a hyaluronic acid capsule that enables binding to the CD44 receptor on epithelial cells [20].

The interaction between these adhesion factors and the host cell cytoskeleton [21,22] can induce the internalisation of *S. pyogenes* within epithelial cells, theoretically enabling the long term persistence of *S. pyogenes* within target tissues [23]. This internalisation prevents the detection of *S. pyogenes* by the host immune system and may protect bacteria from β lactam antibiotics.

S. pyogenes also encodes the FCT pilus (also known as the T-antigen [24]) that consists of a backbone protein , with an ancillary protein at the tip which mediates its binding [25] to factors such as gp340. This compound is found in saliva [26] and gp340 binding promotes aggregation and streptococcal biofilm formation. Biofilms confer protection to *S. pyogenes* against antibiotics and host clearance [27].

These adhesion molecules are important for *S .pyogenes* during superficial tissue infections on the skin or within the nasopharynx. To invade sterile sites and deeper issues, *S. pyogenes* employs a different set of strategies to disseminate within these tissues and to combat the immune response.

1.3. VIRULENCE FACTORS ENABLE *S. PYOGENES* TO EVADE THE IMMUNE SYSTEM.

The production of virulence factors by *S. pyogenes* enables it to evade the immune system. The key to immune defence against *S. pyogenes* is the initiation of neutrophil-mediated killing that requires opsonisation by complement and immunoglobulin. Often, these virulence factors can be directly secreted via specific ABC transporters [28], or through the previously mentioned Sec pathway. They can also be expressed as surface proteins, which later undergo cleavage and release specific portions to interact with the immune system.

Amongst the first secreted virulence factors to be described were the streptolysins, due to their β-haemolytic activity [29]. Streptolysin O forms pores in membranes, which can allow for the entry of virulence factors such as NADase [30], Whilst these can induce cytolysis of red blood cells and neutrophils, at lower concentrations they have been shown to interfere with phagocytosis [31].

Cationic host antimicrobial peptides (AMP) such as LL37, derived from cathelicidin, have lytic activity against streptococci and are found in secretions from the upper respiratory tract as well as within neutrophil granules. It is therefore essential that *S. pyogenes* can combat AMPs and defensins, which is achieved by production of enzymes that can bind, cleave and inactivate these factors, such as the ‘streptococcal inhibitor of complement (SIC) [32].

The relative importance of the various complement pathways to *S. pyogenes* immunity is not clear cut. The complement cascade can recognise *S. pyogenes* via the classical pathway through interaction of C1q with antibody bound to the streptococcal surface. Some studies suggest that C1q can directly bind to *S.*

pyogenes and can facilitate its clearance without the need for classical pathway activation [33]. *S. pyogenes* can also be detected by complement through the recognition of mannose sugars on the streptococcal surface of by the mannose binding lectin pathway. The complement protein C3 is recruited in the process of both these pathways, and can independently initiate the downstream antibacterial activities of the complement cascade via an alternative pathway. This involves the deposition of C3b that recruits other complement factors to form a C3 convertase, leading to bacterial opsonisation and neutrophil phagocytosis [34,35]. *S. pyogenes* can interfere with the complement pathway through binding of endogenous host complement inhibitors, such as complement factor H and C4BP which naturally act to inhibit C3 convertase [36–39]. M-protein also binds to fibrinogen [40], which has been suggested as a way for allowing the deposition of fibrin on the surface of *S. pyogenes*, thus preventing recognition by the complement cascade [41].

The SIC produced by *emm1 S. pyogenes* strains appears to bind and inhibit the function of a number of complement components including C3, and prevents the mobilisation of C5-9 proteins into the membrane attack complex (MAC). The significance of this is unknown as the MAC has no known antibacterial activity in Gram positive bacteria [42]. The chemoattractant activity of C5a is disrupted by *S. pyogenes* via the C5a peptidase scpA [43,44].

The chemoattractant CXCL8/IL-8, and its murine counterparts MIP-2 and KC, act to recruit neutrophils to areas of *S. pyogenes* invasion. *S. pyogenes* encodes a serine protease SpyCEP (Genomic annotation Spy0416, also known as cepA, and ScpC) which cleaves these chemoattractants as well as the entire repertoire of human CXC (neutrophil-active) chemokines [45–47], and prevents the recruitment of neutrophils

to the site of infection. There is also evidence that SpyCEP facilitates the internalisation of *S. pyogenes* into endothelial cells [48].

S. pyogenes also encodes a range of DNases, such as Sda1, which are believed to be protective against neutrophil extracellular traps [49]. Neutrophil extracellular traps are extrusions of a DNA/histone matrix purported to capture bacteria and expose them to bactericidal agents. DNases have been shown to break down this matrix, and prevent the neutrophil killing of *S. pyogenes*.

M-protein binds and activates plasminogen [50,51], causing it to be degraded to plasmin, which can break down fibrin clots and connective tissue [50] and enable *S. pyogenes* to disseminate within the deep tissues of the body. Although severe infection with *S. pyogenes* can trigger disseminated intravascular coagulation, it produces a number of additional virulence factors, such as streptokinase, that interact with the coagulation cascade and can activate the contact system leading to generation of bradykinin, which is a local vasodilator and participant in inflammation [52].

S. pyogenes also utilises molecular mimicry to avoid recognition by the immune system. The tertiary coiled-coil structure of M-protein has immune cross reactivity with myosin and tropomyosin antigens found in the heart and is believed to play a specific role in rheumatic heart disease [53,54]. Cross-reacting antibodies are believed to trigger endothelial and valvular damage and the ensuing immune sensitisation which can then result in cell-mediated autoimmunity and rheumatic heart disease [55].

Capsular hyaluronic acid, in addition to aiding adhesion, also provides a degree of camouflage against the human immune system, as this compound is also produced

naturally by the human host. Unlike other streptococcal capsular polysaccharides, very little antibody is observed in response to the *S. pyogenes* hyaluronic acid capsule. *S. pyogenes* strains isolated from more invasive diseases tend to produce more hyaluronic acid than those isolated from non-invasive disease. This increased production of hyaluronic acid induces enhanced resistance to phagocytosis [56,57].

Superantigens are secreted proteins produced by *S. pyogenes* that, unlike conventional antigenic peptides, bind to the Vβ chain of a restricted proportion of T-cell receptors when presented on HLA class II molecules without requirement for processing or specificity [58]. Superantigens are selective for different subsets of T-lymphocytes based on the type of Vβ receptor. As *S. pyogenes* can produce up to 11 different superantigens, with most strains producing 4-5 such toxins, this interaction causes the widespread activation of T cells, leading to marked cytokine production, systemic inflammation and, in severe cases, streptococcal toxic shock syndrome.

SpeB (streptococcal pyrogenic exotoxin) is a cysteine proteinase that is also believed to aid the dissemination of *S. pyogenes* during infection. It cleaves a number of immune products such as complement factors [59] and immunoglobulins [60]. In addition to this, it cleaves a number of streptococcal proteins, such as M-protein, the superantigen, streptococcal mitogenic exotoxin Z (smeZ) [61], and C5a peptidase [62]. The importance of immunoglobulin in recognition of *S. pyogenes* is underlined by the number of virulence factors expressed to prevent it. In addition to SpeB, proteases such as IdeS and EndoS cleave and inactivate antibodies, while the bacterial cell wall also expresses immunoglobulin binding proteins that capture the Fc segments of immunoglobulins, effectively neutering the ability to opsonise bacteria or interact with neutrophil Fc receptors [63]. The diverse virulence factors produced by *S. pyogenes* enable the bacterium to survive in sterile regions of the

body, and are responsible for the more severe disease manifestations caused by *S. pyogenes*.

1.4. TISSUE TROPISM

The array of different diseases caused by *S. pyogenes* can broadly be described in two classes; non-invasive diseases, such as those that affect the skin and the nasopharynx, and invasive diseases which affect deeper tissues and sterile regions of the body. These different manifestations can to some extent be explained by the genetic factors governing the survival strategies utilised by *S. pyogenes* in these diverse environments.

1.4.1. THE ROLE OF *EMM* TYPES IN DETERMINING TISSUE TROPISM

The two main targets for non-invasive *S. pyogenes* disease are the skin and the upper respiratory tract. The strains of *S. pyogenes* which infect the skin tend to cause a different spectrum of disease and different phenotype to the strains which cause disease in the upper respiratory tract [64].

Historically, clinical isolates of *S. pyogenes* were differentiated by their variant of surface expressed M-protein [65,66] due to its relative heterogeneity. Currently, isolates are identified based on *emm* genotype, as *emm* is the gene encoding the M protein [67]. There are over 200 known *emm* types, but these tend to group structurally into five pattern groups, A-E, based upon the 3' sequence and their chromosomal location. The *emm* patterns broadly map to the tissue tropism patterns of the strains of *S. pyogenes* that express them. Strains with patterns A-C generally infect the upper respiratory tract, pattern D strains primarily infect the skin and strains with Pattern E can infect both of these niches [68,69].

However, the M-protein is only one of many different gene products that play roles in the adhesion of *S. pyogenes* to different tissues. Many of these factors are known to share genetic linkage to specific *emm* patterns and participate in disease initiation, such as serum opacity factor and the FCT pilus [68,70]. The *emm* type can therefore be considered as an indicator of the niche occupied by different strains of *S. pyogenes*. The epidemiology of *S. pyogenes* infection is broadly similar in western developed nations. A study of circulating pharyngitis isolates in the USA revealed that the most common circulating *emm* types tend to be *emm1*, *emm12* and *emm28* (Figure 1.1) [71]. This is broadly the experience within the UK, however there are no published data pertaining to pharyngitis isolates. The most common *emm* types in the UK based on 2009 data from Imperial College were *emm* types 1, 3, 6, 12, 28, 75, and 89, (Figure 1.1.) although the relative importance of *emm*3 has waned in the last two years (Sriskandan, unpublished data).

Despite the broad spectrum of recognised *emm* types, the repertoire of *emm* types causing both invasive and non-invasive infections is in fact surprisingly limited in the industrialised world. This is in contrast to less-developed nations and indigenous communities where there is a greater diversity in the prevalent *emm* types [72,73].

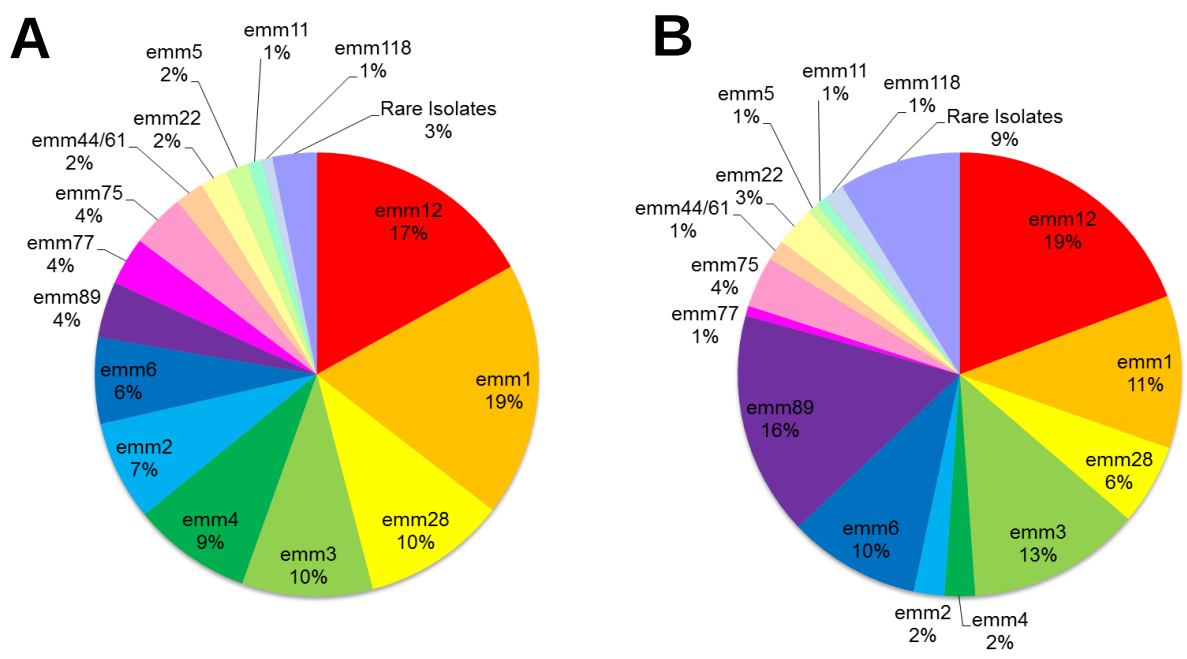


Figure 1.1. Diversity of circulating *emm* types associated with pharyngitis within the USA and the UK. Proportions of different *emm* types collected from cases of non-invasive pharyngitis in multiple hospitals in the USA. Those *emm* types which accounted for <1% of the total collected isolates were classified as "rare" isolates (A). Based on data from [71]. Diversity of circulating *emm* types associated with pharyngitis in West London April-November 2009 (B). Data from Imperial College Healthcare Trust (Sriskandan, unpublished)

Post streptococcal auto-immune sequelae such as rheumatic heart disease, which is characterised by fever and valvular cardiac and joint inflammation, can be triggered by *S. pyogenes* associated with specific *emm* types [74]. It has been suggested that strains of *S. pyogenes* with specific tropisms to the upper respiratory tract tend to cause rheumatic heart disease, and strains with a tropism to the skin tend to cause glomerulonephritis [64]. The molecular and immunological events leading to acute rheumatic fever and post-streptococcal glomerulonephritis are not known, and specific antigens that are targeted by cross-reacting antibodies or T cells remain controversial.

Despite *emm*-specific niche adaptations, *S. pyogenes* across multiple *emm* classes have the capacity to invade deeper tissues and cause invasive disease. The gene regulators which control the expression of these factors play a major role in determining the phenotype of *S. pyogenes* during invasive infection.

1.4.2. REGULATION OF VIRULENCE

The timing of the expression of virulence factors that enable survival of *S. pyogenes* in deeper tissues is controlled by virulence regulators (Table 1.1). Two component regulatory systems enable *S. pyogenes* to detect stimuli within the external environment and to respond to them. They play a crucial role in niche adaptation, such as *SptR/S* which aids survival within saliva [75], and promoting the expression of adhesion factors in the initial stages of colonisation. *RofA*, and the related *nra,* are a set of stand-alone response regulators which increase the production of fibronectin and collagen binding proteins and repress virulence factors such as streptolysin S and SpeB, [76] in response to the presence of oxygen [77].

Regulator Targets / Virulence regulators	covR/S	FasBCAX	Ihk-Irr	SptR/S	TrxR/S	Rgg	RivR	codY	ccpA	mga	rofA	nra
Streptolysin S	↓		↑	↑		↓			↓		↓	↓
Streptolysin O						↓		↑	↑	↑		
SpeA				↑					↑			↓
SpeB	↑			↑			↑		↑		↓	↓
SpeH						↓		↑				
Streptokinase	↓	↑				↓						
Hyaluronic Acid	↓					↓	↓	↓	↑			
SpyCEP	↓							↑	↓			
C5a peptidase	↓				↑			↑		↑		
Sda1	↓								↓			
SIC				↑	↑					↑		
EndoS	↓								↓			
Fibronectin binding protein		↑	↑		↑						↑	↓
NADase	↓					↓						
IdeS	↓			↑		↓		↑				
Mac-2										↑		
M-protein					↑	↓						
Lipoteichoic Acid										↑		
covR/S						↑		↓	↑			
FasBCAX						↑						
Ihk-Irr						↑						
SptR/S								↓				
Mga						↓		↑	↑	↑	↓	↓
Rgg	↓	↓										
codY								↓				
TrxR	↓											
RivR	↓											
References	[78]	[79]	[80]	[75]	[81]	[82,83]	[84]	[85]	[86]	[76]	[76]	[76]

Table 1.1. Virulence regulation. ↑= Positive regulation. ↓= Negative regulation

The first virulence regulatory system described for *S. pyogenes* was *mga,* which is a stand-alone multi-gene activator for which a partner sensor kinase or regulator has not been found. *Mga* promotes the expression of the highly important anti-phagocytic M-protein [87], in addition to streptococcal inhibitor of complement [88], C5a peptidase [89] and a number of other genes within a contiguous operon.

The *covR/S* system (also known as *CsrR/S*) is known to regulate the transcription of 15% of all the chromosomal genes possessed by *S. pyogenes* [78]. Due to its broad coverage of the genome, and its role in repressing an array of important virulence factors, it has been extensively studied. It represses the expression of a number of important virulence factors, such as the hyaluronic acid capsule, DNases, and SpyCEP. While *covR/*S can suppress SpeB protease production in some *S. pyogenes s*trains [78,90] deletion of *covR/S* has been shown to prevent SpeB production in most strains, in particular *emm1 S. pyogenes* [91,92]. There is therefore a reciprocal relationship between SpeB expression and expression of most other virulence factors that are primarily concerned with the prevention of neutrophil-mediated killing. Although *covR/S* primarily plays a role in pathogenicity by varying the phosphorylation status of the repressor component *covR* through kinase activity of the sensor component, c*ovS*, mutations in either component can have a marked irreversible impact on phenotype.

Under ‘normal’ situations in the nasopharynx, it is hypothesised that CovR/S is active; the sensor kinase results in phosphorylation of CovR, which in turn represses expression of virulence factors. It is also believed that exposure to ‘danger’ signals , perhaps from incoming neutrophils, or exposure to blood, results in CovS acquiring phosphatase activity resulting in the de-phosphorylation of CovR. Consequently this leads to the de-repression of virulence factors, such as capsule and SpyCEP,

allowing *S. pyogenes* to defend itself from attack, The signalling molecules recognised by CovS are not characterised but may include Mg^{++} and LL37 [93,94].

Mutations in the *covS* gene are associated with a de-repression of these same virulence factors, leading to a “hypervirulent” phenotype that is associated with invasive streptococcal diseases observed in humans [91,95]. These mutations are known to be selected for during invasive infection in response to immune pressure [49,96] and can be identified in samples from deep tissues in mice where *S. pyogenes* has progressed from a superficial to a more invasive infection, demonstrating a predicted phenotype change to match the acquired genotype [91]. Interestingly, strains of *S. pyogenes* exhibiting this hypervirulent phenotype have impaired biofilm formation [97]. Mutations in *covR* have even more impressive phenotypic effects, increasing the expression of virulence factors such as SpyCEP by 100-1000 fold [45]. Such mutants have been found in cases of invasive infection, but these mutants are not prevalent in the community and have not been identified in outbreak settings [45]. This suggests that the potential for invasiveness is a latent trait that is broadly expressed across all *emm* patterns, but does not become fixed in circulating strains due to the fitness costs it incurs during superficial infection. Despite the fact that *covR/S* mutations appear to favour invasive infection, albeit with likely fitness costs in some settings, there are no data showing that *covR/S* mutation is deleterious to nasopharyngeal infection. One of the aims of this project was to determine if *covR/S* mutation might impact on nasopharyngeal infection using a properly characterised murine model.

1.5. TRANSMISSION

The understanding of the factors governing the transmission of *S. pyogenes* in the human population primarily stems from observational epidemiological studies rather than experimental work. The survival of *S. pyogenes* in saliva [98] likely forms the basis for the transmission of *S. pyogenes* from the respiratory tract. In the process of coughing or sneezing, saliva is converted into airborne infectious droplets [99]. The range and maintenance of *S. pyogenes* as an aerosol is limited by the size of the airborne droplets produced during infection [100].

The dispersal distance of *S. pyogenes* by coughing is believed to be limited compared with sneezing. The spread of bacteria via these routes is dependent on the concentration of bacteria within the saliva, and individuals with high numbers of *S. pyogenes* within their saliva tend to also have more bacteria in other body regions, such as the hands and lower face [101]. Increased physical activity has also been associated with increased aerosolisation [101,102] and crowding is known to be a determining factor in the frequency of transmission in rheumatic heart disease outbreaks [103,104]. There are also reports of transmission and outbreaks from vaginal [105,106] and anal carriers of *S. pyogenes* [107], although these are uncommon reservoirs of infection.

Studies suggest that fomites, such as contaminated bedding and environmental dust particles are not a significant reservoir for streptococcal infection [108,109], as their drying in the environment inhibits infectivity. However nosocomial outbreaks have been linked to contaminated ‘wet’ fomites such as bath and shower fittings, particularly in maternity units [110]. This has led to a recognition that chlorine-based cleaning of such surfaces is a pre-requisite in prevention of nosocomial outbreaks,

as originally proposed over a century ago [111]. *S. pyogenes* outbreaks have also been traced to contaminated food [112,113], but these are uncommon.

As noted earlier, a significant portion of the population carries *S. pyogenes* asymptomatically in the respiratory tract. After the onset of disease, *S. pyogenes* can persist within the respiratory tract in what has been termed a "carrier state" which can potentially last for up to 19 weeks after the initial infection [114,115]. This may be due to the internalisation of *S. pyogenes* within cells of the nasopharynx [23]. This may explain the recurrence of infection even after penicillin treatment, in spite of *S. pyogenes* remaining susceptible to this antibiotic. However, the contribution of this carrier state to *S. pyogenes* spread within the population is debatable, as there is some evidence to suggest that carriers do not harbour streptococci in high numbers, and do not transmit as effectively as compared to patients at the peak of symptomatic infection [116].

1.6. VACCINATION

Rebecca Lancefield described streptococcal M protein as a potentially protective antigen that, when extracted crudely from a broth culture of *S. pyogenes*, could induce protective immunity against challenge with the same strain [16]. The heterogeneity of *S. pyogenes* surface proteins has unfortunately proven to be a formidable barrier against the development of a vaccine. Early attempts to develop a vaccine using attenuated or dead bacteria were unsuccessful [117,118]. The primary safety concern for devising a vaccine against *S. pyogenes* is its immune cross reactivity with the host. This effect could be triggered by the inoculation of dead bacteria or specific antigens, leading to rheumatic carditis [119,120]. Indeed, one early vaccine trial utilising M-protein was implicated in the onset of rheumatic heart

disease in its participants [122,123] and this finding has held back vaccine research by decades.

In spite of this, vaccinations based on M1 [124,125] have demonstrated some protective efficacy, although similar work based on M3 and M12 was not as successful [126]. Further work found that protective antibodies in humans were raised to the variant N-terminal portion of the protein [127]. This poses problems with vaccine coverage when one considers that there are over 200 potentially variant M proteins.

A 26-valent M-protein based vaccine of *S. pyogenes* theoretically provided coverage against 90% of *S. pyogenes* strains circulating in the US [128]. However it lacked sufficient coverage against *S. pyogenes* strains circulating in developing countries, where rheumatic heart disease is an endemic problem [129]. Another approach to target a broad spectrum of M-proteins is to immunise against conserved C-terminal regions of the protein [130,131]. This is the basis for the J8 vaccine, which has been shown to be protective in small animal models, and provides better coverage for developing countries [132]. However the problems of coverage and potential immune sequelae associated with M-proteins has led other candidates to be explored for use in a vaccine.

Adhesion factors have been evaluated for use in a vaccine to prevent *S. pyogenes* pharyngitis. The group A carbohydrate is conserved among multiple *emm* types of *S. pyogenes* and has been shown to be protective in animal models, but is setback by its cross reactivity with human heart antigens [133,134]. Vaccine candidates based on fibronectin binding proteins such as Fbp 54 [135], sfb1 [136–138] have also shown promising results in murine models of infection. The streptococcal T-antigen,

which comprises part of the pilus structure [24], has also been suggested as a vaccine candidate as it is more conserved compared to M-protein [24].

Another strategy is to use streptococcal virulence factors as the basis for vaccines. The advantage of targeting virulence factors is that they are generally highly conserved, due to their essential role in streptococcal infections. The streptolysins are known to be immunogenic, with the anti-streptolysin O antibody titre often being used as an indicator for a previous *S. pyogenes* infection. In recent work, detoxified forms of streptolysin O have shown protective efficacy in mice [139]. A vaccine candidate against streptolysin S has been found to prevent haemolysis, but did not increase opsonophagocytosis [140].

Superantigens such as SpeA and SpeC have been explored as the basis for vaccines, as these toxins play important roles in invasive disease. Vaccines based on superantigenes have been shown to confer protection in rabbit models of streptococcal toxic shock syndrome through mitigating the toxic effects of the disease, rather than facilitating bacterial clearance [141,142].

In general however, cell wall-associated antigens are favoured because antibodies directed to such targets are likely to assist in opsonisation of the bacterium in addition to possibly neutralising the virulence activity of the target. Many such antigens are characterised by the LPXTG sortase anchoring motif at the C terminus of the protein.

A recombinant vaccine based on C5a peptidase has been shown to elicit an antibody response and protection in some mouse models of infection [143]. An additional advantage of this vaccine candidate is the cross reactivity with a C5a peptidase produced by *Streptococcus agalactiae* [144].

The SpyCEP protein is conserved in *S. pyogenes*, and has been identified via proteomic and genomic approaches as a viable candidate for vaccination [145,146]. Vaccination with SpyCEP has been shown to enhance survival in an invasive mouse model of respiratory infection [146]. It also prevents bacterial dissemination in an invasive model of soft tissue infection caused by either *S. pyogenes* or *Streptococcus equi* which expresses a homologous enzyme known as SeCEP [147]. It is likely that future anti-streptococcal vaccines may comprise several antigenic components including proteins such as SpyCEP and C5a peptidase.

A variety of new proteomic approaches have been utilised to screen for surface expressed proteins of *S. pyogenes* [146], using human sera to specifically detect immunogenic candidates [145,148]. Whilst many of these vaccines have shown efficacy in animal models, there are questions as to how appropriately these surrogate hosts have been used to model human infection. Specifically, there is a pressing need for a vaccine against *S. pyogenes* that protects against pharyngeal infection, yet the majority of vaccines evaluated are tested in more invasive animal models. To some extent, this is due to the methods by which vaccines are evaluated. In general, the elicitation of a protective antibody response, and the prevention of deaths in animal models have been the outcomes used to judge the efficacy of vaccines, rather than bacterial clearance (Table 1.2.)

Protein	Vaccine Candidate	Model	Antibody production	Demonstrated protection *in vivo*	Demonstrated reduction in Streptococcal numbers	Reference
M-protein	26-valent (StreptAvax)	Humans	Yes			[149]
		Rabbits	Yes			[128]
	Hexavalent	Mice	Yes	Yes		[150]
		Mice	Yes	Yes		[151]
		Rabbits	Yes			[152]
	30-valent	Rabbits	Yes			[153]
	M5	Mice	Yes	Yes	Yes	[130]
	Salmonella expressing M5	Mice	Yes	Yes		[154]
	Vaccinia expressing M6	Mice	Yes	Yes	Yes	[155]
	M6	Mice	Yes	Yes	Yes	[156]
		Mice	Yes	Yes	Yes	[157]
	M24	Humans, Mice, Rabbits	Yes	Yes		[127]
	J-8	Mice	Yes	Yes	Yes	[158]
		Mice	Yes	Yes		[159]
		Mice	Yes	Yes	Yes	[160]
		Mice	Yes	Yes		[161]
	J-14	Mice	Yes	No		[151]
		Mice	Yes			[131]
		Mice	Yes	Yes	Yes	[158]
		Mice	Yes	Yes	Yes	[162]
		Mice	Yes	Yes		[163]
Lipoteichoic acid		Mice	Yes	Yes	Yes	[164]
Spy0269	Spy0269 (27-849)	Mice	Yes	Yes		[148]
	Spy0269	Mice	Yes	Yes		[145]
Internalin A (spy1361)		Mice	Yes	Yes		[148]
Spy0872		Mice	Yes	Yes		[145]
DacA (spy0292)		Mice	Yes	Yes		[145]
Spy0895		Mice	Yes	Yes		[145]
Spy1536		Mice	Yes	Yes		[145]
Spy0488		Mice	Yes	Yes		[145]
Spy1727		Mice	Yes	Yes		[145]
MraW (spy1666)		Mice	Yes	Yes		[145]
Spy0019	Spy0019	Mice	Yes	Yes		[148]
	Spy0019 /Alum	Mice	Yes	No		[165]
Sse esterase	Sse	Mice	Yes	Yes		[165]
SpeA	SpeA mutants	Rabbit	Yes	Yes		[141]
	SpeA-B fusion protein	Mouse	Yes	Yes		[166]
SpeB	SpeA-B fusion protein	Mouse	Yes	Yes		[166]
SpeC	SpeC mutants	Rabbit	Yes	Yes		[142]
SOF	Recombinant SOF peptides	Rabbit, Mouse	Yes	Yes		[167]
Streptolysin S	SLS(10-30) KLH	Rabbit	Yes			[140]
Streptolysin O	Recombinant SLO (32-571)	Mouse	Yes	Yes		[148]
	Mutant SLO	Mouse	Yes	Yes		[139]
FbaA	GST-FbaA	Mouse	Yes	Yes		[168]
SIB35	rSIB35	Mouse	Yes	Yes		[169]
C5a peptidase	Recombinant SCPAw	Mouse	Yes		Yes	[144]
		Mouse	Yes		Yes	[170]
	ΔSCPA49	Mouse	Yes	Yes	Yes	[143]
SpyCEP	Recombinant SpyCEP (34-898)	Mouse	Yes	Yes		[148]
	SpyCEP	Mouse	Yes	Yes		[145]
	SpyCEP	Mouse	Yes	Yes		[146]
	Recombinant SpyCEP (35-587)	Mouse	Yes		Yes	[147]
Sfb1	FNBR	Mouse	Yes	Yes		[159]
	Sfb1 –CTB	Mouse	Yes	No	No	[136]
Fbp54	rFBP54	Mouse	Yes	Yes		[135]
Streptococcal Haemoprotein Receptor	rSHR	Mouse	Yes	Yes		[171]

Table 1.2. Outcomes utilised to evaluate vaccine candidates

One of the aims of this project was to develop an improved model of *S. pyogenes* upper respiratory tract infection that could be used to screen and evaluate novel vaccine candidates.

1.7. ANIMAL MODELS FOR STREPTOCOCCAL INFECTION AND COLONISATION

Much of the current understanding of *S. pyogenes* pathogenesis has been gained through the utilisation of animal models. Different models have been used in the past to examine different diseases caused by *S. pyogenes* infection. Early studies recognised that rabbits and white mice were more susceptible to *S. pyogenes* infection than other species of animals [3,172]. Mice have become the standard model organism for streptococcal infection, due to degree of characterisation, genetic tractability, relative inexpensiveness and recognised similarities to the human immune system [173].

However, the infectious capability of *S. pyogenes* in many animal hosts, particularly mice, is limited. One of the ways to circumvent this is to adapt *S. pyogenes* to animal hosts through passaging. This selects for strains which thrive in the niche in which they have been passaged, and produces *S. pyogenes* strains that are more infectious to animals [174]. It has been shown that *emm1 S. pyogenes* passaged through an invasive model of infection, acquired mutations within a number of genes, including *covR/S* [96]. Whilst such strains have been useful, the degree to which they change in order to adapt to their new environment may compromise their relevance to the human host. However, whilst these models may have specific limitations, they can reveal interesting new aspects of *S. pyogenes* pathogenesis if properly applied.

1.7.1. ANIMAL MODELS OF SKIN AND SOFT TISSUE INFECTIONS

A number of different animal species and techniques have been utilised to model *S. pyogenes* skin infections. *S. pyogenes* does not survive for long on the surface of human skin [175], and minor trauma may be required to establish an infection [176].

Many models have involved subcutaneous or intradermal instillation of bacteria into surrogate hosts such as hamsters [177,178] or mice [179] to replicate recognised features of streptococcal skin infections. A modification of this infection model involved the injection of an air sac at the site of infection to enable the analysis of immune responses *in vivo* by sampling of fluid within the space [180]. These produced symptoms in animals that were comparable to humans by bypassing the natural barrier of the skin with an injection of a large inoculum. Recently, Svensson and colleagues grafted human foetal foreskin tissue onto SCID mice to produce a so-called 'humanised' mouse model to more accurately reflect the infection process that is believed to occur in humans [181].

However, the subcutaneous model of infection has additional applications, such as the modelling of soft tissue infections. Subcutaneous models of infection have been applied to investigate questions relating to the functions of virulence factors [182] and their regulation [90]; often lesion size is measured as a parameter of infection progression since a dermonecrotic ulcer or abscess can develop. A flaw in such experiments is that the lesion size may relate more to the neutrophil influx than bacterial abundance.

Intramuscular infection models are often used to investigate necrotising fasciitis, due to the characteristic lesions they produce, the size of which relates to the degree of damage occurring within the organ [183]. This model allowed for an estimation of

disease severity of *S. pyogenes* infection by examining the size of the lesions produced, although this too may be biased by neutrophil influx [184]. Hence most investigators choose to quantify bacterial counts at the site of infection, as an objective parameter of infection burden. Nonetheless, such measurement requires the sacrifice of the animal and the timing of measurement may mean that crucial events are missed. To enhance the amount of information gleaned from such experiments, all tissues, including the draining inguinal lymph node, can be harvested for culture [46]. Inevitably, investigators rely on the use of multiple time points to ensure differences between experimental groups are not missed, although this leads to the use of large numbers of animals.

Due to their evolutionary proximity to man, primates have also been infected intramuscularly to simulate necrotising fasciitis [185,186]. These animals developed streptococcal toxic shock syndrome, similar to the disease progression observed in humans. However, primates are seldom utilised for primary research, as their cost of maintenance means they cannot be used in high numbers.

The zebrafish, *Danio rerio*, has been explored as an alternative surrogate host to model soft tissue infection in a higher throughput manner. Intramuscular infection of the zebrafish with *S. pyogenes* produces a soft tissue infection that has some similarities to necrotising fasciitis [187]. The immune systems of the zebrafish and human have enough in common for them to be informative of *S. pyogenes* virulence *in vivo* [188,189].

1.7.2. Animal models of septicaemia and toxic shock syndrome

Whilst the dissemination of *S. pyogenes* from the site of a skin or soft tissue infection can occur, leading to a systemic infection similar to bacteraemia, the injection of bacteria directly into the circulation through intravenous and intraperitoneal routes has also been utilised to directly examine systemic infection. These models of infection have been used for passaging [96], and testing vaccine [160,174] and antibiotic efficacy.

However, the drawback of these models is that mice are relatively resistant to infection compared with the human situation. It has been shown that different strains of mice exhibit different susceptibilities to infection [192,193]. The sex of the mice [194,195], and their age [196] have also been suggested as determinants of systemic infection.

Another issue with mouse models of bacterial infection is that they cannot produce superantigen responses, which are based on the binding of HLA class II subsets that do not occur in mice. One solution is the use of primate models, which are close enough to mimic human responses [190]. However, these models still have the previously discussed resource issues. An alternative approach is the use of human-transgenic mouse models that express the DQ segment of the MHC molecule to enable superantigen activation [191].

1.7.3 Models of respiratory infection

The primary site of *S. pyogenes* colonisation in humans is within the upper respiratory tract. There have been a number of studies in which *S. pyogenes* tonsillitis has been induced in human subjects. Initial work involved the inoculation with secretions from patients [117] and later involved the transfer of *S. pyogenes* in

broth to the tonsils via a cotton applicator [124–126]. Whilst not initially evident, the symptoms of *S. pyogenes* infection were observed to manifest 24-48 hours post infection [109]. It is also important to note that these early methods of experimental inoculation did not necessarily produce infection in all of the unvaccinated subjects [126].

It has been recognised in previous work that baboons can become naturally infected with *S. pyogenes* [197,198]. Indeed, a number of primate species have been utilised to study pharyngitis, such as chimpanzees [199], baboons [200], cynomolgus [201] and rhesus macaques [202], via intranasal instillation, or direct deposition on the tonsils. Whilst *S. pyogenes* colonises these animals effectively, and can result in symptomatic tonsillitis, there are some drawbacks to their use.

Primates are rarely culled at the ends of such experiments; often they receive a course of treatment to clear *S. pyogenes* [202], thus the animals are not dissected at the end of experiments (although there are exceptions [203]). Temperature, blood samples, veterinary scoring and throat swabs provide the primary methods for studying the progression of infection in these animals.

These difficulties, in addition to the challenging ethical issues and high costs of primate maintenance mean that there is a requirement for a higher throughput model for nasopharyngeal infection that can be used to screen vaccine candidates. Mice have been commonly used to model respiratory infection, as they consume few resources, and the conserved nature of the mammalian nasopharynx ensures that they are relevant models [204,205].

However, it is important to recognise that there are some notable differences between the rodent and human nasopharynx. The structure of the nasopharynx

consists of nares, the openings through which air enters, which are lined with tough squamous epithelium and are broadly similar between all mammalian species [206]. The major differences in the structure of the nose come from the complexity of the ethmoturbinates (a scrolled tissue located in the caudal nasopharynx) and the relatively higher proportion of olfactory epithelium in the rodent nasopharynx [205]. Rodents also possess nasal associated lymphoid tissue (NALT) which acts as an immune inductive site in response to inhaled antigens. Whilst NALT has been observed in monkeys and humans, it is fundamentally different in structure to those observed in mice [207,208]. Instead, tonsils are believed to be the human analogue for this tissue [209]. Although rodents do not possess tonsils, some work has shown that the NALT becomes colonised by *S. pyogenes* in a similar way to human tonsils [210].

A number of methods have been utilised to induce infection in mice. Mice have been observed to become infected from *S. pyogenes* at an estimated density of ~150 colony forming units (CFU) per ml of air that was made airborne through the use of a nebuliser and specialised cage system [211]. This infection technique produced variable outcomes, with no infection occurring at all in some instances making viable comparisons between treatments difficult [212]. This unreliability and the need for specialised equipment are the reasons why this method did not become more widely utilised.

A simpler intranasal model was devised using the instillation of inoculum in solution into the nares of a mouse [213]. This model has been more widely adopted to study respiratory infection. A number of works suggest that inoculum volumes of greater than 5µl [214] or 10µl [215] distribute to the lungs, which may cause pneumonia, whereas others state that volumes of 20µl [216] or even 50µl [217] are retained

within the upper respiratory tract. These models of infection have been used to provide insight into infection in the upper respiratory tract [217–219], as well as more severe diseases like pneumonia [220]. However, since the dose distribution varies between studies, many of the models used to study upper respiratory tract infection may also induce severe infection. The various models of respiratory infection that have been used to investigate *S. pyogenes* are summarised in Table 1.3. with particular reference to the dose volumes and number of infecting CFU.

It has been observed that *S. pyogenes* is a poor pathogen of rodents compared to the primary human host. A number of works have adapted strains of *S. pyogenes* to the mouse by passaging them through an intraperitoneal model of infection (Table 1.3.). An *emm*50 strain of *S. pyogenes* that was recovered from mice during an epizootic outbreak in a mouse colony has been widely used [221]. However, this strain was later shown to have a deletion in the *mga* locus [222], a major virulence regulator which is important for human infection.

A number of methods have been utilised to assess infection progression in the upper respiratory tract. Alginate swabs have been used to take throat cultures, but *S. pyogenes* cannot survive for very long on these swabs [223], and only low numbers of the bacteria tend to be recovered. As a result, swabs tend to be used to determine the presence or absence of *S. pyogenes* [224] but often not for quantitative assessments of bacterial numbers. Another method which has been widely used is the monitoring of death as an outcome of infection, but this tends to be a characteristic of invasive infections and cannot be used to measure survivable colonisation. The dissection of the relevant organs can also be used to monitor infection. The lungs and the spleen are useful to monitor the progression of pneumonia and the attendant bacteraemia. The NALT, which has been postulated

as the primary focus of colonisation, has been dissected out as a means to assess nasal carriage. The dissection and culture of the whole nasal tract is the best method to directly assess the numbers of *S. pyogenes*, although the dissection as described in some work would only allow for the extraction of the anterior nasal passages [144]. The various outcomes that have been measured to study upper respiratory tract infection are also described in Table 1.3.

Currently, there are a number of models of respiratory tract infection, few of which focus on infection exclusively in the upper respiratory tract, and there are even fewer techniques with the ability to monitor *S. pyogenes* colonisation non-invasively in living mice. However, in recent years, a new technique has been developed which may enable the direct quantitative monitoring of *S. pyogenes* infection through non-invasive means, which shall be described in more detail below.

Table 1.3. Intranasal models of infection

Dose Volume	Mouse Adapted	*emm type*	CFU	Host	Sex	Age (weeks)	Monitoring method	Sampled Tissues	Ref
5-10µl	Yes	1,3,5,6, 19,24,50	10^1-10^8	CD1	F	7-10 $^+$	Throat cultures, Death		[224]
5µl	Yes	Untyped	10^8	AKR	N/M	3-7		Cervical Lymph Nodes*, Lungs*, Anterior Nasal Tract *	[225]
10µl	Yes	50	10^5	CD1	N/M	12	Throat cultures		[221]
10µl	No	1	10^7	BALB/c & C57BL/6	F	5-6		NALT	[230]
10µl	No	24	10^5-10^7	BALB/c	F	11-14 $^+$	Throat cultures, Death		[20]
10µl	Yes	24	10^7	BALB/c	F	11-14 $^+$	Throat culture, Death		[130]
10µl	No	24	10^7	BALB/c	F	24	Death		[150]
10µl	No	24	10^7	BALB/c	F	11-14 $^+$	Throat culture, Death		[164]
10µl-20µl	Yes	50	10^3-10^8	C3HeB/FeJ	F	4-6	Throat cultures,	Trachea, Lungs, Nasal washings, Meningeal swabs	[226]
10µl-20µl	Yes	50	10^6-10^8	CD1, C57BL/6	F	N/M	Death, Weight Loss		[238]
10µl-20µl	No	2,11,48	10^8	CD1, BALB/c	N/M	4-10	Throat culture, Death		[143]
15µl	No	1,49	10^8	BALB/c	F	6-7	BPI,	NALT, Cervical Lymph node, spleen	[170]
15µl	No	1	10^8	BALB/c background	N/M	N/M		NALT	[228]
15µl	No	1	10^8	C57BL/6	F	6-10		NALT	[229]
15µl	No	1	N/M	C57BL/6	N/M	7-8	Death	NALT	[242]
20µl	No	1, 49	10^8	BALB/c	F	8-11	BPI,	NALT	[216]
20µl	Yes	14	10^9	CD1	F	9	Throat cultures		[156]
20µl	No	1	10^8	CD1	F	8-10		Lungs, Anterior Nasal tract	[144]
20µl	No	24	10^6	BALB/c	F	9	Death	Lungs*	[137]
20µl	No	24	10^7	C3H-HeN, BALB/c	F	12-14	Death	lungs, Blood	[232]
20µl	No	89	10^8	CD1	F	12-14		Spleen, Blood, Thigh muscle, Anterior Nasal tract, NALT and Lungs	[147]
20µl	No	5 ,24	10^7	BALB/c	N/M	N/M	Death		[154]
20µl	Yes	14	10^6	CD1	F	10	Throat culture, Death		[235]
20µl	No	106	10^6	BALB/c	F	9 -20	Death,		[138]
20µl	Yes	6, 50,	10^5	C3HeB/FeJ C57BL/10snJ	M, F	4-5	Throat culture, Death	Blood, Trachea, Lung , Spleen, Nasal washings & meningeal swabs	[220]
20µl	No	81	10^8	CD1	F	6-8		Nasal Tract, NALT, Lung	[46]
20µl	No	3,	N/M	CD1	N/M	3-5 $^+$	Death		[213]
20µl	No	1	10^7	B10.BR	F	8-10	Throat culture, Death		[158]
20µl	Yes	50	10^6	C57BL/6	F	4-6	Throat culture	Pharynx*	[246]
20µl	Yes	6		CD1	F	10-11	Throat culture, death		[157]
20µl	No	6	10^4-10^5	BALB/c nu	F	4-6	Death		[248]
20µl nasally 30µl orally	No	14	10^7	CD1	N/M	4-8	Throat cultures		[217]
20µl-40µl	Yes	1,23,106	N/M	NMRI, CD1	F	11-13	Death		[145]
25µl	No	3	10^7	BALB/c	F	14	Death	lungs, spleen and liver	[231]
25µl	No	1, 3, 12	10^7	BALB/c	F	8	Death,	lungs, spleen liver & kidney	[234]
25µl	No	1	10^7	BALB/c	F	8	Death	Lung, Liver, Spleen, Kidney	[239]
30µl	No	1	N/M	Quackenbush	N/M	N/M	Throat culture, Death		[162]
30µl	No	1	N/M	Quackenbush	N/M	N/M	Throat culture, Death		[161]
30µl nasally 30µl orally	No	12	N/M	BALB/c	F	6	Throat cultures	Head	[227]
40µl	No	106	10^8	BALB/c	F	9-10	Death		[243]
40µl	No	106	10^8	BALB/c	F	9-10	Death		[244]
40µl intranasally 10µl orally	Yes	6	10^6-10^7	CD1	N/M	N/M	Throat culture, Death		[155]
50µl	Yes	50	10^7	NMRI	F	14	Death		[236]
50µl	Yes	50	10^2-10^8	NMRI, CBA	N/M	3-5	Death	Pharynx, Brain, Heart, Lungs, Kidneys, Cervical Lymph Node & Blood	[237]
50µl	No	23	10^6	CD1	F	10	Death		[146]
50µl	No	1,6,12,23	10^8	CD1	F	13	Death		[148]
50µl	No	3	10^7	CD1	M	3-4$^+$	Death	Blood	[241]
50µl	Yes	50	10^7	NMRI	F	14	Death		[218]
50µl	No	1	10^6-10^8	CD1	M	3-4$^+$	Throat culture, Death		[247]
100µl	No	1,3, 49	N/M	CD1	F	5 $^+$	Death		[171]
N/M	No	3	10^7	BALB/c	F	8	Death,	lungs, spleen liver, & kidney	[233]
N/M	No	1	10^8	C57BL/6	N/M	10-12		Nasal tract	[240]
N/M	No	106	10^8	BALB/c	N/M	N/M	Death		[245]
N/M	No	106	10^8	BALB/c	N/M	N/M	Death		[245]

N/M = Not Mentioned, * =Histological Analysis only, $^+$ = Only weight given in reference, Age estimated based on data from Charles River Laboratories

1.8. BIOPHOTONIC IMAGING

Biophotonic imaging (BPI) is a technique based on the detection of light from biological sources, such as fluorescent proteins, or bioluminescence reactions [249]. The incorporation of these light sources into bacteria allows them to be tracked and quantified through the use of sensitive cameras. BPI provides a method to longitudinally monitor infection in a quantitative manner that limits the number of mice required during experiments, and allows mice to act as internal controls throughout a study. The technique therefore fulfils two of the '3Rs' proposed by the National Centre for the Replacement, Refinement and Reduction of Animals in Scientific Research (NC3Rs), namely refinement and reduction [250].

BPI is dependent on the transmission of light through tissue. As light passes through tissue, it is scattered and absorbed, which decreases the signal from any biophotonic source. The wavelength of the light determines the degree to which it is scattered and absorbed within biological tissue. Light with shorter wavelengths, such as blue and green light, is absorbed more than light with longer wavelengths, such as red and infrared [251,252]. The greater the depth of the source, the greater the degree of scattering and absorption occurs. This imposes limits on the ability to detect sources within deep tissues.

1.8.1. FLUORESCENCE

Fluorescence is a physical process which occurs when light of a specific wavelength triggers the excitation of an electron within an atom, which then emits a photon of another wavelength as it returns from this excited state. The wavelength of light emitted from the atom is usually longer than the wavelength of light used to cause excitation.

The green fluorescent protein (GFP), which is produced by the jellyfish *Aequorea victoria*, has been utilised in research to tag proteins to aid visualisation of their expression. These have been useful for studying gene expression in cells through microscopy. The application of this technology to image bacteria within whole animals requires a number of challenges to be overcome.

The absorption of light by biological tissues is one such challenge, as this limits the penetration of light to the fluorescent source, and the detection of light from the source. Biological tissues are inherently fluorescent, and can produce strong signals when the excitation wavelength is applied. This can impair the differentiation of the true source of fluorescence from the high background fluorescence [251].

Most of the fluorescent proteins currently available have excitation wavelengths that are absorbed and scattered readily by human tissue. As discussed earlier, biological tissues transmit infrared light more readily than other wavelengths. Infrared dyes [253] and near infrared emitting fluorescent proteins are currently in development [254] for use in this form of imaging.

1.8.2. BIOLUMINESCENCE

Bioluminescence is a chemical reaction used by biological organisms to produce light. Bioluminescence occurs when a substrate (generically referred to as luciferin) is metabolised by an enzyme (generically referred to as luciferase) in a reaction which causes the emission of a photon.

The gene which encodes the firefly luciferase was amongst the first to be used in research. A number of red-shifted luciferases have also been created, which enable the better detection of light from within biological tissues [255]. Whilst the gene encoding the luciferase is known, the genes which synthesise the luciferin for this

reaction (known as D-luciferin) are not as well defined. Commercial luciferins are synthesised chemically rather than biologically [256]. D-luciferin therefore needs to be applied exogenously to allow for firefly based bioluminescence to occur.

Another form of eukaryotic luminescence has also been characterised in the sea pansy *Renilla reniformis*. The *Renilla* luciferase requires the application of coelentarazine. The source of coelentarazine in nature has been harder to track down, as it is not produced endogenously by the *Renilla*, but from a food source, which is believed to be the copepod *Metridia pacifica* [257]. A number of other organisms produce luciferases which also metabolise coelentarazine, such as the copepod *Gaussia princeps.* The *Renilla* and *Gaussia* luciferases have both been applied to research, and the reactions are notable in that they do not require oxygen in order to occur, and produce brighter signals than the firefly luciferases. However, strong autoluminescent signals have also been observed [258].

Bacteria tagged with a eukaryotic luciferase will only luminesce in the presence of the exogenously applied luciferin. The signal obtained from these bacteria is dependent on the distribution and the concentration of luciferin within their immediate environment. Not knowing the concentration of luciferin at the site of infection makes the enumeration of bacteria using this technique more difficult, especially since different organs absorb the luciferin to different extents [259]. In addition, the reaction is short lived, and multiple applications of reagents are required to image mice over a time course.

The bioluminescent reactions produced by prokaryotes such as the Gram negative bacterium *Photorhabdus luminescens* have also been studied for biophotonic applications. The luminescence trait is conferred by the *luxCDABE* operon, which

encodes the luciferase (*luxAB*) and the enzymes responsible for regenerating a long chain aldehyde (*luxCDE*) that is essential for the reaction to occur. The *luxAB* genes encodes the α and β sub-units of the luciferase enzyme, which binds reduced flavin mononucleotide ($FMNH_2$) to a long chain aldehyde using molecular oxygen [260] (Figure 1.2.). The long chain aldehyde is generated via a transferase, encoded by *luxD*, which transfers long chain fatty acid substrates produced by core metabolic pathways to a synthetase (*luxE*) that acts in concert with a reductase (*LuxC*) to reduce the long chain fatty acid to an aldehyde.

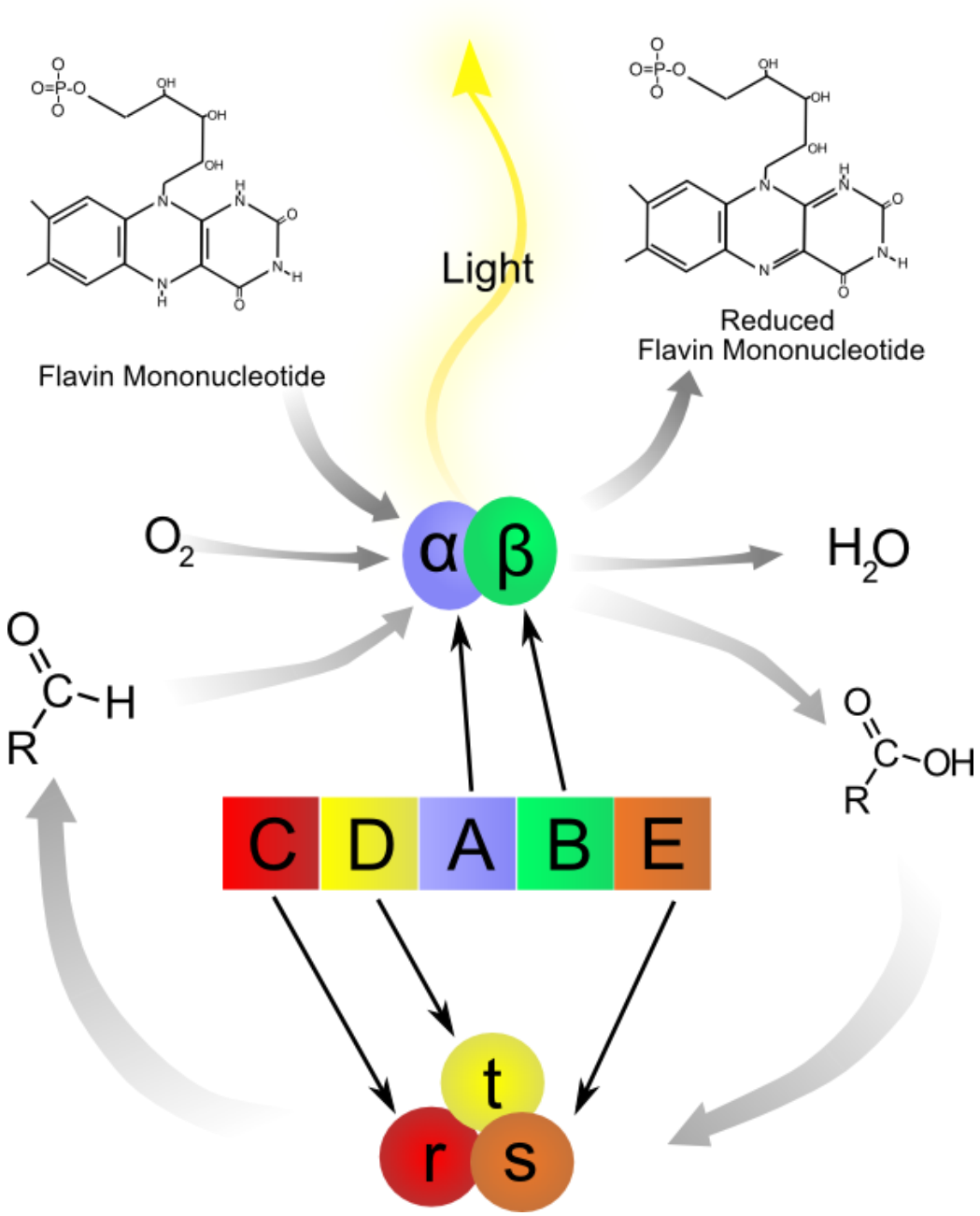


Figure 1.2. The molecular basis of bioluminescence. *LuxAB* genes encode the α and β sub units of the luciferase which combines a fatty acid aldehyde, molecular oxygen and $FMNH_2$ to form an unstable intermediate that decays to produce light, a carboxylic acid, water and reduced flavin mononucleotide [260]. The *LuxCDE* genes encode a reductase, a synthetase and a transferase respectively, which regenerates the long chain aldehyde required for this reaction.

This means that the reaction can only occur in the presence of aerobic respiration in living bacteria. All of the substrates for bacterial bioluminescence are present within the cell, and there is no need to provide exogenous compounds to enable luminescence. It is for this reason that the bacterial *lux* operon has been widely used for BPI studies of bacteria.

The *lux* operon evolved in Gram negative organisms, and so produces very little light when expressed in Gram positive organisms. Rearrangement of the operon as *luxABCDE*, with Gram positive ribosomal binding sites between the genes [261] has allowed the monitoring of infection in a number of Gram positive pathogens, including *Staphylococcus aureus* [262], *Listeria monocytogenes* [263] and *Streptococcus pneumoniae* [264]. These models have enabled investigators to image the colonisation of organs and tumours by *L. monocytogenes* [263], colonisation of *Staphlyococcus epidermidis* in implanted catheters [265], antibiotic efficacy against *S. pneumonia* [266], and the *in vivo* germination of *Bacillus anthracis* [267], to provide a few examples.

The *luxABCDE* operon has previously been integrated onto the chromosome of an *emm49* skin isolate [268] of *S. pyogenes* using a transposon, and the resulting bioluminescent strain has been used to examine systemic [160], and intranasal infection [216]. Following intranasal administration, bioluminescent streptococci were identified in the NALT of infected mice, leading to the proposal that the NALT was a major repository for *S. pyogenes* in mice. However, it is known that isolates derived from the skin have different tissue tropisms from those which infect the nasopharynx, therefore this may not be an appropriate isolate to model nasopharyngeal colonisation. Furthermore, *emm49* strains have not been associated with disease in the west for several decades [71]. The *emm49* bioluminescent isolate is

commercially available but has not been widely used, despite the increasing availability of facilities to image bioluminescence *in vivo*. There is a perceived need to derive newer, clinically relevant bioluminescent derivatives of *S. pyogenes* to model both pharyngeal and invasive infection using *emm* types that reflect those causing disease today. A major aim of this project was to derive such a strain, and determine if BPI could be used to improve or broaden the applications of this model of upper respiratory tract infection with *S. pyogenes*.

1.9. PRELIMINARY WORK TO DEVELOP NEW METHODOLOGY

In preliminary work, new methods to model infections were investigated with the long term aim of improving a model for *S. pyogenes* carriage in the upper respiratory tract.

BPI was used to investigate how the dose volume of bioluminescent *Citrobacter rodentium* [269,270] determined its immediate distribution within the respiratory tract (Figure 1.3). The dose volume retained solely to the nasopharynx was determined to be 5µl, although a volume of 10µl was the highest volume that did not immediately distribute to the lung, confirming previous findings [214,215,225] and demonstrating unequivocally that volumes in excess of 20 µl would reach the lung.

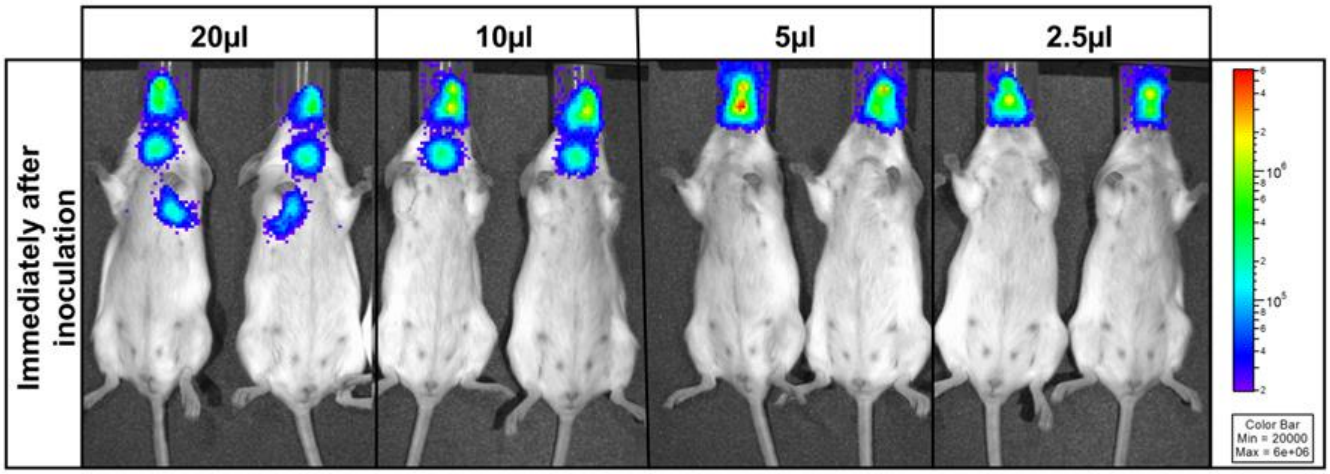


Figure 1.3 Biophotonic imaging of bacterial distribution after intranasal inoculation with bioluminescent *C. rodentium*. 10^8 colony forming units (cfu) of bioluminescent *C. rodentium* were administered intranasally to CD1 outbred mice in 20 µl (n=3), 10 µl (n=2), 5 µl (n=3) and 2.5 µl (n=2) of PBS. Images were acquired using an IVIS spectrum system, and are displayed as images of peak bioluminescence, with variations in colour representing light intensity at a given location. Red represents the most intense light emission, while blue corresponds to the weakest signal. The colour bar indicates relative signal intensity (as photons s^{-1} cm^{-2} sr^{-1}). Two representative mice are shown for each group.

Using a fixed dose volume of 5µl, different pharyngeal and blood culture clinical isolates of *S. pyogenes* from major *emm* types were screened *in vivo* to determine which would result in successful nasopharyngeal infection. In these preliminary studies, groups of 7 BALB/c mice were infected with *emm1*, *emm2*, *emm75*, or *emm81 S. pyogenes* strains. A new technique was used to detect and quantify the carriage of *S. pyogenes* within the nasopharynx. This involved the detection of *S. pyogenes* shed from the mouse nasopharynx via swabbing the anterior nares directly onto Columbia blood agar, a technique which is described in Chapter 2. Strains derived from cases of non-invasive pharyngitis tended to colonise mice more effectively than those derived from invasive diseases. An *emm75* pharyngitis isolate (H347) colonised the upper respiratory tract better than all the others tested (Figure 1.4). However, the overall poor susceptibility of BALB/c mice to infection in the nasopharynx provided an obstacle to further use.



Figure 1.4. Shedding intensity of different serotypes of *S. pyogenes* in BALB/c mice. *Emm1*, *emm2*, *emm81* and *emm75* isolates of *S. pyogenes* were intranasally infected into BALB/c mice (n=7). Nasal shedding was recorded at 24h, 48h, and 72h. Rows indicate individual mice throughout the time course. The colours of each block indicate the numbers of *S. pyogenes* recovered from direct nasal samples with red indicating the highest recorded levels of carriage (≥5000 cfu), green indicating the lowest levels of carriage (1 cfu) and blank blocks indicating no recovery of *S. pyogenes*.

1.10. AIMS

1.10.1. DEVELOPING A MOUSE MODEL OF NASOPHARYNGEAL INFECTION

There is a need for more appropriate mouse models of *S. pyogenes* colonisation of the upper respiratory tract, as current models vary with respect to the bacterial and mouse strains used. Age and gender are also known to exert an effect on invasive *S. pyogenes* infection. The optimisation and balancing of these factors may produce an improved mouse model that is more susceptible to nasopharyngeal colonisation than those currently available. The development of a robust model of murine nasopharyngeal infection will provide a platform from which other features of streptococcal infection can be explored in the future such as, for example, factors affecting transmission of *S. pyogenes* from infected to naive mice, and the aerosolisation of respiratory droplets.

1.10.2. DEVELOPING A BIOLUMINESCENT STRAIN OF *S. PYOGENES*

The currently available bioluminescent strain of *S. pyogenes* is derived from an uncommon skin isolate that may not effectively model pharyngitis. There is a need for a more clinically relevant strain of *S. pyogenes* to be made bioluminescent. It is also important that the bioluminescence expressed by this strain can produce a visible signal *in vivo.*

1.10.3. APPLYING A BIOLUMINESCENT STRAIN OF *S. PYOGENES* TO A MODEL OF NASOPHARYNGEAL INFECTION

The creation of a suitable bioluminescent strain of *S. pyogenes* will enable the study of nasopharyngeal infection. It will be necessary to determine whether BPI can be used to accurately quantify *S. pyogenes* within the nasopharynx.

1.10.4. Determining the effect of virulence regulator dysfunction in a model of nasopharyngeal infection

The switch from colonisation in the nasopharynx to invasive infection is believed to be mediated by mutations or altered phosphorylation status of virulence regulators such as *covR/S*. The use of BPI and direct nasal sampling techniques may provide new insights into the effects of *covR/S* mutation on infection in the nasopharynx.

1.10.5. Utilising a model of nasopharyngeal infection to assess vaccine candidates

The primary benefit of creating a new model of infection is the potential to evaluate the effects of different vaccine candidates on pharyngeal infection by *S. pyogenes*. Evaluation of effect will be based upon monitoring the presence of bacteria in the nasopharynx, rather than on proxies for disease severity. BPI will allow the clearance of *S. pyogenes* to be quantitatively imaged, and used as a criterion for determining vaccine efficacy.

CHAPTER 2. MATERIALS AND METHODS

2.1 MATERIALS

2.1.1. CHEMICALS

Methanol (Fisher)

Microsol (Anachem)

Acetic acid (Fisher)

Agarose (Sigma)

EDTA (Sigma)

Ethanol (Fisher)

Glucose (VWR)

IPTG (Sigma)

Isopropanol (Fisher)

Formalin (VWR)

Pilocarpine (Sigma)

$MgCl_2$ (Sigma)

NaCl (VWR)

$NaHCO_3$ (VWR)

Na_2CO_3 (VWR)

Tris (Sigma)

Sodium Azide (Sigma)

Sodium dodecyl sulphate (Sigma)

SYBR-safe (Invitrogen)

Tween (Sigma)

Dried Milk powder (Sigma)

BSA (VWR)

KH_2PO_4 (VWR)

Mg SO_4.7H2O (Sigma)

Yeast extract (Oxoid)

Glycine (VWR)

DTT (Sigma)

2.1.2. ANTIBODIES

Biotin conjugated Goat Antimouse IgG (Sigma)

Biotin conjugated Goat Antimouse IgA (Abcam)

Streptavidin conjugated HRP (Amersham)

Rabbit Anti SpeB (Abcam)

HRP conjugated Goat anti rabbit (Sigma)

2.1.3. ENZYMES

Proteinase K (Sigma)

Phusion DNA polymerase (Finnzymes)

Mutanolysin (Sigma)

Lysozyme (Sigma)

2.1.3. PRIMERS

Primer Designation	Primer Sequence	Tm°
Aph –A3 F	TTAATTAAAGCGAACCATTTGAGGTGAT	67.5
Aph- A3 R	GAGCTCTGGACAGTTGCGGATGTACT	71.2
Spy0535 F	GAGCTCCAATTAAAAGTTGTGAATTACGAATGA	70.6
Spy0535 R	GGTACCTCCTCACTACTTCTGCCTTTTTG	69.8
Linker Primer F	AATTCGGCGGGACTAGTCGGGGA	75.5
Linker Primer R	GATCTCCCCGACTAGTCCCGCCG	76.0
Spy0535 Diagnostic Primer LF	CAAAAGATGATGTTGTCCTAATTCA	62.8
Spy0535 Diagnostic Primer LR	GTTTTCCCAGTCACGACGTT	63.9
Spy0535 Diagnostic Primer RF	CCGCAACTGTCCATACTCTG	63.3
Spy0535 Diagnostic Primer RR	GCTTTTCTATACTATCCCCTTCTTTC	61.4

Table 2.1. Primers and oligonuceotides

2.1.4. PLASMIDS

Plasmid	Antibiotic resistance	Properties	Source
pUCMUT	Kanamycin		
pET100-CEP	Ampicillin	Expression of a recombinant fragment of SpyCEP	
pICL18	Kanamycin, Ampicillin	Shown in Figure 2.1.	Produced by James Peacock
pICL18^{lux}	Kanamycin	Shown in Figure 2.1.	This study
pICL18^{vlux}	Kanamycin	Shown in Figure 2.1.	This study
pICL18^{0}	Kanamycin	Shown in Figure 2.1.	This study
pTHLK	Kanamycin, Erythromycin	Shown in Figure 2.1.	Produced by Dr Colin Bateman

Table 2.2. Plasmids used in this study

2.1.5. BUFFERS AND STANDARDISED SOLUTIONS

- <u>Electroporation media</u>

  90mls 1mM autoclaved $MgCl_2$

  4.9g D- Glucose filter sterilised into 10mls sterile distilled water, and

  preserved at 4^{o}C.

- <u>SET</u>

  750µl of 5M NaCl

2.5ml 0.5M EDTA

1ml of Tris pH 7.5

This was made up to 50mls with sterile distilled H_2O.

- 50 x TAE buffer stock

  121.0g Tris

  28.6ml acetic acid

  50ml 0.5M EDTA

  This was made up to 500mls with sterile distilled H_2O.

- Fixing Solution

  50mls methanol

  10mls Acetic acid

  40mls Sterile distilled water

- Carbonate coating buffer

  0.53g Na_2CO_3

  0.42 $NaHCO_3$

  0.1g Sodium Azide

  100 mls Sterile distilled water

- Western Wash Buffer

  100mls 10×PBS

  500µl Tween

  This was made up to 1L of sterile distilled water.

- ELISA Wash buffer

  5mls 10× PBS

  5µls Tween

  40mls Sterile distilled water

- Transblot buffer

  0.25M Tris

  1.92g Glycine

- Milk blocking buffer

  50mls PBS

  50µl Tween

  2.5 g Dried milk powder

- BSA Blocking buffer

  0.6g BSA

  60mls PBS

2.1.6. BACTERIAL MEDIA

- Todd Hewitt Yeast (THY) Broth

  7.28g Todd Hewitt broth

  0.4g Yeast extract

  200mls Sterile distilled H_2O

- Todd Hewitt (TH) Agar

  7.28 Todd Hewitt broth

  4.0g Bacterial Agar

  200mls sterile distilled H_2O

- LB broth

  6.4g LB broth

  200mls sterile distilled H_2O

- LB Agar

  7g LB Agar

  200mls sterile distilled H_2O

- C-media

  0.27g - KH_2PO_4

  0.02g - Mg $SO_4.7H_2O$

  0.2g – NaCl

  3g yeast extract

  20mls sterile distilled H_2O

- SOC media (Invitrogen)
- Columbia Blood Agar (Oxoid)

2.1.7. KITS

- PathoDX Streptococcal grouping Kit (Oxoid)
- QIAgen Spin Miniprep Kit
- QIAgen PCR purification Kit
- Novagen His Bind Bugbuster purification Kit
- Fluka Gram staining Kit (Sigma)
- Oxidase Testing Kit (Fisher)
- ECL developing kit (Amersham)
- Invitrogen Colloidal Blue Staining Kit

2.1.8. BACTERIAL STRAINS

An *emm*75 *S .pyogenes* clinical strain, H347, from a pharyngitis case isolated in the Imperial College Healthcare NHS Trust Diagnostic Laboratory was used in all studies. An isogenic *covR/S* mutant of the *emm*75 strain, H494, has been previously described, and is known to have enhanced expression of SpyCEP due to insertional mutagenesis of both *covR* and *covS* [45]. The streptococcal strains used during this work are listed in Table 2.3. All were clinical strains from pharyngitis cases and were

emm typed [67] using standard methods and criteria by Bonita Song (Gram positive pathogenesis group, Imperial College). All streptococcal strains were cultured either in Todd Hewitt Yeast broth (THY), C-media (CM) or on Colombia Blood Agar (CBA). *Lactococcus lactis* strain H826 was used as a negative control for initial vaccination studies. Bioluminescent *Citrobacter rodentium* strain ICC180 [271] was used for nasal dosing studies described in the introduction. Plasmids were propagated in *Escherichia coli* strain DH5α (Invitrogen), and protein production was performed in *E. coli* strain BL21 (Invitrogen), which were both grown in Luria-Bertani (LB) broth.

Strain Designation	***Emm* type**	**Antibiotic resistance(s)**	**Source**
H347	*emm75*		[45]
H494	*emm75*	Erythromycin	[45]
H347^{pTHLK}	*emm75*	Erythromycin, Kanamycin	This study
H347^{vlux}	*emm75*	Kanamycin	This study
H347^{lux}	*emm75*	Kanamycin	This study
H347^{0}	*emm75*	Kanamycin	This study
H494^{lux}	*emm75*	Erythromycin, Kanamycin	This study
H683	*emm1*		This study
H768	*emm2*		This study
H689	*emm3*		This study
H679	*emm4*		This study
H682	*emm6*		This study
H675	*emm12*		This study
H696	*emm22*		This study
H704	*emm28*		This study
H686	*emm89*		This study

Table 2.3. Strains of *S. pyogenes* used in this study

2.2. METHODS

2.2.1. PCR TO AMPLIFY THE KANAMYCIN RESISTANCE GENE APH-A3.

Polymerase chain reactions were performed using Phusion DNA polymerase (0.5µl), ×5 Phusion HF buffer (10µl), 10mM dNTP mix (1µl) and the Aph-a3 primers (1µl each) and 1µl of the template DNA (pUCmut), and 36.5µl of H_2O to make the volume up to 50µl.

Cycles	Temperature	Time
1 cycle	98°C	30 sec
	98°C	10 sec
30 cycles	65°C	30 sec
	72°C	45 sec
1 cycle	72°C	7 minutes
1 cycle	4°C	Hold

2.2.2. PCR TO AMPLIFY THE SPY0535 LOCUS

Polymerase chain reactions were performed using Phusion DNA polymerase (0.5 µl), ×5 Phusion HF buffer (10 µl), 10mM dNTP mix (1 µl) and the spy0535 primers (1 µl each) and 1µl of the template DNA (*S. pyogenes* strain H347 DNA extract), and 36.5µl of H_2O to make the volume up to 50µl.

Cycles	Temperature	Time
1 cycle	98°C	30 sec
	98°C	10 sec
30 cycles	67°C	30 sec
	72°C	30 sec
1 cycle	72°C	7 minutes
1 cycle	4°C	Hold

2.2.3. PCR TO CONFIRM CHROMOSOMAL INSERTION INTO THE SPY0535 LOCUS

Polymerase chain reactions were performed using Phusion flash master mix (10 µl) and primers (1µl each) and 0.5 µl of the template DNA and 7.5 µl of H_2O to make the

volume up to 20µl. Annealing temperatures were set at 10°C below the lowest Tm° of the primers for the first 15 cycles, and then at 3°C below the lowest Tm° of the primers for 30 cycles.

Cycles	Temperature	Time
1 cycle	98°C	10 sec
	98°C	1 sec
15 cycles	55°C	5 sec
	72°C	3 min
	98°C	1 sec
30 cycles	60°C	5 sec
	72°C	3 min
1 cycle	4°C	Hold

2.2.4. PLASMID CONSTRUCTION OF PICL18^{LUX} AND PICL18^{VLUX}

The pTHLK plasmid (Figure 2.1 A) was derived from pIB184, and constructed by Dr Colin Bateman, Imperial College. The pICL18 plasmid was derived from pUC18N during a previous Masters project by Mr James Peacock, Imperial College (shown in Fig 2.1 B). The Aph-A3 gene was amplified from pUCMUT [272] using the Aph- A3 F and Aph-A3 R amplification primers (Table 2.1) and ligated into this vector via a PacI/SacI fragment.

The *Spy0535* gene region was amplified from *emm*75 *S. pyogenes* target DNA using the Spy0535 L and Spy0535 R primers (Table 2.1) before being ligated into the vector as a SacI/KpnI fragment. The *bla* ampicillin resistance was removed via digestion with *PvuI,* and susceptibility to ampicillin was confirmed through successive streaking of transformed *E.coli* onto selective media to make the integrating vector pICL18^{lux} (Figure 2.1 C). The P_{veg} promoter was exchanged for the P_{help} to create pICL18^{vlux} (Figure 2.1 D).

2.2.5. EXCISING LUXABCDE FROM PICL18^{LUX}

Linker primer F and Linker primer R (Table 2.1) were heated to 90^{o}C, and then allowed to cool at room temperature to allow for the linker fragments to form. The *lux* operon was excised via an *EcoR*I/*Bgl*II digest and then the linker was used to ligate the incompatible ends of the vector to create pICL18^{0}. The genomic insertion of the above plasmids was confirmed using the PCR diagnostic primers shown in Table 2.1.

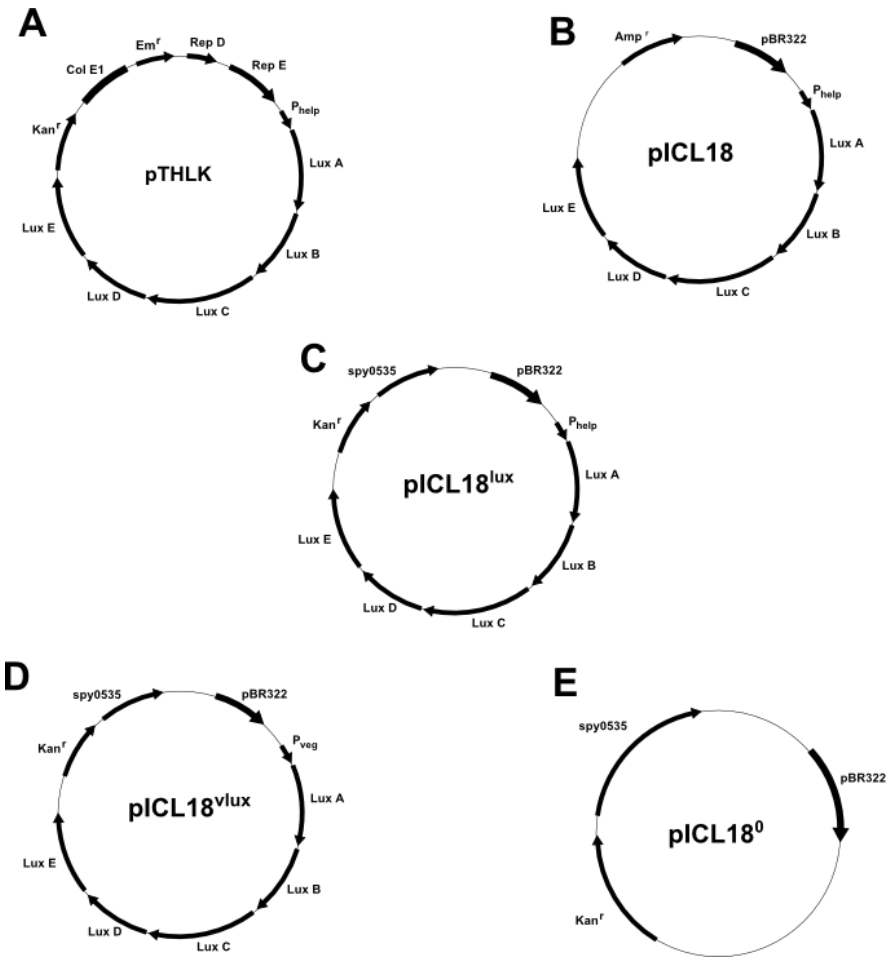


Figure 2.1. Schematic diagrams of plasmids. Arrows indicate locations and orientations of open reading frames. The replicating plasmid construct pTHLK (A), the original pICL18 plasmid (B) and the integrating plasmids pICL18^{vlux} (C) pICL18^{lux} (D) and the pICL18^{0} (E) are shown.

2.2.6. DNA EXTRACTION FROM *S. PYOGENES*

Overnight cultures of *S. pyogenes* in THY broth were spun at 1864×g for 10 minutes at 4^{o}C. The pellet was resuspended in 1 ml of 1×PBS with 20µl mutanolysin (10,000 U ml^{-1}) and 20µl of lysozyme (100 mg ml^{-1}). This was incubated at 37^{o}C for 10 minutes.

The cells were then centrifuged at 200×g for 10 minutes and resuspended in 500 µl SET medium. 50 µl of SDS and 5 µl of proteinase K was added to this mixture, and it was incubated at 55^{o}C with occasional mixing for 2 hours. 175 µl of 5M NaCl and 500 µl of chloroform were added, and incubated for 30 minutes before being centrifuged at 10,000×g for ten minutes. 500 µl of the aqueous phase was removed and added to 500 µl of isopropanol to precipitate the DNA. This was centrifuged at 10,000×g, and the pellet was re-suspended in ethanol and the centrifugation step was repeated. The ethanol was discarded, and the DNA pellet was dried for 30 minutes. It was then dissolved in 200 µl of molecular grade H_2O.

2.2.7. PLASMID EXTRACTION FROM *E.COLI*

The extraction of plasmid was performed using a QIAgen Spin Miniprep Kit utilising a modified protocol to account for the >10Kb sizes of the plasmids used in this work. 40 mls of overnight LB cultures of DH5α were centrifuged at (1294×g), and the pellets were re-suspended in 400 µl buffer P1 and transferred to a 1.5 ml tube. 400 µl of buffer P2 was added and mixed by inversion 4-6 times. 620 µl of buffer N3 was added and mixed in the tube; this was centrifuged for 10min at 15,000×g. 800 µl of the mixture was added to a QIAprep spin column nestled in a collection tube. This was centrifuged for 1 minute and the eluate was discarded after this and each subsequent centrifugation. The remaining 620 µl was then added to the filtration

column and spun once more for 1 minute. 0.5 ml of buffer PB was added to the microfiltration column and centrifuged for 1 minute. 750 µl of buffer PE was added, and centrifuged for 1 minute (15,000×g), and then again for 1 minute to remove excess wash buffer. 30 µl of molecular grade water heated to 70^{o}C was added to the column, and left for 5 minutes. The eluate from this reaction was collected during a 1 minute centrifugation step (15,000×g). 30 µls of 70^{o}C molecular grade water was added again, incubated for 5 minutes and the eluate from the microfiltration columns was collected once more, to produce a 60 µl solution of plasmid DNA.

2.2.8. TRANSFORMATION OF *E.COLI*

DH5α heat competent cells were thawed on ice, and 50 µl was added to 5 µl of plasmid and incubated on ice for 30 minutes before being heat shocked at 42^{o}C for 30 seconds. The mixture was incubated for 5 minutes then 950 µl of SOC media was added prior to incubation at 37^{o}C with shaking for 1 hour, then plating out onto LB agar containing kanamycin (50 µg ml^{-1}), ampicillin (100 µg ml^{-1}) or erythromycin (500 µg ml^{-1}) as appropriate. Plates were incubated overnight at 37^{o}C and 4.5-5% CO_2.

2.2.9. ELECTROTRANSFORMATION OF *S. PYOGENES*

An overnight culture of *S. pyogenes* was diluted 1:20 into THY broth and incubated to an OD_{600} of 0.15-0.17. The bacteria were washed twice in ice cold sterile electroporation medium with re-suspension and centrifuged at 3000×g (Beckman Centrifuge, JA-20 rotor) for 10 minutes at 4^{o}C. After the final wash, the cells were suspended in 750 µl electroporation medium. 75 µl of this suspension were transferred to 1.5 ml tubes containing 5 µl plasmid preparations. This suspension was electroporated at 150 mΩ, 50 µF and 1 kV (Gene Pulser Xcell, Bio-Rad). The time constants which were obtained for this were 6.3-6.5 s^{-1}. The suspension within

the cuvette was added to 10 ml THY broth and incubated for 2 hours at 37^{o}C without antibiotic. This broth was then centrifuged at 1200×g (RTH 750 Rotor, Sorvall) and the supernatant discarded. The remaining pellet was re-suspended in 100 µl THY broth and spread onto selective media containing kanamycin (500 µg ml^{-1}) or erythromycin (50 µg ml^{-1}), as appropriate. Plates were incubated overnight at 37^{o}C and 4.5-5% CO_2.

2.2.10. CEP5 PRODUCTION FROM *E.COLI*

E. coli BL21 were transformed with pET100-CEP, a plasmid expressing his-tagged recombinant CEP5 representing 35-587aa of the SpyCEP protein created in previous work [147]. The transformation mix was aliquoted into 10 ml LB broth, with 100 µg ml^{-1} ampicillin and shaken overnight at 37^{o}C. This was then added to 490 ml of LB with ampicillin and grown for 3 hours (OD_{600} =0.6-0.8) when 250 µl of IPTG was added to make a final concentration of 0.5 mM. 50 ml fractions were centrifuged (RTH-750, Sorvall) at 1294×g for 20 minutes.

Purification of CEP5 protein was performed using the Novagen His Bind kit. The eluted protein was concentrated using Millipore Amicon Ultra-15 centrifuge tubes which were spun at 1294×g for 30 minutes. The solution was cleaned with sterile PBS via three 30 minute centrifugation steps at 1294×g.

Samples taken before and after purification were run on Bis-tris gels as described previously. The gels were incubated with shaking in fixing solution for ten minutes. The fixing solution was discarded and staining solution A for 10 minutes with shaking, followed by the addition of staining solution B. This was incubated with shaking at room temperature for 3 hours. This gel was de-stained overnight in

distilled water. The gel was then imaged using a GelDoc-it imaging system to confirm the production of a 60kDa CEP5 (Figure 2.2).

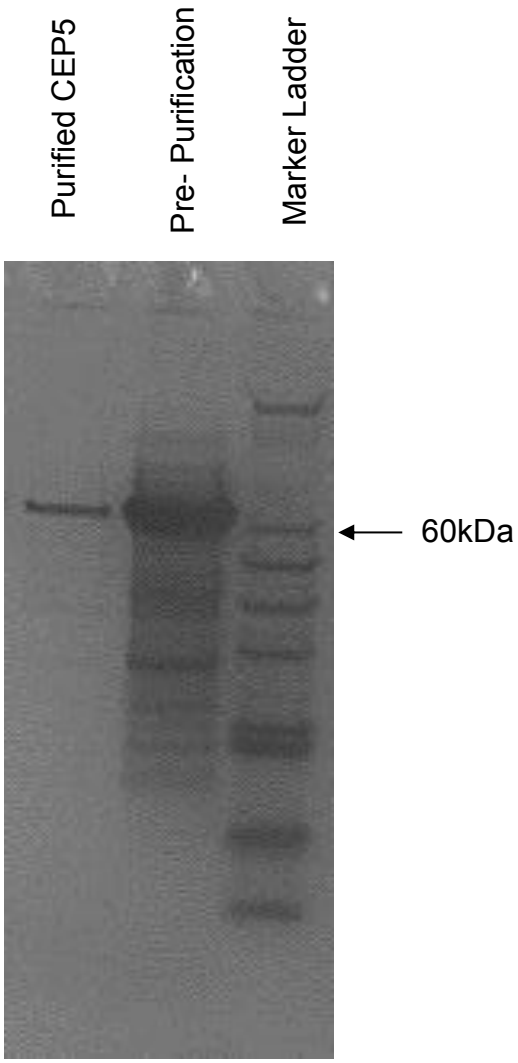


Figure 2.2. SDS PAGE demonstrating production and purification of Recombinant CEP5. 10µl of transformed *E.coli* broth (pre-purification) was compared to 10µl of purified recombinant CEP5 protein.

2.2.11. AGAROSE GEL ELECTROPHORESIS

To analyse DNA products from PCR or from restriction digests, 0.8-1% agarose gels made with 1×TAE were made with SYBR-safe (concentration 1µl SYBR-safe /10mls

agarose.). These were run at 100V for 30 minutes and imaged using a GelDoc-it imaging system (UVP).

2.2.12. SDS GEL ELECTROPHORESIS

Samples were incubated with DTT and LDS sample buffer at 72^{o}C for 10 minutes and run on a 10% Bis-Tris sodium dodecyl sulphate–polyacrylamide gels (NuPAGE) at 200V for 35 minutes with 500 ml MES buffer (NuPAGE) and 500 µl of antioxidant (NuPAGE).

2.2.13. WESTERN BLOT

10µl supernatants obtained from isolates cultured to the early log, mid log, and late log phases of growth in TH were run on a 10% Bis-Tris sodium dodecyl sulphate–polyacrylamide gel electrophoresis (SDS-PAGE) gels (Invitrogen) as described above. A Hybond P membrane (Amersham) was activated in methanol for 10 seconds, soaked in water for 10 minutes. The gel was placed atop the membrane in transblot buffer and then placed in the transblot tank (Mini Trans-Blot Cell, Bio-Rad), and run at 60V for 1 hour at 4^{o}C. On completion of transfer, the membrane was washed 3 times with PBS and milk blocking solution was added and left to incubate with shaking for 1 hour. Rabbit anti-SpeB antibody was added and left to incubate at 4^{o}C overnight. The membrane was then washed with western wash buffer 4 times. Milk blocking solution was added with HRP conjugated- goat anti-rabbit and incubated for 1 hour. The membrane was washed 4 times with wash buffer before being developed using the ECL system (GE Healthcare).

2.2.14. BIOFILM ASSAY

Biofilm assays were performed as described previously [273]. Overnight cultures grown in THY broth were diluted 1:20 into C-media, and incubated at 37^{o}C with 5%

CO_2 for 24 hours. The supernatant was removed from each well and collected in a corresponding 10 ml tube. The wells were washed three times with PBS, and the discarded washes were added to the supernatants for each well, which were then centrifuged at 1864xg (Sorvall RTH-750) to ensure all non-adherent bacteria were collected. The biofilms and supernatants were re-suspended in 0.2% crystal violet (Fluka) for 15 minutes, and then shaken with 1% SDS at 180 rpm (IKA HS 260 Shaker) for 10 minutes. The solutions were diluted 1:10 in PBS in optical cuvettes, and had their OD_{600} measured to assess the presence of bacteria in the biofilms. Serial dilutions of an inoculum containing 10^8 CFU of *S. pyogenes* were made in triplicate, spun down and exposed to the crystal violet staining protocol described previously. Samples from these dilutions were plated out onto CBA to assess the numbers of *S. pyogenes* present, to allow for a standard curve to be drawn.

2.2.15 Growth kinetics and light production kinetics

Growth rates of each strain were assessed through preparing an inoculum as described above, and inoculating it into 50mls THY broth (n=3). The OD_{600} of a 1 ml sample from each culture was taken at hourly intervals. At half hourly intervals, a 50µl sample of culture was taken and was measured using a Modulus Single Tube Luminometer either neat, or diluted 1:10 into PBS.

2.2.16. Light production of the bioluminescent strains

Pellets from overnight cultures of *S. pyogenes* transformed with either the pICL18^{lux} or pTHLK were re-suspended in PBS, and then serial tenfold dilutions were made to determine flux from each well of a 96 well plate, prior to plating onto agar for quantification. These were imaged using the IVIS100 system, and analysed mice using the region of interest (ROI) tool in the Living Image software program.

2.2.17. STABILITY OF BIOLUMINESCENCE EXPRESSION

The stabilities of the replicative and integrated plasmids in *S. pyogenes* were assessed. An inoculum prepared from overnight cultures containing 10^7 colony forming units (CFU) were inoculated into THY broth with and without selection (n=3). Every 24 hours, 1 ml of each culture was inoculated into 49 ml of fresh THY broth with the same growth conditions as the previous culture. Samples were taken at specific time points, from which serial dilutions onto selective and non-selective media were made to assess numbers of bacteria with or without the constructs, which was repeated up to 7 days after the initial inoculation.

2.2.18. ANIMAL HOUSING AND ENRICHMENT

Male and female 5-10 week old CD1, C57BL/6, A/J, BALB/c, FVB/n specific-pathogen free mice (sourced from Harlan or Charles River, UK) were maintained in individually HEPA filtered cages with sterile bedding and free access to sterilised food and water. GLP Mini Fun Tunnels (Lillico), or Des. Res. Mini Mouse Houses (Lillico) were provided in each cage for environmental enrichment. Experiments were performed in accordance with the Animals (Scientific Procedures) Act 1986 and were approved by the local Ethical Review Process. Food and water were provided *ad libitum*, and the facility was maintained on a 12 hour light dark cycle.

Mice were maintained at cage densities between 3-8 mice per cage. Mice older than 10 weeks were not housed in cage numbers greater than 6. Where there was evidence of intraspecific aggression, the aggressors were determined through behavioural observation, and wound analysis, and split into a separate cage. Extra enrichment was added to help ameliorate aggressive behaviour. Mice were weighed

daily for welfare purposes during experiments, and an observed daily weight loss of greater than 20% was a defined humane end point.

2.2.19. INTRANASAL INFECTION

Bacterial inocula were prepared from overnight stationary phase 50 ml THY broth cultures of *S. pyogenes*, with or without antibiotic selection where appropriate. Cultures were spun at 1864×g (Sorvall RT7 Centrifuge with RTH-750 rotor) and re-suspended in PBS to wash twice. A final spin was used to concentrate the bacteria. The optical density at 600nm (OD_{600}) of a 1 in 100 dilution was adjusted to 1, so that a 5 µl sample would contain approximately 10^8 colony forming units (CFU).

To produce bacterial inocula from *S. pyogenes* growing in exponential phase, 3× 50 ml cultures were grown per strain over a 5 hour period. After 5 hours of growth, these were centrifuged, and the pellets were pooled together before being washed twice in PBS. The OD_{600} was adjusted to 1 of a 1 in 100 dilution, so that a 5µl sample would contain approximately 10^8 CFU.

Intranasal inoculation: For streptococcal infection of the nasopharynx, 10^8 CFU of *S. pyogenes* was administered intranasally using a pipette to mice in a volume of 2.5 µl per nostril under 2-5% isoflurane anaesthesia. Mice were weighed daily; reduction by 20% of the original weight was a defined humane end point. Numbers of viable bacteria within the inoculum were retrospectively assessed by plating of the inoculum onto Columbia blood agar.

Intrapulmonary inoculation: An inoculum of approximately 10^7-10^8 CFU in a 5 µl volume prepared as described previously was diluted in sterile PBS to make a 20 µl inoculum suspension. This was then administered to mice under isoflurane

anaesthesia via the intranasal route using a pipette. Numbers of viable bacteria within the inoculum were assessed by retrospective plating onto CBA.

2.2.20 INTRAMUSCULAR INFECTION

10^8 CFU in a volume of 50µl *S. pyogenes* were administered to mice under isoflurane anaesthesia via injection with a 27 gauge needle into the right lateral gastrocnemius muscle within the thigh. Numbers of viable bacteria within the inoculum were assessed by retrospective plating onto CBA.

2.2.21 *IN VIVO* COMPETITION ASSAY

H347, $H347^{lux}$ or $H347^{0}$ cultured overnight were centrifuged (1864×g for 10 min) and washed twice in PBS. The OD_{600} for each strain was adjusted to 100, and suspensions of different isolates were mixed 1:1 pairwise then infected into groups of 8 mice. Bacterial colonies from the nasopharynx were replica plated onto selective media on day 1 (4 mice per group) or day 3 (4 mice per group). Individual colonies were inoculated into THY and bioluminescence quantified after 5 hours of growth (Modulus Single Tube Luminometer). *S. pyogenes* that were either bioluminescent or kanamycin resistant were quantified to determine the proportion of each strain surviving *in vivo*. Competitive Indices (CI) were calculated as follows: CI=(mutant output/WT output)/(mutant input/WT input).

2.2.22 MOUSE IMMUNISATION

Mice were immunised with 50 µl of vaccine comprising either *S. pyogenes* strain H347 heat inactivated at 80°C, or SpyCEP protein (CEP5) intramuscularly 4, 2 and 1 weeks prior to challenge. To make a heat-killed vaccine, a suspension of *S. pyogenes* in sterile PBS was heated for 1 hour at 80ºC and concentrated to a final

density of 2 $\times 10^9$ CFU/ml, yielding a dose of 10^8 CFU per mouse; an aliquot of suspension was plated out prior to heating to quantify CFU. Sterility of this vaccine was verified by plating out onto CBA after heating.

CEP5 (2 mg ml^{-1}) was mixed 1:1 with adjuvant to create the SpyCEP based vaccine. Each mouse therefore received 50µg CEP5 per immunisation. As controls, groups of mice were immunised either with PBS alone, or with PBS mixed 1:1 with adjuvant. For priming vaccinations, Complete Freunds Adjuvant was used, and subsequent boosters used Incomplete Freunds Adjuvant.

2.2.23. SALIVA COLLECTION

Mice were intraperitoneally injected with 100 µl 0.2% pilocarpine. Mice were then anaesthetised with isoflurane at an initial rate of 5%, and then maintained at a rate of 2%. Mice were placed on an angled surface, and saliva was collected. Samples were frozen at 80^oC after collection.

2.2.24. *IN VIVO* BIOPHOTONIC IMAGING

Bioluminescence (presented as photons s^{-1} cm^{-2} steridian $[sr]^{-1}$) from infected animals was assessed after isoflurane anaesthesia using the IVIS 100 camera system (Caliper Life Sciences). The sample shelf was set to a field of view of 10-21.2 cm. A reference image was taken under low illumination prior to quantification of photons emitted from *S. pyogenes* at a binning of 4 over 20-300 seconds using the software program Living Image 2.0 (Xenogen). For anatomical localisation, a pseudocolour image representing light intensity (blue, least intense to red, most intense) was generated using the Living Image software and superimposed over the grayscale reference image. Light intensity on reference image is presented as photons s^{-1} cm^{-2} sr^{-1}, a standardised measure of luminescence.

Bioluminescent signals within specific regions of individual mice were quantified using the region of interest (ROI) tool in the Living Image software program. ROI's to detect light emanating from the nasopharynx were drawn as shown in Figure 2.3. Data collected using ROI is displayed as total flux (p s^{-1})

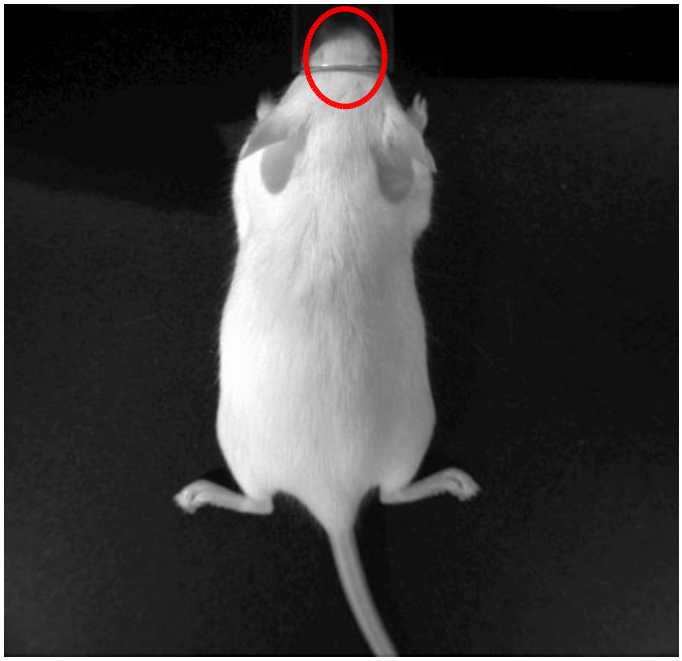


Figure 2.3. ROI for analysing luminescence from the mouse nasopharynx.

2.2.25 DISSECTION

At the end of each experiment, mice were culled by cervical dislocation. To remove the spleen, the peritoneum was exposed and an incision was made to the left side of the mouse halfway between the last rib and the hip joint. To extract the liver, an incision was made to the right side under the last rib, and the liver was pulled away from the diaphragm and dissected out. The extraction of the lung was performed via an incision of the peritoneum underneath the ribcage. The diaphragm was cut away and the ribcage pushed upwards to allow for the dissection of the lung. The inguinal

lymph node was dissected out via peeling back the flank and locating the lymph node adjacent to the deep circumflex iliac artery on the inner surface of the skin.

To ensure complete extraction of the nasopharynx, the skin and mandibles were removed to expose the cranium. This was then sectioned along the coronal plane at the bregma. The brain tissue within the cranium anterior to this incision was removed, exposing the posterior aspect of the nasal cavity, known as the cribriform plate (dissection line shown in Figure 2.4). The orbits were removed from this tissue via sagittal incisions lateral to the pre-maxilla. The remaining tissue comprised the entire nasal cavity, and NALT. This was homogenised into PBS and serial dilutions plated onto CBA to quantify *S. pyogenes* from the whole nasopharynx. Dissection equipment was washed in microsol followed by ethanol before and after the dissection of each organ.

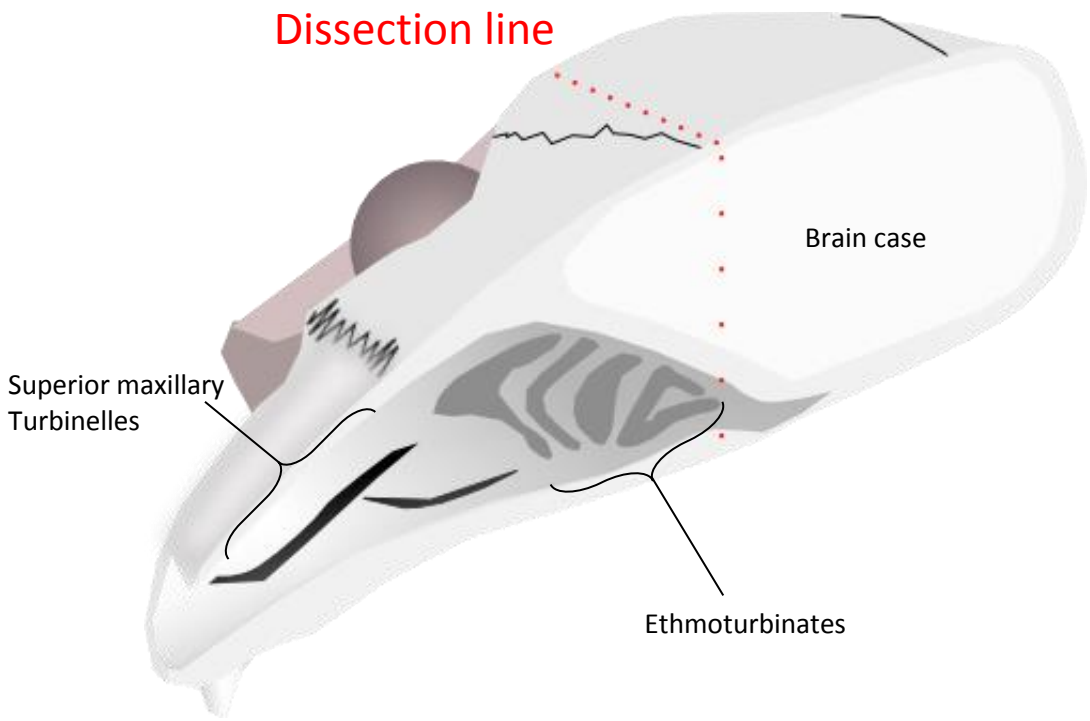


Figure 2.4. Dissection of the mouse nasopharynx. Diagram depicts mouse cranium bisected along the midline, and displaying internal structure of the nasopharynx. Dotted line indicates the plane of the initial cut to separate the nasopharynx. Not shown are the cuts utilised to remove the eye and the maxilla. Anatomy based on [205]

2.2.26. BRONCHO-ALVEOLAR LAVAGE

An incision was made into the neck of the mouse to expose the trachea. A small incision was made to the trachea, into which a lavage tube was inserted and surgical suture thread was looped around the trachea and tightened to secure the lavage tube in place. 1 ml of PBS was injected into the lung, and then aspirated out. Broncho-alveolar lavage fluid was collected in a 1.5ml tube and frozen at -80^{o}C for later use.

2.2.27. COLONY IDENTIFICATION

Colonies plated out onto CBA were checked for the presence of α and β-haemolysis. For further identification, Gram staining, catalase and oxidase testing were used, coupled with Lancefield grouping to confirm Group A *S. pyogenes*

2.2.27.1. GRAM STAINING

Individual colonies were emulsified onto the surface of a glass slide in PBS and air dried before being flooded with crystal violet for 30 seconds. Gram's iodine was added for 30 seconds. The slide was flooded with ethanol/acetone decolouriser for 5 seconds before counterstaining with safranin for 30 seconds. The section was washed under a running tap. Gram-positive bacteria appear purple and Gram-negative bacteria appear pink under microscopic analysis. *S. pyogenes* was used as a positive control and *E.coli* was used as a negative control on each slide.

2.2.27.2. CATALASE TESTING

A bacterial colony was added to 0.1 % hydrogen peroxide on the surface of a glass slide, and the observation of gas bubble formation confirmed the presence of catalase.

2.2.27.3. STREPTOCOCCAL GROUPING

The grouping of streptococci obtained from samples was determined using a PathoDX grouping kit (Oxoid). For conventional testing, the instructions were followed as directed. For confirmation that a β-haemolytic colony is *S. pyogenes*, Individual colonies were emulsified in 20 µl of the extraction enzyme preparation (Oxoid), and incubated at 37^{o}C for 10 minutes. 10 µl samples of this preparation were mixed with 10 µl samples of the latex reagent, and the agglutination reaction was observed as for the initial studies. These modifications allowed for a higher

throughput for testing possible *S. pyogenes* colonies by confirming the presence of the group A carbohydrate.

2.2.27.3. OXIDASE TESTING

A bacterial colony was placed onto filter paper, to which an oxidase reagent (BD biosciences) was added. The rapid production of purple colour after the addition of reagent indicated the presence of oxidase. This was used to differentiate Gram negative bacterial species residing within the nasopharynx.

2.2.28. ENZYME LINKED IMMUNOSORBENT ASSAY FOR IMMUNOGLOBULIN

To assay for immunoglobulin G or A specific for bacteria, 10^8 CFU of heat-killed bacteria (either *L.lactis* or *S.pyogenes*) in 10 ml of carbonate coating buffer was added at 100µl per well of a 96 well plate, and incubated overnight at 4^oC. To assay for immunoglobin specific for CEP5, 400 µl of a solution of 2 mg ml^{-1} of SpyCEP was added to 9.6 ml of carbonate coating buffer and aliquoted at 100 µl per well of a 96 well plate which was incubated overnight at 4^oC.

Plates were then washed (ELx50 Strip Microplate Washer, BioTek) and incubated for two hours with BSA blocking solution before being washed again. Dilutions of samples from serum were incubated in volumes of 100 µl on the plates for two hours. After another wash step, anti-mouse IgG (Sigma) or anti-mouse IgA (AbCam) were added in PBS and incubated for 90 minutes. The plate was washed again, and incubated with a 1:200 dilution of streptavidin conjugated to HRP (R&D systems) in the dark for 20 minutes. The plates were washed, and incubated with 50 µl of TMB for ten minutes, after which 50 µl of a 1M solution of H_2SO_4 was added to stop the reaction. The optical density at 450 nm (OD_{450}) was measured for each well using an ELISA plate reader (µQuant Universal Microplate Spectrophotometer, BioTek).

For analysis of saliva and BAL samples, ELISA was performed as above, except with Milk blocking solution used instead of BSA blocking solution.

2.2.29. HISTOPATHOLOGY

The head of each mouse was removed at the atlanto-occipital joint and sagittally hemi-sected. One half was fixed in formalin and processed routinely to paraffin wax, while the other was homogenised and plated to assess *S. pyogenes* numbers in the nasopharynx. The brain was sectioned coronally at the optic chiasm to image a lesion within it. Paraffin sections were cut at 6 µm and stained with Haematoxylin and Eosin and Gram stains, then reviewed by an experienced histopathologist (Professor Ken Smith, Royal Veterinary College, London).

2.2.30. STATISTICS

Statistics were performed using Prism Graphpad version 5.02. Data are presented as median, ± interquartile range. PS Power and Sample Size calculator was used to prospectively determine the numbers of mice to be used in experiments using >10 mice based on data from preliminary experiments.

2.2.30.1. REGRESSION ANALYSIS

Regression analysis was used to fit data to the appropriate linear, logistic and exponential decay models to determine rate constants and to allow curve comparison. An r^2>0.95 was determined to be a good fit for the data. For curve comparison, *P* values less than 0.05 were defined as significant.

2.2.30.2 MANTEL-COX LOGRANK

For statistical analysis of Kaplan-Meier survival curves, the Mantel-Cox Logrank test was applied. *P* values less than 0.05 were defined as significant.

2.2.30.3 KRUSKAL WALLIS ANALYSIS

For statistical analysis of colony count comparisons, a non-parametric Kruskal-Wallis test and Dunn's post-test were used. To analyse transmission data, *P* values less than 0.05 were defined as significant.

2.2.30.4 MANN WHITNEY

For statistical analysis of colony count comparisons, a non-parametric Mann-Whitney test was used. To analyse transmission data, *P* values less than 0.05 were defined as significant.

2.2.30.5 AREA UNDER THE CURVE ANALYSIS

To compare colony counts taken over a time course, the area under the curve statistics for each individual mouse were calculated. These statistics were compared using either Kruskal-Wallis analysis, or Mann-Whitney tests outlined above. *P* values less than 0.05 were defined as significant.

2.2.30.6. TWO WAY ANOVA

To analyse bioluminescence data over a time course, Two-way ANOVA was performed with Bonferroni correction. *P* values less than 0.05 were defined as significant.

2.3. NEW TECHNIQUES

2.3.1. DIRECT NASAL SAMPLING

The level of shedding of *S. pyogenes* from the nasopharynx was assessed longitudinally using direct nasal sampling. The nares of each mouse were gently pressed onto the surface of a CBA plate ten times. The bacterial colonies were exhaled onto the surface of the plates were spread out using a plastic sterile loop, and the plates were then incubated overnight at 37ºC with 5% CO_2 for bacterial enumeration. Viridans streptococci, staphylococci, pseudomonads and corynebacteria were recovered in preliminary experiments from uninfected mice, but no β haemolytic Group A streptococci were found to naturally colonise the mouse nasopharyngeal tract.

For mice infected with *S. pyogenes,* β-haemolytic colonies were counted for each mouse and confirmed as *S. pyogenes* through Gram staining, catalase testing, oxidase testing, and Lancefield grouping. No other β-haemolytic bacteria were recovered from the mouse nasopharynx. Kaplan-Meier plots were created to analyse the duration of *S. pyogenes* shedding. Mice were determined to have stopped shedding upon the first instance of a nasal sample turning up negative.

2.3.2. SETTLE PLATES IN INDIVIDUALLY VENTILATED CAGES

Airborne bacteria produced by infected mice were detected via the inclusion of CBA plates were placed on the grids of the IVC's in which the mice were housed (n=4 per cage). These were exposed for variable lengths of time of between 8-24 hours for the duration of the experiment. Plates were incubated overnight at 37ºC and the numbers of *S. pyogenes* colonies (identified by Gram staining, catalase testing, and Lancefield grouping) were enumerated.

CHAPTER 3: CHARACTERISING A MODEL OF INFECTION IN THE MURINE NASOPHARYNX

3.1. INTRODUCTION

There is a need for a reproducible mouse model for the infection of the upper respiratory tract by *S. pyogenes* to study the factors underlying infection in this region. Mice are generally less susceptible to streptococcal infection, with the exception of the *emm50 S. pyogenes* strain (B514), which was attenuated at a key virulence regulator locus (*mga*), making it unsuitable for studying human clinical infection [222,226].

The resistance of mice to *S. pyogenes* infection has proven to be a formidable obstacle to investigating transmission. Some early studies utilised a nebuliser system to infuse the air of a mouse cage with droplets of *S. pyogenes* [211] to model airborne transmission. However, the specialised nature of the equipment required for this model, and the variability of the results obtained using it prevented it from being developed further [212]. There are currently no models that can reliably induce mouse to mouse transmission of *S. pyogenes*.

Previous work established that mouse strains differ in their susceptibility to streptococcal infection [192,193], and that age [196] and gender [194,195] can play a role in this susceptibility. As noted earlier (Chapter 1, Table 1.3) a variety of different mouse strains of different ages have been used in previous work to model infection in the respiratory tract. The goal of this work is to assess the effects of these factors and use them to devise a reproducible model of non-invasive nasopharyngeal infection.

To study the progression of nasopharyngeal infection, longitudinal techniques are required that enable non-lethal sampling of the nasopharynx. In previous work, a method for directly sampling bacteria shed from the nasopharynx during an infection was pioneered by quantifying colonies of *S. pyogenes* shed from the nasopharynx directly onto blood agar. It is not known whether the numbers of *S. pyogenes* recovered using this technique accurately represent the abundance of streptococci in the nasopharynx. In this chapter, data will be presented that addresses these questions and lead to the development of a more robust murine model of upper respiratory tract infection.

3.2. RESULTS

3.2.1. COLONY COUNTS OF *S. PYOGENES* SHED BY MICE CORRELATE WITH *S. PYOGENES* COLONY COUNTS FROM DISSECTED NASAL TISSUE.

To longitudinally track bacterial colonisation in the nasopharynx, direct nasal sampling was used to detect the numbers of *S. pyogenes* shed from the nasopharynx during an infection. This utilised the 'direct nasal sampling' technique outlined in Chapter 2.3.1. In previous work (Chapter 1.9.) , an *emm75* strain (H347) had been found to cause nasopharyngeal infection more effectively than other streptococcal strains and hence was used in subsequent experiments. Mice experienced a decrease in weight immediately after nasal inoculation, and occasional conjunctivitis. The numbers of *emm75 S. pyogenes* colonies recovered from the nasal samples at different time points following infection was directly proportional to the numbers of bacteria present in nasal tissues upon dissection at the same time points (Figure 3.1. $r^2<0.95$, n=36).

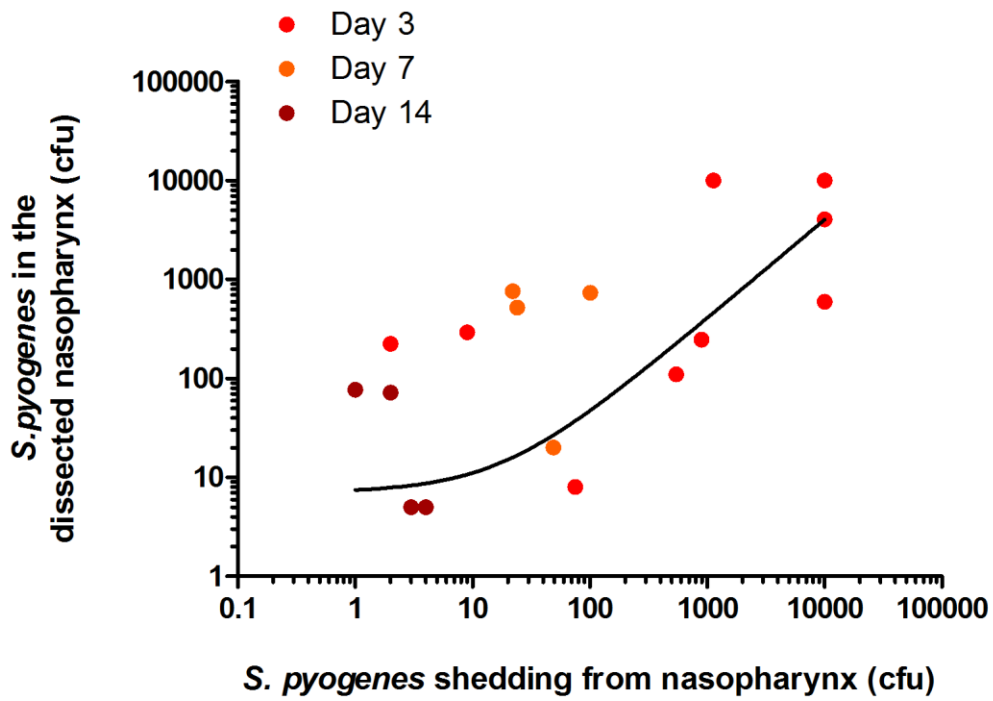


Figure 3.1. Quantitative correlation of *S. pyogenes* (H347) recovered from nasal shedding with *S. pyogenes* recovered from dissection of the nasopharynx. Direct nasal samples taken on days 3, 7, and 14 during intranasal infection were compared to bacterial numbers obtained from dissected samples on the same days. ($r^2 > 0.95$, n=36). Data shown from individual mice.

3.2.2 FVB/N STRAIN MICE CARRY *S. PYOGENES* IN THEIR NASOPHARYNX BETTER THAN OTHER MOUSE STRAINS.

To determine the background nasopharyngeal flora of mice from different strain backgrounds, BALB/c (n=14), CD1 (n=14), FVB/n (n=8), A/J (n=6) and C57BL/6 (n=12) mice were sampled, 5 days before intranasal inoculation with *S. pyogenes* H347, and for the 3 days during infection. The bacteria detected from the nasopharynx by nasal sampling onto CBA were identified through the presence of

haemolysis, Gram staining, catalase testing, oxidase testing and Lancefield grouping. The *emm*75 *S. pyogenes* isolate was administered intranasally to all mice in a in a 5 µl dose containing 10^8 CFU (as 2.5 µl per nostril).

At 5 days prior to inoculation, no *S. pyogenes* was detected in any of the murine strains tested. Viridans streptococci and staphylococci were the species most frequently observed in uninfected mice. *Corynebacter* spp. were also seen infrequently in some of the mouse strains. During the course of intranasal *S. pyogenes* infection, *Pseudomonas spp.* and *Haemophilus spp.* also appeared. (Figure 3.2)

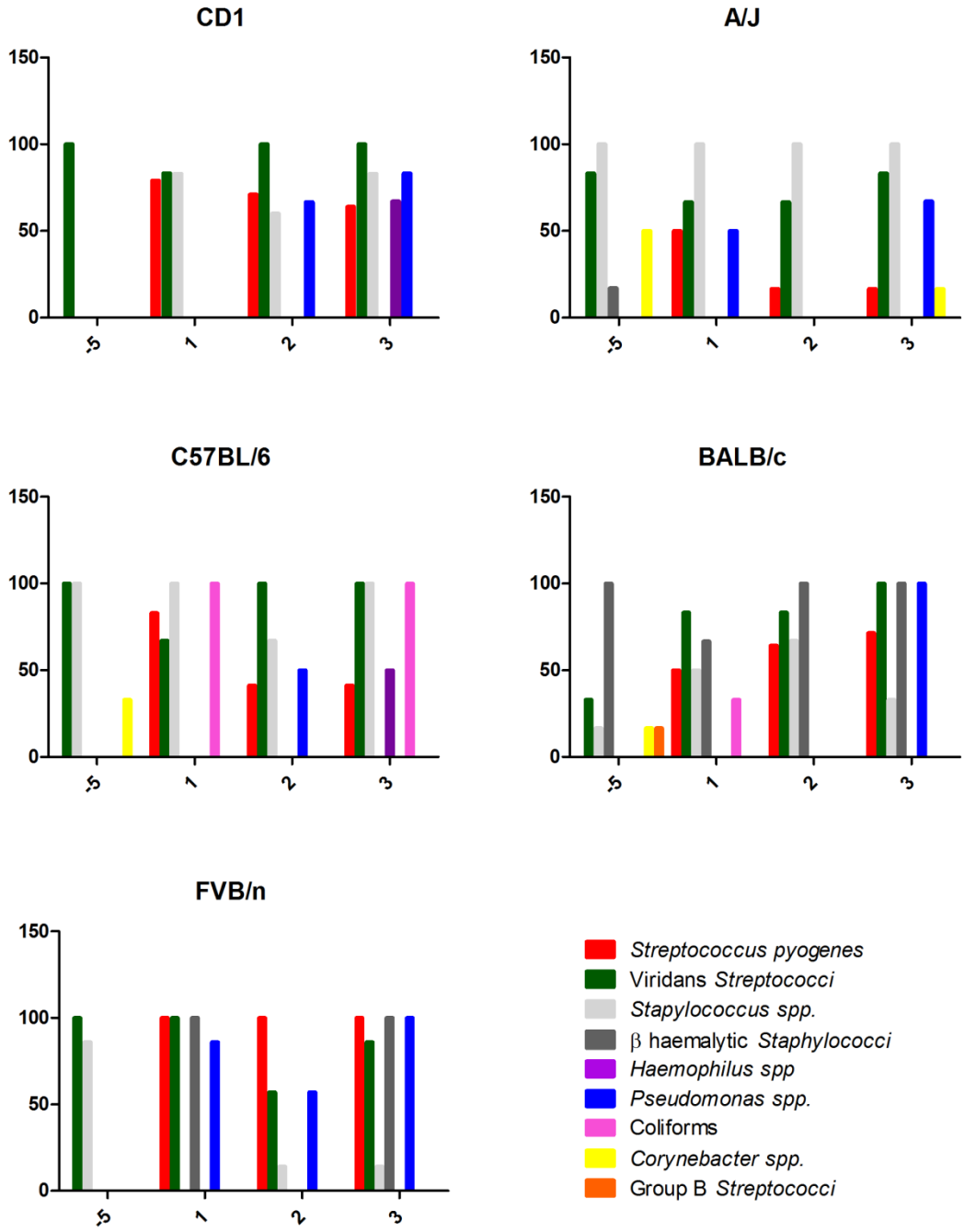


Figure 3.2. Comparison of commensal bacteria in different mouse strains. FVB/n (n=8) CD1 (n=14), BALB/c (n=14), C57BL/6 (n=12) and A/J (n=6) mice were nasally sampled before and during infection with *S. pyogenes* (H347). Colony identification, Gram staining, Catalase Testing, Lancefield Grouping and Oxidase testing were used to identify the bacteria shed by the mice throughout the time course. Bars indicate proportions of mice shedding bacteria.

Of all the mouse strain backgrounds tested, the FVB/n strain was the only group in which all mice had detectable *S. pyogenes* at all time points tested after inoculation (Figure 3.2). FVB/n mice shed significantly more *S. pyogenes* H347 on the final day of the time course than all other strains tested (Figure 3.3 Kruskal-Wallis with Dunns post-test). Thus, the FVB/n mice were used in all further studies.

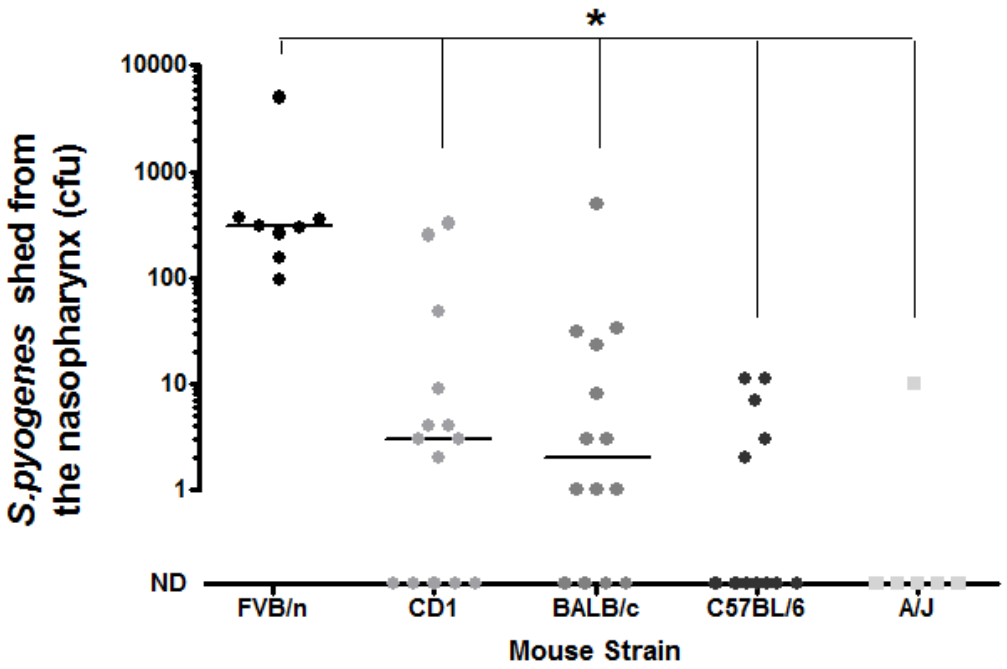


Figure 3.3. Comparison of nasopharyngeal shedding of *S. pyogenes* (H347) between different mouse strains. Bacterial counts shed by FVB/n (n=8) CD1 (n=14), BALB/c (n=14), C57BL/6 (n=12) and A/J (n=6) at 72 hours. Individual points represent individual mice. (Kruskal Wallis with Dunns Post Test $p<0.05$). Bars indicate the median, ND= no detectable bacteria

3.2.3. GENDER HAS AN EFFECT ON THE NASOPHARYNGEAL CARRIAGE OF *S. PYOGENES* THAT IS DEPENDENT ON THE AGE OF THE MICE.

To evaluate the effect gender may have on the duration of shedding of *S. pyogenes* in the nasopharynx, pre pubertal (n= 10 per group, 5 weeks of age) and post pubertal (n= 10 per group, 10 weeks of age) male and female FVB/n mice were challenged intranasally with 10^8 CFU *S. pyogenes* H347.

The duration of shedding from the nasopharynx was measured through direct nasal sampling. A period of continuous shedding persisted immediately after infection, in which no negative nasal samples were recovered, the end of which was defined by the first negative nasal sample, which in most mice correlated to a loss of carriage. However, some mice were observed to become re-infected after this initial period, and resumed shedding *S. pyogenes*. There was no significant difference between the 5 week old males and females over a 21 day period based on the duration of continuous carriage (Figure 3.4 A, Logrank $p>0.05$). The intermittent transmission events which occur after the cessation of continuous shedding were taken into account via a measure of total shedding duration. The total duration of shedding also did not differ significantly between the two groups.

However, the 10 week old male mice were found to shed *S. pyogenes* for significantly longer than 10 week old female mice based on continuous shedding duration (Figure 3.4 C, Logrank test $p<0.05$) and on total shedding (Figure 3.4. D, Logrank test $p<0.05$). The abundance of *S. pyogenes* (H347) present in the nasopharynx of mice tended to “plateau” in the majority of mice at the second or third day after infection, but could last up to the fourth day after infection (Shedding Intensity plot, Appendix 3.2.). Whilst the 10 week old males were better carriers,

they had to be housed separately to ameliorate the effects of aggression. For practical and humane reasons, male mice were not used in further long term carriage experiments.

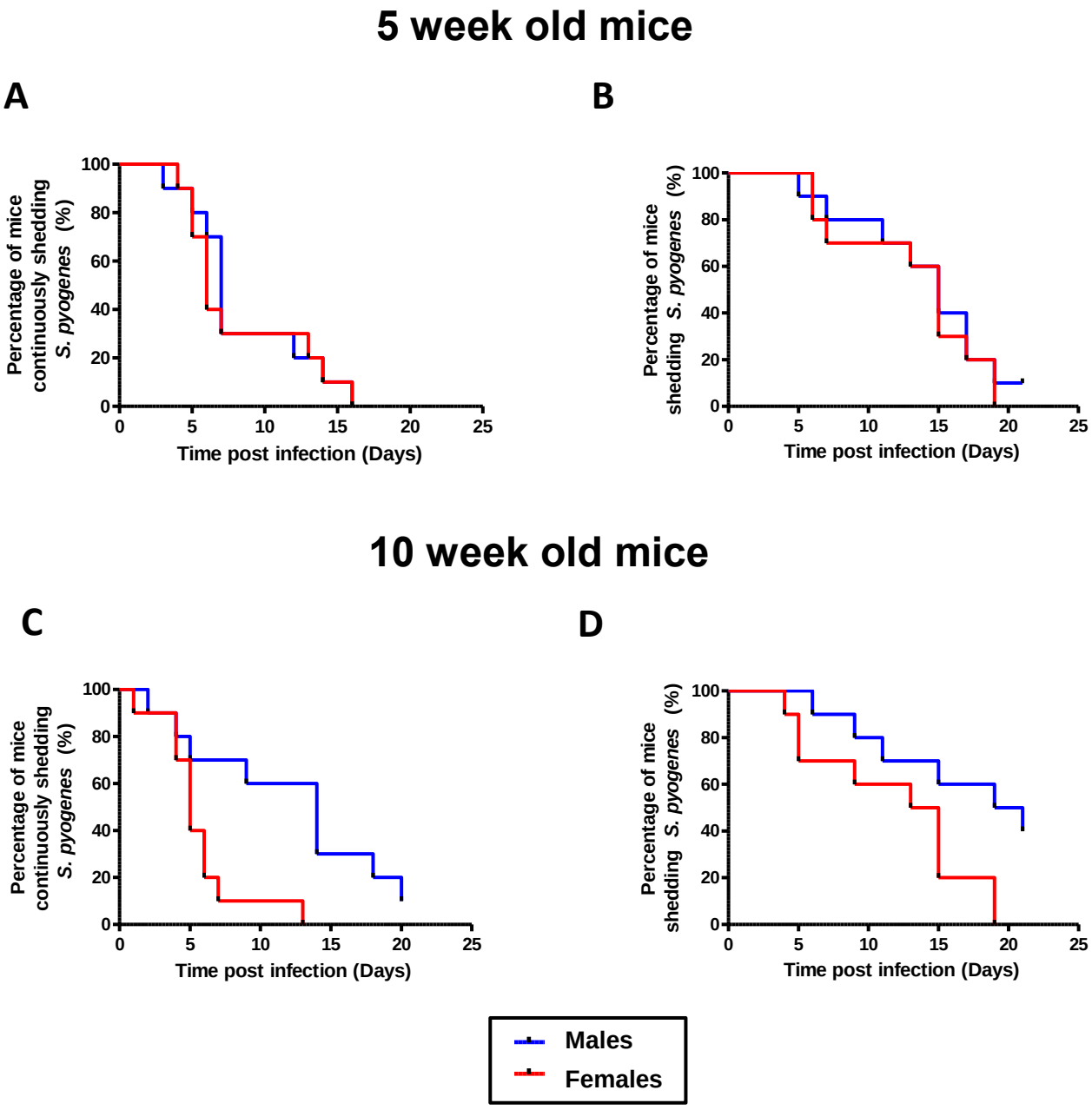


Figure 3.4. Comparison of duration of shedding for *S. pyogenes* H347 between genders in two different age groups. Male and female mice either 5 weeks or 10 weeks of age were infected intranasally and sampled non-invasively through direct nasal sampling over 21 days. The duration that 5 week old mice continuously shed *S. pyogenes* was not significantly different between the genders (A, $p>0.05$ Mantel–Cox Logrank test, n=10). After this period of continuous carriage, mice became re-infected. Thus, the total duration of shedding was determined based on the last positive nasal sample. The difference the total duration of shedding was also not significantly different between the genders in this age group (B, $p>0.05$ Mantel–Cox Logrank test). At 10 weeks of age, Male mice carried *S. pyogenes* H347 significantly longer than female mice based on both the duration of continuous shedding (C, $p<0.05$ Mantel–Cox Logrank test, n=10) and total shedding (D, $p<0.05$ Mantel-cox Logrank test).

3.2.4. INTRANASAL ADMINISTRATION OF *S. PYOGENES* RESULTS IN A SUPPURATIVE UPPER RESPIRATORY TRACT INFECTION THAT RESOLVES OVER 21 DAYS.

5 week old female FVB/n mice infected with *emm75 S. pyogenes* H347 demonstrated inflammatory changes affecting the nasal cavity over the first week of infection, particularly in the caudal (ethmoturbinate) region. A moderate to marked suppurative rhinitis with complete erosion or ulceration of the nasal mucosa and neutrophilic exudate on the mucosal surface (Figure 3.5 A-C) was observed by 72h in all mice, confirming that the infection resulted in an inflammatory process. On days 3 and 7, mice occasionally demonstrated necrosis of underlying turbinate bone and extension of inflammation and infection across the cribriform plate, resulting in a localised meningoencephalitis affecting the olfactory bulbs, although this was limited to single mice. However, by Day 21, the inflammatory damage to the nasal mucosa had resolved (Figure 3.5 D). Semi-quantitative assessment revealed that the observed inflammation decreased throughout the time course consistent with the lowering of the bacterial load (Figure 3.5. E). *S. pyogenes* could still be cultured from the nasopharynx even after the resolution of inflammation had begun.

	Time							
	Day 3		Day 7		Day 15		Day 21	
Strain	Histology grade	Bacterial counts	Histology grade	Bacterial counts	Histology grade	Bacterial counts	Histology grade	Bacterial counts
H347	++	29,000	++++	38,000	+++	1,000	+	10
	++++	1,000	+	2	+	0	ND	0
	++	5,000	+	0	+	1	+	0

Table 3.1. Histopathological analysis of upper respiratory tract tissue from mice infected with *emm75 S. pyogenes* (H347). At each of four time points, 3 mice per group were analysed to determine the severity of infection and assigned a numerical designation. - = No significant abnormality, + =Mild, ++= Moderate, +++ = Marked, ++++ = Severe and ND= Non diagnostic sections. This data was collected concurrently with the histopathological data shown in Table 6.1. Each row represents the findings for one mouse at each of the time points shown.

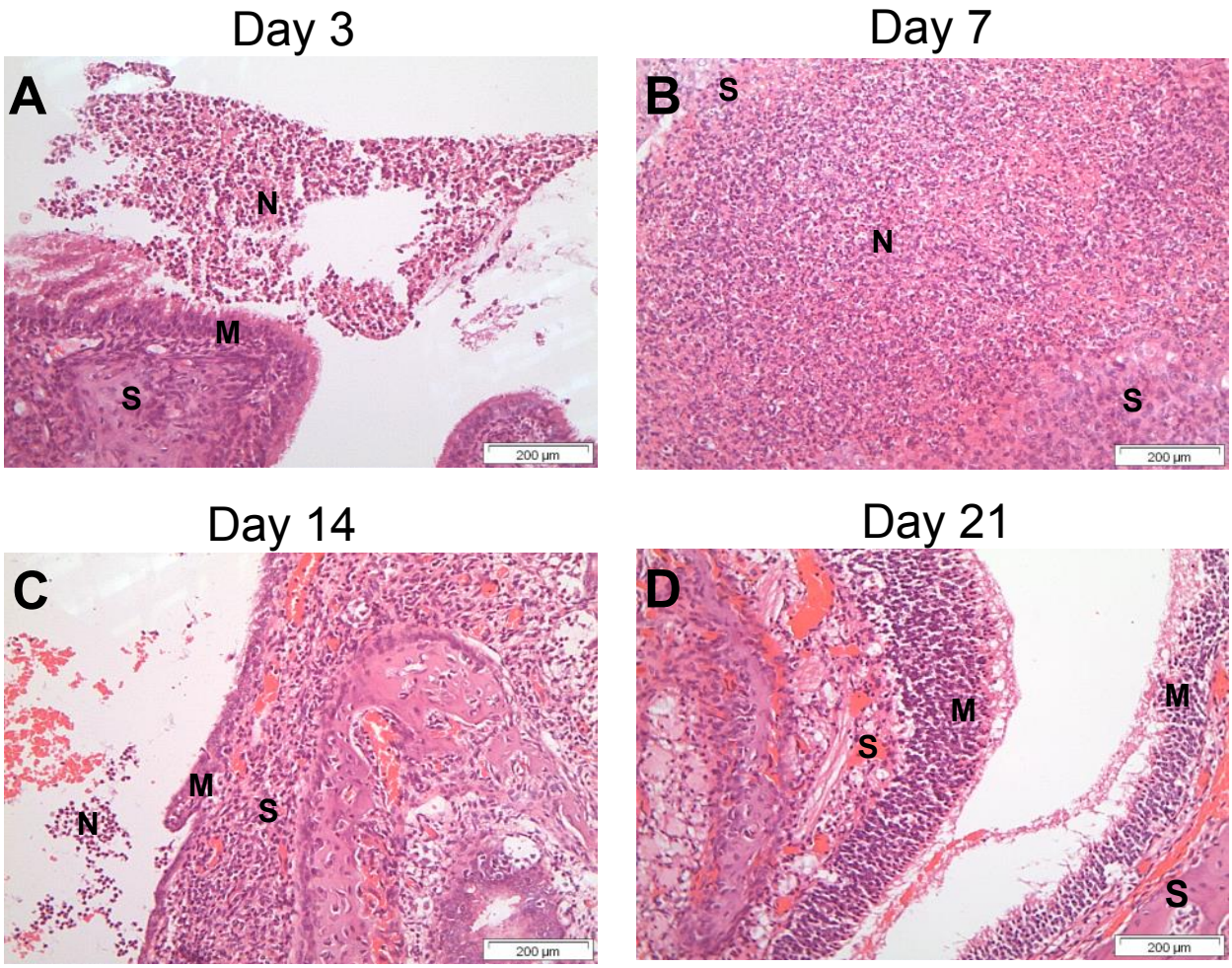


Figure 3.5. Histopathological analysis of upper respiratory tract tissue from mice infected intranasally with *emm75 S. pyogenes* (H347). Photomicrographs demonstrating mice infected with *emm*75 *S. pyogenes* (H347) (n=3 per group) were taken at days 3, 7, 14 and 21 after infection (Haemotoxylin & Eosin staining). **N** = Neutrophilic exudate, **M**= Nasal mucosa, **S**= Nasal stroma. Scale bar as shown. Damage to the nasal mucosa with surface neutrophilic exudate was apparent at day 3 post inoculation (A). The nasal epithelium of mice infected with *S. pyogenes* (H347) was widely eroded or ulcerated by Day 7 (B). At day 14, the inflammation had begun to resolve (C). By day 21, only mild inflammation was observed (D). Representative sections from single mice are shown. This experiment was performed concurrently with histopathological data shown in Figure 6.5.

3.2.5. TRANSMISSION OF *S. PYOGENES* WITHIN A MOUSE CAGE IS DEPENDENT ON THE PROPORTION OF DONOR MICE PRESENT.

When monitoring FVB/n mice infected with *S. pyogenes* over time, infection was occasionally observed to recur in mice after they had cleared the initial infection (see Appendix 3.2.). This raised the possibility that *S. pyogenes* was either present in the nasal tract at concentrations too low to be detected, or that it was being transmitted from infected mice within the cage.

The transmissibility of *S. pyogenes* (H347) in the nasopharynx was investigated through introducing infected “donor” mice into cages of uninfected “recipient” mice (n=8 per cage). Varying the Donor: Recipient (D:R) ratio in a cage was used as a way of altering the exposure of recipients to *S. pyogenes*.

The first direct nasal samples taken at 4 hours post infection revealed transmission had already occurred to all of the recipient mice. Recipient mice in cages with a higher proportion of donor mice acquired higher numbers of *S. pyogenes* (H347) than those with lower densities of donor mice. The recipient mice in the cage with four donors had significantly more bacteria in their nasopharynx compared to the cage with only 2 donors (Figure 3.6. $p<0.05$).

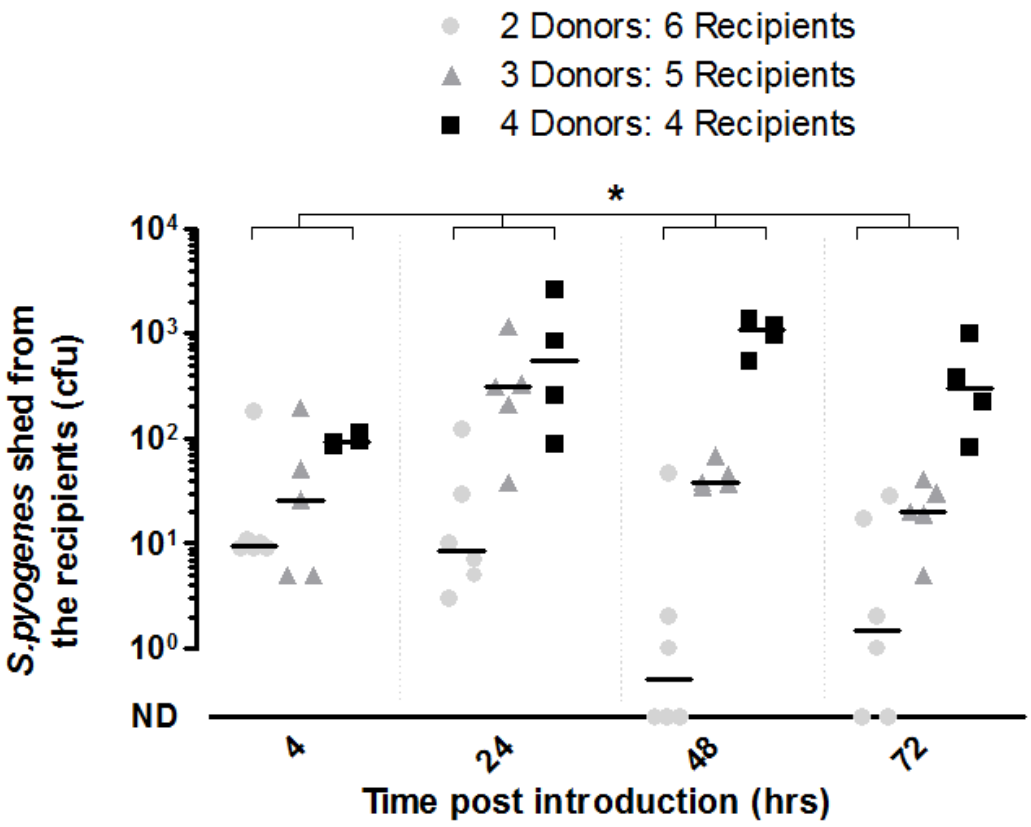


Figure 3.6. Transmission of *S. pyogenes* (H347) occurs more frequently as the density of infected carriers within a cage is increased. Donor mice infected intranasally with *S. pyogenes* H347 were introduced into a cage of naïve recipient mice. The Donor: Recipient (D:R) ratio was varied between 4:4, 3:5 and 2:6 between cages. Recipient mice were sampled at 4, 24, 48, 72 and 96 hours after the introduction of infected donor mice to a cage. Data show counts from direct nasal sampling from recipient mice only. Donor mice had >10,000 cfu recovered at all time points (not shown). The burden of transmitted infection was significantly higher in cages with a D:R ratio of 4:4 compared with cages with a 2:6 ratio. (AUC analysis, followed by Kruskal Wallis with Dunns Post test $p<0.05$). Bars indicate median.

3.2.6. TRANSMISSION BETWEEN MICE AND TO THE AIR IS NOT DEPENDANT ON PASSIVE TRANSFER OF *S. PYOGENES* DIRECTLY AFTER INOCULATION.

The early detection of *S. pyogenes* H347 transmitted between mice in the previous experiment may have been due to droplets of bacterial suspension being transferred between mice directly after inoculation. To rule this out, a transmission experiment involving cages with a D:R ratio of 3:5 where Donors were segregated from the Recipients for 4, 24 and 48 hours post inoculation was conducted.

Transmission was observed within all groups of mice, in spite of any delays in introduction (Figure 3.7 A), which suggests that the mice were actively transmitting *S. pyogenes* H347 throughout their infection.

To determine if *S. pyogenes* H347 was aerosolised from infected mice, settle plates were placed in each cage, at a height that precluded direct contact between mice and blood agar. Settle plates included in each cage revealed that airborne *S. pyogenes* H347 were present after the introduction of the donor mice into each cage (Figure 3.7 B). The time points where the highest levels of *S. pyogenes* were detected in the air coincided with the time points where the highest numbers of bacteria were detected in the recipient mice. The greatest burden of transmission was observed in the cages where the donor mice were introduced at 24 hours after infection. However, it should be noted that transmission was greatest in all of the mice at 24 hours. The differences in transmission to recipients between groups were reflected in the detection of airborne bacteria on settle plates, and are likely due to variation in the behaviours and activity of the mice.

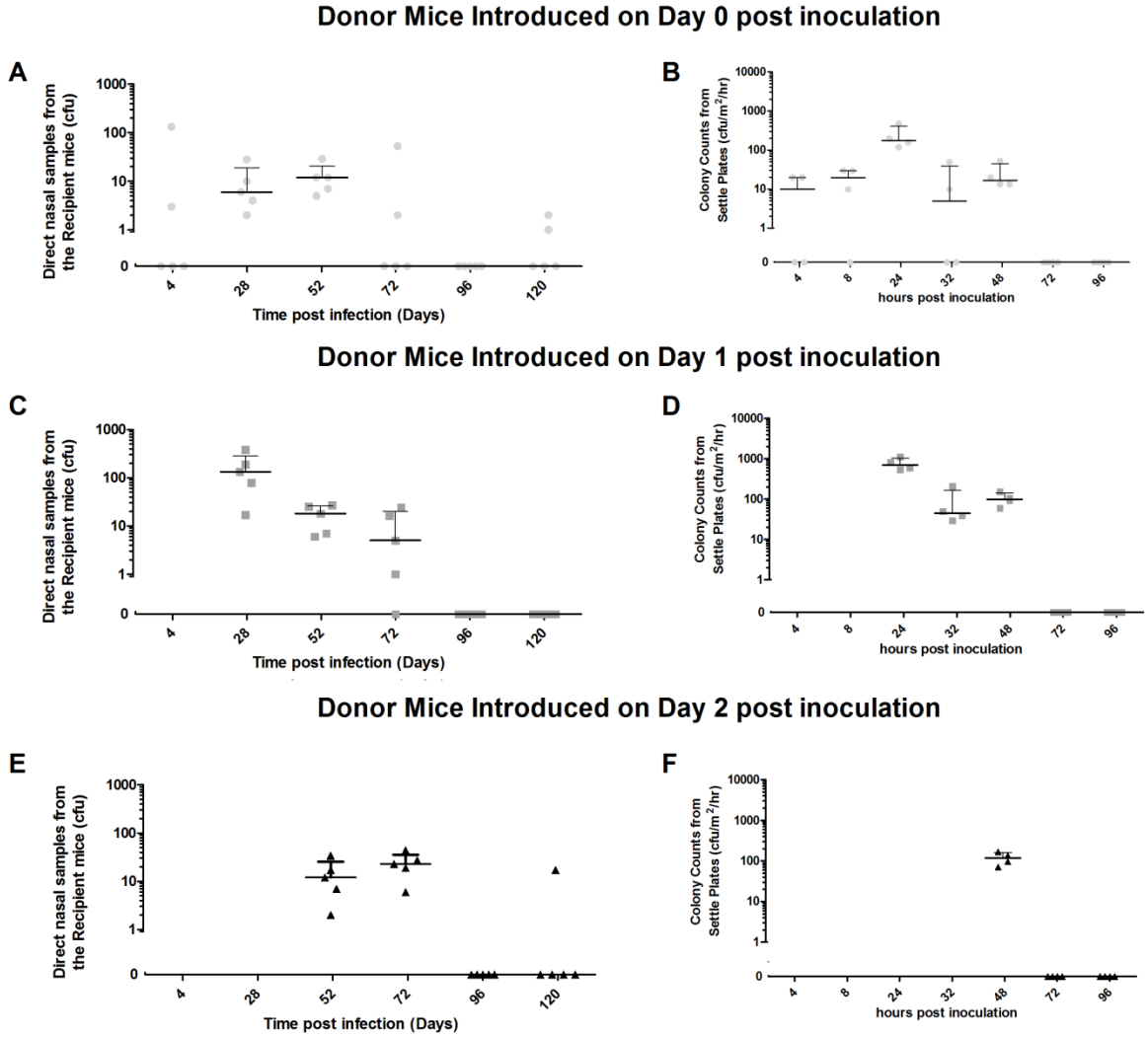


Figure 3.7. Transmission of *S. pyogenes* H347 between mice and to the air is not dependant on passive inoculum transfer. Naïve recipients co-mingled at a D:R ratio of 3:5 with mice infected with *S. pyogenes* H347 and sampled after the introduction of the donor mice (A,C,E, n=5 recipients per group) at 4, 24 and 48 hours post inoculation. Donor mice had >10,000 CFU recovered from direct nasal sampling throughout the experiment. Data shown from individual recipient mice. Settle plates retrieved from each cage (B,D,F, n=4 per cage) revealed the presence of airborne bacteria after the introduction of the donor mice. Data shown for each settle plate.

3.2.7. INFECTION OF DIFFERENT *EMM* TYPES IN THE NASOPHARYNX

The FVB/N model was developed using an *emm*75 *S. pyogenes* strain based on demonstrably superior longevity of carriage in BALB/c mice in preliminary work. To determine if the FVB/n model could support infection with a wider range of *emm* types, clinical pharyngitis isolates of the *emm* types 1, 2, 3, 4, 6, 12, 22, 28, 75 and 89 were inoculated intranasally into FVB/n mice and sampled daily for seven days after (Table 3.2, n=3 per group). The data showed that the model could support infection with all *emm* types up to 48h, however over one week, different *emm* types were cleared or resulted in death. After one week only *emm*2, *emm*75, and *emm*89 *S. pyogenes* were carried by at least 2/3 mice in each group.

The mice carrying the *emm1* and the *emm12* strains had to be culled early due to the severity of the disease in these mice. Lungs, livers and spleens were dissected, and the highest levels bacterial counts were observed within the spleen in mice infected with these isolates (Figure 3.8 A). In one mouse carrying an *emm12* strain, the right hemisphere of the brain demonstrated a macroscopic lesion. This was analysed using histopathology (Figure 3.8 B) and showed a focal meningeal haemorrhage with large numbers of cocci. These data suggest that the *emm1* and *emm12* genotypes can cause a systemic infection in FVB/n mice in spite of being given a dose that is initially confined to the upper respiratory tract.

	Day 1	Day 2	Day 3	Day 4	Day 5	Day 6	Day 7
emm1	3/3	3/3	3/3	1/1			
emm2	3/3	3/3	1/3	1/3	0/3	1/3	2/3
emm3	1/3	3/3	3/3	3/3	3/3	2/3	1/3
emm4	1/3	2/3	0/3	2/3	0/3	0/3	1/3
emm6	3/3	3/3	2/3	3/3	1/3	1/3	1/3
emm12	3/3	3/3	3/3	2/2	1/1		
emm22	2/3	3/3	1/3	1/3	0/3	0/3	2/3
emm28	0/3	1/3	0/3	0/3	0/3	0/3	0/3
emm75	3/3	3/3	2/3	2/3	0/3	1/3	2/3
emm89	1/3	3/3	3/3	2/3	3/3	2/3	3/3

Key
0 carriers
1 carrier
2 carriers
3 carriers
1 Death
2 Deaths

Table 3.2. The carriage of different *S. pyogenes emm* types in the nasopharynx of a mouse over time. Mice (n=3) were inoculated with 10^8 cfu of different *emm* types of *S. pyogenes*, and sampled every day over a week long period. The numbers of carriers present within a cage on a specific day was determined through the use of direct nasal sampling. The fractions show the numbers of carriers per cage (numerator) and the total numbers of mice in the cage (denominator). The colour coded key indicates the numbers of carriers per cage, and the numbers of deaths occurring in each cage.

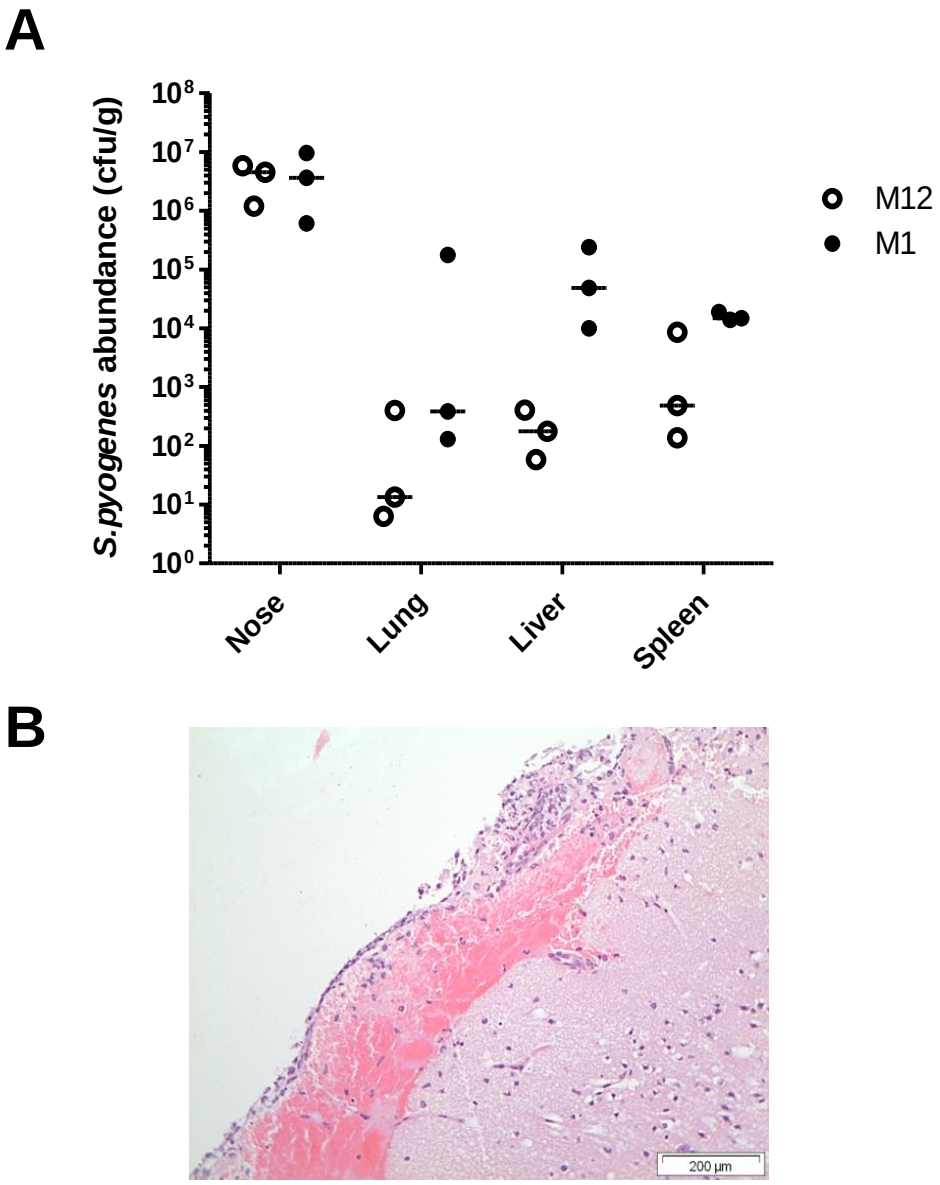


Figure 3.8. Invasive infection in the nasopharynx caused by *emm1* and *emm12* types. Mice (n=3) were inoculated with 10^8 cfu of different *emm* types of *S. pyogenes*, and sampled every day over a week long period (A) Mice infected with the *emm12* and *emm1 S. pyogenes* reached humane endpoints before the end of the experiment. Multiple organs were dissected out, and cultured; as shown. (B) Photomicrograph demonstrating meningeal haemorrhage (Haemotoxylin & Eosin staining) in a mouse infected with *emm12 S. pyogenes*.

3.3. DISCUSSION

To facilitate the investigation of bacterial and host factors that influence *S. pyogenes* in nasopharyngeal infection, a new model of nasopharyngeal colonisation was devised. A mouse host strain sensitive to nasopharyngeal infection was identified using a refined technique for nasal sampling.

The FVB/n mouse strain carried a greater number of bacteria for a longer period of time than other mouse strains tested. The FVB/n mouse is an inbred strain derived from the Swiss mouse based on the presence of the *fv-1*^{b} gene, which confers susceptibility to Friend Virus B through the absence of an interfering *gag* variant [274,275] and the susceptibility to *Citrobacter rodentium* through the *cri-1* locus [276,277].

Crucially, the direct nasal sampling technique employed during this study provided quantitative data that correlated with bacterial burden in the nasopharynx, demonstrating that the method is a valid method for monitoring bacterial burden. The direct nasal sampling technique also provided information regarding other bacteria which colonise the mouse upper respiratory tract. It was important to develop a system to distinguish the infecting *S. pyogenes* from these resident organisms. The dominant species in most of the mouse strains tended to be α-haemolytic viridans streptococci and staphylococci, which have also been shown to be present in the healthy human nasopharynx [278]. However, it should be noted that *Haemophilus* spp. only grew in regions of the blood agar plates that had been subject to β-haemolysis by *S. pyogenes*, and this may be the reason for its increased detection after infection. A similar sampling issue cannot be discounted as the reason for the increase in *Pseudomonas* spp. after *S. pyogenes* infection. The direct nasal

sampling method used in this work was optimised for the recovery of *S. pyogenes*, and whilst trends in commensal bacteria recovered using this method were interesting, and important to distinguish from *S. pyogenes*, a full investigation of the normal mouse nasopharyngeal flora was beyond the scope of the project and would ideally require molecular techniques such as 16S RNA sequencing. Importantly it was easy to distinguish *S. pyogenes* as this was a distinctive β-haemolytic bacterium whose presence could be confirmed by standard microbiological techniques.

It has been suggested in previous work that gender plays a role in the susceptibility of mice to invasive streptococcal disease [58,194]. It was found that gender had an impact on susceptibility to carriage in post pubertal mice only. Data were consistent with other published work demonstrating an increase in susceptibility to infection in male mice [194]. However, the levels of aggression shown by males of the FVB/n strain made them difficult to house in groups, and it is possible that the differences seen here could be due to housing these older mice individually. These welfare issues made male mice of this strain impractical for use in further experiments.

These early characterisation experiments demonstrated that *S. pyogenes* can be shed from the nasopharyngeal tract of mice in great numbers. The numbers of *S. pyogenes* were highest during a “plateau” during the first four days of infection. However, this “plateau” was due to the numbers of *S. pyogenes* retrieved from direct nasal sampling becoming so large that *S. pyogenes* formed a lawn on the surface of the blood agar plates, making accurate counts impossible. As a result, it is likely that this “plateau” defines the upper limit of quantification for this nasal sampling technique, and may be masking a peak of infection that occurs during the first four days of infection.

Multiple apparent re-infection events were observed after the first observed loss of carriage, suggesting transmission was occurring. To determine whether this was indeed the case, co-mingling experiments were conducted.

Co-mingling studies demonstrated that transmission occurred as early as 4 hours post introduction, and the numbers of bacteria recovered from the nares of the recipients increased as the number of infected donor mice in the cage was increased. However, in this initial experiment the donor mice were co-mingled immediately after inoculation, and so it is possible that the actual inoculum may have transferred to the other mice through passive means.

To address this issue, donor mice were segregated from the recipient mice for different lengths of time after inoculation before being re-introduced to the recipient mice. Transmission was still observed between mice after these delays, suggesting that it occurs as a result of an active infection in the donor mice. Settle plates placed in each cage detected airborne *S. pyogenes* in all cages after the introduction of the donor mice.

Importantly, these transmission events may not necessarily result in a productive infection in recipients, as *S. pyogenes* did not reach the same abundance in recipient mice as observed in donor mice, although persistent carriage was detectable for several days in recipients. Further histopathological studies are required to clarify this.

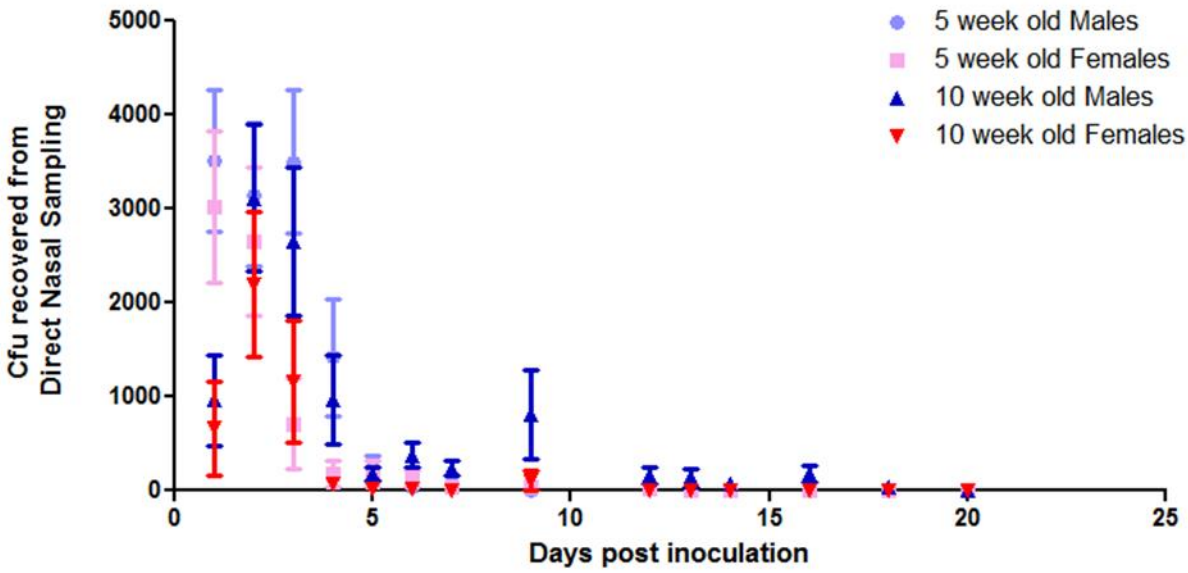
Having demonstrated that transmission to naive mice did occur, the possibility that apparent re-infections during longer term studies were artefacts resulting from the insensitivity of the nasal sampling technique was not formally discounted. However,

this could be addressed in future studies by infecting mice with strains carrying different genetic tags.

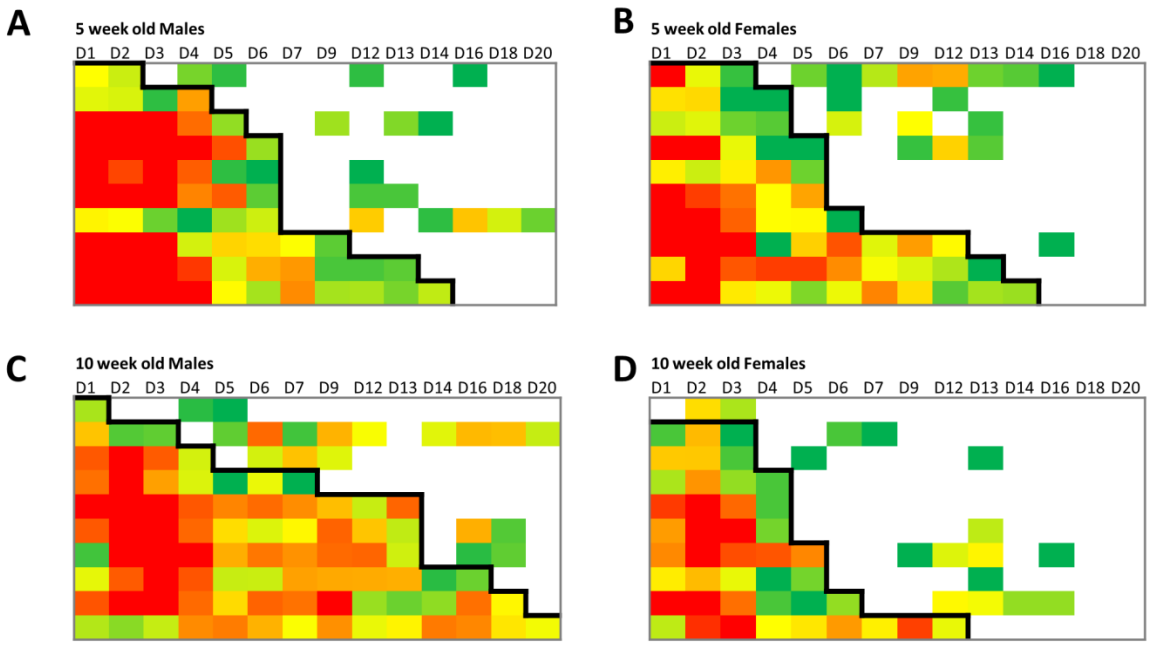
The model was initially developed using an *emm75 S. pyogenes* strain shown to be superior in BALB/c mice. An important consideration for the application of this model is whether it could be used to analyse different *emm* types of *S. pyogenes*. All strains (with the exception of the *emm28*) infected the FVB/n mouse strain for at least 2 days. Furthermore, systemic infections were observed in all the mice infected with the *emm1* and *emm12* genotypes, which are two of the most common causes of *S. pyogenes* infection in Europe, North America, Australia, New Zealand, Japan and Hong Kong [72].

The model described in these experiments allowed the study and quantification of *emm75 S. pyogenes* longitudinally during infection of the FVB/n murine nasopharynx; the model could be extended to alternative *emm* types and could be used to study transmission, something that has not been previously possible.

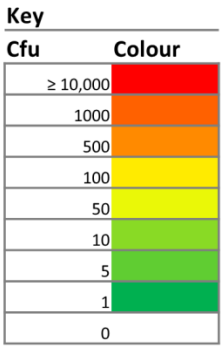
3.4. APPENDIX



Appendix 3.1. Shedding of *S. pyogenes* between genders in two different age groups over a time course. Male and female mice either 5 weeks or 10 weeks of age were infected intranasally and sampled non-invasively via a direct swabbing technique over a 21 day time course. Data points indicate the mean and error bars indicate the standard error of the mean.



Appendix 3.2. Differences in shedding intensity of *S. pyogenes* between genders in two different age groups. Male and female mice either 5 weeks or 10 weeks of age were infected intranasally and sampled non-invasively via a direct swabbing technique over a 21 day time course. Rows indicate individual mice throughout the time course (n=10 per group), colours indicate the numbers of *S. pyogenes* recovered from direct nasal samples with red indicating the highest recorded levels of carriage (≥10,000 cfu) and green indicates the lowest levels of carriage (1 cfu) and blank blocks indicate no recovery of *S. pyogenes*. Black line indicates survival based on the first loss of carriage.



CHAPTER 4: CHARACTERISATION OF A BIOLUMINESCENT STRAIN OF *S. PYOGENES*

4.1. INTRODUCTION

In the preceding chapter, the carriage of *S. pyogenes* in the nasopharynx was assessed through a direct sampling technique to assess the numbers of bacteria shed from the nasopharynx. This technique, whilst sensitive and quantitative, has an upper limit of quantification preventing detailed analysis during the most severe stages of infection.

Bioluminescent reporter genes such as the *lux* operon have been used to tag bacteria, allowing them to be imaged *in vivo* via the use of sensitive cameras. BPI has been used to study a variety of Gram negative [279,280] and Gram positive bacteria [262,281]

BPI has been previously used to observe severe infection using a bioluminescent derivative of an *emm49 S. pyogenes* strain from a skin isolate via an insertion into the Spy0535 locus with no reported fitness cost [170,216,268]. However this strain has not been broadly taken up by investigators studying *S. pyogenes* infection. As described earlier, different strains of *S. pyogenes* exhibit specific tissue tropisms [64,70], with skin isolates rarely being the cause of pharyngitis. For this work, the *emm75* pharyngitis isolate (H347) was chosen to be bioluminescently tagged, as it was not only clinically relevant, but demonstrably produced nasopharyngeal infection in mice.

There are a number of considerations that need to be taken into account when creating a bioluminescent strain for use *in vivo,* the first of which is that it must

express enough light to be detected. The strength of the bioluminescent signal can be boosted by varying the copy number of the genes (for example by expressing from a multi-copy plasmid), the promoter driving expression, or even by codon optimising the luciferase gene, as has been described for *Mycobacterium* spp [258].

For *in vivo* experiments, the expression of bioluminescence must also be stable within *S. pyogenes*, as in the previous characterisation experiments, nasopharyngeal shedding persisted for a median survival time of seven days in the FVB/n mouse strain. As the use of multi-copy plasmids for luciferase expression can require the use of selective media throughout an experiment to ensure a bioluminescence phenotype is maintained, and this can be difficult to deliver *in vivo*, a plasmid conferring bioluminescence was constructed to target and integrate into a pseudogene, spy0535. Spy0535 is present in the chromosome of all sequenced *S. pyogenes* strains and encodes a hypothetical protein of unknown function.

There has been considerable prior research to analyse how light penetrates different tissues [252] but much of this work relies on the wavelengths of light that are more commonly used for fluorescence excitation, rather than the wavelengths of light seen in the production of bioluminescence. The differential light absorption properties of biological tissue have been recognised [282] but their effects on light produced by the bioluminescent reaction have not been quantified. Furthermore, in previous work a background bioluminescent signal has been observed from the mouse nasopharynx [251] and it is likely that this would exert an effect on the sensitivity of bioluminescence imaging. The aim of this chapter was therefore to develop bioluminescent derivatives of *emm75 S. pyogenes* by transforming the parent strain with *luxABCDE* on either a replicating plasmid or through integration into the

bacterial chromosome. The resulting strains were then characterised both *in vitro* and *in vivo* with regard to application in future studies of nasopharyngeal infection.

4.2. RESULTS

4.2.1. EXPRESSION OF BIOLUMINESCENCE IN *S. PYOGENES* WITH A PLASMID BORNE CONSTRUCT

The replicating plasmid pTHLK was constructed with the highly expressed constitutive *Listeria monocytogenes* promoter P_{help} [283] to express *luxABCDE*, kanamycin and erythromycin resistance as described in Chapter 2. The *emm75* isolate, H347, was electroporated with pTHLK, to create the $H347^{pTHLK}$ strain, selected on erythromycin. This strain was grown alongside the H347 parental strain over a ten hour time period, with optical density measured hourly, and luminescence measured at half hourly intervals. Growth data from both strains were fitted to a logistic curve through regression (Figure 4.1 A, r^2>0.95). No significant differences between the growth rates and the carrying capacities for these bacteria were detected. Luminescence was measured in 50 µl samples of the broth culture, either neat, or diluted 1:10 into PBS. The diluted samples produced the highest luminescence readings, and demonstrated that the peak of luminescence occurred after 7 hours of growth (Figure 4.1. B).

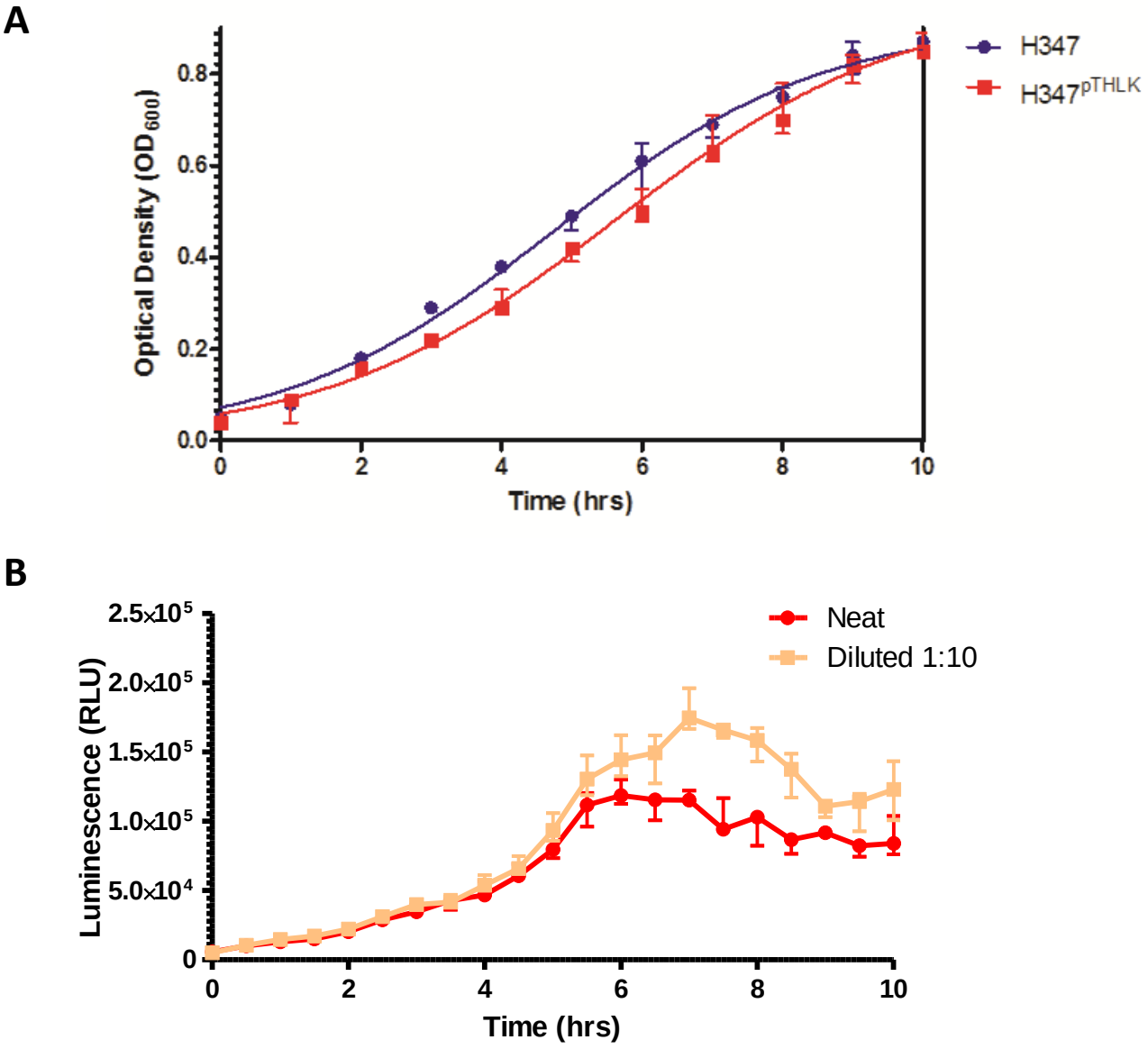


Figure 4.1. Growth kinetics and luminescence production of H347^{pTHLK}

The growth of H347^{pTHLK} was compared with the wild type parental strain (A, n=3 separate cultures per group) and a logistic regression line was fitted to the data (r^2>0.95). Luminescence was quantified during growth either from a neat 50 µl sample, or a 50 µl sample with the same number of bacteria diluted 1:10 into PBS to produce a 500µl sample (B) Error Bars indicate median and interquartile range.

4.2.2. INTEGRATION OF A BIOLUMINESCENT CONSTRUCT INTO *S. PYOGENES*.

A set of plasmids containing the *luxABCDE* operon were created with a region of homology targeting a single crossover with the spy0535 region of the *S. pyogenes* chromosome (Figure 4.2 A). The pICL18^{lux} plasmid utilised the *Listeria* promoter P_{help} to promote bioluminescence, whereas the pICL18^{vlux} plasmid utilised the *Bacillus* promoter P_{veg} instead [284]. These constructs were used to transform the parent *emm75 S. pyogenes* strain H347, and transformants were selected on kanamycin. A control plasmid which did not contain *luxABCDE* but which did contain the Spy0535 region of homology was used to derive a control transformant that had an 'empty' plasmid integrated at the same site.

As pICL derivatives have a Gram negative origin of replication and no Gram positive origin, transformants would only have arisen following chromosomal integration. To confirm integration into Spy0535, primers targeting regions within the pICL based plasmid sequence adjacent to the spy0535, and the genes adjacent to spy0535 on the bacterial chromosome were used to confirm target insertion (Chapter 2, Table 2.1). Three primer pairs were used; LF-LR and RF-RR would amplify products of similar size based on the presence of the construct between the flanking genes spy0534 and spy0536, while the LF-RR pair would only produce a product if spy0535 alone was present, as would be expected in the parent H347 strain (Figure 4.2 A). PCR products revealed successful integrations for the pICL18^{lux}, and pICL18^{0} plasmids (Figure 4.2 B). It should be noted that the pICL18^{vlux} integrated strain did not produce an LF-LR product, although the presence of the RF-RR fragment suggests that the integration was successful. The strains containing the pICL18^{lux},

pICL18^{vlux} and pICL18^{0} plasmids were designated as the H347^{lux}, H347^{vlux} and H347^{0} strains respectively. The wild-type H347 only produced an LF-RR product.

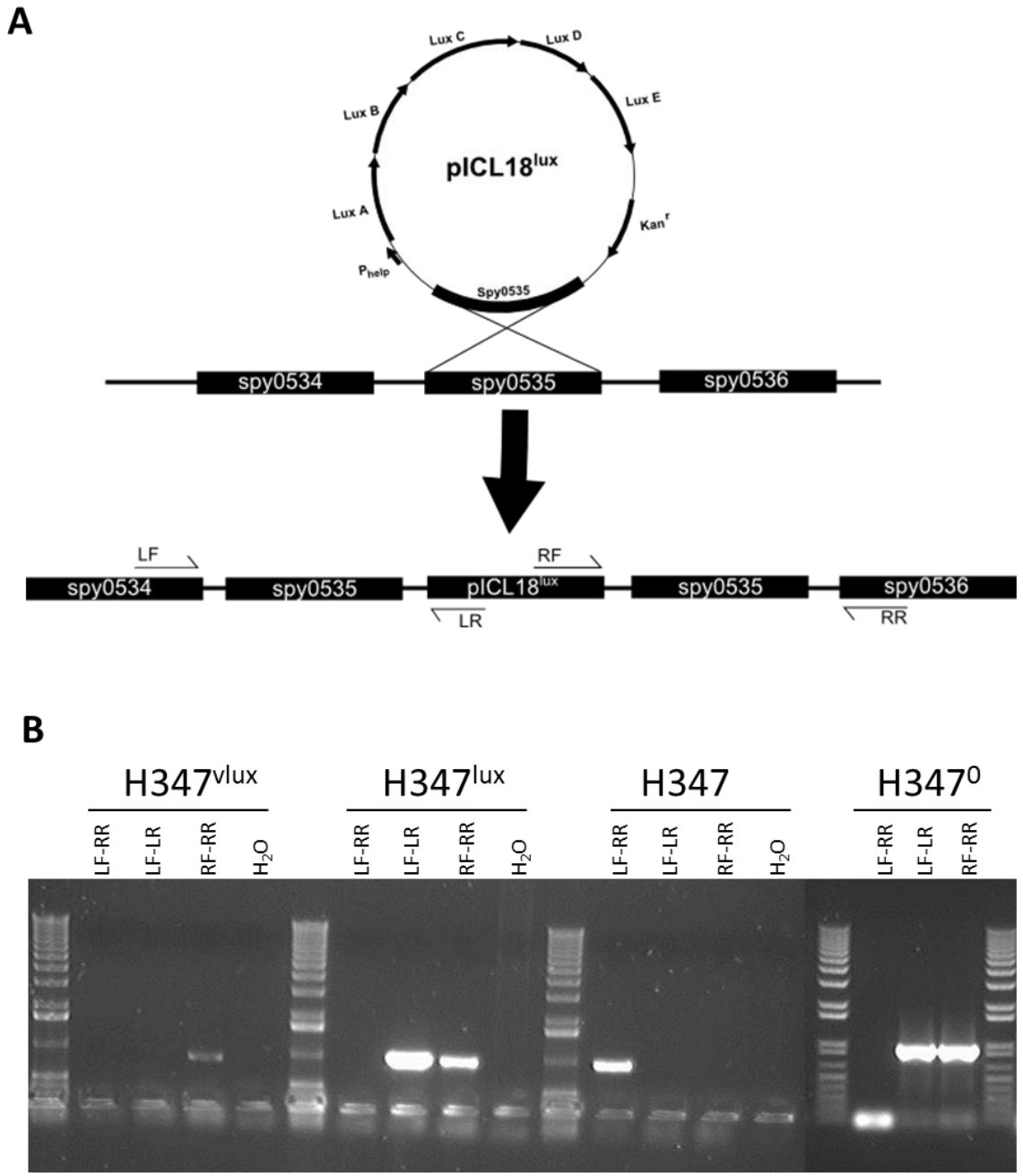


Figure 4.3. Confirmation of integration into the *S. pyogenes* chromosome. A diagrammatic representation of the integration of the plasmid pICL18^{lux} into the *S. pyogenes* chromosome via a single crossover, which would produce two copies of the *spy0535* fragment either side of the integrated plasmid. Primers amplifying from within the integrated pICL18^{lux} and to the adjacent genes are shown on the diagram. An integration will produce positive results for the regions between LF-LR and RF-RR (A). PCR using these primers was performed on DNA purified from H347^{vlux}, H347^{lux}, H347 and the H347^{0} to determine whether a successful integration had occurred (B).

4.2.3. THE GROWTH AND LUMINESCENCE OF THE INTEGRATED CONSTRUCTS IN *S. PYOGENES* .

Two bioluminescent derivatives of strain H347 were derived with different promoters driving the expression of the *luxABCDE* operon. The $H347^{lux}$ and $H347^{vlux}$ strains expressed bioluminescence using the P_{help} and P_{veg} promoters respectively. The growth of these two strains was measured over ten hours, with luminescence readings taken at every half hour (Figure 4.3.). Similar to the strains transformed with replicating plasmids, the peak of luminescence was again observed approximately 7 hours from the start of the experiment. The luminescent signals observed for $H347^{vlux}$ were lower than those observed for $H347^{lux}$, but the difference was not significant.

The growth rate data were fitted to logistic curves through regression (Figure 4.3. $r^2>0.95$) There were no significant differences in the growth rates between the $H347^{lux}$ and $H347^{vlux}$ bioluminescent strains. However, the H347 parental strain had a significantly higher carrying capacity. The carrying capacity is a statistic that defines the maximum population capacity of *S. pyogenes* that can be sustained within a culture. This suggests that the bioluminescent strains had a growth deficit. To determine whether these growth defects were due to the expression of bioluminescence, or the integration into the spy0535 section of the streptococcal chromosome, the non-bioluminescent plasmid $pICL18^0$ was used to transform H347 to create $H347^0$ which had the same plasmid integration into spy0535 (Figure 4.2 B).

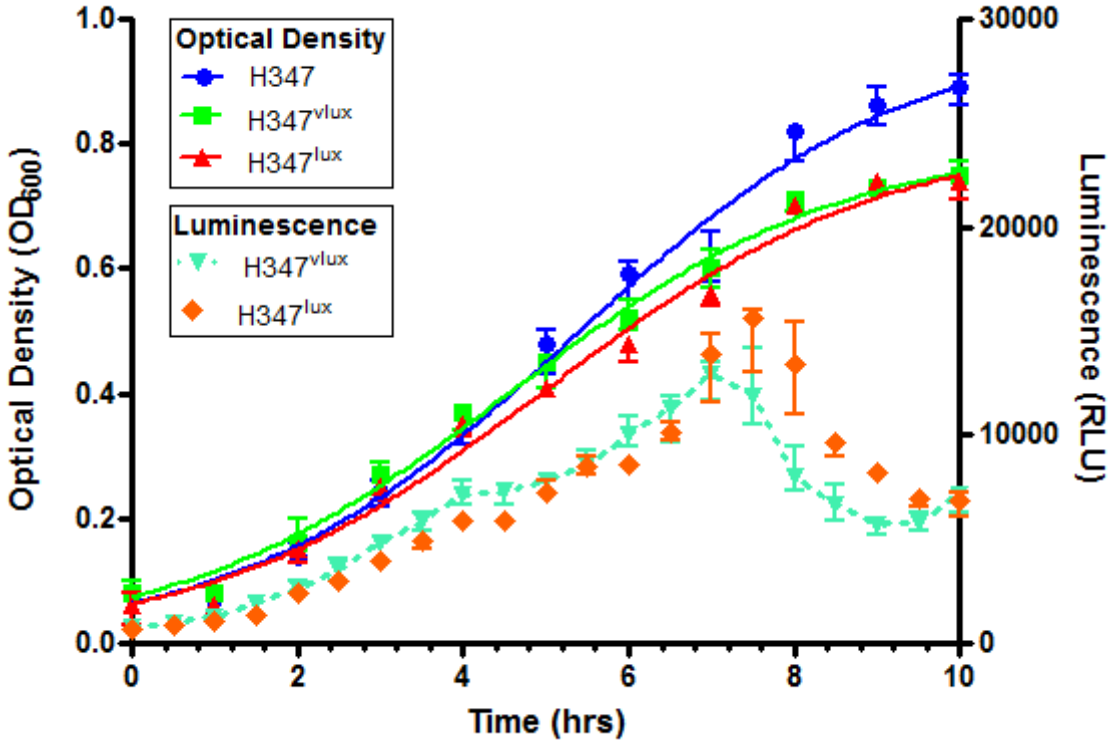


Figure 4.3. Growth kinetics and luminescence production of H347^{vlux} and H347^{lux}. The growth of H347^{vlux}, H347^{lux} and the H347 wild type parental strain were compared over a time course (n=3 separate cultures per group). A logistic curve was fitted to the growth data through regression (r^2>0.95). The luminescent signal from H347^{vlux} and H347^{lux} is also displayed. Error bars indicate median and interquartile range

The H347^{lux}, H347^{0} and H347 parental strains were grown over 10 hours. The data were fitted to a logistic curve (r^2>0.95), which demonstrated that there was no significant difference in growth rate, but there was a significant difference in the µmax between the wild-type and control strains and the bioluminescent strains (Figure 4.4). This suggests that any growth defect is conferred by the expression of bioluminescence, rather than the potential disruption of the spy0535 locus.

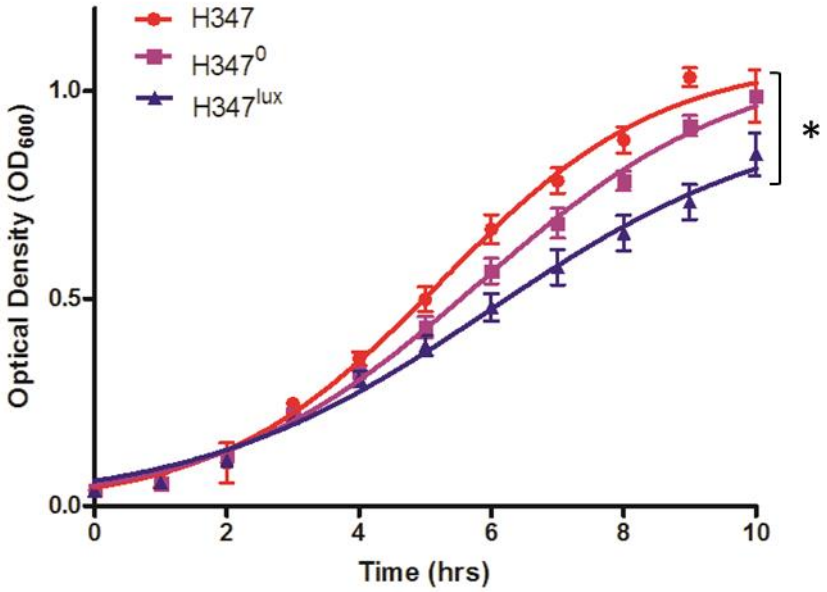


Figure 4.4. Bioluminescence expression confers *in vitro* growth defects. The growth of H347^{lux}, H347^{0}, and H347 wild type strain were compared over a time course (n=6 separate cultures per group). Logistic curves were fitted to the data through regression (r^2>0.95). Error bars indicate median and interquartile range.

4.2.4. COMPARISON OF BIOLUMINESCENCE EXPRESSION BETWEEN *S. PYOGENES* STRAINS TRANSFORMED WITH REPLICATING PLASMID OR INTEGRATED CONSTRUCTS

S. pyogenes carrying pTHLK (H347^{pTHLK}) and *S. pyogenes* with integrated pICL18^{lux} (H347^{lux}) were grown to logarithmic phase and imaged using BPI. There was a significant difference in light production by the two bioluminescent strains (Linear regression $p<0.05$.) H347^{pTHLK} produced on average 26.19 photons ± 0.06 SE per CFU (Figure 4.5), whereas H347^{lux} produced on average 1.062 photons ± 0.012 SE per CFU (Figure 4.5).

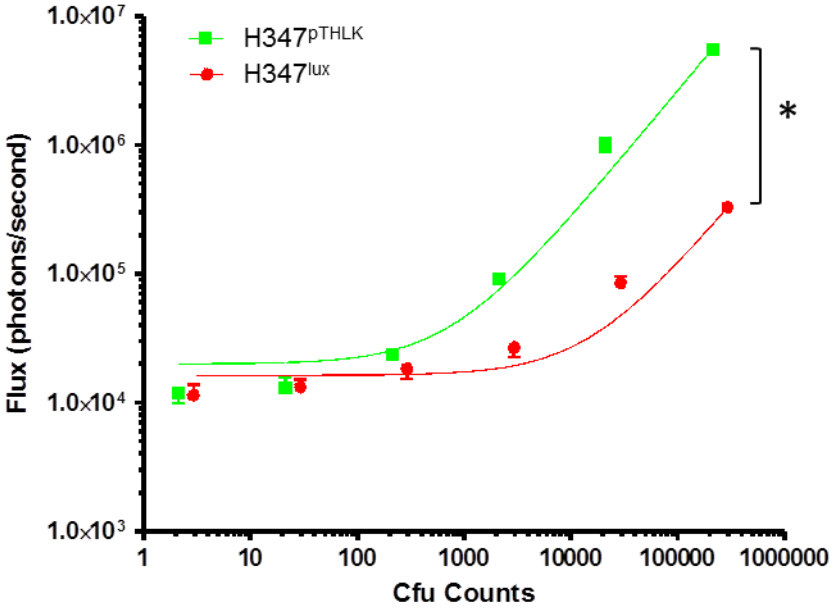


Figure 4.5. Characterisation of Bioluminescent strains. Serial dilutions of the bioluminescent strains with either the bioluminescent plasmid ($H347^{pTHLK}$) or the integrated construct ($H347^{lux}$) were imaged on a 96 well plate (n= 3 separate cultures) using an IVIS 100 system. Colony counts were obtained through serial plating. Error bars indicate median and interquartile range.

4.2.5. THE STABILITY OF THE BIOLUMINESCENT CONSTRUCTS IN *S. PYOGENES*

The H347^{pTHLK} and H347^{lux} strains were passaged daily with and without antibiotics, and plated onto selective and non-selective media daily to assess whether *S. pyogenes* carrying *LuxABCDE* and the Aph-A3 kanamycin resistance gene constructs were still present.

The number of bacteria retaining the replicating plasmid based constructs declined a thousand-fold after each passage, when grown without selection (Figure 4.6 A). In contrast, there was no loss of the bioluminescence constructs when integrated into the chromosome over a seven day period even in the absence of antibiotics (Figure 4.6 B). These data showed that the *luxABCDE* construct integration was stable in the streptococcal chromosome, but the plasmid based construct was unstable. The integrated *luxABCDE* strain was therefore determined to be more suitable for *in vivo* models of infection.

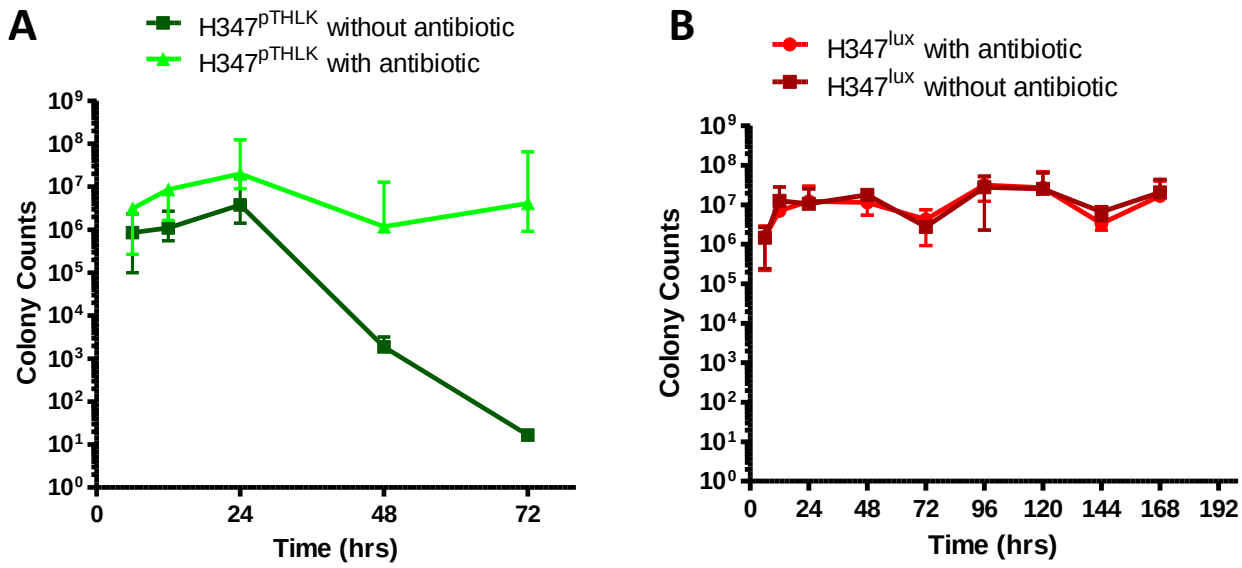


Figure 4.6. Stability of Bioluminescent plasmids. H347^{pTHLK} and H347^{lux} were passaged *in vitro* with or without antibiotic to determine the stability of bioluminescence expression. After 24 hours, the numbers of H347^{pTHLK} containing the plasmid based construct pTHLK declined without antibiotic, whilst bacteria cultured in the presence of antibiotic retained the plasmid (A, n=3 separate cultures). In contrast, H347^{lux} carrying the integrated pICL18^{lux} was maintained in similar numbers whether or not antibiotic was present (B, n=3 separate cultures). Colony counts were obtained through serial plating. Error Bars indicate median and range.

4.2.6. THE EFFECT OF BIOLUMINESCENCE EXPRESSION ON STREPTOCOCCAL BIOFILM FORMATION

As biofilm formation is purported to underlie the successful colonisation of the pharynx, the H347^{lux}, H347^{0} and H347 strains were assessed for their ability to form biofilms through the crystal violet staining method [273]. A standard curve was constructed to ensure that the optical density measured by the previous method correlated to the numbers of bacteria (Figure 4.7 A). H347^{lux} were significantly less abundant in biofilms compared to the H347 parental strain and the H347^{0} (Figure 4.7 B, p <0.05 Kruskal-Wallis with Dunns post test).

Total numbers of bacteria within the entire well were calculated based on measurements taken from non-adherent as well as adherent bacteria (Figure 4.7 C). When bacterial CFU in biofilm were adjusted to take into account the total number of bacteria, it transpired that the lower abundance of H347^{lux} in biofilm resulted from a generalised lower abundance in cultures. This suggests that the expression of bioluminescence impairs *S. pyogenes* growth, but not its ability to form biofilms.

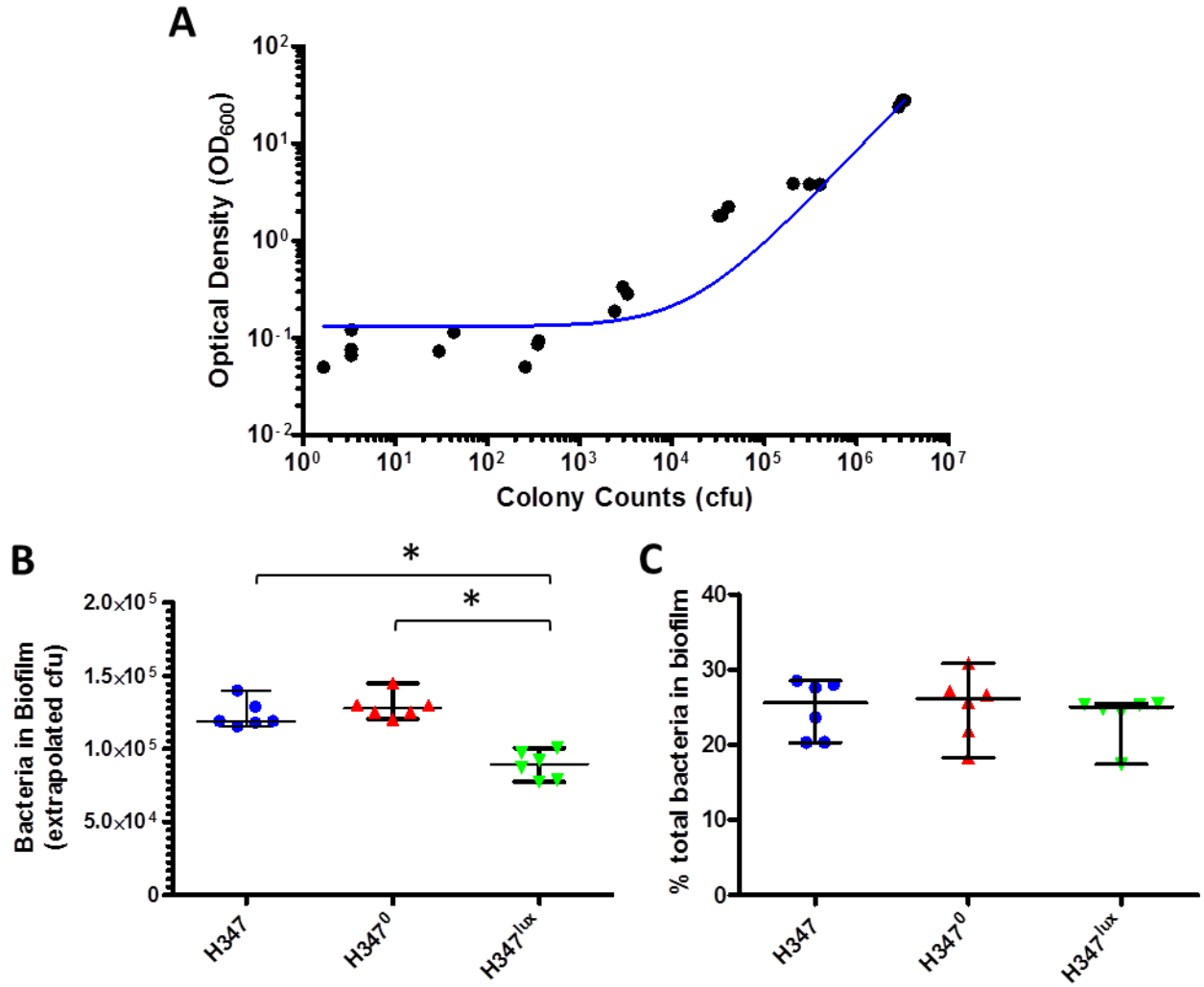


Figure 4.8. Biofilm forming capacity of Bioluminescent strains. The biofilm forming ability of H347, H347^{0} and H347^{lux} *S.pyogenes* strains were assessed through a crystal violet staining technique. A standard curve comparing measured OD_{600} from crystal violet straining to *S. pyogenes* counts showed a significant correlation (A, n=18, Linear regression, r^2>0.95). H347^{lux} was significantly less abundant in biofilms than the other strains tested (B, n=6, Kruskal-Wallis with Dunns post test p<0.05).
The total percentage of bacteria in the biofilm, calculated as a fraction of the bacteria in the biofilm and non-adherent bacteria in the supernatant, revealed no significant difference.(C). Data shown for independent cultures, Error bars indicate median and range

4.3. DISCUSSION

A suite of plasmids carrying bioluminescence reporter genes were constructed with the purpose of creating a bioluminescent derivative of the *emm75* strain of *S. pyogenes* H347 used in the preceding chapter to characterise a model of intranasal infection.

The replicating plasmid pTHLK showed initial promise, as the strain H347^{pTHLK} did not show any specific growth defects, and produced a 25-fold stronger luminescent signal than the H347^{lux}. The pTHLK plasmid was however shown to be unstable when passaged in the absence of antibiotic, making it unsuitable for use in an *in vivo* model. Luminescent signals needed to be diluted 1:10 in order to prevent the effects of quenching and obtain accurate readings. A reduction in the bioluminescent signal was observed as the *S. pyogenes* cultures entered stationary phase. This effect has been observed for *S. pneumoniae* [285] and *S. aureus* [281], and is suspected to be due to a lack of available $FMNH_2$ in Gram positive bacteria during this phase of growth.

The luminescent strains H347^{lux} and H347^{vlux}, in which the bioluminescence operon was integrated alongside spy0535 in the chromosome, had lower carrying capacities compared to the wild type strain. The reduction in carrying capacity observed in the bioluminescent strains could conceivably be due to the changes to the spy0535 locus of the chromosome incurred by the integration of a plasmid into the region. To determine whether this was the case, a control plasmid pICL18^{0} that did not confer bioluminescence was integrated into this region. H347^{0} did not demonstrate any growth defect *in vitro* confirming that the site of integration per se was not harmful.

Despite using different promoters to drive *luxABCDE* expression, there was no significant difference found in bioluminescence between these strains. The H347^{lux} strain with the P_{help} promoter was used for further studies as this allowed for a better comparison with the H347^{pTHLK} strain, and because its bioluminescence appeared to be stronger than the H347^{vlux} which used the P_{veg} promoter.

The integrated strains were assessed for defects in growth and biofilm formation. Although raw numbers of H347^{lux} in biofilm were lower than the non-bioluminescent strains, analysis of the non-adherent bacteria revealed that this was a manifestation of the defect in carrying capacity seen during growth. Importantly, the lack of any biofilm formation, or growth defect in the H347^{0} strain suggest that the fitness cost is incurred by the expression of bioluminescence itself. This may explain why the replicative plasmid pTHLK was so rapidly lost, as *S. pyogenes* that stop expressing bioluminescence would have a fitness advantage.

However, this fitness deficit appears to only affect the maximum numbers of *S. pyogenes* present within culture, and it is possible that this may not manifest during infection in the nasopharynx.

CHAPTER 5: *IN VIVO* CHARACTERISATION OF BIOLUMINESCENT *S. PYOGENES*

5.1 INTRODUCTION

Isogenic bioluminescent derivatives of the *emm75* clinical pharyngitis isolate H347 could enable the quantification of *S. pyogenes in vivo* using biophotonic imaging. However, a number of considerations must be addressed before such strains can be used *in vivo.*

Previous studies have found that many living organisms can themselves produce weak bioluminescent signals [286,287]. In mice, the main source of signal has been identified as the gastrointestinal tract, due to the presence of chlorophyll in alfalfa diets contributing to a chemiluminescent signal [251].

In the previous chapter, a *S. pyogenes* strain carrying a non-integrating plasmid pTHLK (H347^{pTHLK}) produced a higher bioluminescent signal *in vitro* compared with the signal from *S. pyogenes* transformed with integrated pICL18^{lux} (H347^{lux}). The use of this brighter bioluminescent strain could allow for the more sensitive detection of *S. pyogenes.* However the bioluminescent construct of this strain was unstable without antibiotics, in contrast to H347^{lux}, and required regular antibiotic application in order for it to be maintained.

The expression of bioluminescence attenuated the *in vitro* growth of *S. pyogenes* H347^{lux} (Chapter 4.2.3 and 4.2.6), hence the degree to which growth attenuation exerts an effect *in vivo* required determination.

5.2. RESULTS

5.2.1. CHARACTERISATION OF THE BACKGROUND LUMINESCENT SIGNAL FROM THE MURINE NASOPHARYNX

Uninfected FVB/n mice were imaged using an IVIS camera. The background bioluminescent signal was not homogenously distributed throughout the anatomy of the mouse. The background luminescence from the nose and the lungs were determined through imaging FVB/n mice from both dorsal and ventral viewpoints, with an integration time of 300 seconds (Figure 5.1 A & B). The luminescent signals from the nasopharynx did not exceed 10^4 photons s^{-1} cm^{-2} sr^{-1}.

The luminescent signals taken from the nose (Figure 5.1 C, ROI as described in Chapter 2) and the lung (Figure 5.1 D, ROI as described in Chapter 2) were quantified from both the dorsal and ventral viewpoints. The background luminescence from the dorsal viewpoints in the lung and the nose were found to be significantly higher than that detected from the ventral viewpoints. The nasal tracts of the mice were dissected out, and a background signal was observed in the anterior portion of the nasopharynx (Figure 5.1 E). The mean background luminescence was found to be 15952 photons s^{-1} (± 2571 SE).

To account for this background, any signal obtained from the nasopharynx of around 2×10^4 p/s was treated as background, and images are displayed with a set luminescence threshold of at least 4000 p $s^{-1}cm^{-2}sr^{-1}$.

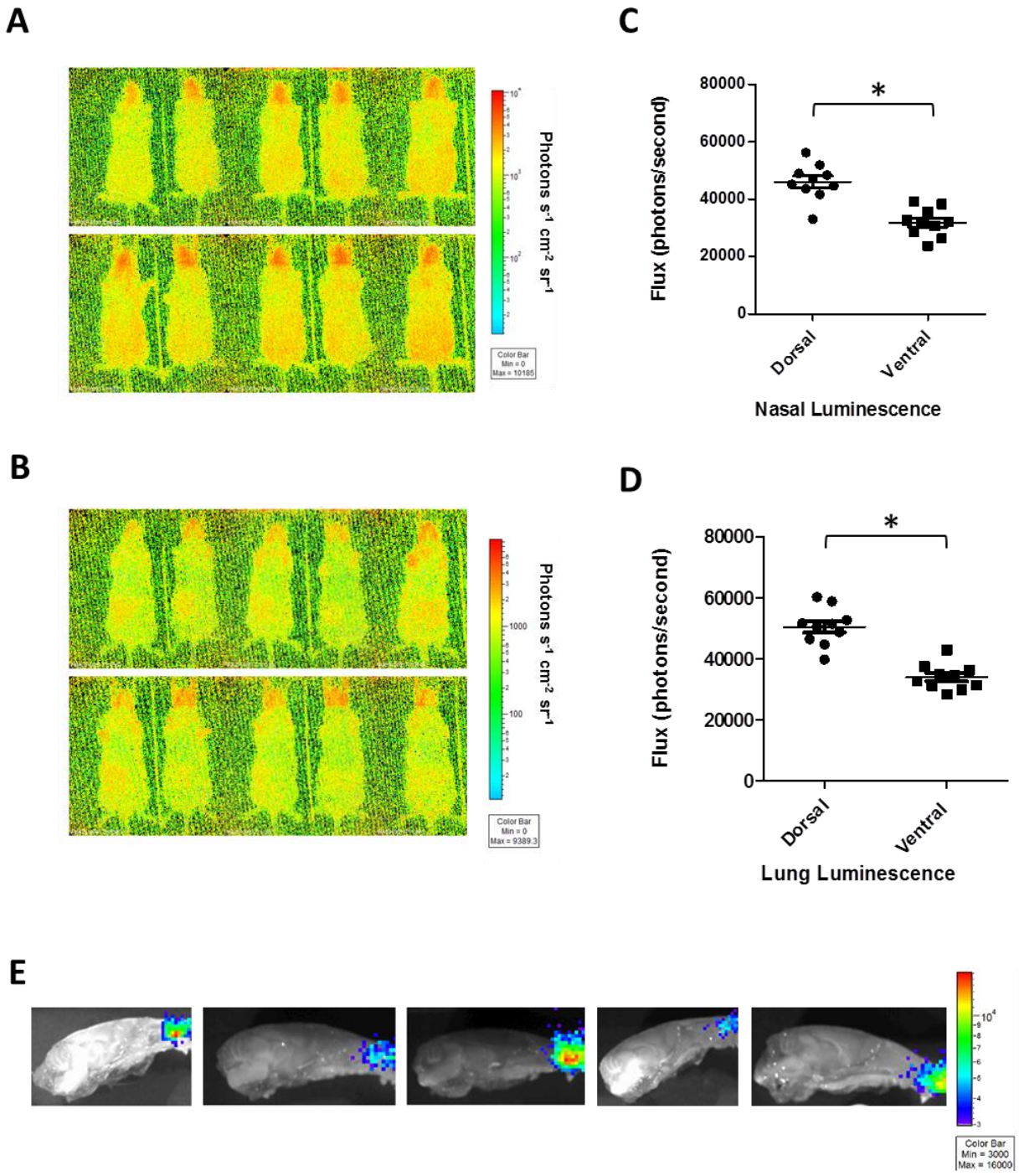


Figure 5.1. Background luminescence from mice. FVB/n strain mice (n=10) were imaged using the IVIS 100 system with an integration time of 300 seconds both dorsally (A) and ventrally (B). The background luminescent signals from the nasal tract (C, Mann-Whitney U $p<0.05$) and the lung (D, Mann Whitney U, $p<0.05$) were quantified both dorsally and ventrally. Images from the dissected nasopharynx of controls revealed the origin of the background bioluminescent signal (E). Data shown for individual mice, bar indicates median.

5.2.2. *IN VIVO* INSTABILITY OF THE MULTI-COPY PLASMID IN *S. PYOGENES* ANTIBIOTIC APPLICATION

Whilst the *in vitro* work suggested that the H347^{pTHLK} was unstable without antibiotics, the possibility remained that it could be maintained *in vivo* with the application of antibiotics. H347^{pTHLK} was inoculated intranasally into FVB/n mice (n=4) that were exposed to antibiotics (2.5mg/kg, intraperitoneal erythromycin) 6 hours before the inoculations, and at 12 hour intervals afterwards.

Mice were imaged on the day of inoculation and every day after inoculation for 72 hours (Fig. 5.2 A). The luminescence from the dorsal view of the nose was assessed (Fig 5.2 B), direct nasal samples taken daily onto CBA to assess *S. pyogenes* shedding, and then onto selective medium to determine the numbers of bacteria still carrying the pTHLK plasmid (Fig 5.2. C). H347^{pTHLK} rapidly lost the plasmid pTHLK *in vivo,* despite repeated antibiotic application. Only one mouse had erythromycin resistant bacteria 24 hours post inoculation, and this was the only mouse that showed any bioluminescent signal. This same mouse had high numbers of *S. pyogenes* the day afterwards, but none of the bacteria retained the plasmid. The poor stability of this plasmid *in vivo* precluded its use in further *in vivo* experiments.

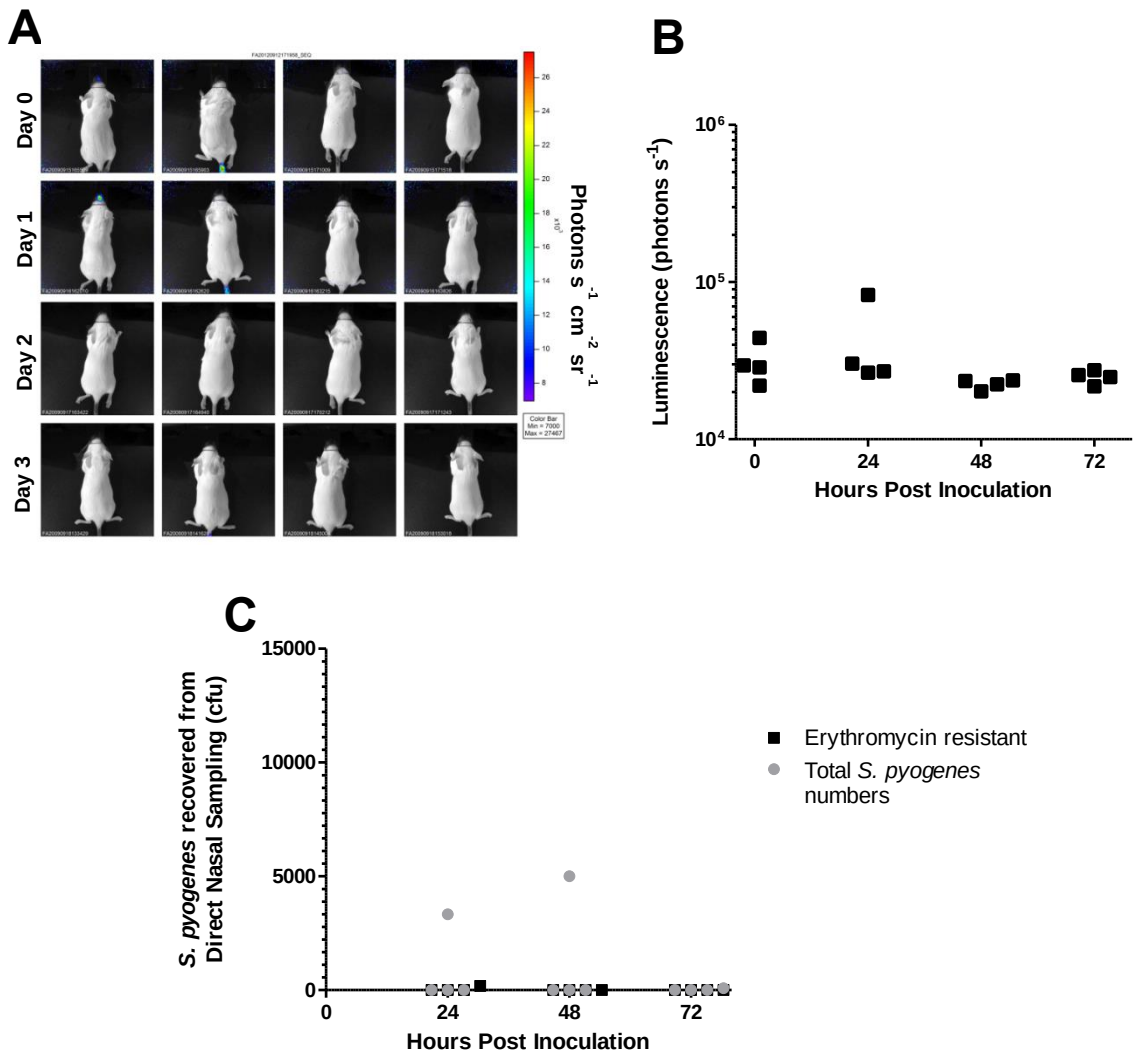


Figure 5.2. Instability of the pTHLK replicating plasmid *in vivo*. Mice inoculated with H347^{pTHLK} were imaged over 72 hours post inoculation (A, n=4). Luminescent signal was assessed from the dorsal view (B). An autoluminescent signal was obtained from the red dye used to mark the tail of one mouse. Direct nasal samples were taken daily onto CBA to determine total *S. pyogenes* numbers, and onto THA with erythromycin to determine the numbers of *S. pyogenes* still carrying pTHLK (C). Data shown for individual mice.

5.2.3. INTRANASAL INFECTION WITH STABLY BIOLUMINESCENT *S. PYOGENES* OVER A LONGITUDINAL TIME COURSE

S. pyogenes strain H347^{lux} that was transformed with a chromosomally-integrated *luxABCDE* operon, was inoculated intranasally into FVB/n mice and imaged over a five day time course (Figure 5.3 A, n=6). In contrast to bacteria transformed with a replicating plasmid, H347^{lux} retained visible bioluminescent properties *in vivo* without antibiotic treatment. The bioluminescent signal obtained from the dorsal viewpoint was found to be much higher than that obtained from the ventral viewpoint. In the majority of mice, the signal declined to background levels by day four post inoculation (Figure 5.3 B), a decline that was matched by direct nasal samples that were taken daily (Figure 5.3 C). Throughout the experiment, 100% of the colonies tested remained bioluminescent and antibiotic resistant, demonstrating that the construct was stable even without antibiotic treatment.

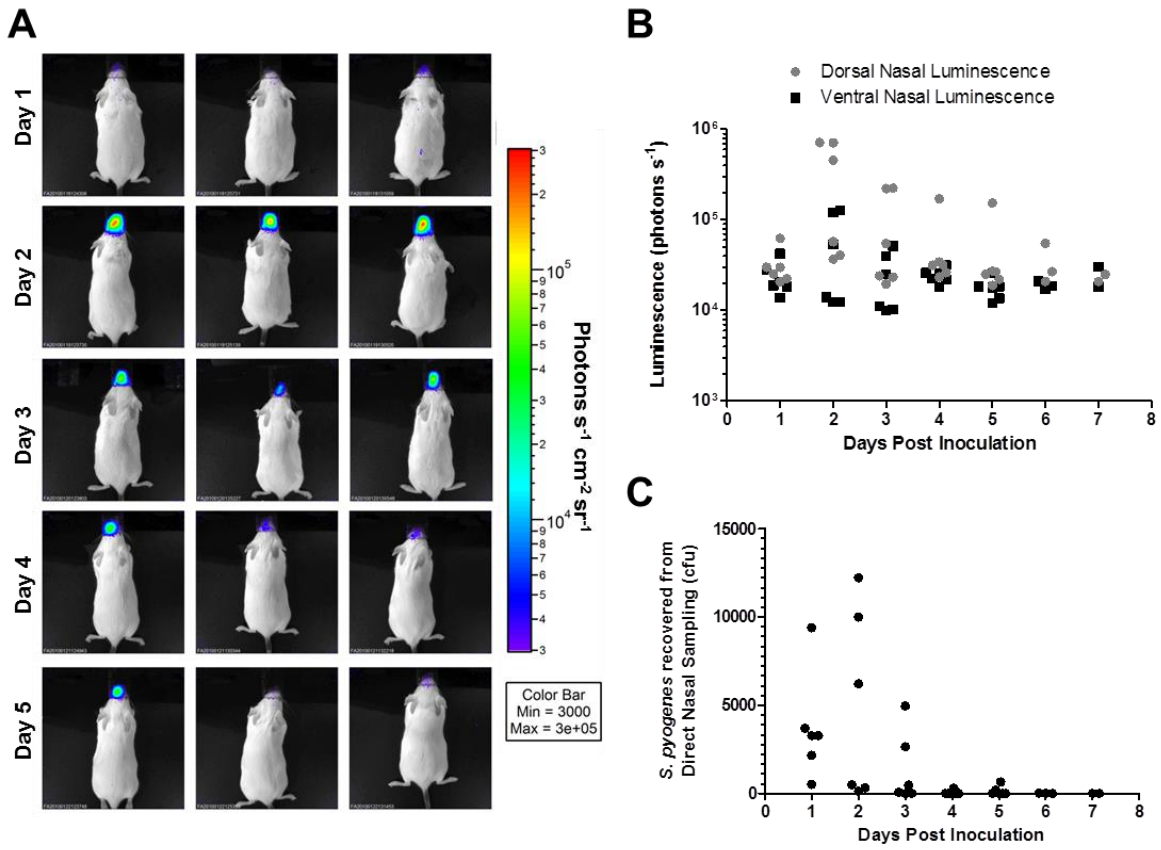


Figure 5.3. Imaging of S*. pyogenes* H347 with a stably integrated *lux* operon over a time course. Mice intranasally inoculated with *S. pyogenes* (H347^{lux}) were imaged over five days (A, three representative mice shown), and had luminescence from the nasal tract quantified from the dorsal and ventral viewpoints (B, n=6), alongside direct nasal samples that were taken daily (C, n=6). Data shown for individual mice.

5.2.4. CORRELATION OF BIOLUMINESCENT *S. PYOGENES* WITH THE BIOLUMINESCENT SIGNAL DETECTED FROM THE NASOPHARYNX

The bioluminescent signal from $H347^{lux}$ in the nasopharynx was quantified from the dorsal and ventral viewpoints. Nasal tracts were dissected out and total *S. pyogenes* numbers were quantified.

Bioluminescence data, mapped to lines determined by linear regression, demonstrating that the signal from the dorsal viewpoint was significantly higher than that obtained from the ventral viewpoint (Figure 5.4 A, n= 18, $r^2>0.95$, $p<0.05$). The surface luminescence from the dorsal viewpoint was 0.022 photons per CFU (± 2.864×10^{-4} SE), compared with 0.006 photons per CFU (±7.547×10^{-5} SE) obtained from the ventral viewpoint. Dissection revealed that the primary anatomical location of *S. pyogenes* during the first 3 days of nasal infection was within the ethmoturbinates (Figure 5.4 B). The luminescent signal was from a different location from the background luminescence, and much brighter.

The nasal associated lymphoid tissues (NALT) from each mouse, previously reported to be a major site for *S. pyogenes* infection, were imaged *ex vivo.* No correlation was found between the signal obtained from this organ and streptococcal numbers within it (Figure 5.4. C, Spearman correlation, $p>0.05$). In contrast, the bioluminescent signal from the *ex vivo* nasal tract correlated linearly to streptococcal numbers within it (Figure 5.4.D, $r^2>0.95$).

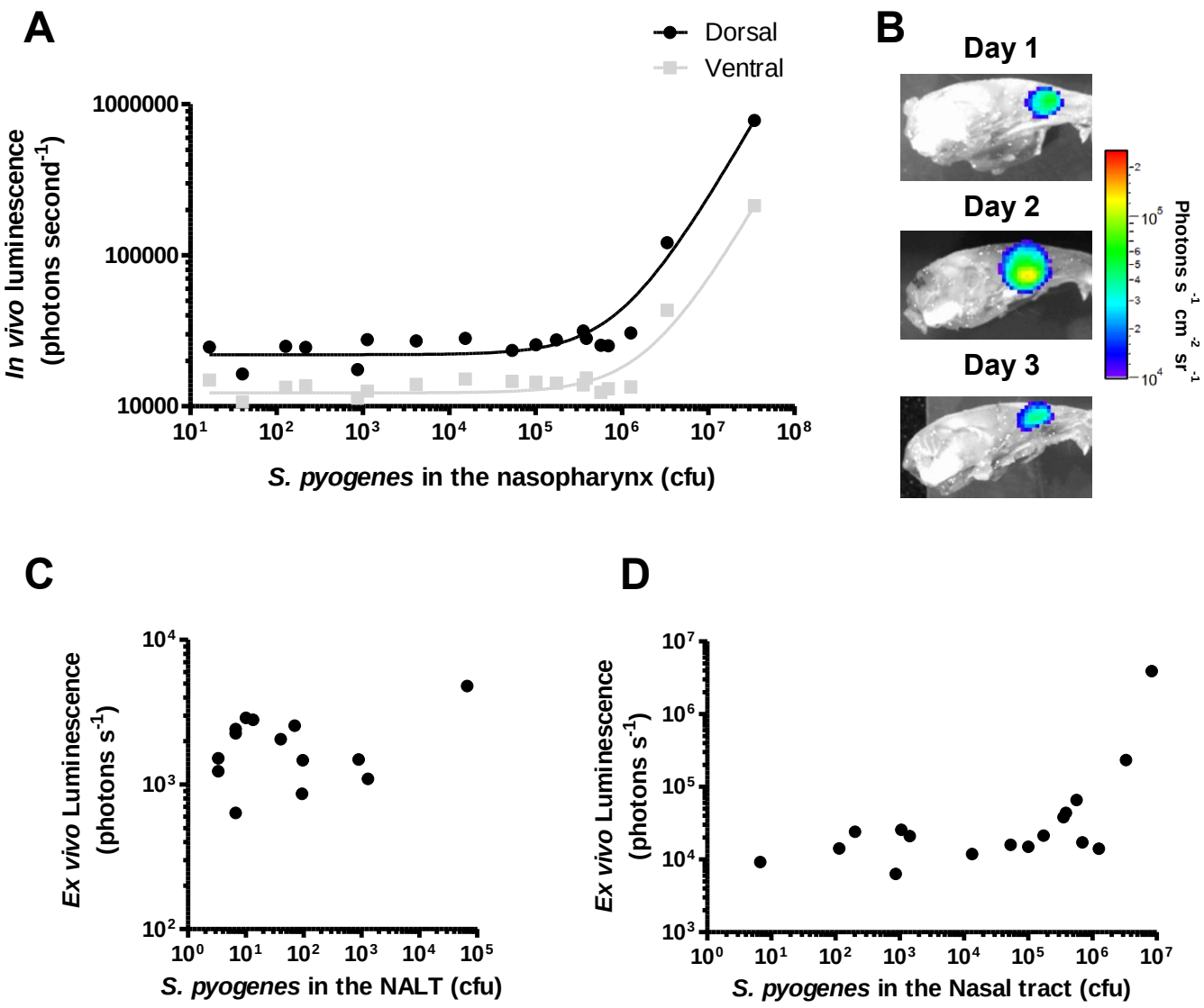


Figure 5.4. Correlation of bioluminescent signal to *S. pyogenes* numbers within the nasopharynx. Bioluminescence measurements from the dorsal and ventral viewpoints taken during an intranasal infection were compared to bacterial numbers obtained on dissection on the same day and a linear trend was fitted to the data using regression (A, r^2 >0.95, n=18). The nasal tract was extracted and imaged (B) NALT was extracted upon dissection and imaged, and the signal from this tissue was plotted against *S. pyogenes* obtained from this tissue (C). The nasal tract was also dissected out and imaged, and the bioluminescent signal from this tissue was plotted against the numbers of bacteria obtained from it (D).

5.2.5. THE EXPRESSION OF BIOLUMINESCENCE *IN VIVO* CONFERS A COMPETITIVE DISADVANTAGE IN THE NASOPHARYNX.

To determine if the site of integration of the *lux* construct (spy0535) was in itself harmful, a control strain was constructed that had an integrated plasmid at spy0535 but no bioluminescent operon ($H347^0$). A growth defect that was ascribed to bioluminescence expression had already been detected *in vitro* (Chapter 4).

Inocula containing pairwise mixes of H347, $H347^{lux}$ and $H347^0$ were administered intranasally to determine competitive survival *in vivo* (Figure 5.5 A). Mice were culled on days 1 and 3 post inoculation (n=4 per group per time point) and the nasal tracts were extracted for bacteriology. *S. pyogenes* recovered from these mice were tested for antibiotic resistance (Kanamycin, 500µg/ml) and luminescence production. The competitive indices were calculated for $H347^{lux}$ and $H347^0$ (Figure 5.5 B) and showed that $H347^{lux}$ was significantly attenuated over the time course compared to $H347^0$ (Two way ANOVA $p<0.05$). There was however no significant difference between H347 and $H347^0$, confirming that the chromosomal site of integration was not in itself harmful.

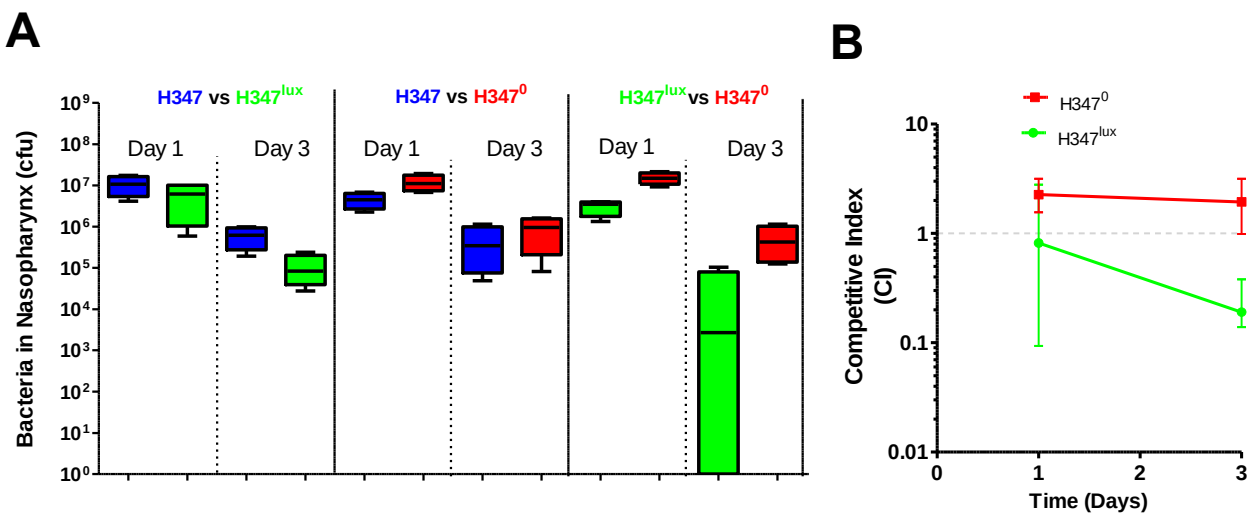


Figure 5.5. Bioluminescence confers *in vivo* growth defects. Mice were intranasally administered with mixed inoculation combinations of the bioluminescent strain ($H347^{lux}$), the wild type control (H347), and the spy0535 integrated control ($H347^{0}$). Mice were culled at day 1 post inoculation, and at day 3 and the relative abundance of each strain was assessed through replica plating onto selective media (A, n=8 per group). Based on these, the relative abundance of the bioluminescent strain and the spy0535 integrant were calculated relative to the wild type. (B) The bioluminescent strain was less competitive compared to the non-bioluminescent integrant.

5.2.6. BIOLUMINESCENT *S. PYOGENES* OCCASIONALLY CAUSES A SUPPURATIVE UPPER RESPIRATORY TRACT INFECTION

Mice intranasally infected with H347 ^{lux} were euthanised at days 3, 7, and 15 (n=3 per group per time point) and sagittal sections of the head, including the nasal cavity, nasopharynx and the brain were examined. At day 3 post inoculation, only one mouse out of three exhibited marked rhinitis, while on day 15, one mouse had mild rhinitis (Table 5.1.). *S. pyogenes* counts taken from each mouse nasopharynx revealed that *S. pyogenes* were present, even when no significant abnormality was detected. The inflammation caused by H347^{lux} was less than had been observed with the wildtype H347 (see Chapter 3.2.3).

Strain	Time					
	Day 3		Day 7		Day 15	
	Histology grade	Bacterial counts	Histology grade	Bacterial counts	Histology grade	Bacterial counts
H347^{lux}	-	796	-	520	-	5
	+++	10,000	-	10	-	0
	-	0	-	0	+	10,000

Table 5.1. Histopathological analysis of upper respiratory tract tissue from mice infected with bioluminescent *S. pyogenes*. At each of three time points, 3 mice per group, infected with H347^{lux} , were analysed histopathologically to determine the severity of infection and assigned a numerical designation. - = No significant abnormality, + =Mild , ++= Moderate, +++ = Marked, ++++ = Severe and ND= Non diagnostic sections. Bacterial counts from the same nasopharynx are also shown. This data was collected concurrently with the histopathological data shown in Table 6.2. Individual mice are shown on each row, for each time point.

5.2.7. THE EFFECT OF INTRANASAL INFECTION WITH STATIONARY VS EXPONENTIAL PHASE *S. PYOGENES*

S. pyogenes ($H347^{lux}$) grown to either stationary or exponential phases were concentrated into inocula. 10^8 CFU were dosed intranasally into FVB/n mice, which were then imaged over a 48 hour time course (Figure 5.6 A & B, n=6 per group, per time point). The bioluminescent signal obtained from the nasopharynx was compared to the bacterial numbers obtained on dissection using linear regression. The exponential phase *S. pyogenes* produced a significantly lower signal *in vivo* than bacteria used for infection whilst in stationary phase (Figure 5.6 C, $r^2 > 0.95$, $p<0.05$). Streptococcal counts from nasal tracts extracted over the 48 hour time course revealed that mice infected with *S. pyogenes* carried the bacterium less well where exponential phase inocula were used, than where stationary phase inocula were used (Figure 5.6. D).

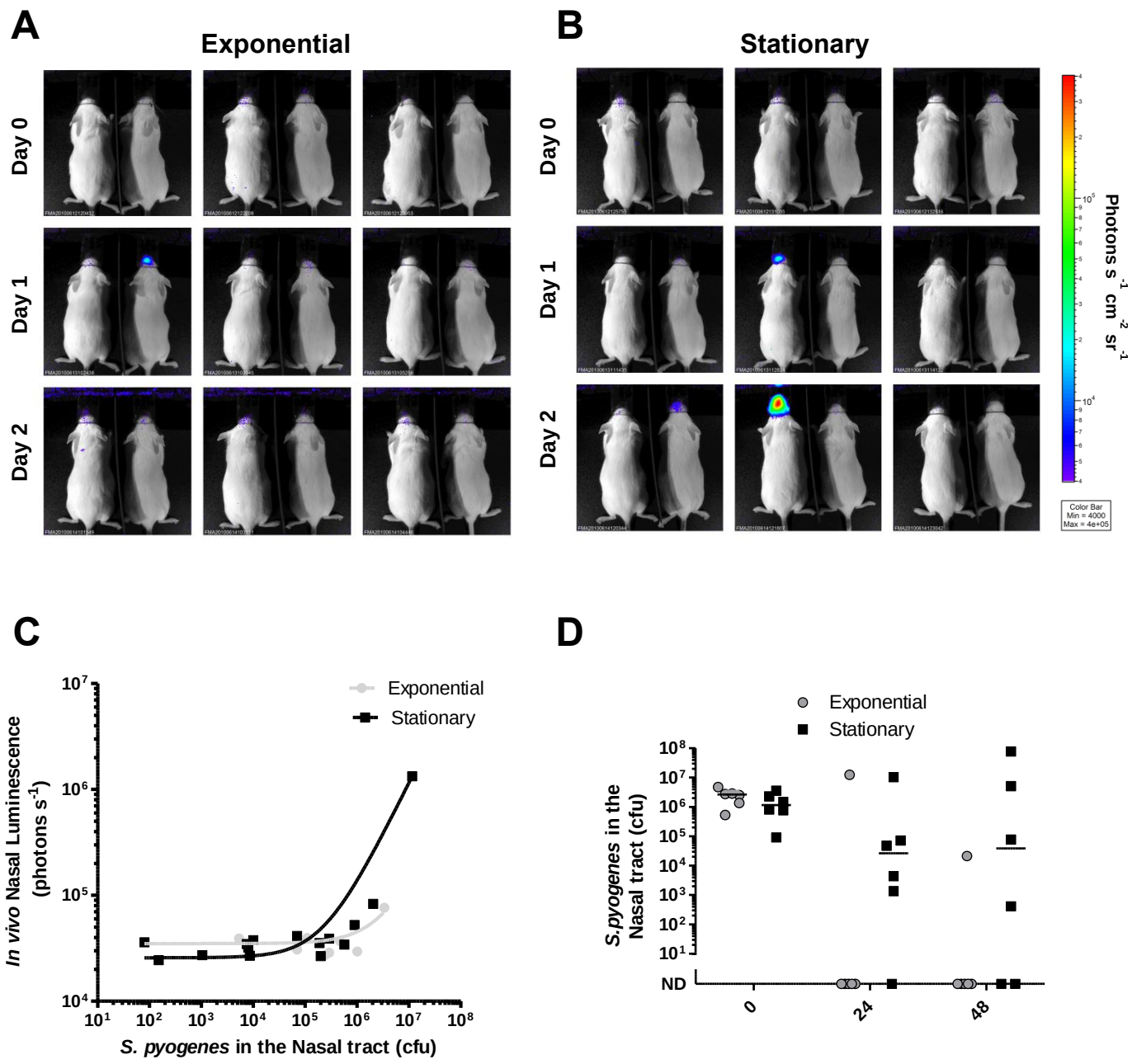


Figure 5.6. Biophotonic imaging of mice inoculated with either exponential or stationary phase grown *S. pyogenes*. Mice inoculated with bioluminescent *S. pyogenes* ($H347^{lux}$) in either the exponential (A) or the stationary phase (B) were imaged over 48 hr. The *in vivo* bioluminescence was compared to cfu present within the nasopharynx in both groups at all time points (C, r^2>0.95). The bacterial numbers obtained on dissection from each group over the time course were enumerated for each day (D). Data shown for individual mice.

5.3. DISCUSSION

A number of different factors need to be considered when examining streptococcal infection using bioluminescence in an *in vivo* situation. The first consideration for this model is the natural background luminescence exhibited by living organisms. A previous study discovered a signal emanating from the nasopharynx [251]. The control mice imaged in this study also exhibited luminescence from the nasopharynx, and this luminescence was stronger from the dorsal viewpoint compared to the ventral viewpoint, suggesting the source of the luminescence was closer to the dorsal surface of the mouse. Dissection of the mouse heads confirmed that the source of this background bioluminescent signal was towards the anterior portion of the nasopharynx. The actual tissue causing this bioluminescent signal could not be determined within this study, but was important to take into consideration given the likely reduction in sensitivity of bioluminescence imaging for the detection of bioluminescent *S. pyogenes* in the nasopharynx.

In the preceding chapter, two bioluminescent derivatives of the *S. pyogenes* clinical throat isolate H347 were characterised. The H347^{pTHLK} isolate carrying a replicating plasmid was more bioluminescent *in vitro*, but the plasmid was unstable. The regular application of antibiotics failed to maintain the plasmid, and the expression of bioluminescence, *in vivo*. *S. pyogenes* expressing *luxABCDE* from the integrated construct, H347^{lux}, was found to express bioluminescence for up to five days post inoculation, and paradoxically produced a higher signal *in vivo*. Therefore, the H347^{lux} strain was used for further characterisation studies.

The luminescent signal expressed by H347^{lux} *in vitro* was found to be around 1 photon per CFU (see Chapter 4.2.4). The surface bioluminescence measured *in vivo* however

was lower, due to the attenuation of the signal as it travels through the tissue. The signal detected *in vivo* was found to be approximately 0.022 photons per CFU when taken from the dorsal viewpoint, and 0.006 from the ventral view. This equates to approximately a 50-fold reduction in signal when collected from the dorsal viewpoint, and an approximate hundred fold reduction when collected from the ventral viewpoint. The presence of the jaw obscures the pathway of light from the nasopharynx when images are taken from the ventral viewpoint, causing a greater degree of absorption and scattering than from the dorsal viewpoint, in which only the skull skin and fur obstruct the passage of light.

Previous reports using bioluminescence to study *S. pyogenes* suggested that the primary site of *S. pyogenes* colonisation in mice was within the NALT [216]. However for H347, a clinical isolate, the primary point of infection was within the caudal nasal tract, in the ethmoturbinates (Chapter 3.2.4). Bioluminescence imaging of the nasopharynx revealed that this was the primary point of colonisation for the bioluminescent H347^{lux} strain as well. Although earlier studies identified the NALT as harbouring *S. pyogenes*, the reports did not described any consistent attempt to identify *S. pyogenes* in other tissues of the upper respiratory tract.

NALT did not produce any bioluminescent signal that correlated with the presence of *S. pyogenes*. However, the bioluminescent signal from dissected nasal tissue produced a much higher bioluminescent signal that did correlate to the presence of *S. pyogenes*, providing further evidence that this was the primary site of colonisation.

Previous work (see Chapter 4.2.3 & 4.2.6) demonstrated that the expression of bioluminescence confers a growth cost *in vitro.* These growth costs contributed to a lack of competitiveness of the H347^{lux} strain in the nasopharynx with respect to the wild

type (H347) and its isotypic control ($H347^0$). Furthermore, the disease caused by the bioluminescent strain was less severe than that of the wild type (Chapter 3.2.4) with the majority of infected mice not showing inflammation over a long term time course.

The metabolic state of *S. pyogenes* influenced its bioluminescence expression *in vitro,* with the brightest signal being obtained whilst it was in its exponential phase of growth. However, infecting mice with *S. pyogenes* in exponential phase did not result in an increased luminescent signal immediately after infection. Furthermore, mice infected with *S. pyogenes* in the exponential phase tended to clear it more quickly than mice infected with *S. pyogenes* in stationary phase.

The primary focus of this chapter was to define the limits of bioluminescence imaging *in vivo*. The background bioluminescent signal exhibited by the FVB/n mice impacted on the sensitivity of this technique. The expression of bioluminescence by *S. pyogenes* exerted fitness costs *in vivo*. This contributed to the instability of the pTHLK plasmid *in vivo*, decreased competitiveness in the $H347^{lux}$ strain and its reduced invasiveness relative to the wildtype. These factors are essential to consider in all studies utilising recombinant bacteria that express bioluminescence. Taken together, the data suggest that $H347^{lux}$ could be used for shorter (<5 day) BPI studies involving nasopharyngeal infection to address therapeutic or vaccination studies where bacterial clearance is being measured

CHAPTER 6: IMPACT OF *COVR/S* MUTATION ON NASOPHARYNGEAL *S. PYOGENES* INFECTION AND TRANSMISSION

6.1 INTRODUCTION

The survival of *S. pyogenes* during invasive infection is dependent on the expression of virulence factors. The two component regulator CovR/S represses a variety of virulence factors concerned with resistance to neutrophil mediated killing such as hyaluronic acid capsule, DNase and SpyCEP [45,49,78,91,96]. Mutations in *covR/S* de-repress these virulence genes, which can confer a selective advantage to *S. pyogenes* in mouse models of invasive infection, leading to greater mortality [96,288].

Although naturally occurring mutations in *covR/S* have been described among invasive clinical *S. pyogenes* strains, in particular of the *emm1* type, the impact of such mutations on nasopharyngeal infection, and hence transmission in the community and the clinical setting, is unclear.

The role of *covR/S* mutations in the nasopharynx have not been well characterised experimentally, in part due to a paucity of available animal models. In chapter 3, one such model was devised using a clinical *emm75* pharyngitis isolate H347. In previous work, an isogenic derivative of H347 was constructed that had undergone inactivation of *covR/S* by insertion mutagenesis [45]. This *covR/S* mutant (designated strain H494) produced markedly higher levels of SpyCEP compared to wild type H347 [45]. In this chapter the effects of changing *covR/S* expression were investigated with regard to *S.*

pyogenes persistence in the nasopharynx and transmission using the tools devised in the preceding chapters.

6.2. RESULTS

6.2.1 THE *IN VITRO* CHARACTERISATION OF A *COVR/S* MUTANT

The CovR/S regulatory system promotes the repression of up to 15% of the *S. pyogenes* genome, but paradoxically promotes the expression of cysteine protease SpeB [289]. Therefore, the SpeB production by the *covR/S* mutant (H494) should be impaired compared to the parental strain if *covR/S* has been fully inactivated. To determine if H494 demonstrated the predicted phenotype, supernatants taken from *S. pyogenes* cultures grown to early log, mid log, late log and stationary phase were analysed for SpeB production (Figure 6.1). The wild type *S. pyogenes* (H347) produced higher levels of SpeB at all time points compared to the *covR/S* mutant (H494). This did not reflect a general loss of fitness in H494, since this strain produced far more SpyCEP than the wildtype [45].

Strains of *S. pyogenes* with mutations in *covR/S* have, in previous studies, shown defects in biofilm formation [97]. To confirm this finding for the *emm*75 *S. pyogenes* isolate used, crystal violet biofilm binding assays were performed as described previously (Chapter 4.3.4) to determine the presence of adherent bacteria within biofilms (Figure 6.2 A). To ensure that the difference observed was not due to a growth defect (as was observed in Chapter 4.2.), the supernatants were also collected to assess the percentage of adherent bacteria within each well (Figure 6.2. B). The *covR/S* mutant not only produced less biofilm, but also produced less as a percentage of the bacteria present, suggesting that the biofilm forming capacity is specifically impaired.

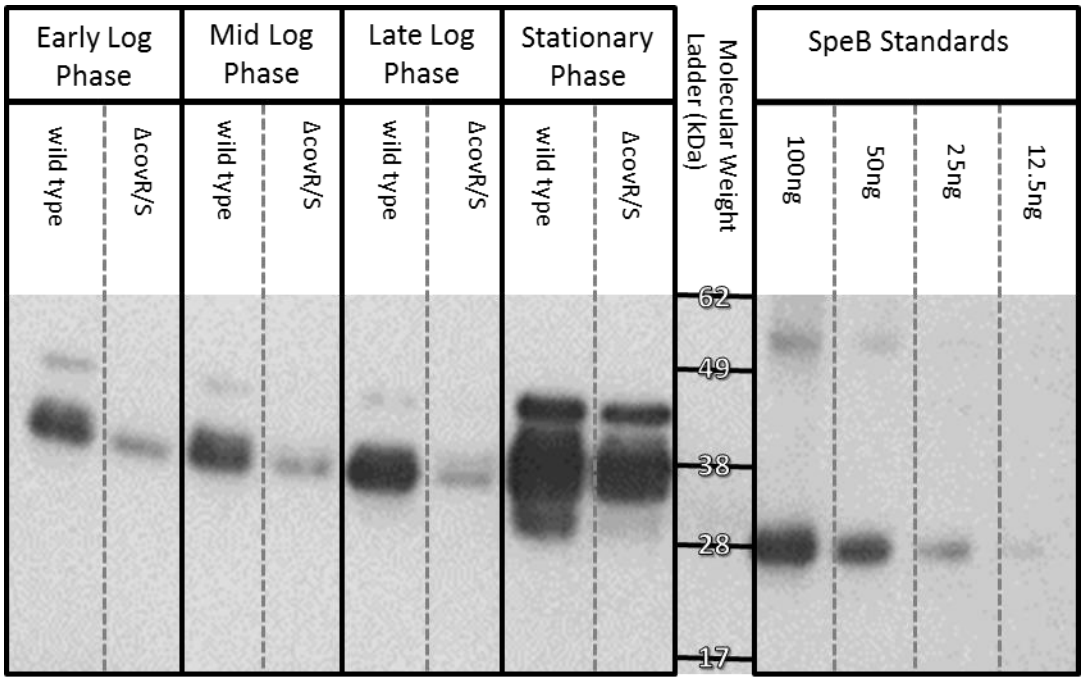


Figure 6.1 Inactivation of CovR/S results in loss of cysteine protease SpeB expression. Western blot analysis for SpeB in the culture supernatant from the wild type *emm75 S. pyogenes* isolate H347 and *ΔcovR/S* (H494) grown to early-log, mid-log, late log and stationary phase cultures revealed a difference in SpeB expression. *ΔcovR/S* consistently produced less SpeB than the wild-type strain. Purified recombinant SpeB (28kDa domain) standards are shown for reference.

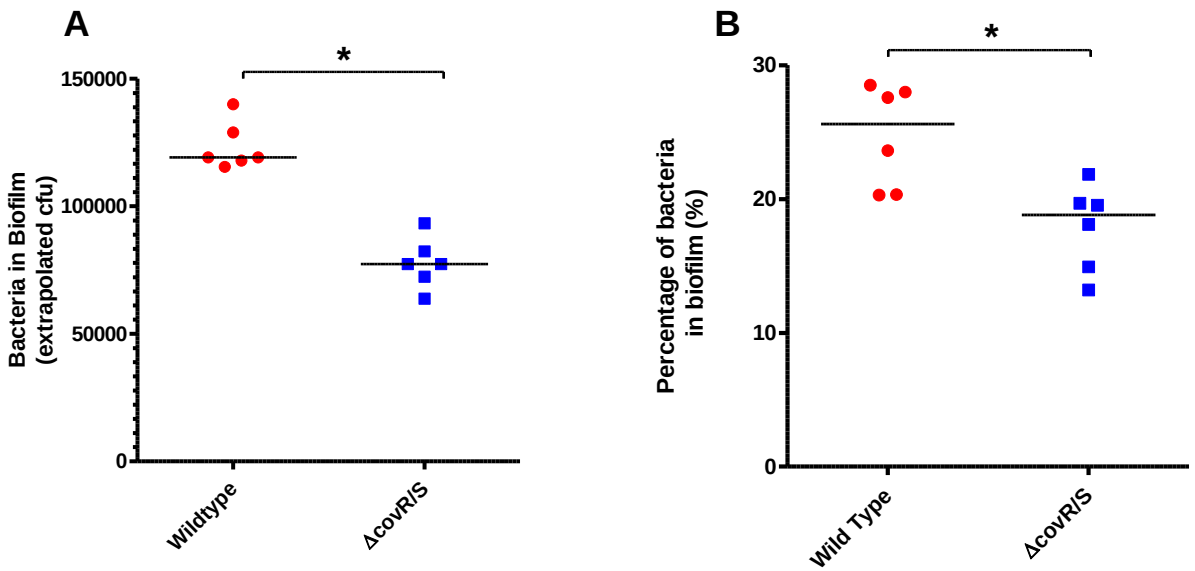


Figure 6.2. Biofilm formation is affected by the loss of CovR/S regulation. Bacteria grown in stationary cultures were incubated for 24 hrs in C-media. There were significantly less *ΔcovR/S S. pyogenes* (H494) present in biofilms compared to the wild type (H347) (A). The percentage of *S. pyogenes* adhered in biofilms as a percentage of total bacteria present was also reduced, demonstrating that this difference was not due to any specific growth defect caused by the mutation (B). Data shown for individual wells with median indicated.

6.2.2 CovR/S mutation confers enhancement of virulence in an invasive model of *S. pyogenes* infection.

To ensure that the *covR/S* mutation conferred an invasive phenotype during invasive streptococcal infection, groups of mice were infected either with the wild type H347 strain or the *covR/S* mutant (H494) intramuscularly into the gastrocnemius muscle (n=12 per group). There was no quantitative difference between isogenic *S. pyogenes* strains cultured from the muscle after 72h (Figure 6.3.A). Whilst fewer wild type H347 disseminated to the Liver (Figure 6.3 C) and the Spleen (Figure 6.3 D) compared to the *ΔcovR/S* strain, the difference was not significant. However the Δ*covR/S* strain did disseminate to the ipsilateral inguinal lymph node in greater numbers than its wild type counterpart (Figure 6.3.B, $p<0.05$ Mann-Whitney). This confirmed that Δ*covR/S* strain was, as expected, more invasive than the wild type strain, due to increased expression of invasive virulence factors.

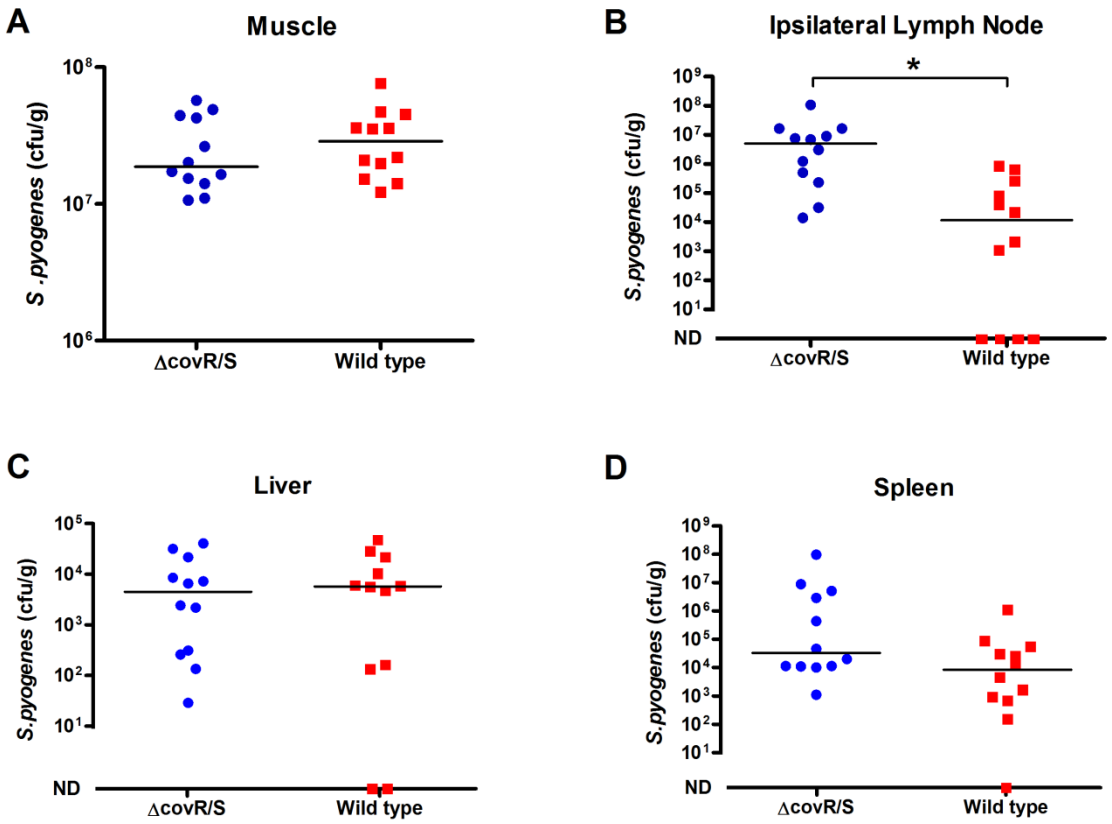


Figure 6.3. The loss of virulence factor regulation aids bacterial dissemination in invasive infection. FVB/n mice (n=12) were inoculated intramuscularly into the right thigh with either wildtype *S. pyogenes* strain (H347) or the *covR/S* mutant (H494). After three days there was no significant difference in growth within the thigh (A), but there was a significant difference in bacterial numbers in the ipsilateral inguinal lymph node (Mann Whitney U $p<0.05$) (B). No significant difference was found in the numbers of bacteria disseminating to the Liver (C) and the Spleen (D) Data shown for individuals with median indicated.

6.2.3. MUTATION OF *COVR/S* IS DETRIMENTAL TO LONG TERM *S. PYOGENES* COLONISATION IN THE NASOPHARYNX.

To determine whether the phenotype conferred by *covR/S* mutation is beneficial during *in vivo* infection in the nasopharynx, two groups of mice (n=20) were infected intranasally with 10^8 CFU of either H347 or H494 in 5 µl and observed over 21 days. Survival curves based on daily nasal samples demonstrated that the *covR/S* mutant H494 was shed from the nasopharynx for a shorter length of time compared to its wild type counterpart. (Figure 6.4 A, Mantel Cox Logrank $p<0.05$). The duration of continuous shedding was determined to have terminated upon the first negative sample. However, as was seen previously (Chapter 3.2.2) this was followed by a period of intermediate shedding, where *S. pyogenes* numbers were either too low to be detected, or mice became re-infected. When the end point of this stage was used to define the end point of infection, a significant difference was still observed between the two groups (Figure 6.4 B Mantel Cox Logrank, $p<0.05$). The raw data from the nasal samples is represented by heat maps (See Appendix 6.1.). Taken together, data confirmed that the *covR/S* mutant strain H494 was carried less well in the nasopharynx than an isogenic wild type parental strain H347.

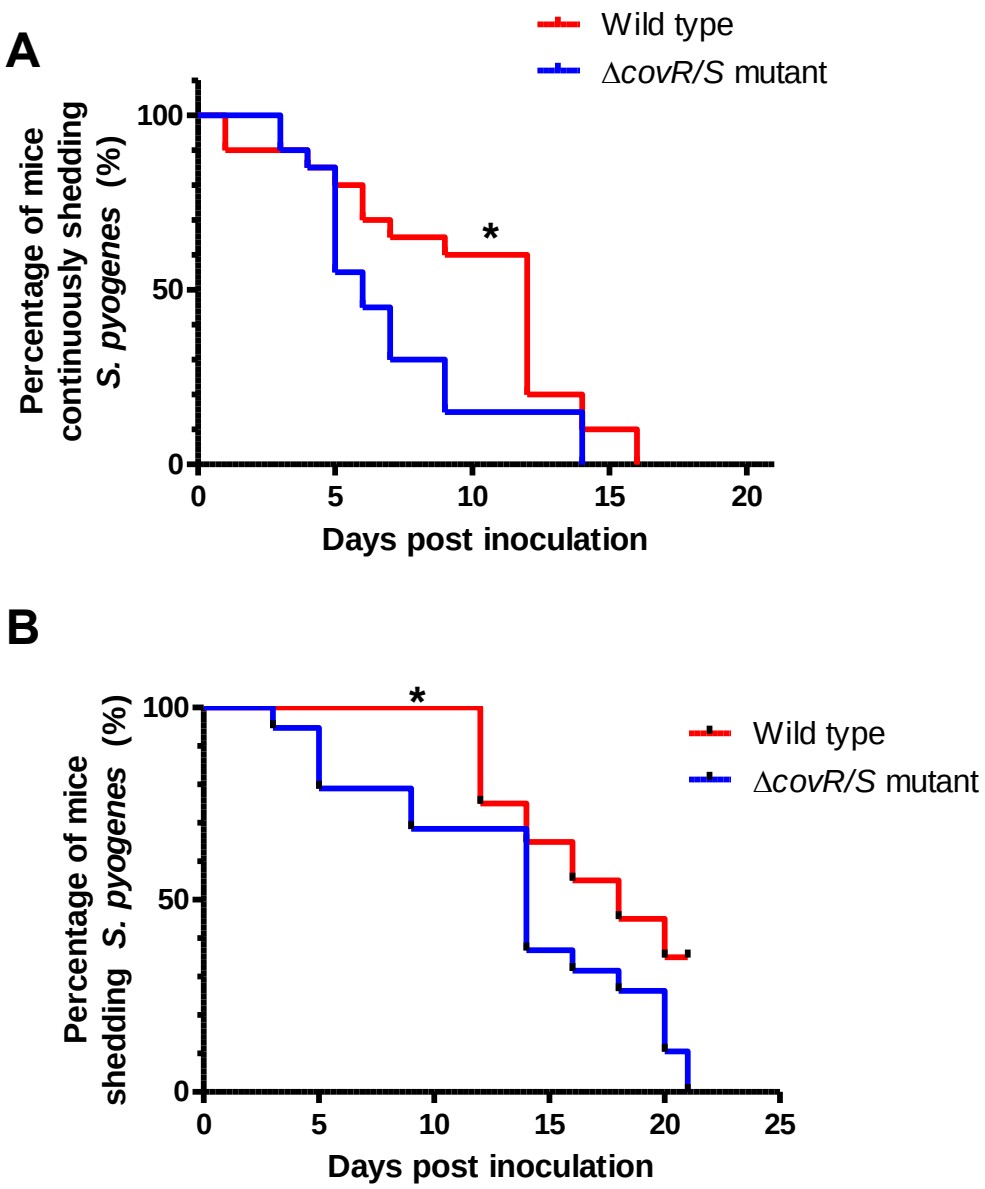


Figure 6.4. Nasopharyngeal infection is adversely affected by *covR/S* mutation. FVB/n mice were inoculated intranasally with either the wild type, or the Δ*covR/S* strain (n=20 per group). To determine the duration of shedding, direct nasal samples were taken over a 21 day period. The duration of continuous shedding was plotted based on the first negative nasal sample (A) and the total duration of shedding was determined based on the last positive nasal sample (B). The wild type strain was shed over a significantly longer time period than the Δ*covR/S* strain based on both criteria. (Logrank Mantel Cox $p<0.05$).

6.2.4. *S. PYOGENES* WITH A *COVR/S* MUTATION CAN CAUSE AN ATTENUATED SUPPURATIVE UPPER RESPIRATORY TRACT INFECTION.

To better understand any differences between nasopharyngeal infection caused by the wild type and Δ*covR/S* strains, mice were intranasally infected with the *covR/S* mutant (Figure 6.5) and then euthanised at days 3, 7, 14 and 21 (n=3 per group per time point);sagittal sections of the head, including the nasal cavity, nasopharynx and brain were examined.

These mice demonstrated inflammatory changes affecting the nasal cavity over the first week of infection, particularly in the ethmoturbinate region, which had been demonstrated previously as the primary site of *S. pyogenes* infection within the nasopharynx.

Mice infected with the *S. pyogenes covR/S* mutant H494 demonstrated mild to marked suppurative rhinitis at days 3 and 7 post inoculation. However by day 14 the majority of mice had normal nasal mucosa, and at day 21, the mice infected with H494 had normal nasal mucosa or showed only mild inflammation (Table 6.1) despite still carrying *S. pyogenes*. The inflammation seen in mice infected with H494 was however less severe and less protracted than the inflammation caused by the wild type strain H347 alone (See Chapter 3.2.3). The differences seen between these two strains with regard to pathology were consistent with what was observed with regard to the bacterial load.

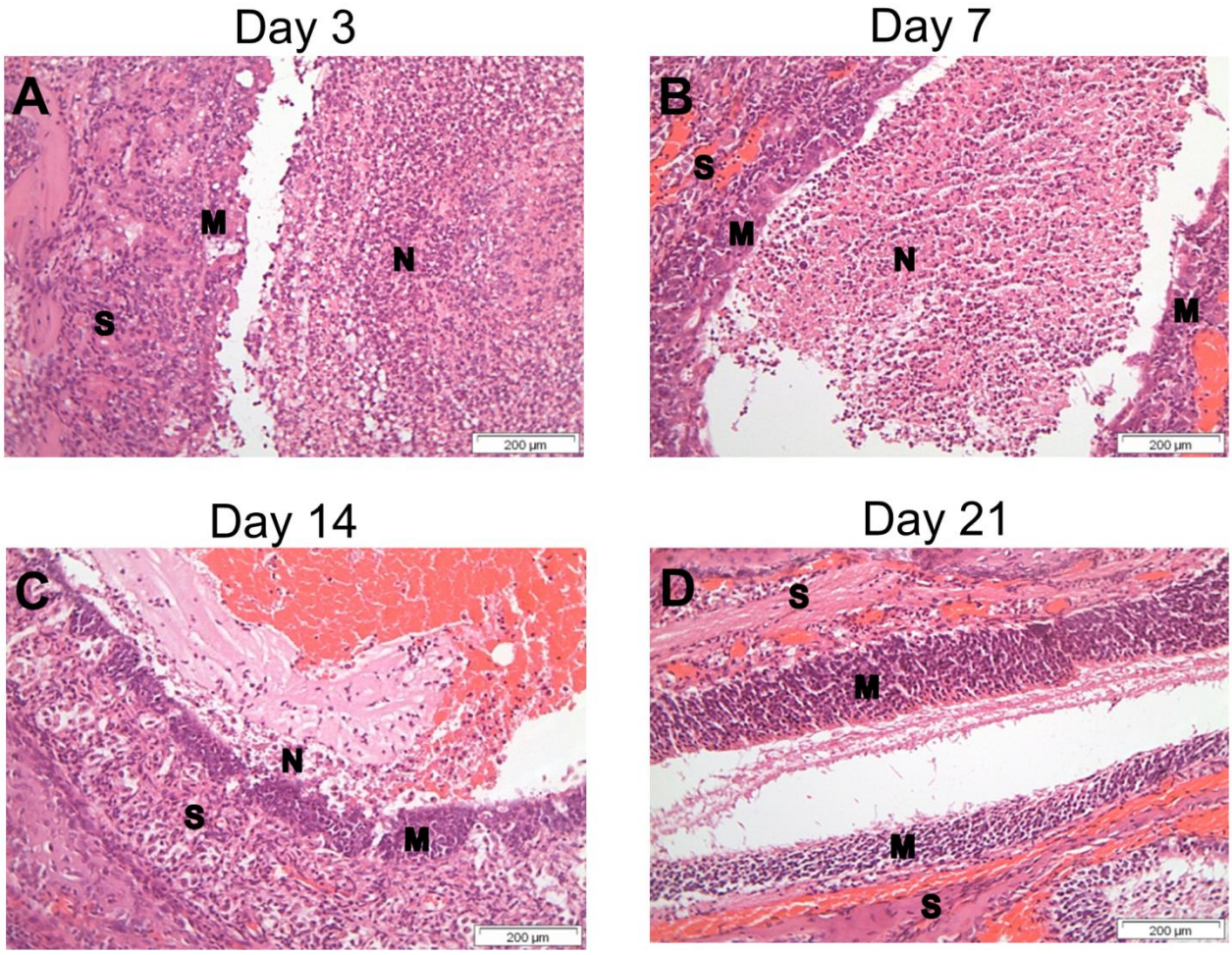


Figure 6.5. Histopathological analysis of the ethmoturbinates during nasal infection. Nasal tissues from mice infected with a *covR/S* mutant of *S. pyogenes* (H494) (n=3 per group) were taken at days 3, 7, 14 and 21 after inoculation (Haemotoxylin & Eosin staining). **N** = Neutrophilic Exudate, **M**= Nasal mucosa, **S**= Nasal stroma. Scale bar as shown. Damage to the nasal mucosa with surface neutrophilic exudate was apparent at day 3 post inoculation (A) This exudate was still present at day 7 (B) At day 14 the inflammation had begun to resolve (C). By day 21, the no abnormality was observed in the nasal mucosa (D). Representative sections from single mice are shown. Semi quantitative results are shown in Table 6.1. This experiment was performed concurrently with the histopathological data shown in Figure 3.3.

	Time							
	Day 3		Day 7		Day 15		Day 21	
Strain	Histology grade	Bacterial counts	Histology grade	Bacterial counts	Histology grade	Bacterial counts	Histology grade	Bacterial counts
H494	+	45,000	+++	1,000	-	2	ND	0
	+	31,000	++	12,000	-	242	+	0
	+++	25,000	++	2,000	++	84	-	0

Table 6.1. Histopathological analysis of upper respiratory tract tissue from mice infected with the *covR/S* mutant H494. At each of four time points**,** 3 mice per group, infected with the Δ*covR/S* strain, were analysed histopathologically to determine the severity of infection and assigned a numerical designation. - = No significant abnormality, + =Mild , ++= Moderate, +++ = Marked, ++++ = Severe and ND= Non diagnostic sections. This experiment was performed concurrently with the histopathological data shown in Table 3.1.

6.2.5. INVESTIGATION OF *covR/S* MUTATION USING BIOLUMINESCENCE:

INTENSITY OF INFECTION IN NASOPHARYNX AND LUNGS

A bioluminescent derivative of the *ΔcovR/S* strain was developed through the integration of the pICL18^{lux} plasmid into the spy0535 region of the H494 chromosome to create H494^{lux}. Mice were infected intranasally with either H347^{lux} or H494^{lux}, to determine whether any differences conferred by the *covR/S* mutation could be observed using bioluminescence imaging (Figure 6.6 A & B). Mice were infected with either 5 µl to deposit bacteria within the nasopharynx (n=3 per group, per time point), or 20 µl to trigger a pulmonary infection (n=3 per group, per time point). It should be noted that one of the mice infected with 20 µl of the *covR/S* mutant H494^{lux} reached a humane end point and had to be culled before it could be imaged. No significant difference was found between bioluminescent signals for each strain within in the nasopharynx (Figure 6.6. C, r^2 >0.95). This finding was confirmed using traditional quantitative bacteriology. Indeed, no significant difference was observed between the carriage of H347^{lux} and H494^{lux} in the nasopharynx in mice infected with 5 µl (Figure 6.6. D), or in the lung, in groups infected with 20 µl (Figure 6.6. E) These results contrasted with those obtained when comparing non-bioluminescent *S. pyogenes* wild type and *covR/S* mutant strains.

Mice that were administered 20 µl inocula were imaged from the ventral viewpoint to examine the lung (Figure 6.7 A). However, a signal was only visible from the lungs of one mouse in the group infected with the wild-type derived strain, H347^{lux}. One of the mice infected with the bioluminescent Δ*covR/S* strain, H494^{lux} demonstrated multiple regions to which bacteria had disseminated on imaging (Figure 6.7. B). Dissection revealed that the inguinal lymph nodes were amongst the regions affected, and bacteriology revealed the presence of *S. pyogenes*. However, such events were

sporadic and not statistically significant. Interestingly, one of the mice infected with H347^{lux} showed colonisation originating from the genital tract.

Overall, there was no quantitative difference in *S. pyogenes* infection of the nasopharynx or the lung between the bioluminescent derivatives H347^{lux} and H494^{lux} despite differences in functional *covR/S*, in contrast to findings for the non-bioluminescent strains H347 and H494.

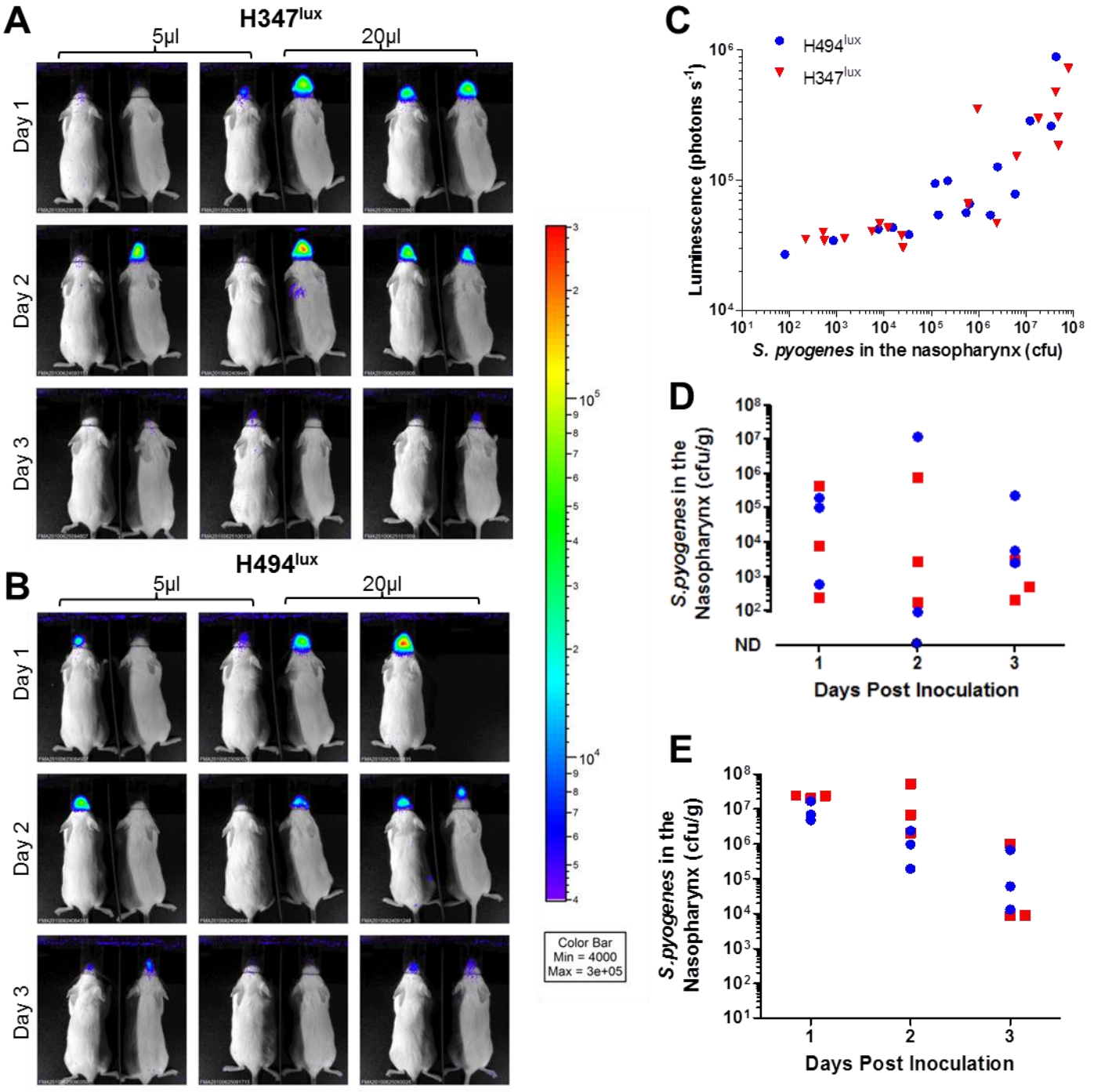


Figure 6.6. Imaging of a bioluminescent *covR/S* mutant during nasopharyngeal infection. Mice were infected with 5 µl or 20 µl of either the H347^{lux} or the H494^{lux} then were imaged for three days post inoculation (A & B, n=3 mice per treatment group, per time point). The bioluminescent signal obtained from the dorsal view was correlated to the numbers of *S. pyogenes* present on direct culture of nasal tissues for both strains at all time points (C, $r^2 > 0.95$). The colony counts from the nasopharynx of mice infected with 5µl (D) and 20µl (E) showed no significant difference in bacterial numbers between strains. Data shown for individual mice.

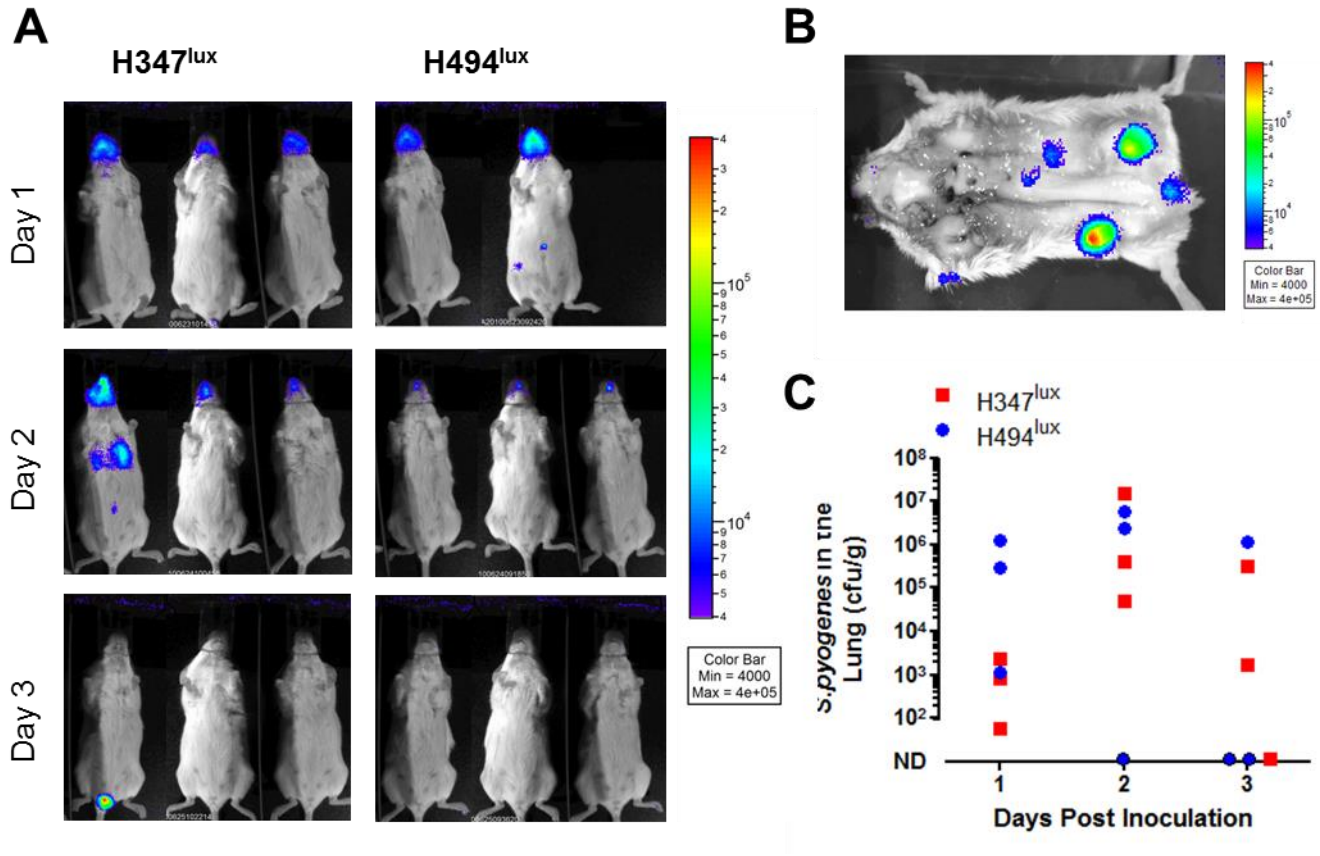


Figure 6.7. Imaging of a bioluminescent c*ovR/S* mutant during intrapulmonary infection. Mice were infected with 20 µl of either the H347^{lux} or the H494^{lux} were imaged for three days post inoculation (A, n=3 mice, per group, per time point). One mouse infected with H494^{lux} showed dissemination to a variety of areas, including the inguinal lymph nodes, which were positive for *S. pyogenes* upon dissection on day 1 post inoculation (B). The colony counts from the lungs of mice infected with 20µl showed no significant difference in *S. pyogenes* carriage between strains (C). Data shown for individual mice.

6.2.6. *CovR/S* MUTATION MAY PARTIALLY COMPENSATE FOR GROWTH DEFECTS CONFERRED BY BIOLUMINESCENCE DURING LONG TERM *S. PYOGENES* COLONISATION IN THE NASOPHARYNX.

The bioluminescent derivatives of the wild type and *covR/S* mutant ($H347^{lux}$ and $H494^{lux}$, respectively) were infected intranasally and compared with regard to streptococcal shedding over a 15 day time course.

In contrast to results obtained when comparing non-bioluminescent strains, the duration of continuous shedding for the Δ*covR/S* $H494^{lux}$ strain was significantly longer than that for the $H347^{lux}$ strain (Figure 6.8 A, Mantel Cox Logrank $p<0.05$). However, when looking at the total duration of shedding (Figure 6.8 B) there was no significant difference between the groups. Mice from each group had the nasopharynx dissected at Days 3, 7 and 15 post-inoculation, and demonstrated no significant difference in bacterial counts between these groups (Figure 6.8.C).

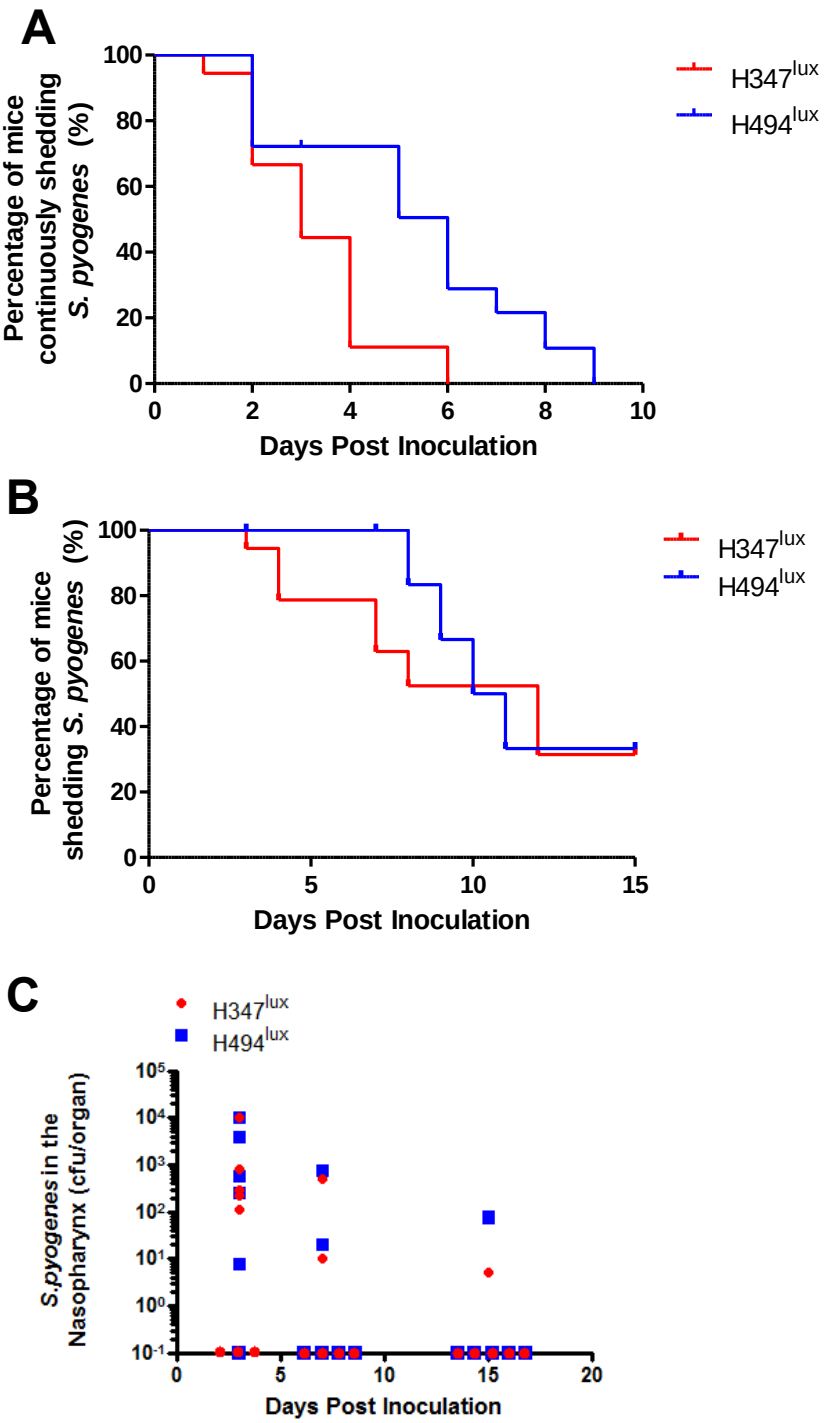


Figure 6.8. Expression of bioluminescence alters the impact of *covR/S* mutation. FVB/n mice were inoculated intranasally with either H347^{lux} or H494^{lux} (n=18 per group). To determine the duration of shedding, direct nasal samples were taken over a 15 day period. The period of continuous shedding for the H494^{lux} strain was significantly longer than for H347^{lux} (A, Mantel Cox Logrank $p<0.05$). However, for the total period of shedding, there was no significant difference between the strains (B). *S. pyogenes* in the nasopharynx were enumerated from mice dissected on Day 3, Day 7 and Day 15 (C).

6.2.7. BIOLUMINESCENT Δ*COVR/S S. PYOGENES* CAUSES A SUPPURATIVE UPPER RESPIRATORY TRACT INFECTION

Mice intranasally infected with H494^{lux} were euthanized at days 3, 7, and 15 (n=3 per group per time point) and sagittal sections of the head, including the nasal cavity, nasopharynx and the brain were examined (Table 6.2). Bacterial counts taken from each mouse nasopharynx revealed that bacteria were present, even when no significant abnormality was detected. Interestingly even when bacteria had cleared, the inflammation did not fully resolve. The inflammation observed in this strain was less severe than the non-bioluminescent H494 isolate (Table 6.1), but paradoxically was greater than the H347^{lux} strain (Table 5.1). As bioluminescence expression appeared to confound the impact of *covR/S* mutation, further experiments that examined virulence traits and CovR/S excluded the use of bioluminescent strains.

	Time					
	Day 3		Day 7		Day 15	
Strain	Histology grade	Bacterial counts	Histology grade	Bacterial counts	Histology grade	Bacterial counts
$H494^{lux}$	+++	10,000	-	0	+	0
	+	92	-	83	+	0
	+	596	+	732	+	77

Table 6.2. Histopathological analysis of upper respiratory tract tissue from mice infected with a bioluminescent Δ*covR/S S. pyogenes* strain ($H494^{lux}$). At each of four time points**,** 3 mice per group, infected with the *emm*75 Δ*covR/S* strain $H494^{lux}$, were analysed histopathologically to determine the severity of infection and assigned a numerical designation. - = No significant abnormality, + =Mild , ++= Moderate and +++ = Marked. This experiment was performed concurrently with the histopathological data shown in Figure 5.1.

6.2.8. *CovR/S* MUTATION IS DETRIMENTAL TO THE TRANSMISSION OF *S. PYOGENES* IN A MOUSE MODEL.

Mice infected with either the wildtype (H347) or the *covR/S* mutant (H494) strains were introduced into cages at a D:R ratio of 3:5 to determine whether the expression of virulence factors has an effect on transmission. To eliminate the effects of passive inoculum transfer, mice were separated for six hours after inoculation. Direct nasal samples taken from recipient mice revealed that transmission occurred more frequently from donors carrying the wild-type strain than from the *covR/S* mutant (Figure 6.9. A, AUC analysis with Mann Whitney U $p<0.05$). Settle plates incubated in each cage detected no significant difference in airborne *S. pyogenes* (Figure 6.9 B). However, in previous studies the differences in burden of colonisation between mice infected with the *covR/S* mutant and the wild type manifested after three days, and may have accounted for the observed difference in transmission.

To eliminate this potential confounding factor, mice were observed over a shorter time course of three days. A power calculation was used to determine the correct experimental numbers to allow for the detection of differences in transmission, and aerosolisation at this stage of infection. The transmission of the wild type strain to recipient mice was significantly higher than the transmission of the Δ*covR/S* strain (n=24 at a D;R ratio of 3:5, Figure 6.10.A, AUC analysis, with Mann Whitney U $p<0.05$). However, the settle plates revealed no significant difference between the levels of airborne wildtype *S. pyogenes* H347, or the Δ*covR/S* strain H494 (Figure 6.10 B).

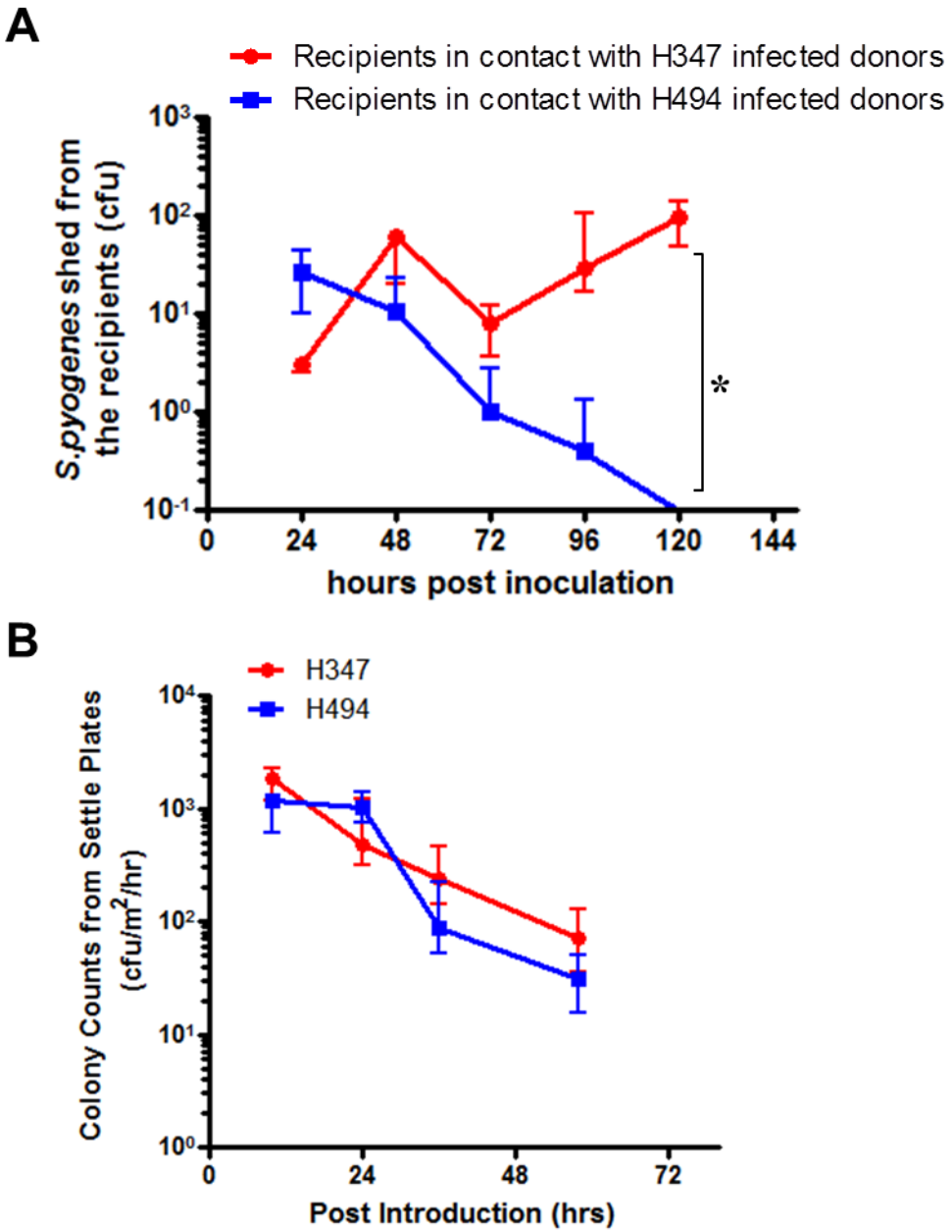


Figure 6.9. Transmission of S. pyogenes is hampered by the loss of covR/S regulation Naïve recipients co-mingled at a D:R ratio of 3:5 with mice infected with either the wild type strain or the Δ*covR/S* mutant and sampled for five days after the introduction of the donor mice. (n=5 recipients per group). Donor mice had >5000 cfu recovered from direct nasal sampling throughout the experiment. Donor mice infected with the H494 Δ*covR/S* mutant transmitted significantly less well to recipients compared to the H347 wild type strain (AUC analysis, followed by Mann-Whitney U test). Data from settle plates taken from the first 58 hours after introduction revealed that there were no significant differences in the bacteria deposited on the surface of the plates by mice infected with the wild type, or the Δ*covR/S* mutant (B) Error Bars indicate median and interquartile range

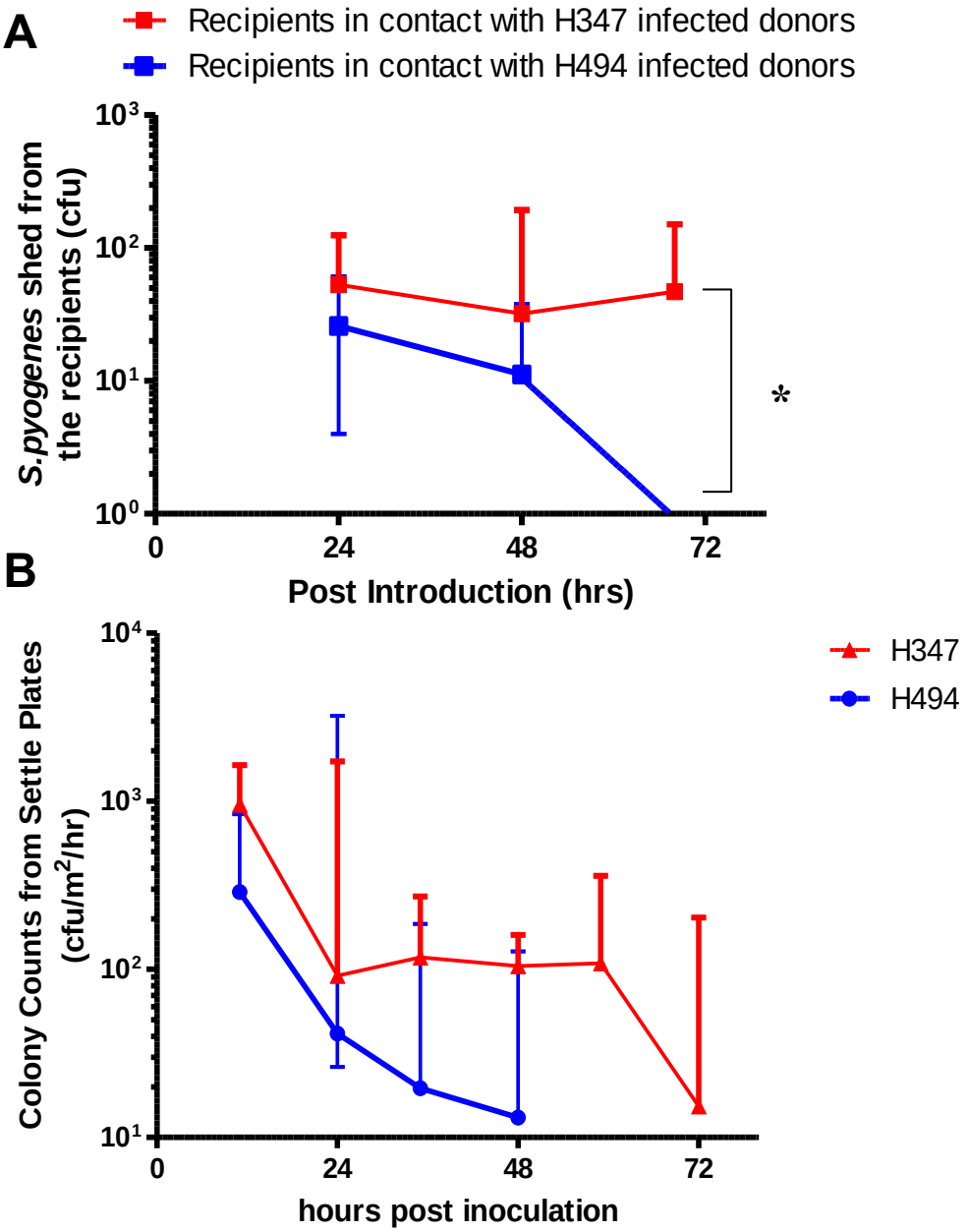


Figure 6.10. Transmission of *S. pyogenes* is hampered by the loss of CovR/S regulation. Naïve recipients co-mingled at a D:R ratio of 3:5 with mice infected with either the wild type strain H347 or the Δ*covR/S* strain H494 and sampled after the introduction of the donor mice. (n=15 recipients per group from 3 identical studies). Donor mice had >5000 cfu recovered from direct nasal sampling throughout the experiment. Donor mice infected with H494 transmitted significantly less well to recipients compared to H347 (AUC analysis, followed by Mann-Whitney U test). Data shown from settle plates through the time course revealed that there were no significant differences in the bacteria deposited on the surface of the plates by mice infected with H347 or H494 (B) Error Bars indicate median and interquartile range.

6.3. DISCUSSION

An isogenic derivative of the *emm*75 strain with a *covR/S* mutation was created in previous work and was shown to have increased SpyCEP production [45]. Here, it has been demonstrated to have impaired SpeB production and biofilm formation, similar to *emm1* strains with *covS* mutations reported recently [97,289]. The *covR/S* mutation in the strain studied here (H494) was derived by a single crossover homologous recombination event [45]. Such a mutation can have polar effects on bacterial gene function that are distinct from the specific inactivation events intended. A global polar effect in fitness was considered highly unlikely since the strain was known to have no growth defect *in vitro* [45] and is known to have an almost complete block in transcription of *covR* and *covS*, resulting in a 100 fold increase in the transcription of the IL-8 cleaving enzyme SpyCEP.

The *covR/S* mutant was demonstrably more invasive as it disseminated to the inguinal lymph nodes in greater numbers than its wild type counterpart during intramuscular infection. This again corroborated the effects of the mutation of the *covR/S* gene as described in other work [96] as it is known to de-repress a large number of genes essential for defence against neutrophil mediated killing.

However, whilst the *covR/S* mutation confers advantages during invasive infection, the converse was observed during infection in the nasopharynx. The duration of both continuous shedding and total shedding was shorter in mice infected with the Δ*covR/S* strain (H494) compared to those infected with wild type (H347). The inflammation caused by infection with the Δ*covR/S* strain (H494) was less severe and resolved faster than observed for the wild type in Chapter 3, which could be due to the lower numbers of *S. pyogenes* present.

To determine whether bioluminescent imaging could offer greater insight into the impact of *covR/S* mutation, a bioluminescent derivative of the *covR/S* mutant was created through the integration of the pICL18^{lux} plasmid into the spy0535 region of the chromosome to create H494^{lux}. Mice infected with the Δ*covR/S* bioluminescent derivative (H494^{lux}) showed no significant difference in bioluminescence *in vivo* compared to mice infected with the parent bioluminescent strain, H347^{lux} in the nasopharynx. When infected at a volume in which the bacteria would be delivered to the lungs, no significant difference in carriage could be found in this region, or the nasopharynx. However, one mouse infected with H494^{lux} had to be culled early due to the severity of its illness, and multiple dissemination events were observed after infection with the H494^{lux} strain in another mouse.

Importantly, the expression of bioluminescence in *S. pyogenes* led to different outcomes in the nasopharynx when observed over a longer time course. In the preceding chapter, the expression of bioluminescence conferred growth defects *in vitro*, and within the nasopharynx. In light of this, the reduced duration of continuous and total shedding of the H347^{lux} strain when compared to its wild-type non-bioluminescent counterpart was to be expected. The finding that this H347^{lux} strain had a reduced duration of continuous shedding when compared to its isogenic bioluminescent Δ*covR/S* counterpart, H494^{lux} was surprising.

Earlier work in this chapter showed that the non-bioluminescent strain H347 led to protracted carriage and transmission. The duration of total shedding was not significantly different to the wild type, which is reflected in the data from dissection. The inflammation caused by this strain in the nasopharynx was also lower, but greater than that seen following infection with the H347^{lux} strain. This highlights an important and broadly relevant consideration when exploiting bioluminescent strains

to determine the importance of single gene differences. The fitness burden conferred by bioluminescence may outweigh the impact of any additional genetic changes.

The removal of *covR/S* regulation, in conjunction with the metabolic cost conferred by bioluminescence may modulate the expression of virulence factors to a level that allows for H494^{lux} to be carried longer than H347^{lux}. It should be noted that the differences between continuous carriage duration and total carriage duration are defined by the probability of re-infection, and that these differences could be explained by a general impairment in transmissibility caused by a *covR/S* mutation.

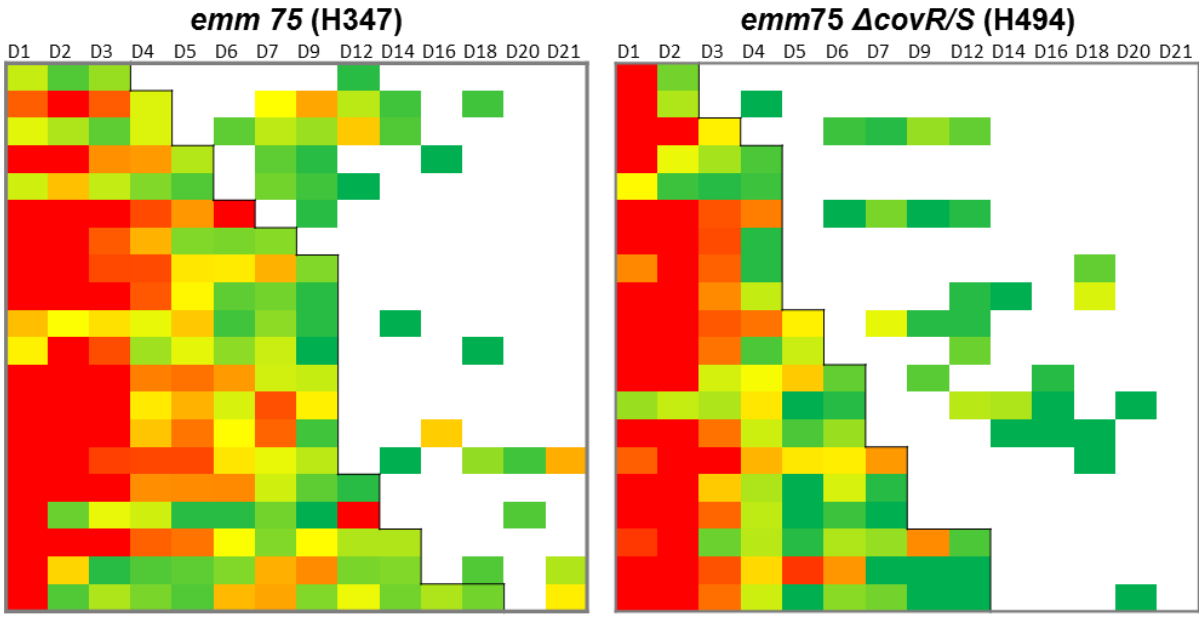
In either event, the differences in the behaviour of H494^{lux} when compared to its non-bioluminescent counterpart suggest that it would not be appropriate to use this strain for further study of the effects of *covR/S* mutation.

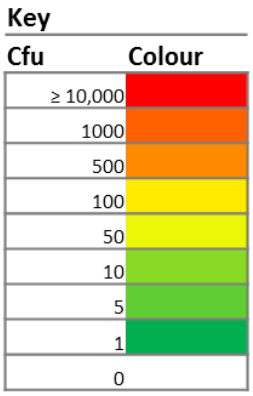
Co-mingling was then used to examine the impact of *covR/S* on transmission using the non-bioluminescent strains. Over time courses of five and three days, the Δ*covR/S* strain was less transmissible than wild-type *S. pyogenes*, despite the fact that the infection burden (as measured by direct nasal sampling) was similar between the two donor groups in the first 72h. Furthermore, settle plates placed in each cage revealed no significant difference in aerosolisation between the two strains. This suggests that either the bacteria are primarily transmitted via close contact between recipients and donors, or that the *covR/S* mutant is impaired when infecting mice from a droplet borne state.

There is thus a fitness cost conferred by *covR/S* mutation specific to the nasopharynx that may explain why such bacteria have not become prevalent in community *S. pyogenes* infections despite being advantageous in invasive infection.

covR/S mutation impacts the longevity of infection pathology in the nasopharynx and transmissibility from it. Biophotonic imaging failed to detect a phenotype imparted by *covR/S* mutation, and this is likely related to the global fitness burden conferred by expression of bioluminescence, a drawback that is important to underline in molecular microbiology since it is of relevance to both fluorescently and bioluminescently-labelled bacteria.

6.4. APPENDIX





Appendix 6.1. Shedding intensity is adversely affected by a *covRS* mutation. FVB/n mice were inoculated intranasally with either *S. pyogenes*, or an isogenic Δ*covR/S* in a 5µl dose. To determine the duration of shedding, direct nasal samples were taken over a 21 day period. Rows indicate individual mice (n=20 per group) throughout the time course, colours indicate the numbers of *S. pyogenes* recovered from direct nasal samples with red indicating the highest recorded levels of carriage (≥10,000 cfu) and green indicates the lowest levels of carriage (1 cfu) and blank blocks indicate no recovery of *S. pyogenes*. Black line indicates survival based on the first loss of carriage.

CHAPTER 7: THE UTILITY OF BIOPHOTONIC IMAGING IN ASSESSING VACCINE EFFICACY

7.1. INTRODUCTION

The models of nasopharyngeal infection utilised in many studies tend to cause invasive infection, and often studies use death as the outcome to evaluate the protection conferred by a vaccine [137,138,231]. However an effective vaccine against *S. pyogenes* must also curb the onset of non-invasive diseases such as pharyngitis, particularly if the aim of vaccination is to reduce the incidence of acute rheumatic fever.

The application of bioluminescence to study *S. pyogenes* infection in the nasopharynx allows for the progression of infection to be studied non-invasively. Although conferring a fitness burden on the infecting bacterium, BPI provides a longitudinal method that can be used to evaluate the efficacy of new vaccine candidates through direct measurements of *S. pyogenes* in the nasopharynx.

Subunits of SpyCEP, a cell wall-associated IL-8 protease, have demonstrated efficacy as vaccines against *S. pyogenes* during intravenous, intramuscular and lower respiratory tract infections [145–148]. The model of non-invasive infection, and the bioluminescent *S. pyogenes* developed and utilised in the preceding chapters provide an opportunity to assess the protective efficacy of this vaccine candidate during non-invasive upper respiratory infection.

Whilst the preceding chapters have revealed a few disadvantages to the use of BPI in certain situations, this chapter sets out to illustrate the application of BPI to vaccine development.

7.2. RESULTS

7.2.1 INTRAMUSCULAR BUT NOT INTRANASAL IMMUNISATION CONFERS PROTECTION AGAINST INTRANASAL CHALLENGE AGAINST *S. PYOGENES*

The efficacy of intranasal and intramuscular vaccination in protection against *S. pyogenes* nasopharyngeal infection was assessed, using heat-killed *L. lactis* as a control for non-specific responses, and heat-killed *S. pyogenes* as the protective vaccine. A vaccine comprising heat-killed *S. pyogenes* can act as a positive control for any vaccine study, since the vaccine should provide protection against infection with live bacteria of the same strain.

Mice were intranasally immunised with either heat-killed *emm*75 *S. pyogenes* or heat-killed *L. lactis* at 4, 2 and 1 weeks prior to intranasal challenge with live *emm*75 *S. pyogenes*. Serum IgG taken after the final immunisation revealed no specific immune response to either *S. pyogenes* or *L. lactis* (Figure 7.1. A). Broncho-alveolar lavage (BAL) samples taken at the time of dissection did not show the presence *S. pyogenes*-specific IgG (Figure 7.1. B) or IgA (Figure 7.1.C).

Mice were challenged intranasally with bioluminescent *S. pyogenes* ($H347^{lux}$), and imaged for two days post infection (Figure 7.1 D). Intranasal immunisation with either heat killed *S. pyogenes* or *L. lactis* followed by *S. pyogenes* challenge resulted in similar levels of bacterial infection in both groups (Figure 7.1. E) Hence, intranasal immunisation with heat killed bacteria did not result in systemic or mucosal immune responses, nor did it confer any specific protection *in vivo* against intranasal infection.

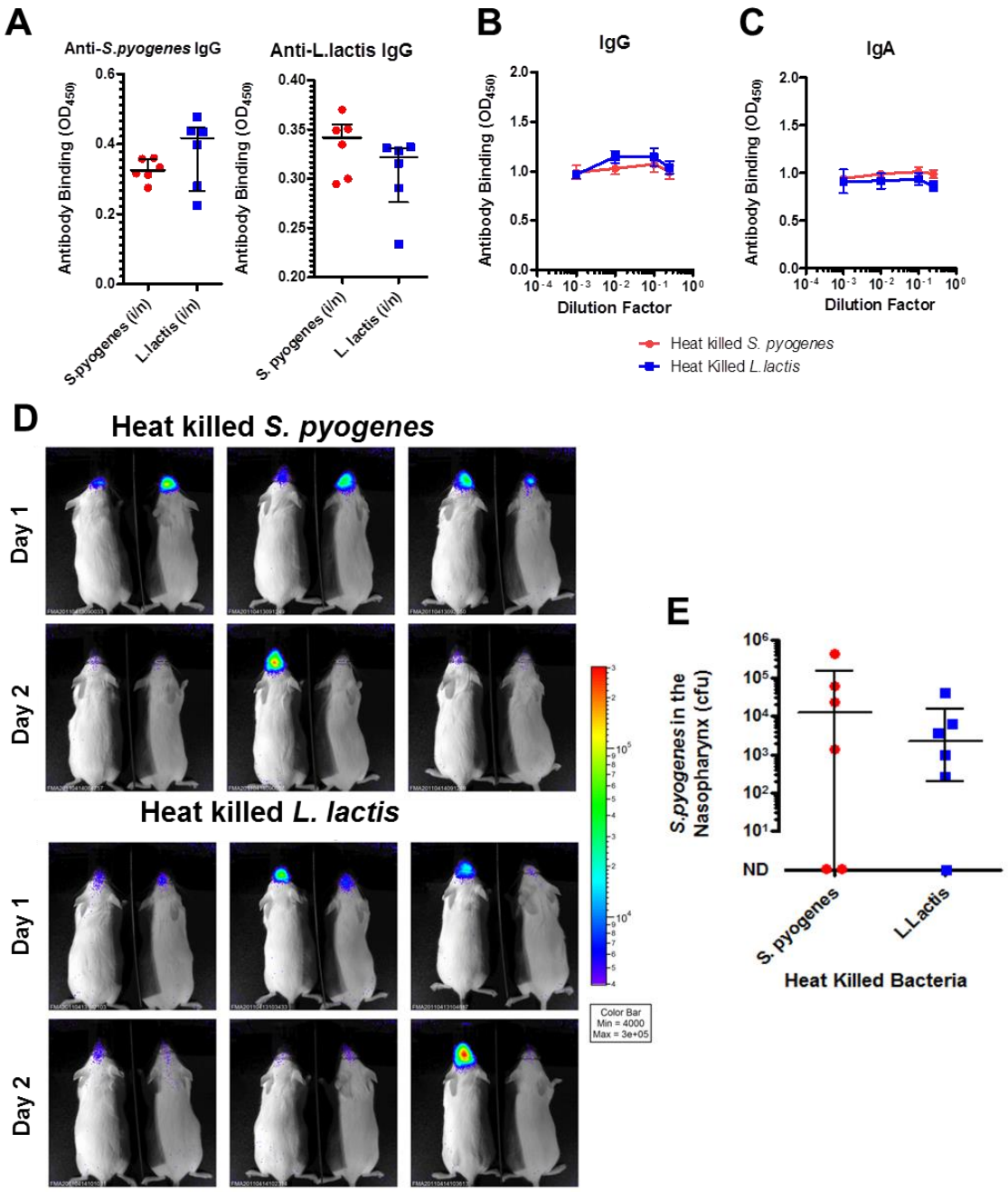


Figure 7.1. Intranasal immunisation with heat killed *S. pyogenes* or *L. lactis* and the resultant immune response. (A) Serum IgG response to either heat killed *S. pyogenes* of heat-killed *L.lactis* following immunisations. Samples were taken prior to challenge. (B) IgG and (C) IgA response in BAL fluid following vaccination with heat killed *S. pyogenes* or heat killed *L. lactis* ; Lavages taken at the time of dissection at 48 hours following challenge with live *S. pyogenes*. (D) Bioluminescent signal following live *S. pyogenes* ($H347^{lux}$) challenge in mice vaccinated with either heat killed *S. pyogenes* or heat killed *L. lactis.* (E) Quantitative *S. pyogenes* numbers obtained from dissected nasal tissues at the end of the previous experiment. Data shown for individual mice (n=6), lines and error bars indicated median and interquartile range.

Mice were then immunised intramuscularly with either heat killed *S. pyogenes* or *L. lactis*. Serum taken after the final vaccination revealed the presence of specific immune responses against *S. pyogenes* and *L. lactis* in mice immunised with each preparation (Figure 7.2. A). BAL fluid taken on dissection showed an *S.pyogenes*-specific IgG response (Figure 7.2. B), but no specific IgA response in *S. pyogenes* vaccinated mice (Figure 7.2. C).

Following intramuscular vaccination, mice were then challenged intranasally with bioluminescent *S. pyogenes* ($H347^{lux}$) and imaged for two days post inoculation (Figure 7.2. D). Whilst streptococcal numbers were lower in the mice immunised with *S. pyogenes*, this difference was not significant (Figure 7.2 C). Taken together, it appeared that intramuscular immunisation resulted in a specific and detectable immune response that could not be reproduced using intranasal vaccination.

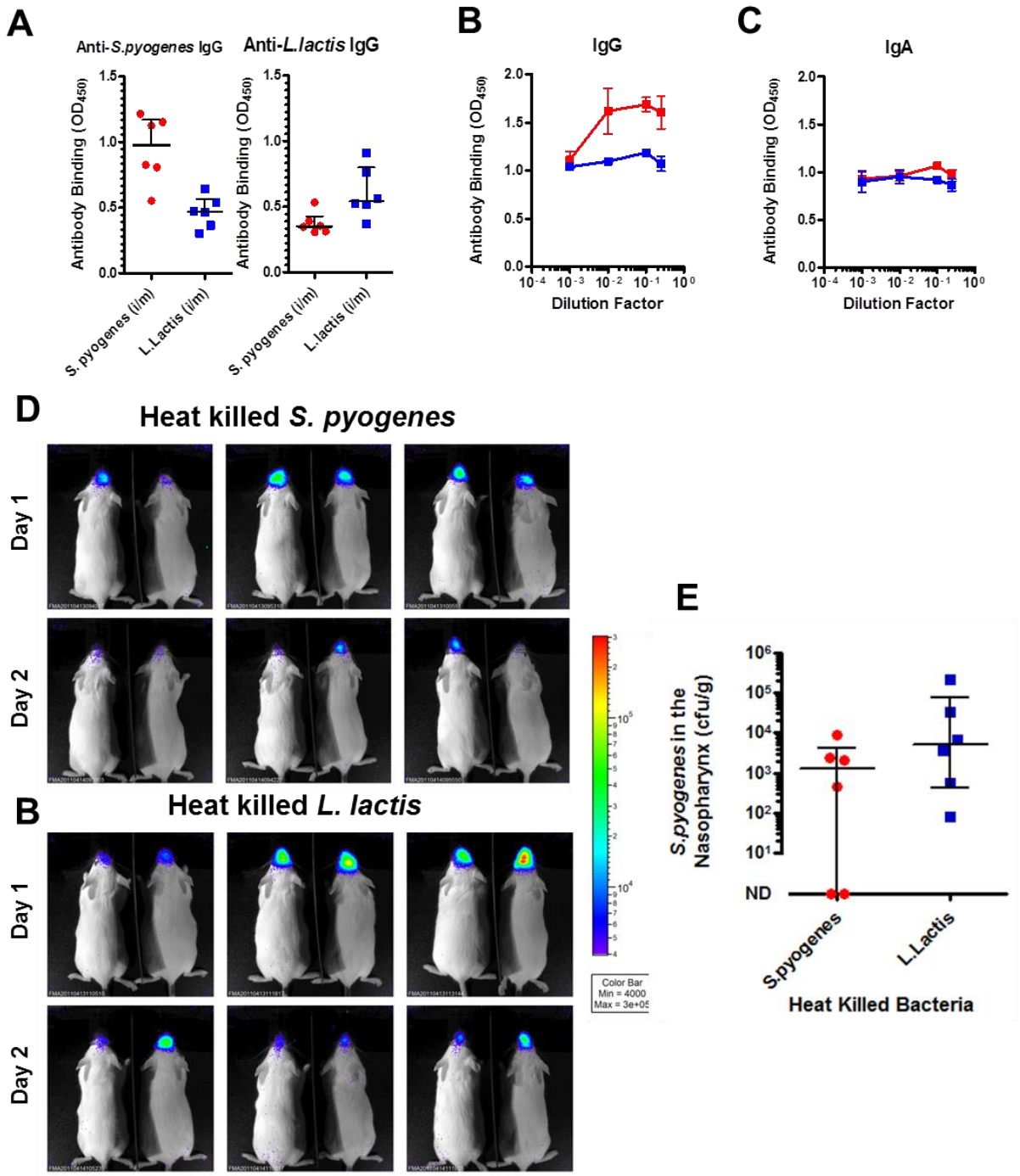


Figure 7.2. Intramuscular immunisation with heat killed *S. pyogenes* or *L. lactis* and the resultant immune response. (A) Serum IgG response to either heat killed *S. pyogenes* of heat-killed *L.lactis* following immunisations. Samples were taken prior to challenge. (B) IgG and (C) IgA response in BAL fluid following vaccination with heat killed *S. pyogenes* or heat killed *L. lactis* ; Lavages taken at the time of dissection at 48 hours following challenge with live *S. pyogenes*. (D) Bioluminescent signal following live *S. pyogenes* ($H347^{lux}$) challenge in mice vaccinated with either heat killed *S. pyogenes* or heat killed *L.lactis.* (E) Quantitative *S. pyogenes* numbers obtained from dissected nasal tissues at the end of the previous experiment. Data shown for individual mice (n=6), lines and error bars indicated median and interquartile range.

To determine whether a nasopharyngeal mucosal response could be elicited by immunisation, mice were immunised either intranasally or intramuscularly with heat-killed *S. pyogenes* (n=8 per group). Saliva samples were taken from these mice before immunisation, and after the final vaccination. These revealed no differences in the presence of IgA in all groups, but mice immunised intramuscularly had IgG specific for *S. pyogenes* (Figure 7.3.). These findings indicated that intramuscular immunisation with heat killed *S. pyogenes* produced an IgG response in both serum, BAL fluid, and saliva.

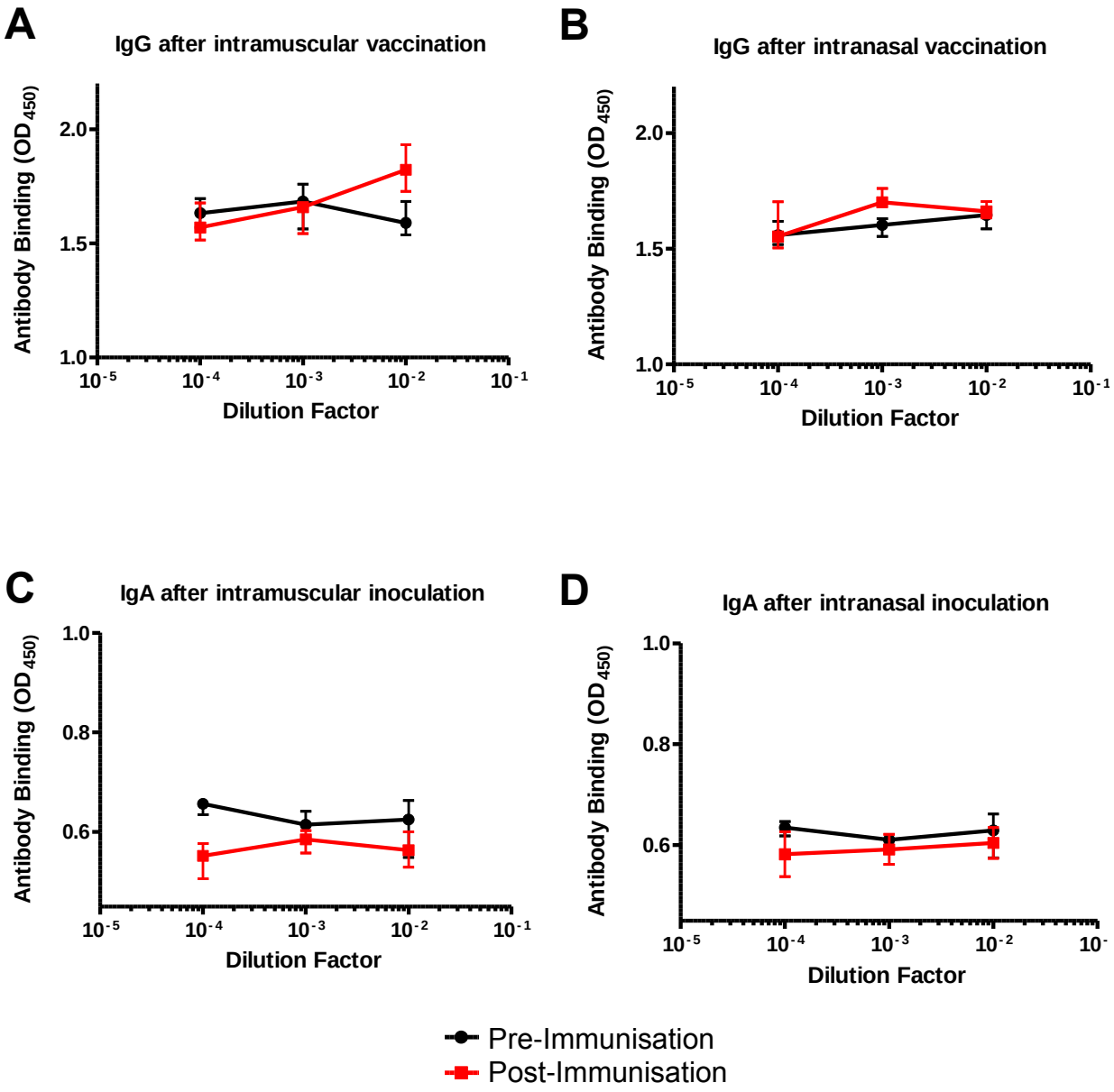


Figure 7.3. Salivary IgA and IgM responses following vaccination with heat killed *S. pyogenes* administered intramuscularly or intranasally. (A) Anti *S. pyogenes* IgG in saliva prior of following intramuscular vaccination with heat killed *S. pyogenes*. (B) Anti *S. pyogenes* IgG in saliva prior of following intranasal vaccination with heat killed *S. pyogenes*. (C) Anti *S. pyogenes* IgA in saliva prior of following intramuscular vaccination with heat killed *S. pyogenes*. (D) Anti *S. pyogenes* IgA in saliva prior of following intranasal vaccination with heat killed *S. pyogenes*. Lines indicate median, error bars indicate interquartile range.

7.2.2 USE OF BPI TO DETERMINE THE PROTECTIVE EFFICACY OF A HEAT KILLED *S. PYOGENES* BASED VACCINE.

The previous experiments demonstrated that intramuscular vaccination with heat killed *S. pyogenes* produced a detectable IgG immune response and may be protective. Data from this study were used to power a more substantive study evaluating protection.

Intramuscular vaccination with either heat-killed *S. pyogenes* or a PBS control was performed at 4, 2, and 1 week prior to intranasal challenge with bioluminescent *S. pyogenes.* Serum samples taken a week before challenge revealed the presence of specific IgG reactive against heat killed *S. pyogenes* in vaccinated mice compared with controls (Figure 7.4 A).

Mice were imaged for four days after intranasal challenge (Figure 7.4 B). Mice immunised with heat-killed *S. pyogenes* emitted significantly less bioluminescence compared to the controls immunised with PBS (Figure 7.4 C, Two-Way ANOVA $p<0.05$). On the final day, mice were culled and nasal tissue was extracted for quantitative bacteriology (Figure 7.4. D). There were significantly fewer *S. pyogenes* in the nasopharynx of the mice immunised with heat killed *S. pyogenes* compared with controls. (Mann-Whitney Test $p<0.05$). The experiment provided proof that heat killed *S. pyogenes* can protect against nasopharyngeal carriage, and that BPI was a robust tool for evaluating vaccine efficacy.

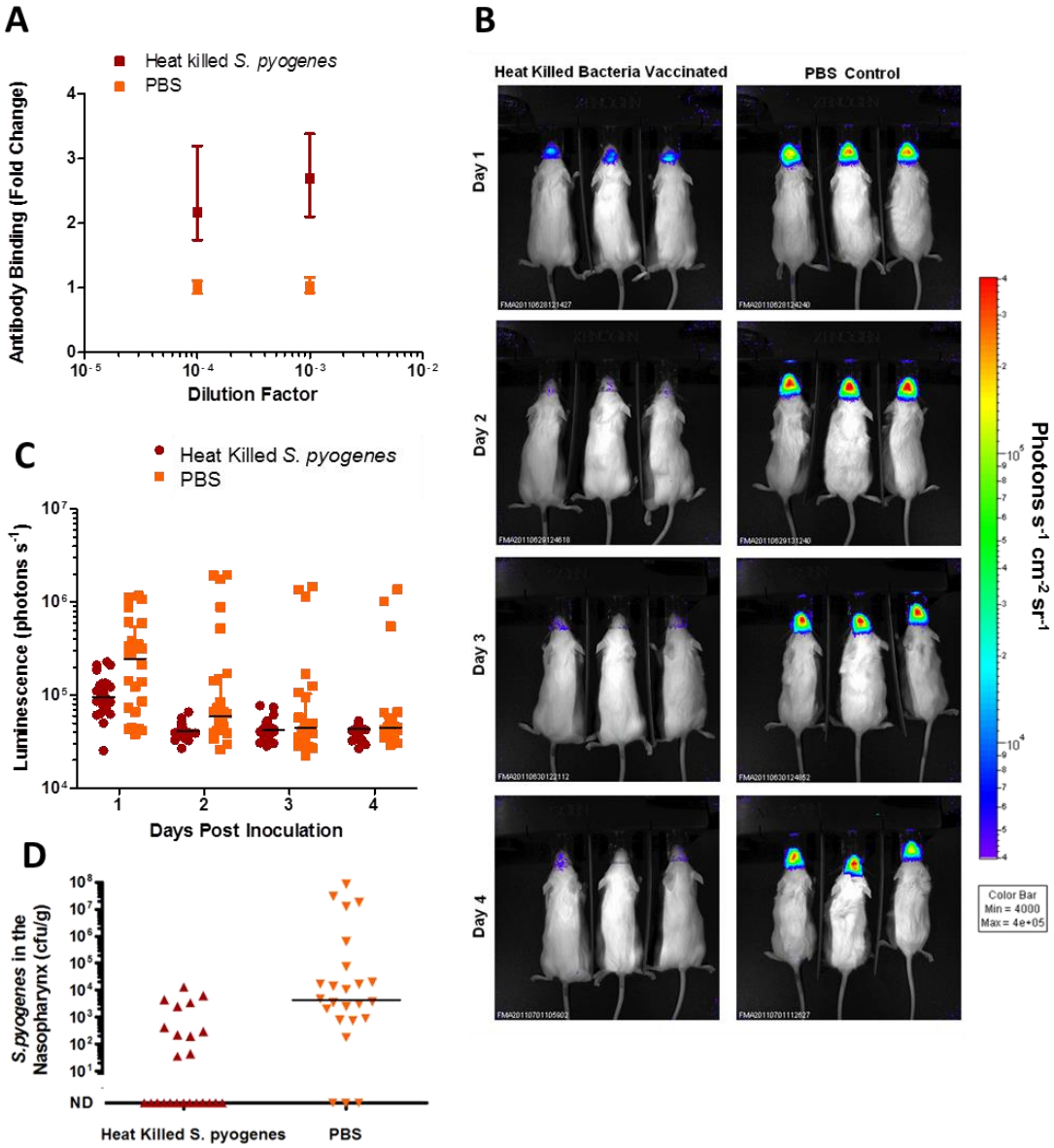


Figure 7.4. BPI revealed the protective efficacy of a vaccine based on heat-killed bacteria. Mice were immunised with either PBS or with heat-killed *S. pyogenes* strain H347. A serum IgG response against heat-killed *S. pyogenes* was detected in the vaccinated group (A). Mice challenged with bioluminescent *S. pyogenes* were imaged for four days post infection using an IVIS 100 system (B)**.** The luminescent signal recovered from the mice immunised with PBS was significantly higher than that recovered from mice immunised with heat-killed bacteria (C, Two way ANOVA $p<0.05$). Colony counts obtained from dissections performed on the final day confirmed that mice immunised with heat-killed *S. pyogenes* had significantly less bacteria than mice immunised with PBS alone (D, Mann-Whitney $p<0.05$). Data is shown for individual animals, bars indicate median.

7.2.3. THE USE OF BPI TO DETERMINE THE PROTECTIVE EFFICACY OF A VACCINE BASED ON SPYCEP

The same immunisation protocol was then used to determine the protective efficacy of a vaccine candidate based on SpyCEP. A mix of recombinant CEP5 (a sub-unit of SpyCEP) with complete Freunds adjuvant was intramuscularly injected 4 weeks prior to infection, followed by boosters at 2 and 1 weeks prior to intranasal challenge using Freunds incomplete adjuvant. Controls received vaccination with Freunds mixed with PBS. Serum samples taken a week before challenge revealed the presence of specific IgG reactive against SpyCEP (CEP5) in vaccinated mice compared with controls (Figure 7.5 A).

Mice were imaged over a four day period post infection (Figure 7.5. B). The luminescent signal retrieved from the nasopharynx revealed that the mice immunised with SpyCEP carried significantly fewer bacteria than the controls (Figure 7.5. C. Two-way ANOVA $p<0.05$). This was confirmed at the end of the experiment, when mice were culled and nasal tissue cultured to determine *S. pyogenes* burden (Figure 7.5. D**,** Mann-Whitney test $p<0.05$). The data demonstrated that inclusion of SpyCEP as a vaccine confers additional protection compared to the vehicle alone. However, it must be noted that the protection conferred was less dramatic than that conferred by heat killed bacteria.

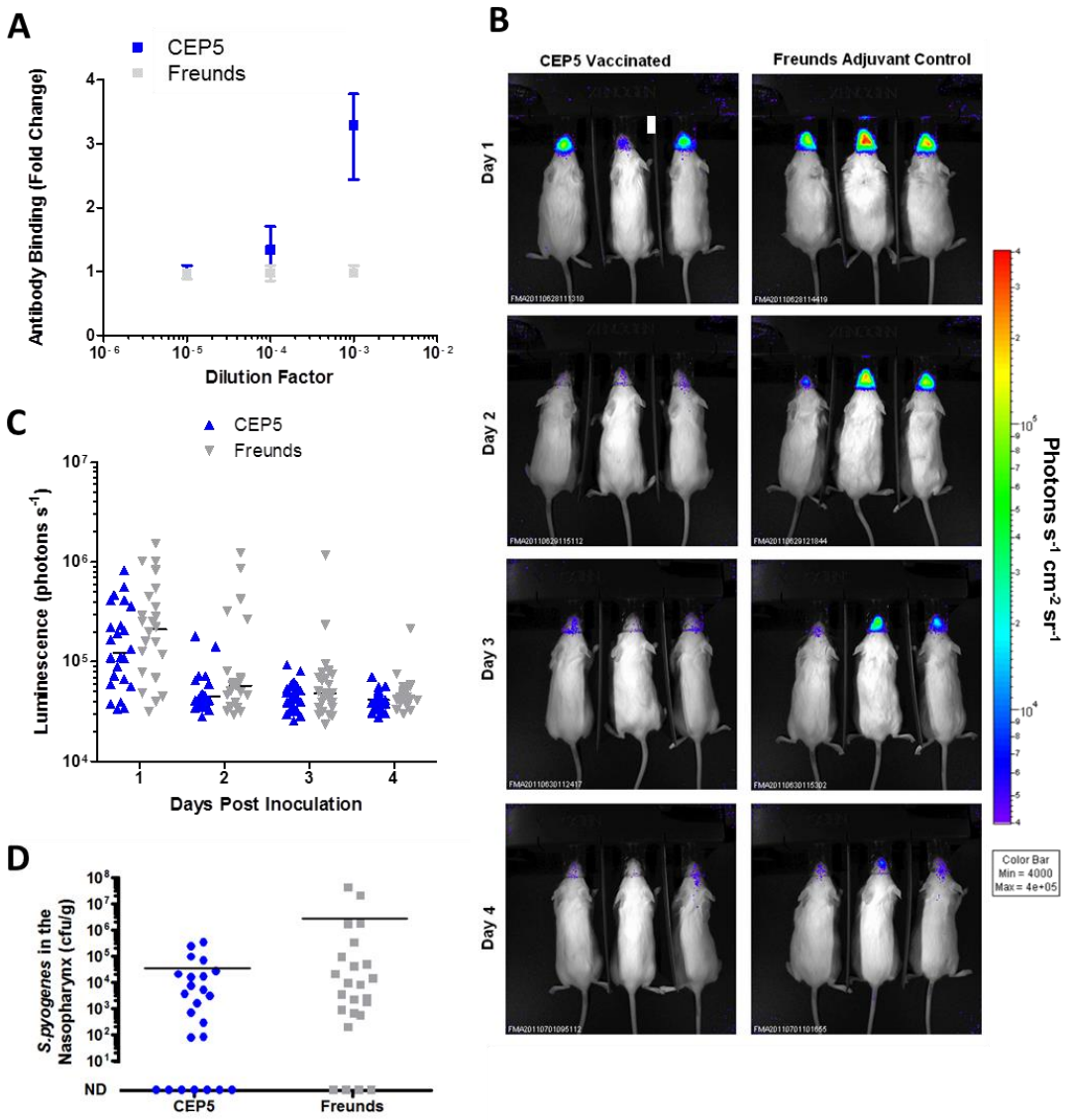


Figure 7.5. BPI revealed the protective efficacy of a vaccine based on SpyCEP. Mice were immunised with either Freunds adjuvant or CEP5 + Freunds adjuvant. A serum IgG response against CEP5 was detected in the vaccinated group (A). Mice challenged with bioluminescent *S. pyogenes* were imaged for four days post infection using an IVIS 100 system (B)**.** The luminescent signal recovered from the mice immunised with Freunds adjuvant was significantly higher than that recovered from mice immunised with CEP5 (C, Two way ANOVA $p<0.05$). Colony counts obtained from dissections performed on the final day confirmed that mice immunised with CEP5 had significantly less bacteria than mice immunised with Freunds adjuvant alone (D, Mann-Whitney $p<0.05$). Data is shown for individual animals, bars indicate median.

7.3. DISCUSSION

The unique benefit of BPI is that it allows quantitation of bacterial load at the site of infection non-invasively. This capability provided an opportunity to study the efficacy of vaccination in a way that was not possible before.

BPI was used to study the effects of immunisation with heat killed bacteria administered either via intramuscular inoculation or intranasal application. Whilst heat-killed *S. pyogenes* are unsuitable for use in human vaccines due to issues of safety and poor coverage, they can be used as a proof of principle to test how well BPI can gauge vaccine efficacy.

Vaccination with heat-killed *L. lactis* was used as a control to allow for a more specific analysis of the immune response against *S. pyogenes*. *L. lactis* has a similar cell wall to *S. pyogenes* comprising peptidoglycan and teichoic acid, yet does not have the repertoire of immunogenic proteins that *S. pyogenes* possesses.

Intriguingly, there may even be some cross species protection, for example through conserved antigens expressed by different Gram positive species. A recent report suggested that the conserved DLDH and P5CDH proteins may be protective against both *Staphylococcus aureus* and *Streptococcus pneumoniae* [290]. Live *L. lactis* has been investigated as a method for vaccine delivery [235], and may also produce a cross protective immune response.

In this study it was not possible to elicit any protection following intranasal vaccination with *S. pyogenes* and this was associated with a failure to elicit any specific immune response. This contrasts with previous studies using *S. pyogenes* in intranasal vaccines [157,243], and although it could be related to strain differences, or differences in end-points, the lack of any response was surprising. Adjuvants are

often required for intranasal vaccination with proteins, however this was considered unnecessary when administering heat killed whole bacteria.

Whilst some antigens expressed by *S. pyogenes* do not appear to require the presence of adjuvants to confer protection [138], adjuvants such as alum [148,160], or the cholera toxin B sub-unit [156,159] are used in the majority of vaccines targeted to the nasopharynx [170]. It is possible that an adjuvant is necessary for a vaccine to be effective in the nasopharynx, although it was expected that a whole cell vaccine would provide such an adjuvant stimulus. It is also possible that the strain of *S. pyogenes* used in this study may not be amenable for use as an intranasal vaccine candidate, since other studies have demonstrated protection when *emm24 S. pyogenes* was used as a vaccine [224]. However, the previous study used PBS as a control, and it is possible that there is a non-specific immune reaction caused by both *L. lactis* and *S. pyogenes*, which would make a comparison between the two invalid. It should also be noted that in that study, bacteria were heat killed at a temperature of 56^{o}C, whereas a temperature in excess of 80^{o}C was used in these studies due to safety regulations to ensure all the bacteria are reliably killed.

For mice immunised via the intramuscular route, IgG responses were seen in the serum, saliva and BAL fluid. A specific anti-streptococcal IgA response, which tends to be associated with mucosal immunity [224], was not observed in this study. The production of IgA is thought to derive from the induction of immunity at mucosal sites, and so the lack of this response after intramuscular immunisation may not be surprising [291]. The lack of IgA response after intranasal immunisation suggests that mucosal specific adjuvants are necessary, and the heat killed vaccination preparation used in this study is not sufficiently immunogenic on its own.

These initial studies were not powered to detect a protective effect against *S. pyogenes* in the respiratory tract. A larger study was performed, with mouse numbers determined by a power calculation based on the previous data, to demonstrate protection by a heat-killed *S. pyogenes* vaccine. The mice were also followed over a longer period of infection, and PBS was used as a control instead of *L. lactis*. These data demonstrated that heat-killed *S. pyogenes* applied in an immunisation protocol can confer *in vivo* protection against nasal challenge over a four day observation period. In previous studies bioluminescent *S. pyogenes* was used to investigate the efficacy of a C5a peptidase vaccine during intranasal infection [170], and the efficacy of passive immunisation with anti-serum raised against a conserved C-terminal sub-unit of M-protein [160]. In the latter study, bioluminescence could only be assessed post mortem on dissected organs, which provides no better insight than simply performing quantitative bacteriology on the dissected organs. In both of these studies, the strain utilised was derived from an *emm49* skin isolate, and none of these studies directly looked at the presence of bacteria in the whole nasal tract.

SpyCEP is but one of a number of different conserved proteins found via genomic [145,148] and proteomic [146] approaches which may become the basis for a combination vaccine. Such candidates have been shown to improve survival after intrapulmonary, intravenous and intraperitoneal infection [145,146,148] . The application of BPI allows for the measurement of bacterial clearance, as opposed to death, making it both a more humane and more relevant method for assessing the protectiveness of a vaccine.

BPI was successfully used in this study to demonstrate that vaccination against SpyCEP can reduce *S. pyogenes* numbers in the nasopharynx. This method could

just as effectively be applied to measure the efficacy of other vaccine candidates in a similar way.

CHAPTER 8: GENERAL DISCUSSION

The work described in this thesis was performed to fulfil the need for a reproducible model of nasopharyngeal infection that can be analysed longitudinally, and that can be used to determine the factors that influence carriage, infection, and transmissibility in future studies. The model was used to demonstrate the effects of global virulence factor de-repression on *S. pyogenes* survival and transmission within this niche. A new bioluminescent strain of *S. pyogenes* was developed from an isolate known to cause nasopharyngeal infection in humans and mice; the resultant model was used to demonstrate its potential as a model to screen vaccine candidates. In this work, the efficacy of a vaccine candidate based on SpyCEP was evaluated.

Whilst working towards these aims, a fitness cost conferred by the expression of bioluminescence in *S. pyogenes* was uncovered, new methods for non-invasively measuring bacterial carriage without the need for expensive equipment and genetically modified bacteria were tested, and a model for mouse to mouse transmission was devised. In the following section these results will be discussed with respect to their broader applicability to previously published work, and possible future avenues of investigation.

8.1. THE SUSCEPTIBILITY OF MICE TO *S. PYOGENES* INFECTION IN THE NASOPHARYNX IS BASED ON THE HOST STRAIN, GENDER AND AGE

It was noted earlier that a variety of different methods have been utilised to investigate *S. pyogenes* in the nasopharynx using mouse models (Chapter 1, Table 1.1). A major issue for these models was the resistance of mice to streptococcal infection, and thus followed the requirement for high doses of inocula. A number of

studies have established that the host background of mice can determine outcome of invasive infection induced by intraperitoneal, or intravenous injection [192,193], along with a gender difference. Mouse background and gender also impacted upon the model of intranasal infection devised in the current work, and the FVB/n mouse strain was found to be most susceptible to *S. pyogenes* infection. This strain is not known to suffer from any immune deficiencies, save for the presence of the *cri-1* locus conferring susceptibility to *C. rodentium* infection [276,277], and the genetic susceptibility to the strain B Friend mouse leukaemia virus that was used to differentiate this strain from its progenitors [274]. Conversely, other studies have found that this strain is more resistant to infection in the lungs based on the numbers of bacteria recovered from this region [292]. The experiments performed in the current work were specifically designed to avoid lung involvement, and thus do not contradict these findings. However, the findings raise the possibility that susceptibility to infection arose after the derivation of this strain, and certain populations of this mouse strain may not possess the susceptibility observed in this thesis. Importantly, the FVB/n mice used in these studies were sourced from two separate breeding colonies, Harlan and Charles-River, and no discernible difference in susceptibility was observed.

Other studies have also determined that male mice tend to be more susceptible to invasive infection with *S. pyogenes* compared to female mice [192–194]. The reasons for this difference have been suggested to be due to the presence of a locus for susceptibility carried on the X-chromosome [192] or the presence of testosterone causing some inhibition to the immune response of male mice [194]. This latter evidence is supported by the finding that female mice tend to be more reactive to superantigen mediated toxic shock than male mice [195]. As observed in humans,

enhanced susceptibility to autoimmune disease is observed in female mice. Conversely, generally enhanced protection from sepsis is observed in females compared with males [293,294]. This ties in with globally enhanced immune responses, whether cytokine, immunoglobulin, or T cell –derived, to immune stimulus in females [295,296]

The findings reported in this thesis support the findings from previous research studies, although the difference observed herein in susceptibility was detectable only after the mice had reached ten weeks of age, compared with pre-pubertal mice. Other work has similarly indicated that the susceptibility of female mice to intranasal infection decreases after they age past 11-12 weeks [156] which supports the findings described here. Earlier work examining the effects of age tended to examine much later time points of the mouse life cycle, and is not directly comparable to the work performed here [193,196].

The critical difference between mice aged 5 weeks and mice aged 10 weeks is the onset of puberty. This could support the hypothesis that sex hormones to some degree define mouse susceptibility to *S. pyogenes* infection. However, the male mice in the older age group had to be separated due to aggression. These mice tended to carry *S. pyogenes* for longer in spite of the lack of potential for re-infection caused by this situation. Previous studies have shown that individually housed mice show greater humoral immunity, and thus greater resistance to infections, which would suggest that separation is not responsible for enhanced susceptibility to infection [297].

The documentation of sex specific determinants of *S. pyogenes* susceptibility supports the proposition that puberty may be a significant factor in the development of resistance to infection in female mice.

It should be noted that the *emm75 S. pyogenes* strain utilised in these studies was chosen based on its ability to survive in the nasopharynx of BALB/c mice in initial studies. Importantly, pharyngitis strains of different *emm* types were found to cause infection in the FVB/n nasopharynx to an equivalent, if not greater, degree than the *emm75* strain used to characterise the model.

Whilst there are a number of studies in humans which support the findings that males are more susceptible to infection than females [294,298–301], and are more susceptible to toxic shock [195,302], there are some differences that need to be acknowledged. In humans, susceptibility to infection decreases after the onset of puberty, a finding that only appears to be corroborated by female mice in this model, as the male mice appeared to become more susceptible to experimentally induced pharyngitis after this period. This has not been observed in human adults, but the sheer prevalence of *S. pyogenes* infection in early life may be a confounding factor.

These general issues stem from the differences in biology between the mouse and the human, and apply to the discussion of any findings from a mouse model. The questions that these models are used to investigate must be framed with these issues in mind.

8.2 THE CHARACTERISATION OF *S. PYOGENES* INFECTION IN THE MOUSE

The *emm75 S. pyogenes* was found to cause a suppurative infection in the nasopharynx of the FVB/n mice. The numbers of bacteria recovered from the nasopharynx tended to be highest in most mice during the first four days of infection

(Appendix 3.1). This finding was corroborated through BPI; high numbers of bacteria were detectable by imaging during the first four days after infection, but thereafter were only detectable by conventional microbiological techniques. After an initial phase of suppurative infection, mice remained colonised with *S. pyogenes* at much lower levels but with no visible symptoms or distress for up to 21 days post inoculation (Figure 3.5.).

In artificial *S. pyogenes* infections induced in humans, the presence of bacteria on the tonsils was found to peak between 2-4 days post infection [109,124], although it should be noted that the period of observation in these studies was limited, and the cessation of infection was caused by penicillin prescription rather than the natural induction of immunity, for obvious ethical reasons. However, in clinical cases of *S. pyogenes* pharyngitis, an asymptomatic carrier state is recognised to follow, after the cessation of suppurative infection [114,116,298]. The similarities between the infection described in humans and the infection observed in mice during this study are striking.

Whilst similarities exist between clinical and experimental infection, the fundamental differences in the anatomy between human and the inbred mouse must be taken into account when extrapolating the findings from this model to the human condition. The primary focus of infection in humans is within the tonsils. However, the rodent equivalent of the tonsils, the NALT, is situated above the hard palate, within the nasopharynx [209]. The suppuration induced by *S. pyogenes* occurred primarily within this tissue, and the highest numbers of *S. pyogenes* were found within the ethmoturbinates within the posterior nasopharynx. Whether this is due a specific preference, or simply because the high surface area of the ethmoids allowed for more *S. pyogenes* to colonise than the other portions of the nasopharynx was not

discovered in this study. This heavy colonisation of the posterior nasopharynx was documented to lead to damage to the cribriform plate, the bone which separates the brain from the nasopharynx, and the entry of *S. pyogenes* into the olfactory bulb. Although recognised to occur in invasive sinus infections associated with the *S. milleri* group and *S. pneumoniae*, this form of invasion has not been observed in *S. pyogenes* human infection, and may only occur due to anatomical differences in the distribution of *S. pyogenes* colonisation in mice compared with humans.

8.3. THE TRANSMISSION OF *S. PYOGENES* BETWEEN MICE

In the initial studies of *S. pyogenes* nasopharyngeal infection, direct nasal sampling allowed for the decline of *S. pyogenes* carriage to be examined. There was a curious trend that occurred during the latter stages of infection, whereby mice would appear to clear infection, only to later demonstrate apparent relapse or re-infection with *S. pyogenes*. Although it is possible that low level carriage of *S. pyogenes* fell below the limit of detection for the direct nasal sampling technique for a short period, there was the possibility that these were transmission events. This provided two potentially different end points when judging the time at which *S. pyogenes* infection ended.

The most rigorous end point was the time point when the first negative sample was obtained from each mouse, eliminating any potential effects of re-infection events on nasal carriage, and ignoring any further positive cultures occurring after the level of carriage fell below the level of detection. This represented the period of continuous shedding.

The period of intermittent shedding was, however, of biological interest, as the impact of transmission events had possible relevance to the human populations. This was evaluated by measuring the total duration of shedding, in which the last

positive sample of *S. pyogenes* was used to define the cessation of carriage. The fact that the duration of continuous shedding often differed from the total duration of shedding suggests that transmission may play a role in the maintenance of nasopharyngeal infection in this mouse model.

S. pyogenes is thought to be transmitted in airborne respiratory droplets, although direct contact may also contribute. The transmission of *S. pyogenes* between mice would provide an opportunity to study transmission in a way not previously possible, The resistance of mice to *S. pyogenes* infection described in previous works have necessitated the administration of inocula containing large numbers of *S. pyogenes* to individual mice by direct intranasal inoculation rather than by aerosolised droplets [303] . The exception to this is a set of work produced during the 1950's, in which a nebuliser system was utilised to infect Swiss mice [211,212,304,305]. In one study, the spread of *S. pyogenes* between mice in separate cages was observed [304]. Later studies indicated that there were differences in the susceptibility of mice to infection by the nebuliser technique, and it was later abandoned [212]. The outbred nature of the strains used and the inconsistent environmental conditions likely played roles in this inconsistency. The use of inbred strains of mice in the current work, and the standardised environmental controls implemented in the housing and care of the mice in these studies mean that the current study is not subject to those particular sources of variability.

A co-mingling model was implemented to study transmission, as it has been long recognised that transmission via the airborne route may not the primary mode of transmission.

Transmission was observed to occur rapidly, with recipient mice acquiring *S. pyogenes* in the nasopharynx within 4 hours of the introduction of donor mice. The numbers of *S. pyogenes* were observed to increase in the recipients when more donor mice were present. Furthermore, the deferred introduction of infected donor mice revealed that transmission was not simply an artefact of inoculum transfer.

The acquisition of *S. pyogenes* in the nasopharynx of the recipient mice did not result in bacterial loads of the levels reached in mice that were inoculated directly. Importantly histopathological studies on recipient mice were not undertaken and it cannot be said whether the acquisition resulted in a productive inflammatory infection. In the human situation, asymptomatic carriers of *S. pyogenes* have been observed during outbreaks of infection [306,307]. The persistence of *S. pyogenes* in this state may aid its persistence in a cage of infected mice in a similar manner to which it enables persistence within a community. However, there is a strong behavioural component to transmission in mice via this co-mingling model which cannot be ignored. Mice tend to maintain a social hierarchy that is reinforced by grooming and subtle demonstrations of aggression. In the studies described, donor mice had to be separated from their cage mates for specific periods of time, which had the potential to upset this hierarchy, causing increased subtle aggression in some cages upon the reintroduction of the donor mice and introducing a source of variability when investigating transmission.

The transmission events demonstrated did not differentiate between transmission due to direct contacts and transmission due to aerosolised droplets. Nonetheless, the potential for airborne transmission was ably demonstrated by the transmission of beta haemolytic streptococci to the settle plates in the upper levels of cages, at a height of 10cm above the cage floor. Future studies will necessarily involve

segregation of infected donor and naïve recipient mice by panels that prevent direct contact and grooming, but allow passage of air.

8.4. Efficacy of different methods for determining the presence of *S. pyogenes* in the nasopharynx longitudinally

The primary focus in this work was the development of non-invasive techniques for assessing long term *S. pyogenes* colonisation in mice. During a previous Master's project, a technique was developed utilising direct nasal sampling from the nasopharynx onto agar plates. In the current study, the numbers of exhaled *S. pyogenes* recovered using this technique were found to correlate with the actual numbers of bacteria within the nasopharynx of the mice. This technique allowed for the course of an infection to be tracked, and for the infection to be assessed on the basis of the survival of *S. pyogenes* within the nasopharynx, rather than the survival of the infected hosts after infection. However, whilst this technique was sensitive, the upper limit of accurate quantification was sometimes restricted during the first three days of infection. During the point of greatest carriage, *S. pyogenes* colonies from direct nasal sampling could reach 100% confluence on the surface of the sampling plates, making the precise assessment of *S. pyogenes* numbers impossible. This prevented the study demonstrating how the *S. pyogenes* numbers exhaled from the nasopharynx change quantitatively over this period. Thus, although the technique provided quantitatively useful information at certain levels of carriage, the main value of the technique was to longitudinally monitor the presence or absence of group A streptococci, rather than quantities.

There was no such upper limit of quantification when biophotonic imaging was used to study *S. pyogenes* infection. Bioluminescent derivatives of an *emm75* isolate were

created for use in this study. Whilst a strain bearing a non-integrating plasmid, H347^{pTHLK}, was found to be brighter *in vitro*, the instability of this plasmid made this strain unsuitable for use *in vivo*. A strain of *S. pyogenes* with the *luxABCDE* operon integrated into the spy0535 locus, H347^{lux}, was found to stably produce bioluminescence both *in vitro* and *in vivo*.

During the course of intranasal infection, the bioluminescent signal was detectable within the first four days of infection, the period of infection where direct nasal sampling could not be used to reliably assess bacterial numbers. However, BPI could not be used when there were less than 10^3 bacteria present in the nasopharynx, as the attenuation caused by the tissues of the mouse and the presence of a background signal limited the sensitivity of detection.

In addition to this, it was found that the bioluminescent isolate utilised in this study, H347^{lux}, was attenuated in growth relative to the wild type parental strain. The creation of an isogenic strain with a plasmid insertion in the same spy0535 locus confirmed that this attenuation was not due to the disruption of this gene region. The expression of bioluminescence itself was the reason for the fitness cost.

The basis for the bioluminescence conferred by the *luxABCDE* operon comes from two reactions, of which the *luxAB* genes are the only ones which are essential for bioluminescence expression, as the products of the *luxCDE* reaction can be supplied exogenously. This could reduce the energy cost of bioluminescence by up to 67%, but the *luxAB* reaction still demands energy from intracellular stores of $FMNH_2$ [308]. While the long chain fatty acid aldehyde decanal can be supplied to enable *luxAB* to function, administration of this compound *in vivo* is complicated by its toxicity to animals.

In spite of this fitness deficit, bioluminescent *S. pyogenes* still maintained the ability to grow within the nasopharynx, and thus provide some useful information about infection.

8.5. THE UTILITY OF BIOLUMINESCENCE IMAGING FOR EVALUATING VACCINES AND IMAGING INFECTION

Non-invasive pharyngitis accounts for a large portion of *S. pyogenes* disease that is estimated to afflict 616 million people worldwide per year [1] and incurs an estimated cost of 224-539 million dollars per year to the USA [309]. To effectively prevent these diseases, vaccine candidates must ensure bacterial clearance during *S. pyogenes* pharyngitis [145,146,148].

In a number of previous studies, vaccines based on SpyCEP have shown some degree of efficacy in preventing death after the onset of pneumonia, and dissemination from an invasive disease. Few studies have demonstrated that immunisation against SpyCEP can facilitate bacterial clearance from the nasopharynx [147].

BPI enables real time assessment of bacterial numbers in the nasopharynx, and was used to show that an immunisation strategy utilising SpyCEP could facilitate bacterial clearance from the nasopharynx using the previously described model of infection. The data suggest that this vaccine candidate may not only ensure protection against invasive disease, but may also prevent less invasive infections, making it an ideal component of any future developmental vaccine. Indeed, this antigen is included in a vaccine being developed by the company Novartis[310].

The real advantage of BPI is in the discovery of new niches and foci of infection that would not have been revealed in other situations. During the course of this work, it

was discovered that colonisation of the female urogenital tract regularly occurred following intranasal infection. It appeared likely that *S. pyogenes* was deposited genitally during the course of grooming. The mice which became infected in this region did not demonstrate any outward indication of infection such as inflammation or distress. Preliminary studies which involved administration of β-estradiol to control the oestrus cycle suggest that there may be a hormonal component to susceptibility. Further investigations are required in order to fully characterise how genital infection develops, and the underlying factors that govern it, and these will be discussed with regards to further work. It is known that *S. pyogenes* can cause vaginitis in pre pubertal children [106,311] and to a lesser extent in adults [312,313]. However, there are very few mouse models available to study this form of infection. The infection of the urogenital tract was only discovered in mice through the use of BPI, and demonstrates how readily *S. pyogenes* can spread between mucosal epithelial sites.

8.6. *CovR/S* MUTATIONS IMPAIR *S. PYOGENES* COLONISATION OF THE NASOPHARYNX

Mutations in the *CovR/S* gene regulator are known to facilitate a change to a phenotype that is considered to be more virulent [78,91,95,96,288]. Mutations in *CovR/S* have been shown to promote survival of *S. pyogenes* in mouse models of invasive infection [49,314]. Increased invasiveness was confirmed in a murine model of intramuscular infection in the current study using the *emm75* pharyngitis isolate (H347) and an isogenic *covR/S* mutant (H494). As expected, the *covR/S* mutant was found to disseminate more readily to other organs than the wild type counterpart. In the context of infection in the nasopharynx however, the deletion of *covR/S* and the expression of a “hypervirulent” phenotype led to a different outcome.

In terms of both continuous carriage and the total duration of carriage, the *covR/S* mutant survived significantly less well than the wild type counterpart. The inflammation caused by the *covR/S* mutant was also diminished compared to the wild type when analysed histopathologically. The utilisation of the previously described co-mingling model of transmission repeatedly showed that recipients housed with mice carrying *covR/S* mutant *S. pyogenes* did not acquire it as readily as those housed with mice carrying the wild type strain. This suggests a general deficit in the ability of the *covR/S* mutant to survive within, and transmit from the nasopharynx. Settle plates were used to evaluate the presence of airborne *S. pyogenes* within these cages, and demonstrated no difference in the presence of either the wild type or the *covR/S* mutant in the air. This suggests that during the early stages of nasopharyngeal infection both the *covR/S* mutant and the wild type strains are aerosolised equally from the nasopharynx, but that, nonetheless, transmission occurs more readily from mice infected with the wild type strain. The numbers of *S. pyogenes* shed from the nasopharynx during the earlier phases of infection were above the upper limit of quantification by direct nasal sampling, and thus made it very difficult to determine whether contact-related shedding differed between the groups. Given that airborne transmission was similar in these early stages, it seemed likely that shedding would be similar. Taken together, the data suggest that transmission of wild-type bacteria was greatest because the wild type bacterium is better able to productively infect recipient mice.

Whilst the *covR/S* mutant survived less well than its wild type counterpart within the nasopharynx, the question of whether it could disseminate systemically from this region remained open. A bioluminescent derivative of the *covR/S* mutant was generated to answer this. In initial intranasal infection studies, dissemination to

various lymph nodes was observed in one mouse. However, further characterisation of this bioluminescent *covR/S* mutant revealed a worrying discrepancy. With regard to the total duration of shedding, there was no significant difference between the bioluminescent *covR/S* mutant and the isogenic bioluminescent counterpart expressing a functional *covR/S* locus. Indeed, in contrast to findings with non-bioluminescent strains, the bioluminescent *covR/S* mutant survived longer in the nasopharynx than the bioluminescent strain expressing wild type *covR/S*. It appeared likely that any fitness cost or advantage imparted by the deletion in *covR/S* was compensated for by the overwhelming fitness cost of expression of the bioluminescence operon. The energy cost incurred by bioluminescence could be implicated, as it would consume resources that would otherwise be used to produce virulence factors and ensure bacterial survival. The loss of *covR/S* could conceivably upregulate the production of these factors to levels that match the wild type. Whilst the duration of continuous carriage was longer, the total duration of carriage was not different to the wild type. This may suggest that in this situation the *covR/S* mutant is impaired in its capacity to transmit and re-infect after the initial cessation of shedding. This is speculation, and further work will be required to fully elucidate the interfering effects of bioluminescence expression on *S. pyogenes* pathogenesis.

In spite of these issues, it was clear that *covR/S* mutation in non-bioluminescent *S. pyogenes* impaired bacterial survival within the nasopharynx. Previous studies have revealed that the inactivation of *covR/S* impairs biofilm formation and adhesion to cells derived from the nasopharynx and the skin [97]. The *covR/S* mutant utilised in this study was also attenuated with respect to biofilm formation. This impairment with respect to biofilm formation may explain why the *covR/S* mutant survives less well within the nasopharynx. The failure to produce biofilm may allow bacteria to be

cleared by the host in spite of their increased virulence factor production. *covR/S* mutant *S. pyogenes* strains produce an abundance of virulence proteins related to resistance to phagocytosis such as SpyCEP and the hyaluronic acid capsule biosynthesis enzymes. It is conceivable that capsule may impede colonisation of the nasopharynx by concealing important adhesion ligands. The deficit in nasopharyngeal survival and transmissibility conferred by mutations in *covR/S* may explain why such bacteria have not become prevalent in community *S. pyogenes* infections despite being advantageous in invasive infection.

8.7. SUMMARY

The models described in this work represent refinements of previous systems to study upper respiratory tract infection by *S. pyogenes*; each model is non-invasive and allows longitudinal monitoring of bacterial infection, using the same mice throughout the study. This has facilitated research which might have otherwise required prohibitively large numbers of animals.

The direct nasal sampling technique and the co-mingling model of transmission have revealed similarities between mouse and human infection, and some differences that needed to be accounted for when translating the findings of this research into the human setting. The studies have also revealed for the first time that *covR/S* mutation impedes infection of, and transmission from the nasopharynx.

Through application of BPI to study infection in the nasopharynx this work demonstrated that immunisation with a vaccine candidate based on SpyCEP provides protection during infection in the nasopharynx. The capacity of BPI to directly quantify bacterial numbers during the course of infection enabled vaccine efficacy to be assessed based on bacterial clearance rather than host survival.

Importantly, the expression of bioluminescence was not in itself neutral to the pathogenesis of *S. pyogenes*. It was found to confer a slight fitness defect *in vitro*, and impaired the competitiveness of *S. pyogenes in vivo*. Furthermore the change in the infectious phenotype caused by the expression of bioluminescence interfered with the effects of *covR/S* mutation in this model.

BPI has the potential for providing useful insights into the pathogenesis of infection. However these insights must be tempered by the knowledge of its flaws, and the acknowledgement that its applicability may be limited in certain situations. BPI is a powerful technique, but must be utilised with care and precision if it is to fulfil its potential.

8.8. Further Work.

8.8.1. Characterisation of the FVB/n mouse strain susceptibility to *S. pyogenes*

In this work, the FVB/n mouse strain was found to be susceptible to *S. pyogenes* colonisation. However, the reasons for this susceptibility remain unknown. Other work investigating the relative susceptibility of different strains of mice to *S. pyogenes* infection such as BALB/k and C3H/HeN have been linked to the variants of MHC class II molecules encoded by the $H2^k$ region. Whilst this locus of susceptibility has been shown to be important in the course of invasive infection, it is not known whether this has a significant effect during the course of nasopharyngeal infection. Differences in innate immunity, for example in complement or AMP's, are most likely to impact upon susceptibility to infection with bacteria such as *S. pyogenes*. In addition to simple cytometric comparisons of neutrophil numbers, and absolute concentrations of complement and AMP, simple *ex vivo* bacterial killing

experiments comparing serum opsonic activity using donor neutrophils could address this potentially. Comparative whole genome sequencing of the FVB/n mouse should reveal candidate loci. If a different locus is responsible for the susceptibility of the FVB/n strain to *S. pyogenes*, its characterisation may provide a useful insight into the underlying factors governing the susceptibility of humans to *S. pyogenes* infection. In addition to this, without more detailed knowledge of the factors governing the susceptibility of the FVB/n mouse, this trait may accidentally be bred out of the strain.

8.8.2. THE STUDY OF THE COMMENSAL BACTERIA WITHIN THE MURINE NASOPHARYNX BEFORE AND DURING *S. PYOGENES* INFECTION

The presence of commensal bacteria within the nasopharynx was briefly investigated during this study with the sole aim of differentiating commensal bacteria from exogenously administered *S. pyogenes*. None of the commensal strains documented in this study were fully speciated, and the use of CBA for direct nasal sampling may have biased the findings in favour of bacteria that are better able to grow on CBA. Certain classes of commensals, such as *Haemophilus* and *Pseudomonas* were more frequently recovered after the onset of *S. pyogenes* infection. Whether this was due to an actual increase in the presence of these bacteria after infection, or whether it was a recovery artefact due to the extensive haemolysis caused by the presence of *S. pyogenes* onto CBA is unclear. It is believed that *S. pyogenes* can interact with other commensal species such as *Streptococcus salivarius* via the production of signalling peptides [315] and lantibiotics which can inhibit the growth of commensal bacteria within the nasopharynx [316]

To better investigate this, direct nasal sampling onto a number of different media could be performed, and genomic techniques could be utilised to speciate the commensals which naturally inhabit the nasopharynx, and observe how the presence of *S. pyogenes* in this region alters the abundance of these commensals and determine whether this interaction plays a role in infection.

8.8.3. THE CHARACTERISATION OF *S. PYOGENES* INFECTION OF THE UROGENITAL TRACT AFTER INFECTION IN THE NASOPHARYNX

In the course of these studies, colonisation of the mouse urogenital tract was observed to occur in some mice as a consequence of nasopharyngeal infection. In preliminary studies, mice that had been pre-treated with β-estradiol showed an increased susceptibility to urogenital colonisation. There are a number of factors which need to be further understood before this could be used to devise a model of *S. pyogenes* vaginitis. The phase of oestrus in which the mouse urogenital tract becomes susceptible to infection needs to be characterised. The bacterial content of this tract must also be studied, in order to see whether any other bacteria take advantage of this susceptibility. Isolates of *S. pyogenes* from cases of vaginitis would need to be tested, in order to determine whether they have a greater tendency to colonise this region than other strains, and whether there are any aspects of their phenotype which enable their infection of this region.

S. pyogenes has also been long known to cause puerperal sepsis, an invasive disease which generally occurs after childbirth. Sepsis is believed to result from an ascending *S. pyogenes* infection that exploits the recently parturient genital tract as a portal of entry. However, strains that cause puerperal sepsis are not generally carried in the genital tract prior to childbirth and appear to be acquired shortly before

invasive infection occurs, from the respiratory tract of either the patient, family member, or healthcare worker[317]. The factors, including strain type, that govern transmission from the respiratory tract to the genital tract are therefore important. An extension to the characterisation of a mouse model of vaginitis would be to develop a mouse model of puerperal sepsis using pregnant mice to dissect the factors which underlie the susceptibility to this disease.

8.8.4. Further studies on transmission, and the relative impact of mouse behaviour

The *emm75* isolate used in this study was found to be readily transmitted from infected mice to uninfected recipients housed in the same cage. Whilst these recipient mice carried *emm75 S. pyogenes*, it appeared that this represented asymptomatic carriage as opposed to clinical infection. However, other pharyngitis strain types of *S. pyogenes,* such as the *emm1* and *emm12* strains studied in this work, showed a greater capacity for virulence during nasopharyngeal infection. As has been shown in this work, the numbers of bacteria shed from the nose correlate with actual bacterial abundance in the nasopharynx. The *emm1* and *emm12* strains may prove to be more transmissible and better able to result in a productive infection than the *emm*75 strain utilised in this study, and may thus be better suited to represent the entire transmission and infection cycle of *S. pyogenes*. Such a transmission model could then be used to test whether vaccinated recipients are more susceptible to infection than adjuvant vaccinated or unvaccinated recipients. The model could also be used to develop a system to study outbreaks that have been strongly associated with highly virulent emm types such as *emm*1.

The model was used in this work to demonstrate the relative impairment of a *covR/S* mutation with respect to transmission. The phenotypic effect was dramatic enough to be detected in spite of the relative variability in transmission between mice. As a result of this variability, mutations which exert more subtle effects may not be as readily detectable.

One of the sources of variability stems from the behaviour of the mice themselves, and the manner in which they interact. To control for this, specialised equipment may be required. The construction of housing in which a partition prevents infected donor mice from physically interacting with recipient mice, but allowing for the free passage of air would enable this to some extent. But even in this situation, the activity of mice would be a source of variability. In studies in humans, airborne transmission of bacteria such as *S. pyogenes* and *S. aureus* was found to be increased during physical exercise [101,318]. A number of technologies could be adapted to monitor the relative effects of this movement. Piezoelectric sensors could be employed to gauge the total movement within a cage during different time periods, and the difference this exerts on the production of airborne *S. pyogenes* could be detected using settle plates. Recent advances in motion tracking using high frame rate cameras can potentially be used to track the interactions of mice with each other and their surroundings and comprehensively control for the effects of movement and aggressive behaviours. However, this particular technology has not yet been developed for such a purpose.

The development of a standardised model of transmission that more accurately represents the *S. pyogenes* pathogenic cycle will enable the more effective testing of strategies to prevent outbreaks of infection and lead to a greater understanding of how this lethal organism spreads within households and institutions.

REFERENCES

1. Carapetis JR, Steer AC, Mulholland EK, Weber M. The global burden of group A streptococcal diseases. Lancet Infectious Diseases **2005**; 5:685–694.

2. Van Arsdale WW On the Present State of Knowledge in Bacterial Science in Its Surgical Relations (Continued). Annals of Surgery **1886**; 3:221–226.

3. Ogston A. Micrococcus poisoning. Journal of Anatomy and Physiology **1882**; 17:24.

4. Quirk WF, Sternbach G. Joseph Jones: Infection with Flesh Eating Bacteria. Journal of Emergency Medicine **1996**; 14:747–753.

5. Klein E. The Etiology of Scarlet Fever. Proceedings of the Royal Society of London **1887**; 42:158–161.

6. Poynton FJ, Paine A. The Present Position Of The Bacteriology Of Rheumatic Fever. British Medical Journal **1901**; 2:779–781.

7. Rammelkamp CH, Weaver RS. Acute Glomerulonephritis. The Significance of the Variations in the Incidence of the Disease. Journal of Clinical Investigation **1952**; 8:345–358.

8. Faber HK, Murray V. Studies in Glomerulonephritis III. An Attempt to Produce Glomerulonephritis by Repeated Injections of Bacteria. Journal of Experimental Medicine **1917**; 26:707–720.

9. Carapetis JR, Gardiner D, Currie BJ, Mathews JD. Multiple strains of *Streptococcus pyogenes* in skin sores of aboriginal Australians. Journal of clinical microbiology **1995**; 33:1471–2.

10. Shaikh N, Leonard E, Martin JM. Prevalence of Streptococcal Pharyngitis and Streptococcal Carriage in Children : A Meta-analysis. Pediatrics **2010**;

11. Strömberg A, Schwan A, Cars O. Throat carrier rates of beta-hemolytic streptococci among healthy adults and children. Scandinavian Journal of Infectious Diseases **1988**; 20:411–7.

12. Anisimova M, Bielawski J, Dunn K, Yang Z. Phylogenomic analysis of natural selection pressure in Streptococcus genomes. BMC Evolutionary Biology **2007**; 7:154.

13. Banks DJ, Beres SB, Musser JM. The fundamental contribution of phages to GAS evolution, genome diversification and strain emergence. Trends in Microbiology **2002**; 10:515–21.

14. Rosch JW, Caparon MG. The ExPortal: an organelle dedicated to the biogenesis of secreted proteins in *Streptococcus pyogenes*. Molecular microbiology **2005**; 58:959–968.

15. Raz A, Fischetti VA. Sortase A localizes to distinct foci on the *Streptococcus pyogene*s membrane. Proceedings of the National Academy of Sciences **2008**; 105:18549–54.

16. Hirst GK, Lancefield RC. Antigenic properties of the type-specific substance derived from group A hemolytic streptococci. Journal of Experimental Medicine **1939**; 69:425..

17. Navarre WW, Schneewind O. Surface Proteins of Gram-Positive Bacteria and Mechanisms of Their Targeting to the Cell Wall Envelope. Microbiology and Molecular Biology Reviews **1999**; 63:174

18. Courtney HS, Von Hunolstein C, Dale JB, Bronze MS, Beachey EH, Hasty DL. Lipoteichoic acid and M protein: dual adhesins of group A streptococci. Microbial Pathogenesis **1992**; 12:199–208.

19. Courtney HS, Hasty DL, Dale JB. Molecular mechanisms of adhesion , colonization , and invasion of group A streptococci. Annals of Medicine **2002**; 34:77–87.

20. Wessels MR, Bronze MS. Critical role of the group A streptococcal capsule in pharyngeal colonization and infection in mice. Proceedings of the National Academy of Sciences **1994**; 91:12238.

21. Dombek PE, Cue D, Sedgewick J, et al. High-frequency intracellular invasion of epithelial cells by serotype M1 group A streptococci : M1 protein- mediated invasion and cytoskeletal rearrangements. Molecular Microbiology **1999**; 31:859–870.

22. Cue D, Dombek PE, Lam H, Cleary PP. *Streptococcus pyogenes* serotype M1 encodes multiple pathways for entry into human epithelial cells. Infection and Immunity **1998**; 66:4593–601.

23. Osterlund A, Engstrand L. An intracellular sanctuary for *Streptococcus pyogenes* in human tonsillar epithelium--studies of asymptomatic carriers and *in vitro* cultured biopsies. Acta Oto-laryngologica **1997**; 117:883–8.

24. Falugi F, Zingaretti C, Pinto V, et al. Sequence variation in group A Streptococcus pili and association of pilus backbone types with lancefield T serotypes. Journal of Infectious Diseases **2008**; 198:1834–41.

25. Becherelli M, Manetti AGO, Buccato S, et al. The ancillary protein 1 of *Streptococcus pyogenes* FCT-1 pili mediates cell adhesion and biofilm formation through heterophilic as well as homophilic interactions. Molecular Microbiology **2012**; 83:1035–47.

26. Edwards AM, Manetti AGO, Falugi F, et al. Scavenger receptor gp340 aggregates group A streptococci by binding pili. Molecular microbiology **2008**; 68:1378–94.

27. Baldassarri L, Creti R, Recchia S, et al. Therapeutic failures of antibiotics used to treat macrolide-susceptible *Streptococcus pyogenes* infections may be due to biofilm formation. Journal of Clinical Microbiology **2006**; 44:2721–7.

28. Nizet V, Beall B, Bast DJ, et al. Genetic Locus for Streptolysin S Production by Group A Streptococcus. Infection and Immunity **2000**;68:4245

29. Ruediger GF. A Study of the Nature of Streptolysin: Second Contribution. Journal of Infectious Diseases **1907**; 1001:277–281.

30. Michos A, Gryllos I, Håkansson A, Srivastava A, Kokkotou E, Wessels MR. Enhancement of streptolysin O activity and intrinsic cytotoxic effects of the group A streptococcal toxin, NAD-glycohydrolase. The Journal of Biological Chemistry **2006**; 281:8216–23.

31. Logsdon LK, Håkansson AP, Cortés G, Wessels MR. Streptolysin O Inhibits Clathrin-Dependent Internalization of Group A Streptococcus. mBio **2011**; 2:1–9.

32. Fernie-King BA, Seilly DJ, Lachmann PJ, Immunology M. The interaction of streptococcal inhibitor of complement (SIC) and its proteolytic fragments with the human beta defensins. Immunology **2004**;111:444–452.

33. Yuste J, Ali S, Sriskandan S, Hyams C, Botto M, Brown JS. Roles of the alternative complement pathway and C1q during innate immunity to *Streptococcus pyogenes*. Journal of Immunology **2006**; 176:6112–20.

34. Sarma JV, Ward P A. The complement system. Cell and Tissue Research **2011**; 343:227–35.

35. Rus H, Cudrici C, Niculescu F. The Role of the Complement System in Innate Immunity. Immunologic Research **2005**;33 :103–112.

36. Blackmore TK, Fischetti VA, Sadlon TA, Ward HM, Gordon DL. M Protein of the Group A Streptococcus Binds to the Seventh Short Consensus Repeat of Human Complement Factor H. Infection and Immunity **1998**; 66:1427–1431.

37. Horstmann RD, Sievertsen HJ, Knobloch J, Fischetti VA. Antiphagocytic activity of streptococcal M protein: selective binding of complement control protein factor H. Proceedings of the National Academy of Sciences **1988**; 85:1657–61.

38. Morfeldt E, Berggård K, Persson J, Johnsson E, Lindahl E, Linse S. Isolated Hypervariable Regions Derived from Streptococcal M Proteins Specifically Bind Human C4b-Binding Protein: Implications for Antigenic Variation. Journal of Immunology **2001**; 167:3870–3877.

39. Thern A, Stenberg L, Dahlback B, Lindahl G. Ig-Binding Surface Proteins of *Streptococcus pyogenes* also bind human C4b-Binding Protein (C4BP), a Regulatory Component of the Complement System. Journal of Immunology **1995**; :375–386.

40. Hryniewicz W, Lipinski B, Jeljaszewicz J. Nature of the interaction between M protein of *Streptococcus pyogenes* and fibrinogen. Journal of Infectious Diseases **1972**; 125:626.

41. Whitnack E, Beachey EH. Inhibition of complement-mediated opsonization and phagocytosis of *Streptococcus pyogenes* by D fragments of fibrinogen and fibrin bound to cell surface M protein. Journal of Experimental Medicine **1985**; 162:1983.

42. Åkesson P, Sjo AG, Bjo L. Protein SIC , a Novel Extracellular Protein of *Streptococcus pyogenes* Interfering with Complement Function. Journal of Biological Chemistry **1996**; 271:1081–1088.

43. Ji Y, Mclandsborough L, Kondagunta A, Cleary PP. C5a peptidase alters clearance and trafficking of group A streptococci by infected mice. Infection and Immunity **1996**; 64:503.

44. Cleary PP, Prahbu U, Dale JB, Wexler DE, Handley J. Streptococcal C5a Peptidase Is a Highly Specific Endopeptidase. Infection and Immunity **1992**; 60:5219.

45. Turner CE, Kurupati P, Jones MD, Edwards RJ, Sriskandan S. Emerging role of the interleukin-8 cleaving enzyme SpyCEP in clinical *Streptococcus pyogenes* infection. Journal of Infectious Diseases **2009**; 200:555–63.

46. Kurupati P, Turner CE, Tziona I, et al. Chemokine-cleaving *Streptococcus pyogenes* protease SpyCEP is necessary and sufficient for bacterial dissemination within soft tissues and the respiratory tract. Molecular Microbiology **2010**; 76:1387–1397.

47. Hidalgo-Grass C, Mishalian I, Dan-Goor M, et al. A streptococcal protease that degrades CXC chemokines and impairs bacterial clearance from infected tissues. The EMBO journal **2006**; 25:4628–37.

48. Jeet Kaur S, Nerlich A, Bergmann S, et al. The CXC chemokine-degrading protease SpyCEP of *Streptococcus pyogene*s promotes its uptake into endothelial cells. Journal of Biological Chemistry **2010**; 285:27798–805.

49. Walker MJ, Hollands A, Sanderson-Smith ML, et al. DNase Sda1 provides selection pressure for a switch to invasive group A streptococcal infection. Nature Medicine **2007**; 13:981–5.

50. Sanderson-Smith ML, Dinkla K, Cole JN, et al. M protein-mediated plasminogen binding is essential for the virulence of an invasive *Streptococcus pyogene*s isolate. The FASEB Journal **2008**; 22:2715–22.

51. Broeseker TA, Boyle MD, Lottenberg R. Characterization of the interaction of human plasmin with its specific receptor on a group A streptococcus. Microbial Pathogenesis **1988**; 5:19–27.

52. Sriskandan S, Cohen J. Kallikrein-kinin system activation in streptococcal toxic shock syndrome. Clinical Infectious Diseases **2000**; 30:961–2.

53. Fenderson PG, Fischetti VA, Cunningham MW. Tropomyosin shares immunologic epitopes with group A streptococcal M proteins. Journal of Immunology **1989**; 142:2475.

54. Cunningham MW, Hall N, Krisher K, Spanier A. A study of anti-group A streptococcal monoclonal antibodies cross-reactive with myosin. Journal of Immunology **1986**; 136:293–8.

55. Guilherme L, Faé KC, Oshiro SE, Tanaka a C, Pomerantzeff PM a, Kalil J. Rheumatic fever: how *S. pyogenes*-primed peripheral T cells trigger heart valve lesions. Annals of the New York Academy of Sciences **2005**; 1051:132–40.

56. Foley J, Wood WB. Studies on the pathogenicity of Group A streptococci II. The antiphagocytic effects of the M protein and the Capsular Gel. Journal of Experimental Medicine **1959**;110 :617–629.

57. Rothbard S. Protective effect of hyaluronidase and type specific Anti-M serum on experimental Group A streptococcal infections. Journal of Experimental Medicine **1948**;88:325-42

58. Sriskandan S, Faulkner L, Hopkins P. *Streptococcus pyogenes*: insight into the function of the streptococcal superantigens. The International Journal of Biochemistry & Cell biology **2007**; 39:12–19.

59. Kuo C-F, Lin Y-S, Chuang W-J, Wu J-J, Tsao N. Degradation of complement 3 by streptococcal pyrogenic exotoxin B inhibits complement activation and neutrophil opsonophagocytosis. Infection and Immunity **2008**; 76:1163–9.

60. Collin M, Olsen A. Effect of SpeB and EndoS from *Streptococcus pyogene*s on Human Immunoglobulins. Infection and Immunity **2001**; 69:7187–7189.

61. Nooh MM, Aziz RK, Kotb M, et al. Streptococcal mitogenic exotoxin, SmeZ, is the most susceptible M1T1 streptococcal superantigen to degradation by the streptococcal cysteine protease, SpeB. The Journal of Biological Chemistry **2006**; 281:35281–8.

62. Berge A, Björck L. Streptococcal Cysteine Proteinase releases Biologically Active Fragments of Streptococcal Surface Proteins. Journal of Biological Chemistry **1995**; 270:9862–9867.

63. Collin M, Olsén A. Extracellular enzymes with immunomodulating activities: variations on a theme in *Streptococcus pyogenes*. Infection and Immunity **2003**; 71:2983.

64. Wannamaker LW. Differences between Streptococcal Infections of Throat and of Skin. New England Journal of Medicine **1970**; 282:23.

65. Lancefield RC. The Significance of M and T antigens in the cross reactions between certain types of group A streptococci. Journal of Experimental Medicine **1940**; :539–550.

66. Lancefield RC, Todd E. Antigenic Differences Between Matt Hemolytic Streptococci and Their Glossy Variants. Journal of Experimental Medicine **1928**; 48:769–790.

67. Facklam R, Beall B, Efstratiou A, et al. emm Typing and Validation of Provisional M Types for Group A Streptococci. Emerging Infectious Diseases **1999**; 5:247–253.

68. Bessen DE, Izzo MW, Fiorentino TR, Caringal RM, Hollingshead SK, Beall B. Genetic Linkage of Exotoxin Alleles and *emm* Gene Markers for Tissue Tropism in Group A Streptococci. Journal of Infectious Diseases **1999**; 179:627–636.

69. Bessen DE, Sotir CM, Readdy TL, Hollingshead SK. Genetic Correlates of Throat and Skin Isolates of Group A Streptococci. Journal of Infectious Diseases **1996**; 173:896–900.

70. Bessen DE, Kumar N, Hall GS, et al. Whole-genome association study on tissue tropism phenotypes in group A Streptococcus. Journal of Bacteriology **2011**; 193:6651–63.

71. Jaggi P, Tanz RR, Beall B, Shulman ST. Age Influences the *emm* Type Distribution of Pediatric Group A Streptococcal Pharyngeal Isolates. The Pediatric Infectious Disease Journal **2005**; 24:1089–1092.

72. Steer AC, Law I, Matatolu L, Beall BW, Carapetis JR. Global *emm* type distribution of group A streptococci: systematic review and implications for vaccine development. Lancet Infectious Diseases **2009**; 9:611–6.

73. Parks T, Smeesters PR, Steer AC. Streptococcal skin infection and rheumatic heart disease. Current Opinion in Infectious Diseases **2012**; 25:145–53.

74. Hirata AA, Terasaki PI. Cross-reactions between streptococcal M proteins and human transplantation antigens. Science **1970**; 168:1095.

75. Shelburne III SA, Sumby P, Sitkiewicz I, Granville C, DeLeo FR, Musser JM. Central role of a bacterial two-component gene regulatory system of previously unknown function in pathogen persistence in human saliva. Proceedings of the National Academy of Sciences **2005**; 102:16037–42.

76. Kreikemeyer B, Mciver KS, Podbielski A. Virulence factor regulation and regulatory networks in *Streptococcus pyogenes* and their impact on pathogen – host interactions. Trends in Microbiology **2003**; 11:224–232.

77. Fogg GC, Caparon MG. Constitutive expression of fibronectin binding in *Streptococcus pyogenes* as a result of anaerobic activation of rofA . Journal of Bacteriology **1997**; 179:6172-6180

78. Graham MR, Smoot LM, Migliaccio CA, et al. Virulence control in group A Streptococcus by a two-component gene regulatory system: global expression profiling and *in vivo* infection modeling. Proceedings of the National Academy of Sciences **2002**; 99:13855–60.

79. Kreikemeyer B, Boyle MD, Buttaro BA , Heinemann M, Podbielski A. Group A streptococcal growth phase-associated virulence factor regulation by a novel operon (Fas) with homologies to two-component-type regulators requires a small RNA molecule. Molecular Microbiology **2001**; 39:392–406.

80. Kobayashi SD, Braughton KR, Whitney AR, et al. Bacterial pathogens modulate an apoptosis differentiation program in human neutrophils. Proceedings of the National Academy of Sciences **2003**; 100:10948–53.

81. Leday T V, Gold KM, Kinkel TL, Roberts S a, Scott JR, McIver KS. TrxR, a new CovR-repressed response regulator that activates the Mga virulence regulon in group A Streptococcus. Infection and Immunity **2008**; 76:4659–68.

82. Chaussee MS, Sylva GL, Sturdevant DE, et al. Rgg Influences the Expression of Multiple Regulatory Loci To Coregulate Virulence Factor Expression in *Streptococcus pyogenes*. Infection and Immunity **2002**;70:762-70

83. Dmitriev A V, McDowell EJ, Kappeler K V, Chaussee M a, Rieck LD, Chaussee MS. The Rgg regulator of *Streptococcus pyogenes* influences utilization of nonglucose carbohydrates, prophage induction, and expression of the NAD-glycohydrolase virulence operon. Journal of Bacteriology **2006**; 188:7230–41.

84. Roberts SA, Scott JR. RivR and the small RNA RivX : the missing links between the CovR regulatory cascade and the Mga regulon. Molecular Microbiology **2007**; 66:1506–1522.

85. Malke H, Ferretti JJ. CodY-affected transcriptional gene expression of *Streptococcus pyogenes* during growth in human blood. Journal of Medical Microbiology **2007**; 56:707–14.

86. Shelburne III SA, Keith D, Horstmann N, et al. A direct link between carbohydrate utilization and virulence in the major human pathogen group A Streptococcus. Proceedings of the National Academy of Sciences **2008**;105:1698-1703

87. Chen C, Bormann N, Cleary PP. VirR and Mry are homologous trans-acting regulators of M protein and C5a peptidase expression in group A streptococci. Molecular and General Genetics **1993**;241 :685–693.

88. Podbielski A, Flosdorff A, Weber-Heynemann J. The group A streptococcal virR49 gene controls expression of four structural vir regulon genes .Infection and Immunity **1995**; 63:9-20

89. McIver KS, Heath AS, Green BD, et al. Specific binding of the activator Mga to promoter sequences of the *emm* and scpA genes in the group A streptococcus Journal of Bacteriology. **1995**; 177:6619-6624

90. Heath A, DiRita VJ, Barg NL, Engleberg NC. A two-component regulatory system, CsrR-CsrS, represses expression of three *Streptococcus pyogenes* virulence factors, hyaluronic acid capsule, streptolysin S, and pyrogenic exotoxin B. Infection and Immunity **1999**; 67:5298.

91. Sumby P, Whitney AR, Graviss EA, DeLeo FR, Musser JM. Genome-Wide Analysis of Group A Streptococci Reveals a Mutation That Modulates Global Phenotype and Disease Specificity. PLoS Pathogens **2006**; 2:0041–0049.

92. Shelburne S a, Olsen RJ, Suber B, et al. A combination of independent transcriptional regulators shapes bacterial virulence gene expression during infection. PLoS Pathogens **2010**; 6:e1000817.

93. Gryllos I, Levin JC, Wessels MR. The CsrR/CsrS two-component system of group A Streptococcus responds to environmental Mg2+. Proceedings of the National Academy of Sciences **2003**; 100:4227–32.

94. Froehlich BJ, Bates C, Scott JR. *Streptococcus pyogenes* CovRS mediates growth in iron starvation and in the presence of the human cationic antimicrobial peptide LL-37. Journal of Bacteriology **2009**; 191:673–7.

95. Ikebe T, Ato M, Matsumura T, et al. Highly frequent mutations in negative regulators of multiple virulence genes in group A streptococcal toxic shock syndrome isolates. PLoS Pathogens **2010**; 6:e1000832.

96. Kansal RG, Datta V, Aziz RK, Abdeltawab NF, Rowe S, Kotb M. Dissection of the molecular basis for hypervirulence of an *in vivo*-selected phenotype of the widely disseminated M1T1 strain of group A Streptococcus bacteria. Journal of Infectious Diseases **2010**; 201:855–65.

97. Hollands A, Pence MA, Timmer AM, et al. Genetic switch to hypervirulence reduces colonization phenotypes of the globally disseminated group A Streptococcus M1T1 clone. Journal of Infectious Diseases **2010**; 202:11-9.

98. Shelburne III SA, Granville C, Tokuyama M, Sitkiewicz I, Patel P, Musser JM. Growth characteristics of and virulence factor production by group A Streptococcus during cultivation in human saliva. Infection and Immunity **2005**; 73:4723.

99. Hamburger M, Robertson OH. Expulsion of group A hemolytic streptococci in droplets and droplet nuclei by sneezing, coughing, and talking. American Journal of Medicine **1948**; 4:690–701.

100. Gralton J, Tovey E, McLaws M-L, Rawlinson WD. The role of particle size in aerosolised pathogen transmission: a review. The Journal of infection **2011**; 62:1–13.

101. Rubbo S, Benjamin M. Transmission of haemolytic streptococci. Journal of Hygiene **1953**; 51:278–292.

102. McKee W, Di Caprio JM, Roberts CE, Sherris JC. Anal carriage as the probable source of a streptococcal epidemic. Lancet **1966**; 2:1007–9.

103. Wannamaker LW. The epidemiology of streptococcal infections. In: McCarty M, ed. Streptococcal Infections. New York: Columbia University Press, 1954.

104. Jaine R, Baker M, Venugopal K. Acute rheumatic fever associated with household crowding in a developed country. The Pediatric Infectious Disease Journal **2011**; 30:315–9.

105. Sherertz RJ, Bassetti S, Bassetti-Wyss B. “Cloud” health-care workers. Emerging infectious diseases **2001**; 7:241–4.

106. Hansen MT, Sanchez VT, Eyster K, Hansen KA. *Streptococcus pyogenes* pharyngeal colonization resulting in recurrent, prepubertal vulvovaginitis. Journal of Pediatric and Adolescent Gynecology **2007**; 20:315–317.

107. Asnes RS, Vail D, Grebin B, Sprunt K. Anal Carrier Rate of Group A Beta-Hemolytic Streptococci in Children With Streptococcal Pharyngitis. Pediatrics **1973**; 52:438.

108. Perry WD, Siegel AC, Rammelkamp CH, Wannamaker LW, Marple EC. Transmission of group A streptococci. I. The role of contaminated bedding. American Journal of Hygiene **1957**; 66:85–95.

109. Rammelkamp CH, Morris AJ, Catanzaro FJ, Wannamaker LW, Chamovitz R, Marple EC. Transmission of group A streptococci: III. The effect of drying on the infectivity of the organism for man. Journal of Hygiene **1958**; 56:280.

110. Claesson BE, Claesson UL. An outbreak of endometritis in a maternity unit caused by spread of group A streptococci from a showerhead. Journal of Hospital Infection **1985**; 6:304–311.

111. Cullingworth CJ. Introductory Address on Puerperal Fever a Preventable Disease: a Plea for the More General Adoption of Antiseptics in Midwifery Practice. British Medical Journal **1888**; 2:743–747.

112. Falkenhorst G, Bagdonaite J, Lisby M, et al. Outbreak of group A streptococcal throat infection: don't forget to ask about food. Epidemiology and Infection **2008**; 136:1165–71.

113. Kanno T, Sakaguchi K, Suzuki J. Time course of virulence factors produced by group A streptococcus during a food-borne epidemic. Journal of infection and Chemotherapy **2012**; 18:35–40.

114. Krause RM, Rammelkamp Jr CH, Denny Jr FW, Wannamaker LW. Studies of the carrier state following infection with group A streptococci. I. Effect of climate. Journal of Clinical Investigation **1962**; 41:568.

115. Kirkbride MB, Wheeler MW, West CD. A Comparative Study of Hemolytic Streptococci from Patients Convalescent from Scarlet Fever. Journal of Infectious Diseases **1930**; 47:16–29.

116. Krause RM, Rammelkamp CH. Studies of the carrier state following infection with group A streptococci II. Infectivity of the streptococci isolated during acute pharyngitis and during the carrier state. Journal of Clinical Investigation **1962**; 41:575–578.

117. Richey DG. Experimental Streptococcic Tonsillitis: The Apparent Inefficacy of Streptococcic Vaccine as Prophylactic. Journal of Infectious Diseases **1919**; 25:299–305.

118. Boughton TH. Injections of Homologous Streptococci Killed by Galactose in the Treatment of Suppurative Complications of Contagious Diseases. Journal of Infectious Diseases **1910**; 7:99.

119. Davis WC, Pachman LM. The effect of heat-killed streptococci on the survival of heart grafts in inbred strains of mice. Journal of immunology **1976**; 116:86.

120. Fiedel B a., Jackson RW. Nephropathy in the rabbit associated with immunization to a group a streptococcal Lipoteichoic acid. Medical Microbiology and Immunology **1979**; 167:251–260.

121. Snider LA, Swedo SE. Post-streptococcal autoimmune disorders of the central nervous system. Current Opinion in Neurology **2003**; 16:359–65.

122. Massell BF, Gabriel Michael J, Amezcua J, Siner M. Secondary and Apparent Primary Antibody Responses After Group A Streptococcal Vaccination of 21 children. Applied Microbiology **1968**; 16:509–518.

123. Massell BF, Honikman LH, Amezcua J. Rheumatic Fever Following Streptococcal Vaccination Report of Three Cases. Journal of the American Medical Association **1969**; 207:1115–1119.

124. Fox EN, Waldman RH, Wittner MK, Mauceri AA, Dorfman A. Protective Study with a Group A Streptococcal M Protein Vaccine. Journal of Clinical Investigation **1973**; 52:1885–1892.

125. Polly S, Waldman R, High P, Wittner MK, Dorfman A, Fox EN. Protective studies with a group A streptococcal M protein vaccine. II. Challenge of volunteers after local immunization in the upper respiratory tract. Journal of Infectious Diseases **1975**; 131:217.

126. D'Alessandri R, Plotkin G, Kluge R, et al. Protective studies with group A streptococcal M protein vaccine. III. Challenge of volunteers after systemic or intranasal immunization with Type 3 or Type 12 group A. Journal of Infectious Diseases **1978**; 138:712–718.

127. Beachey EH, Stollerman GH, Johnson RH, Ofek I, Bisno AL. Human Immune response to immunization with a structurally defined polypeptide fragment of Streptcoccal M-Protein. Journal of Experimental Medicine **1979**; 150:862–877.

128. Hu MC, Walls MA, Stroop SD, Reddish MA, Beall B, Dale JB. Immunogenicity of a 26-valent group A streptococcal vaccine. Infection and Immunity **2002**; 70:2171.

129. Carapetis JR. Group A streptococcal vaccine development : current status and issues of relevance to less developed countries. World Health Organization: Discussion Papers on Child Health **2005**;

130. Bronze MS, Courtney HS, Dale JB. Epitopes of group A streptococcal M protein that evoke cross-protective local immune responses. Journal of Immunology **1992**; 148:888–93.

131. Bauer MJ, Georgousakis MM, Vu T, et al. Evaluation of novel *Streptococcus pyogenes* vaccine candidates incorporating multiple conserved sequences from the C-repeat region of the M-protein. Vaccine **2012**; 30:2197–205.

132. Steer AC, Magor G, Jenney AWJ, et al. emm and C-repeat region molecular typing of beta-hemolytic Streptococci in a tropical country: implications for vaccine development. Journal of clinical microbiology **2009**; 47:2502–9.

133. Cunningham MW, Krisher K, Graves DC. Murine monoclonal antibodies reactive with human heart and group A streptococcal membrane antigens. Infection and Immunity **1984**; 46:34–41.

134. Dudding BA, Ayoub EM. Persistence of Streptococcal Group A antibody in patients with rheumatic Valvular Disease. Journal of Experimental Medicine **1968**; 128:1081–1098.

135. Kawabata S, Kunitomo E, Terao Y, et al. Systemic and mucosal immunizations with fibronectin-binding protein FBP54 induce protective immune responses against *Streptococcus pyogenes* challenge in mice. Infection and Immunity **2001**; 69:924.

136. McArthur JD, Medina E, Mueller A, et al. Intranasal vaccination with streptococcal fibronectin binding protein Sfb1 fails to prevent growth and

dissemination of *Streptococcus pyogenes* in a murine skin infection model. Infection and Immunity **2004**; 72:7342.

137. Guzman C. A, Talay SR, Molinari G, Medina E, Chhatwal GS. Protective immune response against *Streptococcus pyogenes* in mice after intranasal vaccination with the fibronectin-binding protein SfbI. Journal of Infectious Diseases **1999**; 179:901–906.

138. Schulze K, Medina E, Chhatwal GS, Guzman C. A. Stimulation of long-lasting protection against *Streptococcus pyogenes* after intranasal vaccination with non adjuvanted fibronectin-binding domain of the SfbI protein. Vaccine **2003**; 21:1958–1964.

139. Chiarot E, Faralla C, Chiappini N. Targeted Amino Acid Substitutions Impair Streptolysin O Toxicity and Group A Streptococcus Virulence. mBio **2013**; 4: e00387-12

140. Dale JB, Chiang EY, Hasty DL, Harry S, Courtney HS. Antibodies against a Synthetic Peptide of SagA Neutralize the Cytolytic Activity of Streptolysin S from Group A Streptococci. Infection and Immunity **2002**;70:2166

141. Roggiani M, Stoehr J a, Olmsted SB, et al. Toxoids of streptococcal pyrogenic exotoxin A are protective in rabbit models of streptococcal toxic shock syndrome. Infection and Immunity **2000**; 68:5011–7.

142. McCormick JK, Tripp TJ, Olmsted SB, et al. Development of streptococcal pyrogenic exotoxin C vaccine toxoids that are protective in the rabbit model of toxic shock syndrome. Journal of Immunology **2000**; 165:2306–12.

143. Ji Y, Carlson B, Kondagunta A, Cleary PP, Cleary PP. Intranasal immunization with C5a peptidase prevents nasopharyngeal colonization of mice by the group A Streptococcus . Infection and Immunity **1997**; 65:2080.

144. Cleary PP, Matsuka Y V, Huynh T, Lam H, Olmsted SB. Immunization with C5a peptidase from either group A or B streptococci enhances clearance of group A streptococci from intranasally infected mice. Vaccine **2004**; 22:4332–41.

145. Fritzer A, Senn BM, Minh DB, et al. Novel conserved group A streptococcal proteins identified by the antigenome technology as vaccine candidates for a non-M protein-based vaccine. Infection and Immunity **2010**; 78:4051–67.

146. Rodriguez-Ortega M, Norais N, Bensi G, et al. Characterization and identification of vaccine candidate proteins through analysis of the group A Streptococcus surface proteome. Nature Biotechnology **2006**; 24:191–197.

147. Turner CE, Kurupati P, Wiles S, Edwards RJ, Sriskandan S. Impact of immunization against SpyCEP during invasive disease with two streptococcal species: *Streptococcus pyogenes* and *Streptococcus equ*i. Vaccine **2009**; 27:4923–4929.

148. Bensi G, Mora M, Tuscano G, et al. Multi high-throughput approach for highly selective identification of vaccine candidates: the Group A Streptococcus case. Molecular & Cellular Proteomics **2012**;11: M111.015693.

149. McNeil S , Halperin S , Langley JM, et al. Safety and immunogenicity of 26-valent group a streptococcus vaccine in healthy adult volunteers. Clinical Infectious Diseases **2005**; 41:1114–22.

150. Hall MA, Stroop SD, Hu MC, et al. Intranasal Immunization with Multivalent Group A Streptococcal Vaccines Protects Mice against Intranasal Challenge Infections. Infection and Immunity **2004**; 72:2507–2512.

151. Penfound T A, Chiang E Y, Ahmed E A, Dale JB. Protective efficacy of group A streptococcal vaccines containing type-specific and conserved M protein epitopes. Vaccine **2010**; 28:5017–22..

152. Dale JB. Multivalent group A streptococcal vaccine designed to optimize the immunogenicity of six tandem M protein fragments. Vaccine **1999**; 17:193-200

153. Dale JB, Penfound T A, Chiang EY, Walton WJ. New 30-valent M protein-based vaccine evokes cross-opsonic antibodies against non-vaccine serotypes of group A streptococci. Vaccine **2011**; 29:8175–8.

154. Poirier TP, Kehoe MA, Beachey EH. Protective immunity evoked by oral administration of attenuated aroA Salmonella typhimurium expressing cloned streptococcal M protein. Journal of Experimental Medicine **1988**; 168:25–32.

155. Fischetti VA, Hodges WM, Hruby DE. Protection Against Streptococcal Pharyngeal Colonization with a Vaccinia: M Protein Recombinant. Science **1989**; 244:1487–1490.

156. Bessen DE, Fischetti VA. Synthetic peptide vaccine against mucosal colonization by group A streptococci. I. Protection against a heterologous M serotype with shared C repeat region epitopes. Journal of Immunology **1990**; 145:1251–6.

157. Bessen D, Fischetti VA. Influence of intranasal immunization with synthetic peptides corresponding to conserved epitopes of M protein on mucosal colonization by group A streptococci . Journal of Experimental Medicine **1988**; 56:1945–1950.

158. Olive C, Clair T, Yarwood P, Good MF. Protection of mice from group A streptococcal infection by intranasal immunisation with a peptide vaccine that contains a conserved M protein B cell epitope and lacks a T cell autoepitope. Vaccine **2002**; 20:2816–2825.

159. Schulze K, Olive C, Ebensen T, Guzmán C a. Intranasal vaccination with SfbI or M protein-derived peptides conjugated to diphtheria toxoid confers protective immunity against a lethal challenge with *Streptococcus pyogenes*. Vaccine **2006**; 24:6088–95.

160. Sheel M, Pandey M, Good MF, Batzloff MR. Correlation between bioluminescence and bacterial burden in passively protected mice challenged with a recombinant bioluminescent M49 group A streptococcus Strain. Clinical and Vaccine Immunology **2010**; 17:127–33.

161. Batzloff MR, Hayman WA, Davies MR, et al. Protection against Group A streptococcus by immunization with J8 Diptheria toxoid : Contribution of J8 and Diphtheria toxoid specific Antibodies to Protection. Journal of Infectious Diseases **2003**; 187:1598–1608.

162. Batzloff MR, Hartas J, Zeng W, Jackson DC, Good MF. Intranasal Vaccination with a Lipopeptide Containing a Conformationally Constrained Conserved Minimal Peptide , a Universal T Cell Epitope , and a Self-Adjuvanting Lipid Protects Mice from Group A Streptococcus Challenge and Reduces Throat Colonization. Journal of Infectious Diseases **2006**; 194:325–330.

163. Abdel-Aal A-BM, Zaman M, Fujita Y, Batzloff MR, Good MF, Toth I. Design of three-component vaccines against group A streptococcal infections: importance of spatial arrangement of vaccine components. Journal of Medicinal Chemistry **2010**; 53:8041–6.

164. Dale JB, Baird RW, Courtney HS, Hasty DL, Michael S, Bronze MS. Passive Protection of Mice against Group A Streptococcal Pharyngeal Infection by Lipoteichoic Acid. Journal of Infectious Diseases **1994**; 169:319–323.

165. Liu M, Zhu H, Zhang J, Lei B. Active and passive immunizations with the streptococcal esterase Sse protect mice against subcutaneous infection with group A streptococci. Infection and Immunity **2007**; 75:3651–7.

166. Ulrich RG. Vaccine based on a ubiquitous cysteinyl protease and streptococcal pyrogenic exotoxin A protects against *Streptococcus pyogenes* sepsis and toxic shock. Journal of immune Based Therapies and Vaccines **2008**; 6:8.

167. Courtney HS, Hasty DL, Dale JB. Serum Opacity Factor (SOF) of *Streptococcus pyogenes* Evokes Antibodies That Opsonize Homologous and Heterologous SOF-Positive Serotypes of Group A Streptococci. Infection and Immunity **2003**;71:9:5097

168. Ma C, Li C, Wang X, et al. Similar Ability of FbaA with M Protein to Elicit Protective Immunity Against Group A Streptococcus Challenge in Mice. Cellular and Molecular Immunology **2009**; 6:73–77.

169. Okamoto S, Tamura Y, Terao Y, Hamada S, Kawabata S. Systemic immunization with streptococcal immunoglobulin-binding protein Sib 35 induces protective immunity against group A Streptococcus challenge in mice. Vaccine **2005**; 23:4852–9.

170. Park HS, Cleary PP. Active and passive intranasal immunizations with streptococcal surface protein C5a peptidase prevent infection of murine nasal

mucosa-associated lymphoid tissue, a functional homologue of human tonsils. Infection and Immunity **2005**; 73:7878.

171. Huang Y-S, Fisher M, Nasrawi Z, Eichenbaum Z. Defense From the Group A Streptococcus by Active and Passive Vaccination With the Streptococcal Hemoprotein Receptor. Journal of Infectious Diseases **2011**; 203:1595–1601.

172. La Rue Robinson J. Streptococcic Infections. California State Journal of Medicine **1915**; 227–230.

173. Buer J, Balling R. Mice, microbes and models of infection. Nature Reviews Genetics **2003**; 4:195–205.

174. Gay FP, Stone R. Experimental Streptococcus Empyema: Attempts at Prevention and Therapy by Means of Vaccines and Serum. Journal of Infectious Diseases **1920**; 26:265–284.

175. Burtenshaw JML. The mortality of the haemolytic Streptococcus on the skin and on other surfaces. Journal of Hygiene **1938**; 38:575.

176. Leyden JJ, Stewart R, Kligman AM. Experimental infections with group A streptococci in humans. Journal of Investigative Dermatology **1980**; 75:196–201.

177. Dajani AS, Wannamaker LW. History of the Infection Infection of the Skin in the Hamster Simulating Human Experimental Impetigo . I . Natural History of the Infection. Journal of Infectious Diseases **1970**; 122:196–204.

178. Dajani AS, Wannamaker LW. Experimental infection of the skin in the hamster simulating human impetigo III. interaction between staphyococci and group A streptococci. Journal of Experimental Medicine **1971**; 134:588–599.

179. Ashbaugh CD, Warren HB, Carey VJ, Wessels MR. Molecular Analysis of the Role of the Group A Streptococcal Cysteine Protease , Hyaluronic Acid Capsule , and M Protein in a Murine Model of Human Invasive Soft-Tissue Infection. Journal of Clinical Investigation **1998**;102;550-560

180. Raeder R, Boyle MD. Association between Expression of Immunoglobulin G-Binding Proteins by Group A Streptococci and Virulence in a Mouse Skin Infection Model. Infection and Immunity **1993**;61:1378-84

181. Svensson MD, Scaramuzzino DA, Frank C, Debra E, Olse A. Role for a secreted cysteine proteinase in the establishment of host tissue tropism by group A streptococci. Molecular Microbiology **2000**; 38:242–253.

182. Starr C, Engleberg NC. Role of hyaluronidase in subcutaneous spread and growth of group A streptococcus. Infection and Immunity **2006**; 74:40.

183. Selbie FB, Simon RD. Virulence to mice of Staphylococcus pyogenes: its measurement and its relation to certain *in vitro* properties. British Journal of Experimental Pathology **1952**; 33.

184. Sriskandan S, Moyes D, Buttery LK, et al. Streptococcal pyrogenic exotoxin A release, distribution, and role in a murine model of fasciitis and multiorgan failure due to *Streptococcus pyogenes*. Journal of Infectious Diseases **1996**; 173:1399–407.

185. Taylor FB, Bryant AE, Blick KE, et al. Staging of the Baboon Response to Group A Streptococci Administered Intramuscularly : A Descriptive Study of the Clinical Symptoms and Clinical Chemical Response Patterns. Clinical Infectious Diseases **1999**; 29:167–177.

186. Olsen RJ, Sitkiewicz I, Ayeras A, et al. Decreased necrotizing fasciitis capacity caused by a single nucleotide mutation that alters a multiple gene virulence axis. Proceedings of the National Academy of Sciences **2010**; 107:888–93.

187. Neely MN, Pfeifer JD, Caparon MG. Streptococcus-zebrafish model of bacterial pathogenesis. Infection and Immunity **2002**; 70:3904.

188. Phelps H a, Neely MN. SalY of the *Streptococcus pyogenes* lantibiotic locus is required for full virulence and intracellular survival in macrophages. Infection and Immunity **2007**; 75:4541–51.

189. Miller JD, Neely MN. Zebrafish as a model host for streptococcal pathogenesis. Acta Tropica **2004**; 91:53–68.

190. Stevens DL, Bryant a E, Hackett SP, et al. Group A streptococcal bacteremia: the role of tumor necrosis factor in shock and organ failure. Journal of infectious diseases **1996**; 173:619–26.

191. Sriskandan S, Unnikrishnan M, Krausz T, et al. Enhanced susceptibility to superantigen-associated streptococcal sepsis in human leukocyte antigen-DQ transgenic mice. Journal of Infectious Diseases **2001**; 184:166–73.

192. Medina E, Goldmann O, Rohde M, Lengeling A, Chhatwal GS. Genetic control of susceptibility to group A streptococcal infection in mice. Journal of Infectious Diseases **2001**; 184:846–852.

193. Murphy WH, Watson DW. Susceptibility of Inbred mice to Group A Streptococcal Infection. Proceedings of the Society for Experimental biology and Medicine **1957**; 94:755–758.

194. Willoughby DS, Watson DW. Host-Parasite Relationships among Group A Streptococci II. Influence of sex on the susceptibility of inbred mice toward streptococcal infection. Journal of bacteriology **1964**; 87:1457–1461.

195. Faulkner L, Altmann DM, Ellmerich S, Huhtaniemi I, Stamp G, Sriskandan S. Sexual dimorphism in superantigen shock involves elevated TNF-alpha and

TNF-alpha induced hepatic apoptosis. American Journal of Respiratory and Critical Care Medicine **2007**; 176:473–82.

196. Goldmann O, Lehne S, Medina E. Age-related susceptibility to *Streptococcus pyogenes* infection in mice : underlying immune dysfunction and strategy to enhance immunity. Journal of Pathology **2010**; :521–529.

197. Pomales-Lebron A, Morales-Otero P. Hemolytic streptococci from the throat of normal monkeys. Proceedings of the Society for Experimental Biology and Medicine **1940**; 45:509–511.

198. Seegal BC, Heller G, Jablonowitz J. Incidence of Hemolytic Streptococci and Pneumococci in the Pharyngeal Flora of Normal Rhesus Monkeys. Proceedings of the Society for Experimental Biology and Medicine **1936**; 34:812–816.

199. Zimmerman RA, Krushak DH, Wilson E, Douglas JD. Human streptococcal disease syndrome compared with observations in chimpanzees. II. Immunologic responses to induced pharyngitis and the effect of treatment. Journal of Infectious Diseases **1970**; 122:280–289.

200. Ashbaugh CD, Moser TJ, Shearer MH, White GL, Kennedy RC, Wessels MR. Bacterial determinants of persistent throat colonization and the associated immune response in a primate model of human group A streptococcal pharyngeal infection. Cellular Microbiology **2000**; 2:283–92.

201. Virtaneva K, Porcella S. Longitudinal analysis of the group A Streptococcus transcriptome in experimental pharyngitis in cynomolgus macaques. Proceedings of the National Academy of Sciences **2005**; 102:9014–9019.

202. Skinner JM, Caro-Aguilar IC, Payne AM, Indrawati L, Fontenot J, Heinrichs JH. Comparison of rhesus and cynomolgus macaques in a *Streptococcus pyogenes* infection model for vaccine evaluation. Microbial Pathogenesis **2011**; 50:39–47.

203. Olsen RJ, Ashraf M, Gonulal VE, et al. Lower respiratory tract infection in cynomolgus macaques (Macaca fascicularis) infected with group A Streptococcus. Microbial Pathogenesis **2010**; 49:336–47.

204. Hillenius WJ. The evolution of nasal turbinates and mammalian endothermy. Paleobiology **1992**; 18:17–29.

205. Harkema JR, Carey S a, Wagner JG. The nose revisited: a brief review of the comparative structure, function, and toxicologic pathology of the nasal epithelium. Toxicologic Pathology **2006**; 34:252–69.

206. Reznik GK. Comparative Anatomy , Physiology , and Function of the Upper Respiratory Tract. Environmental Health **1990**; 85:171–176.

207. Loo SK, Chin KN. Lymphoid tissue in the nasal mucosa of primates , with particular reference to intraepithelial lymphocytes. Journal of Anatomy **1974**; 117:249–259.

208. Debertin AS, Tschernig T, Tönjes H, Kleemann WJ, Tröger HD, Pabst R. Nasal-associated lymphoid tissue (NALT): frequency and localization in young children. **2003**; :503–507.

209. Wu HY, Nguyen H, Russell MW. Nasal lymphoid tissue (NALT) as a mucosal immune inductive site. Scandinavian Journal of Immunology **1997**; 46:506–513.

210. Cleary PP, Zhang Y, Park H. Nasal associated lymphoid tissue & M cells , a window to persistent streptococcal infections. Indian Journal of Medical Research **2004**; 119:57–60.

211. Coburn A, Evans J, Nathan J. Pathogenicity of *Streptococcus pyogenes*. I. The Experimental Induction of Respiratory Tract Infections in Swiss Albino Mice with Group A Haemolytic Streptococcus. British Journal of Experimental Pathology **1954**;35:270-278

212. Coburn A, Frank P, Nolan J. pathogenicity of *Streptococcus pyogenes*. IV. The relation between the capacity to induce fatal respiratory infections in mice and epidemic respiratory diseases in man. British Journal of Experimental Pathology **1957**;38:256-267

213. Glaser RJ, Berry JW, Loeb LH. Production of Group A Cervical Lymphadenitis in Mice. Proceedings of the Society for Experimental Biology and Medicine **1953**; 82:87–92.

214. Southam DS, Dolovich M, O'Byrne PM, Inman MD. Distribution of intranasal instillations in mice: effects of volume, time, body position, and anesthesia. American Journal of Physiology. Lung Cellular and Molecular Physiology **2002**; 282:L833–9.

215. Eyles JE, Spiers ID, Williamson ED, Alpar HO. Tissue distribution of radioactivity following intranasal administration of radioactive microspheres. Journal of Pharmacy and Pharmacology **2001**; 53:601–7.

216. Park HS, Francis KP, Yu J, Cleary PP. Membranous cells in nasal-associated lymphoid tissue: a portal of entry for the respiratory mucosal pathogen group A streptococcus. Journal of Immunology **2003**; 171:2532.

217. Nelson D, Loomis L, Fischetti VA. Prevention and elimination of upper respiratory colonization of mice by group A streptococci by using a bacteriophage lytic enzyme. Proceedings of the National Academy of Sciences **2001**; 98:4107–12.

218. Stjernquist-Desatnik A, Kurl DN, Schal C, Christensen P. Protective effect of heterologous Gram-positive vaccine against lethal upper respiratory tract

infection with type M50 group A streptococci in mice. Vaccine **1990**; 8:150–152.

219. Batzloff MR, Yan H, Davies MR, et al. Toward the Development of an Antidisease , Transmission-Blocking Intranasal Vaccine for Group A Streptococcus. Journal of Infectious Diseases **2005**; 192:1450.

220. Husmann LK, Yung DL, Hollingshead SK, Scott JR. Role of putative virulence factors of *Streptococcus pyogenes* in mouse models of long-term throat colonization and pneumonia. Infection and Immunity **1997**; 65:1422–30.

221. Hook EW, Wagner RR, Lancefield RC. An epizootic in Swiss mice caused by a group A streptococcus, newly designated type 50. American Journal of Epidemiology **1960**; 72:111.

222. Yung DL, McIver KS, Scott JR, Hollingshead SK. Attenuated expression of the mga virulence regulon in an M serotype 50 mouse-virulent group A streptococcal strain. Infection and Immunity **1999**; 67:6691.

223. Dadd A, Dagnall V, Everall P, Jones A. The survival of *Streptococcus pyogenes* on bacteriological swabs made from various fibres. Journal of Medical Microbiology **1970**; 3:561.

224. Bronze MS, McKinsey DS, Beachey EH, Dale JB. Protective immunity evoked by locally administered group A streptococcal vaccines in mice. Journal of Immunology **1988**; 141:2767–70.

225. Jordan RT, Ohno S. Comparative pathological changes in AKR mice following intranasal instillation of tumor cells and streptococci. Cancer Research **1958**; 18:47–50.

226. Husmann LK, Dillehay DL, Jennings VM, Scott JR. *Streptococcus pyogenes* infection in mice. Microbial Pathogenesis **1996**; :213–224.

227. Broudy TB, Fischetti VA. *In vivo* Lysogenic Conversion of Tox - S*treptococcus pyogenes* to Tox + with Lysogenic Streptococci or Free Phage. Infection and Immunity **2003**; 71:3782–3786.

228. Costalonga M, Cleary PP, Fischer LA, Zhao Z. Intranasal bacteria induce Th1 but not Treg or Th2. Mucosal immunology **2009**; 2:85–95.

229. Hyland KA, Brennan R, Olmsted SB, et al. The early interferon response of nasal-associated lymphoid tissue to *Streptococcus pyogenes* infection. Cell **2009**; 55:422–431.

230. Wang B, Dileepan T, Briscoe S, et al. Induction of TGF-beta1 and TGF-beta1–dependent predominant Th17 differentiation by group A streptococcal infection. Proceedings of the National Academy of Sciences **2010**; 107:5937.

231. Okamoto S, Kawabata S, Fujitaka H, Uehira T. Vaccination with formalin-inactivated influenza vaccine protects mice against lethal influenza *Streptococcus pyogenes* superinfection. Vaccine **2004**; 22:2887–2893.

232. Siegert J, Sastalla I, Chhatwal GS, Medina E. Vaccination equally enables both genetically susceptible and resistant mice to control infection with group A streptococci. Microbes and Infection **2006**; 8:347–353.

233. Okamoto S, Kawabata S. A model of invasive type of *Streptococcus pyogenes* infection after intranasal superinfection in influenza A virus-infected mice. International Congress Series **2004**; 1263:733 – 736.

234. Okamoto S, Kawabata S, Nakagawa I, et al. Influenza A virus-infected hosts boost an invasive type of *Streptococcus pyogenes* infection in mice. Journal of Virology **2003**; 77:4104.

235. Mannam P, Jones KF, Geller BL. Mucosal vaccine made from live, recombinant Lactococcus lactis protects mice against pharyngeal infection with *Streptococcus pyogenes*. Infection and Immunity **2004**; 72:3444.

236. Kurl DN, Stjernquist-Desatnik A, Schalen C, Christensen P. Induction of local immunity to group A streptococci type M50 in mice by non-type-specific mechanisms. Acta Pathologica Microbiologica Scandinavica **1985**; 93:401–5.

237. Wildfeuer A, Heymer B, Schäfer H. The cervical lymph nodes in *Streptococcus pyogenes*, group A, type 50, infection in mice. Medical Microbiology and Immunology **1978**; 137:129–137.

238. Limbago B, McIver KS, Penumalli V, Weinrick B, Scott JR. Restoration of Mga function to a *Streptococcus pyogenes* strain (M Type 50) that is virulent in mice. Infection and Immunity **2001**; 69:1215.

239. Okamoto S, Kawabata S, Terao Y, Fujitaka H, Okuno Y, Hamada S. The *Streptococcus pyogenes* capsule is required for adhesion of bacteria to virus-infected alveolar epithelial cells and lethal bacterial-viral superinfection. Infection and Immunity **2004**; 72:6068.

240. Zinkernagel AS, Timmer AM, Pence MA, et al. The IL-8 protease SpyCEP/ScpC of group A Streptococcus promotes resistance to neutrophil killing. Cell Host & Microbe **2008**; 4:170–8.

241. Lukomski S, Montgomery C a, Rurangirwa J, et al. Extracellular cysteine protease produced by *Streptococcus pyogenes* participates in the pathogenesis of invasive skin infection and dissemination in mice. Infection and Immunity **1999**; 67:1779–88.

242. Dileepan T, Linehan JL, Moon JJ, Pepper M, Jenkins MK, Cleary PP. Robust antigen specific th17 T cell response to group A Streptococcus is dependent on IL-6 and intranasal route of infection. PLoS pathogens **2011**; 7:e1002252.

243. Olive C, Schulze K, Sun HK, et al. Enhanced protection against *Streptococcus pyogenes* infection by intranasal vaccination with a dual antigen component M protein/SfbI lipid core peptide vaccine formulation. Vaccine **2007**; 25:1789–97.

244. Schulze K, Medina E, Guzmán C a. Intranasal immunization with serum opacity factor (SOF) of *Streptococcus pyogenes* fails to protect mice against lethal mucosal challenge with a heterologous strain. Vaccine **2006**; 24:1446–50.

245. Schulze K, Medina E, Towers RJ, Chhatwal GS, Guzman C. A. Characterization of the domain of fibronectin-binding protein I of Streptococcus pyogenes responsible for elicitation of a protective immune response. Infection and Immunity **2001**; 69:622.

246. Cywes C, Stamenkovic I, Wessels MR. CD44 as a receptor for colonization of the pharynx by group A Streptococcus. Journal of Clinical Investigation **2000**; 106:995–1002.

247. Lukomski S, Hoe NP, Abdi I, et al. Nonpolar Inactivation of the Hypervariable Streptococcal Inhibitor of Complement Gene (sic) in Serotype M1 *Streptococcus pyogenes* Significantly Decreases Mouse Mucosal Colonization. Infection and Immunity **2000**; 68:535.

248. Bessen D, Fischetti VA. Passive acquired mucosal immunity to Group A Streptococci by secretory Immunoglobulin A. Journal of Experimental Medicine **1988**; 167:1945–1950.

249. Andreu N, Zelmer A, Wiles S. Noninvasive biophotonic imaging for studies of infectious disease. FEMS Microbiology Reviews **2011**; 35:360–94.

250. Russell WMS, Burch RL. The Principles of Humane Experimental Technique. Methuen, 1959: 238.

251. Troy T, Jekic-McMullen D, Sambucetti L, Rice BW. Quantitative comparison of the sensitivity of detection of fluorescent and bioluminescent reporters in animal models. Molecular Imaging **2004**; 3:9–23.

252. Cheong WF, Prahl SA, Welch AJ. A review of the optical properties of biological tissues. IEEE journal of quantum electronics **1990**; 26:2166–2185.

253. Hilderbrand S a, Weissleder R. Near-infrared fluorescence: application to *in vivo* molecular imaging. Current opinion in chemical biology **2010**; 14:71–9.

254. Shcherbo D, Shemiakina I, Ryabova A. Near-infrared fluorescent proteins. Nature **2010**; 7:1–4.

255. Branchini BR, Southworth TL, Khattak NF, Michelini E, Roda A. Red- and green-emitting firefly luciferase mutants for bioluminescent reporter applications. Analytical biochemistry **2005**; 345:140–8.

256. White EH, McCapra F, Field GF. The Structure and Synthesis of Firefly Luciferin. Journal of the American Chemical Society **1963**; 42.

257. Oba Y, Kato S-I, Ojika M, Inouye S. Biosynthesis of coelenterazine in the deep-sea copepod, Metridia pacifica. Biochemical and biophysical research communications **2009**; 390:684–8.

258. Andreu N, Zelmer A, Fletcher T, et al. Optimisation of bioluminescent reporters for use with mycobacteria. PloS one **2010**; 5:e10777.

259. Berger F, Paulmurugan R, Bhaumik S, Gambhir SS. Uptake kinetics and biodistribution of 14C-D-luciferin--a radiolabeled substrate for the firefly luciferase catalyzed bioluminescence reaction: impact on bioluminescence based reporter gene imaging. European Journal of Nuclear Medicine and Molecular Imaging **2008**; 35:2275–85.

260. Meighen E a. Bacterial bioluminescence: organization, regulation, and application of the lux genes. The FASEB journal **1993**; 7:1016–22.

261. Hill M, James A, Maxted W. Some physical investigations of the behaviour of bacterial surfaces: IX. Studies on the streptococcal cell wall. Biochimica et biophysica acta **1963**; 75:264–274.

262. Francis KPP, Joh D, Bellinger-Kawahara C, Hawkinson MJJ, Purchio TFF, Contag PR. Monitoring bioluminescent *Staphylococcus aureus* infections in living mice using a novel luxABCDE construct. Infection and Immunity **2000**; 68:3594.

263. Riedel CU, Monk IR, Casey PG, et al. An improved luciferase tagging system for *Listeria monocytogenes* allows real-time monitoring *in vivo* and *in vitro*. Applied and Environmental Microbiology **2007**; 73:3091–3094.

264. Henken S, Bohling J, Ogunniyi a D, et al. Evaluation of biophotonic imaging to estimate bacterial burden in mice infected with highly virulent compared to less virulent *Streptococcus pneumoniae* serotypes. Antimicrobial Agents and Chemotherapy **2010**; 54:3155–60.

265. Vuong C, Kocianova S, Jun Y. Development of real-time *in vivo* imaging of device-related *Staphylococcus epidermidis* infection in mice and influence of animal immune status on susceptibility to. Journal of Infectious Diseases **2008**; 198:9–12.

266. Henken S, Bohling J, Martens-Lobenhoffer J, et al. Efficacy profiles of daptomycin for treatment of invasive and noninvasive pulmonary infections with *Streptococcus pneumoniae*. Antimicrobial Agents and Chemotherapy **2010**; 54:707–17.

267. Sanz P, Teel LD, Alem F, Carvalho HM, Darnell SC, O'Brien AD. Detection of *Bacillus anthracis* spore germination *in vivo* by bioluminescence imaging. Infection and immunity **2008**; 76:1036–47.

268. Beyer-Sehlmeyer G, Kreikemeyer B, Hörster A, Podbielski A. Analysis of the growth phase-associated transcriptome of *Streptococcus pyogenes*. International Journal of Medical Microbiology **2005**; 295:161–177.

269. Wiles S, Clare S, Harker J, et al. Organ specificity, colonization and clearance dynamics *in vivo* following oral challenges with the murine pathogen *Citrobacter rodentium*. Cellular Microbiology **2004**; 6:963–72.

270. Wiles S, Crepin VF, Childs G, Frankel G, Kerton A. Use of biophotonic imaging as a training aid for administration of substances in laboratory rodents. Laboratory Animals **2007**; 41:321–8.

271. Wiles S, Pickard KM, Peng K, MacDonald TT, Frankel G. *In vivo* bioluminescence imaging of the murine pathogen *Citrobacter rodentium*. Infection and Immunity **2006**; 74:5391.

272. Sriskandan S, Unnikrishnan M, Krausz T, Cohen J. Molecular analysis of the role of streptococcal pyrogenic exotoxin A (SPEA) in invasive soft-tissue infection resulting from *Streptococcus pyogenes*. Molecular Microbiology **1999**; 33:778–790.

273. Manetti AGO, Zingaretti C, Falugi F, et al. *Streptococcus pyogenes* pili promote pharyngeal cell adhesion and biofilm formation. Molecular Microbiology **2007**; 64:968–983.

274. Taketo M, Schroeder AC, Mobraaten LE, et al. FVB/N: an inbred mouse strain preferable for transgenic analyses. Proceedings of the National Academy of Sciences **1991**; 88:2065.

275. Goff SP. Operating under a Gag order: a block against incoming virus by the Fv1 gene. Cell **1996**; 86:691–3.

276. Teatero SA, Thomassin J-L, Zhu L, Diez E, Malo D, Gruenheid S. The Cri1 Locus is the common genetic cause of susceptibility to *Citrobacter rodentium* infection in C3H and FVB mouse strains. Gut Microbes **2011**; 2:173–177.

277. Diez E, Zhu L, Teatero S a, et al. Identification and characterization of Cri1, a locus controlling mortality during *Citrobacter rodentium* infection in mice. Genes and Immunity **2011**; 12:280–90.

278. Konno M, Baba S, Mikawa H, et al. Study of upper respiratory tract bacterial flora : first report . Variations in upper respiratory tract bacterial flora in patients with acute upper respiratory tract infection and healthy subjects and variations by subject age. Journal of Infection and Chemotherapy **2006**; :83–96.

279. Wiles S, Dougan G, Frankel G. Emergence of a “hyperinfectious ” bacterial state after passage of *Citrobacter rodentium* through the host gastrointestinal tract. Cellular Microbiology **2005**; 7:1163–1172.

280. Flentie KN, Qi M, Gammon ST, et al. Stably integrated luxCDABE for assessment of Salmonella invasion kinetics. Molecular Imaging **2008**; 7:222–233.

281. Qazi SNA, Counil E, Morrissey J, et al. *agr* expression precedes escape of internalized *Staphylococcus aureus* from the host endosome. Infection and Immunity **2001**; 69:7074.

282. Rice BW, Stearns DG, Troy T. Method and Apparatus for Determining target depth, brightness and size within a body region. EP Patent 1,402,243. 2010;

283. Riedel CU, Monk IR, Casey PG, et al. Improved Luciferase Tagging System for *Listeria monocytogenes* Allows Real-Time Monitoring *in vivo* and *in vitro* Applied and Environmental Microbiology **2007**;73:3091-3094

284. Biswas I, Jha JK, Fromm N. Shuttle expression plasmids for genetic studies in *Streptococcus mutans*. Microbiology **2008**; 154:2275.

285. Beard S, Salisbury VC, Lewis RJ, Sharpe J, MacGowan AP. Expression of lux genes in a clinical isolate of *Streptococcus pneumoniae*: using bioluminescence to monitor gemifloxacin activity. Antimicrobial Agents and Chemotherapy **2002**; 46:538.

286. Kobayashi M, Kikuchi D, Okamura H. Imaging of Ultraweak Spontaneous Photon Emission from Human Body Displaying Diurnal Rhythm. PLoS One **2009**; 4:e6256.

287. Devaraj B, Usa M, Inaba H. Biophotons: ultraweak light emission from living systems. Current Opinion in Solid State and Materials **1997**; 2:188–193.

288. Engleberg NC, Heath A, Miller a, Rivera Starr C, DiRita VJ. Spontaneous mutations in the CsrRS two-component regulatory system of *Streptococcus pyogenes* result in enhanced virulence in a murine model of skin and soft tissue infection. Journal of Infectious Diseases **2001**; 183:1043–54.

289. Treviño J, Perez N, Ramirez-Peña E, et al. CovS simultaneously activates and inhibits the CovR-mediated repression of distinct subsets of group A Streptococcus virulence factor-encoding genes. Infection and Immunity **2009**; 77:3141–3149.

290. Lijek RS, Luque SL, Liu Q, Parker D, Bae T, Weiser JN. Protection from the acquisition of *Staphylococcus aureus* nasal carriage by cross-reactive antibody to a pneumococcal dehydrogenase. Proceedings of the National Academy of Sciences of the United States of America **2012**; 109:13823–8.

291. Mcghee JR, Mestecky J, Dertzbaugh MT, Eldridge JH. The mucosal immune system : from fundamental concepts to vaccine development. Vaccine **1992**; 10:75–88.

292. Hollingsworth JW, Whitehead G, Berman KG, et al. Genetic basis of murine antibacterial defense to streptococcal lung infection. Immunogenetics **2007**; 59:713–24.

293. Klein SL. The effects of hormones on sex differences in infection: from genes to behavior. Neuroscience and Biobehavioral Reviews **2000**; 24:627–38.

294. Martin GS, Mannino DM, Eaton S, Moss M. The Epidemiology of Sepsis in the United States from 1979 through 2000. New England Journal of Medicine **2003**; 348:1546–1554.

295. Lee T-P, Chiang B-L. Sex differences in spontaneous versus induced animal models of autoimmunity. Autoimmunity Reviews **2012**; 11:A422–9.

296. Barna M, Komatsu T, Bi Z, Reiss CS. Sex differences in susceptibility to viral infection of the central nervous system. Journal of Neuroimmunology **1996**; 67:31–9.

297. Edwards EA, Dean LM. Effects of Crowding of Mice on Humoral Antibody Formation and Protection to Lethal Antigenic Challenge. Psychosomatic Medicine **1977**; 39:19–24.

298. Brown WA, Allison VD. Carriers and Return Cases in Scarlet Fever. Journal of Hygiene **1935**; 35:283–99.

299. Lamagni TL, Darenberg J, Luca-Harari B, et al. Epidemiology of severe *Streptococcus pyogenes* disease in Europe. Journal of clinical microbiology **2008**; 46:2359–67.

300. Siljander T, Lyytikäinen O, Vähäkuopus S. Epidemiology , outcome and *emm* types of invasive group A streptococcal infections in Finland. European Journal of Clinical Microbiology & Infectious Diseases **2010**;29 :1229–1235.

301. Inthorn D, Andress H. Incidence and mortality of severe sepsis in surgical intensive care patients : the influence of patient gender on disease process and outcome. Intensive Care Medicine **2000**;26 :167–172.

302. Hajjeh RA, Reingold A, Weil A, Shutt K, Schuchat A, Perkins BA. Toxic Shock Syndrome in the United States: Surveillance Update 1976-1996. Emerging Infectious diseases **1999**; 5:1997–2000.

303. Medina E. Models of group A streptococcal diseases: a review of current status. Drug Discovery Today: Disease Models **2004**; 1:65–71.

304. Coburn A, Evans J, Nathan J. Studies on the Pathogenicity of *Streptococcus pyogenes.* II. Factors Which Influence the Infectivity of Group A Haemolytic Streptococcus in Swiss Albino Mice. British Journal of Experimental Pathology **1954**;35 :279–293..

305. Slade HD, Coburn AF, Simich L. Studies on the pathogenicity of *Streptococcus pyogenes* III. The utilisation of 59-Fe, 65-Zn and 32-P by Group A Streptococcus and the quantitative determination of the air-borne infection of mice with “tagged” cells. British Journal of Experimental Pathology **1955**;36 :566–572.

306. Ayoub EM, Anthony BF, Mauceri AA, Sanders WE. Asymptomatic Epidemic Acquisition of Group A Streptococcus : Antibody Response to Extracellular and Type-Specific Antigens. Journal of Infectious Diseases **1975**; 132:20–27.

307. Roberts AL, Connolly KL, Kirse DJ, et al. Detection of group A Streptococcus in tonsils from pediatric patients reveals high rate of asymptomatic streptococcal carriage. BMC pediatrics **2012**; 12:3.

308. Meer JR Van Der, Tropel D, Jaspers M. Illuminating the detection chain of bacterial bioreporters. Environmental microbiology **2004**; 6:1005–1020.

309. Pfoh E, Wessels MR, Goldmann D, Lee GM. Burden and economic cost of group A streptococcal pharyngitis. Pediatrics **2008**; 121:229–34.

310. Grandi G, Margarit IYR, Capo S, Bensi G, Manetti AGO. Combination GAS Vaccines and Therapeutics. United States Patent and Trademark Office, **2010** Patent no: US 2010/0136041 A1,

311. Morris C. Seasonal variation of streptococcal vulvo-vaginitis in an urban community. Journal of Clinical Pathology **1971**; 24:805–7.

312. Ugurlu G, Van der Houwen C, Brandenburg A, Schreuder I, Bogchelman D. *Streptococcus pyogenes* vaginitis in a postmenopausal woman. European Journal of Obstetrics & Gynecology and Reproductive Biology **2008**; 138:115.

313. Verstraelen H, Verhelst R, Vaneechoutte M, Temmerman M. Group A streptococcal vaginitis: an unrecognized cause of vaginal symptoms in adult women. Archives of Gynecology and Obstetrics **2011**; 284:95–8.

314. Cole JN, Pence M a, Von Köckritz-Blickwede M, et al. M Protein and Hyaluronic Acid Capsule Are Essential for *In vivo* Selection of covRS Mutations Characteristic of Invasive Serotype M1T1 Group A Streptococcus. mBio **2010**; 1:e00191.

315. Upton M, Tagg JR, Wescombe PA, Jenkinson H. F. Intra-and interspecies signaling between *Streptococcus salivarius* and *Streptococcus pyogenes* mediated by SalA and SalA1 lantibiotic peptides. Journal of bacteriology **2001**; 183:3931.

316. Hynes W, Tagg J. Production of Broad-Spectrum Bacteriocin-Like Activity by Group A Streptococci of Particular M-Types. Zentralblatt für Bakteriologie, Mikrobiologie, und Hygiene. Series A **1985**; 259:155–164.

317. Sriskandan S. Severe peripartum sepsis. The Journal of the Royal College of Physicians of Edinburgh **2011**; 41:339–46.

318. Hare R, Thomas CG. The transmission of *Staphylococcus aureus*. British Medical Journal **1956**; 2:840–4.

OPEN ACCESS Freely available online

PLOS ONE

Inactivation of the CovR/S Virulence Regulator Impairs Infection in an Improved Murine Model of *Streptococcus pyogenes* Naso-Pharyngeal Infection

Faraz M. Alam[1], Claire E. Turner[1], Ken Smith[2], Siouxsie Wiles[1,3], Shiranee Sriskandan[1]*

1 Section of Infectious Diseases and Immunity, Department of Medicine, Imperial College London, London, United Kingdom, **2** Department of Pathology and Infectious Diseases, Royal Veterinary College, Hertfordshire, United Kingdom, **3** Department of Molecular Medicine and Pathology, University of Auckland, Auckland, New Zealand

Abstract

Streptococcus pyogenes is a leading cause of pharyngeal infection, with an estimated 616 million cases per year. The human nasopharynx represents the major reservoir for all *S. pyogenes* infection, including severe invasive disease. To investigate bacterial and host factors that influence *S. pyogenes* infection, we have devised an improved murine model of nasopharyngeal colonization, with an optimized dosing volume to avoid fulminant infections and a sensitive host strain. In addition we have utilized a refined technique for longitudinal monitoring of bacterial burden that is non-invasive thereby reducing the numbers of animals required. The model was used to demonstrate that the two component regulatory system, CovR/S, is required for optimum infection and transmission from the nasopharynx. There is a fitness cost conferred by *covR/S* mutation that is specific to the nasopharynx. This may explain why *S. pyogenes* with altered *covR/S* have not become prevalent in community infections despite possessing a selective advantage in invasive infection.

Citation: Alam FM, Turner CE, Smith K, Wiles S, Sriskandan S (2013) Inactivation of the CovR/S Virulence Regulator Impairs Infection in an Improved Murine Model of *Streptococcus pyogenes* Naso-Pharyngeal Infection. PLoS ONE 8(4): e61655. doi:10.1371/journal.pone.0061655

Editor: Adam J. Ratner, Columbia University, United States of America

Received December 1, 2012; **Accepted** March 12, 2013; **Published** April 25, 2013

Copyright: © 2013 Alam et al. This is an open-access article distributed under the terms of the Creative Commons Attribution License, which permits unrestricted use, distribution, and reproduction in any medium, provided the original author and source are credited.

Funding: This work was supported by the Biotechnology and Biological Sciences Research Council via the Centre for Integrative Mammalian Physiology and Pharmacology [DDDH.PS0618] and the National Centres for Replacement, Refinement and Reduction of Animals in Research. The funders had no role in study design, data collection and analysis, decision to publish, or preparation of the manuscript.

Competing Interests: The authors have declared that no competing interests exist.

* E-mail: s.sriskandan@imperial.ac.uk

Introduction

Streptococcus pyogenes is estimated to cause 616 million cases of pharyngeal infection per year, and 663,000 cases of invasive disease [1]. As the human nasopharynx represents the major reservoir for all types of *S. pyogenes* infection, it is essential to develop a better understanding of the factors that influence upper respiratory tract infection.

Despite their limitations, mice play an important role in infectious diseases research [2]. The mouse nasopharynx has structural similarities to the nasal turbinate system in humans [3], although mice lack tonsils [4]. Instead, mice possess nasal associated lymphoid tissue (NALT), which shares some similarity to the tonsils [5] and has been shown to be a target for infection by *S. pyogenes* [6]. Indeed, mice have been used by several groups to investigate *S. pyogenes* in the upper respiratory tract, although there is no consensus on which is the most appropriate strain, sex or age of animal to use [6,7,8,9,10]. Furthermore, the maximum dose volume posited for establishing infection by previous studies ranges from 5 µl, as determined by administration of colored dye [8,11], 10 µl as determined by radioactive microspheres [10,12], to 20 µl volumes [6]. This is an important consideration, as aspiration of the bacteria into the lungs has the potential to trigger a more invasive disease and systemic infection.

It is known that phenotypic differences can exist between nasopharyngeal and invasive *S. pyogenes* isolates, and these have been ascribed to altered activity or mutation of the streptococcal two component regulatory system, *covR/S* [13]. As a result of signalling from the sensor kinase, CovS, CovR represses a range of virulence factors concerned with resistance to phagocytosis, such as the capsule synthesis operon *has*ABC, the DNase, *sda*, and the CXC chemokine protease, SpyCEP [13,14,15,16,17]. Mutations in *covR/S* de-repress these virulence genes, conferring a selective advantage to *S. pyogenes* in mouse models of invasive infection, leading to greater mortality [15,18]. However, the impact of such mutations on nasopharyngeal infection is unclear. Isolates of *S. pyogenes* with *covS* mutations bind less well to skin cells in vitro and in vivo than those without the mutation [19]. Furthermore, *S. pyogenes* with mutations in *covS* lack competitiveness in the saliva relative to wild type [20].

In this work, we set out to produce a longitudinally monitored murine model of nasopharyngeal infection, by examining the effect of mouse strain, age and sex on *S. pyogenes* carriage. We evaluated *S. pyogenes* pharyngitis isolates from patients rather than a previously-described mouse-pathogenic strain that lacks a functional copy of the multigene activator, *mga* [21,22]. The improved nasopharyngeal infection model was used to evaluate the impact of the *S. pyogenes* CovR/S two component regulatory system on longevity and transmission of *S. pyogenes* upper respiratory tract infection.

Methods

Ethics Statement

In vivo experiments were performed in accordance with the Animals (scientific Procedures) Act 1986, subject to protocols set

Table 1. Bacterial strains used in this study.

Strain Designation	Emm type	Species	Description	Ref.
H305	*emm1*	*S. pyogenes*	Scarlet fever reference strain	[23]
H343	*emm2*	*S. pyogenes*	Pharyngitis isolate	[16]
H292	*emm81*	*S. pyogenes*	Blood isolate	[16]
H347	*emm75*	*S. pyogenes*	Pharyngitis isolate	[16]
H494	*emm75*	*S. pyogenes*	Strain H347 with an inactivated *covR/S* operon	[16]
ICC180		*C. rodentium*	Bioluminescent derivative of ICC169	[24]

doi:10.1371/journal.pone.0061655.t001

out in PPL 70/7379 that were approved by the Imperial College Ethical Review Process (ERP) panel and the UK Home Office.

Bacterial Strains

The bacterial strains used in this study are given in Table 1 [16,23,24]. Streptococcal strains were cultured in Todd Hewitt Yeast broth (THY) or on Columbia Blood Agar (CBA), while Luria Bertani (LB) medium was used for culturing *C. rodentium* ICC180. All strains were grown at 37°C. For animal experiments, *S. pyogenes* was grown without shaking with 5% CO_2 overnight, centrifuged at 1864×g, (Sorvall RTH 750 Rotor), washed twice in phosphate buffered saline (PBS), and re-suspended in PBS to produce an inoculum of $1–7\times10^8$ colony forming units (cfu) per 5 µl. Numbers of viable bacteria within the inoculum were retrospectively assessed by plating of 10^{-6}–10^{-8} dilutions of the inoculum onto agar.

Animals

Male and female 5–10 week old CD1, C57BL/6, A/J, BALB/c, FVB/n specific-pathogen free mice (Harlan, UK) were maintained in individually HEPA filtered cages with sterile bedding and free access to sterilized food and water. GLP Mini Fun Tunnels (Lillico), or Des. Res. Mini Mouse Houses (Lillico) were provided in each cage for environmental enrichment.

Intranasal Infection

Pilot experiments were conducted using $\sim10^9$ cfu in doses of 2.5 µl–20 µl bioluminescent *C. rodentium* ICC180 [24] to determine the correct dosing strategy to deliver bacteria to the murine nasopharynx without lung involvement. Bioluminescence (as photons s^{-1} cm^{-2} steridian [sr] $^{-1}$) from living animals was performed as previously described [24] using an IVIS® 100 system (Perkin Elmer).

For streptococcal infection of the nasopharynx, $1–7\times10^8$ cfu of *S. pyogenes* was administered intranasally using a pipette to mice in a volume of 2.5 µl per nostril under 2–5% isoflurane anaesthesia. Mice were weighed daily; reduction by 20% of original weight was a defined humane endpoint.

Intramuscular Infection

6×10^8 cfu *S. pyogenes* were administered to mice under isoflurane anaesthesia via injection with a 27 gauge needle into the right lateral thigh. Numbers of viable bacteria within the inoculum were assessed by retrospective plating of 10^{-6}–10^{-8} dilutions. At 72 hours, the right thigh muscle and ipsilateral inguinal node were extracted, weighed and homogenized into PBS and then plated out onto CBA for bacterial enumeration.

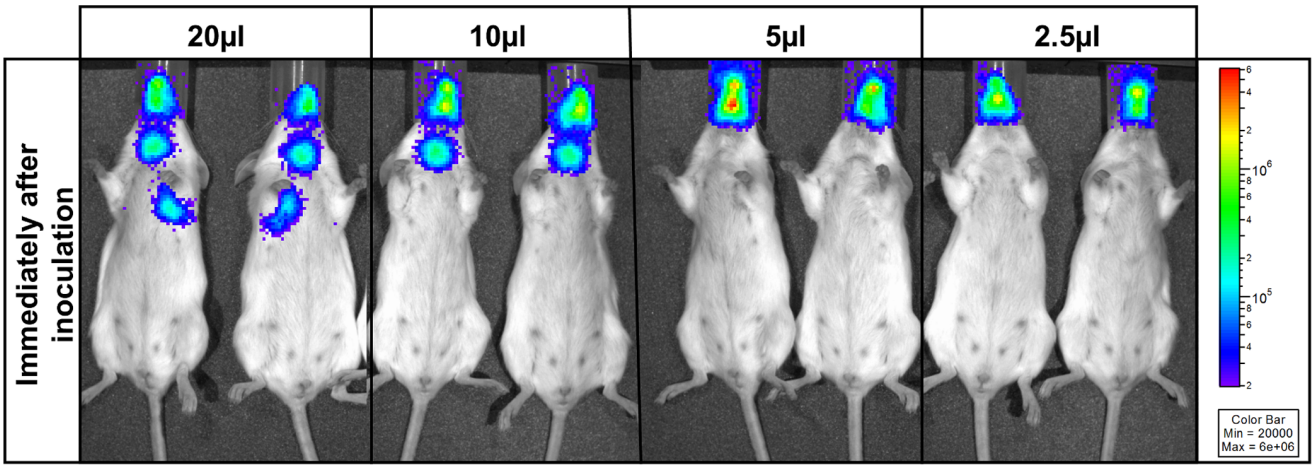


Figure 1. Bioluminescence imaging of bacterial distribution after intranasal inoculation with bioluminescent *C. rodentium*. 10^9 colony forming units (cfu) of bioluminescent *C. rodentium* were administered intranasally to 8 week old CD1 outbred female mice in 20 µl (n = 3), 10 µl (n = 2), 5 µl (n = 3) and 2.5 µl (n = 2) of PBS. Images were acquired using an IVIS spectrum system, and are displayed as images of peak bioluminescence, with variations in colour representing light intensity at a given location. Red represents the most intense light emission, while blue corresponds to the weakest signal. The colour bar indicates relative signal intensity (as photons s^{-1} cm^2 sr^{-1}). Two representative mice shown for each group.
doi:10.1371/journal.pone.0061655.g001

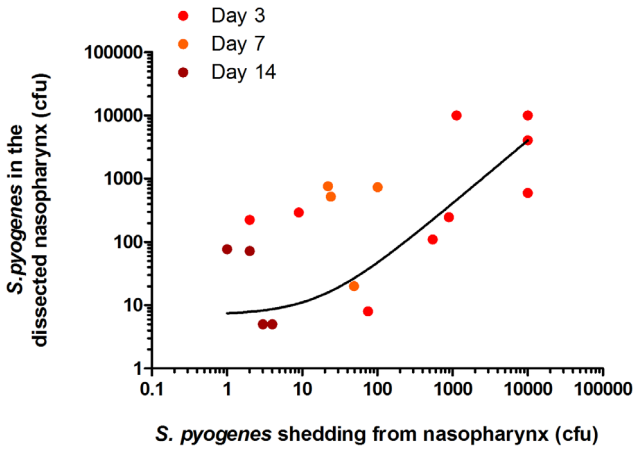


Figure 2. Correlation between *S. pyogenes* recovered from nasal shedding and from nasopharyngeal dissection. Data are pooled from direct nasal samples taken on days 3, 7, and 14 from five week old female FVB/n mice during intranasal infection with *emm75 S. pyogenes* (1.3×10^8 cfu) were compared to bacterial numbers obtained on dissection on the same days. ($r^2>0.95$, n = 36). Data shown from individual mice.
doi:10.1371/journal.pone.0061655.g002

Nasal Sampling

The level of shedding of *S. pyogenes* from the nasopharynx was assessed longitudinally using direct nasal sampling. The nares of each mouse were gently pressed onto the surface of a CBA plate ten times. Exhaled particulates were streaked out, and the plates were then incubated overnight at 37°C with 5% CO_2 for bacterial enumeration. In preliminary experiments using naive, non-infected mice, α-hemolytic streptococci, staphylococci, pseudomonads and corynebacteria were recovered, but no β hemolytic Group A streptococci were found to naturally colonize the mouse nasopharyngeal tract.

For experiments where mice had been infected with *S. pyogenes*, β-hemolytic colonies were counted for each mouse and confirmed as *S. pyogenes* through Gram staining, catalase testing, oxidase testing, and Lancefield grouping. No other β-haemolytic bacteria were recovered from the mouse nasopharynx. Kaplan-Meier plots were created to analyse the duration of *S. pyogenes* shedding. Nasal samples were taken for 21 days post inoculation. Mice were determined to have stopped shedding upon the first instance of a nasal sample turning up negative.

In some studies, the nasopharynx was dissected and removed at fixed time points for microbiological culture. To ensure complete extraction of the nasopharynx, the skin and mandibles were removed to expose the cranium. This was then sectioned along the coronal plane at the bregma. The brain tissue within the cranium anterior to this incision was removed, exposing the posterior aspect of the nasal cavity, known as the cribriform plate. The orbits were removed from this tissue via sagittal incisions lateral to the premaxilla. The remaining tissue comprised the entire nasal cavity, and NALT. This was homogenized into PBS and serial dilutions plated onto CBA to quantify *S. pyogenes* from the whole nasopharynx.

Settle Plates

To detect the presence of airborne bacteria within cages of infected mice, CBA plates were placed in the upper rack of the individually HEPA filtered cages (n = 4 plates per cage) and exposed for defined time periods throughout each experiment.

Table 2. Duration of shedding of different strains of *S. pyogenes* (7×10^8 cfu per 5 µl dose) in 8 week old male BALB/c mice after intranasal infection.

	Number of mice shedding *S. pyogenes*		
	Day 1	**Day 2**	**Day 3**
***emm*1**	0/7	0/7	0/7
***emm*2**	1/7	1/7	1/7
emm75	4/7	3/7	2/7
***emm*81**	1/7	0/7	0/7

doi:10.1371/journal.pone.0061655.t002

Plates then incubated overnight at 37°C and the numbers of *S. pyogenes* colonies, (identified by Gram staining, catalase testing, and Lancefield grouping) were enumerated.

Histopathology

The head of each mouse was removed at the atlanto-occipital joint and sagittally hemi-sected. One half was fixed in formalin and processed routinely to paraffin wax, while the other was homogenised and plated to assess *S. pyogenes* numbers in the nasopharynx. Paraffin sections were cut at 6 µm and stained with Haematoxylin and Eosin and Gram stains. The degree of nasal damage and inflammation was scored as : No significant abnormality (Intact nasal mucosa and absence of inflammation), Mild (Focal erosion of the mucosa with local neutrophil exocytosis across the affected epithelium), Moderate (Focal necrosis and ulceration of the mucosa with local neutrophilic exocytosis and surface neutrophilic exudation), Marked (Extensive necrosis and ulceration of the mucosa with widespread neutrophilic exocytosis and surface neutrophilic exudation) and Severe (Extensive necrosis and ulceration of the mucosa with widespread neutrophilic exocytosis and surface neutrophilic exudation and with extension of necrosis into underlying stroma). Slides were reviewed and scored by an experienced histopathologist (KS).

Statistics

For statistical analysis of Kaplan-Meier curves, the Mantel-Cox Logrank test was applied. For statistical analysis of colony count comparisons, a non-parametric Kruskal-Wallis test and Dunn's post-test were used. *P* values less than 0.05 were defined as significant. Statistics were performed using Prism Graphpad version 5.02. Data are presented as median, ± interquartile range.

Results

Volume of Inoculum Determines Distribution within the Respiratory Tract

Bioluminescence imaging demonstrated that dose volumes of 20 µl volume delivered bacteria to the lungs, whereas this was not shown with lower volumes (Figure 1). Any dose volume above 10 µl was deposited in the trachea. Dose volumes of 5 µl and 2 µl did not distribute bacteria to the lungs. As the optimal dose volume for nasopharyngeal deposition without lung involvement or significant nasal clearance was 5 µl (2.5 µl per nostril), this was the volume used in subsequent experiments.

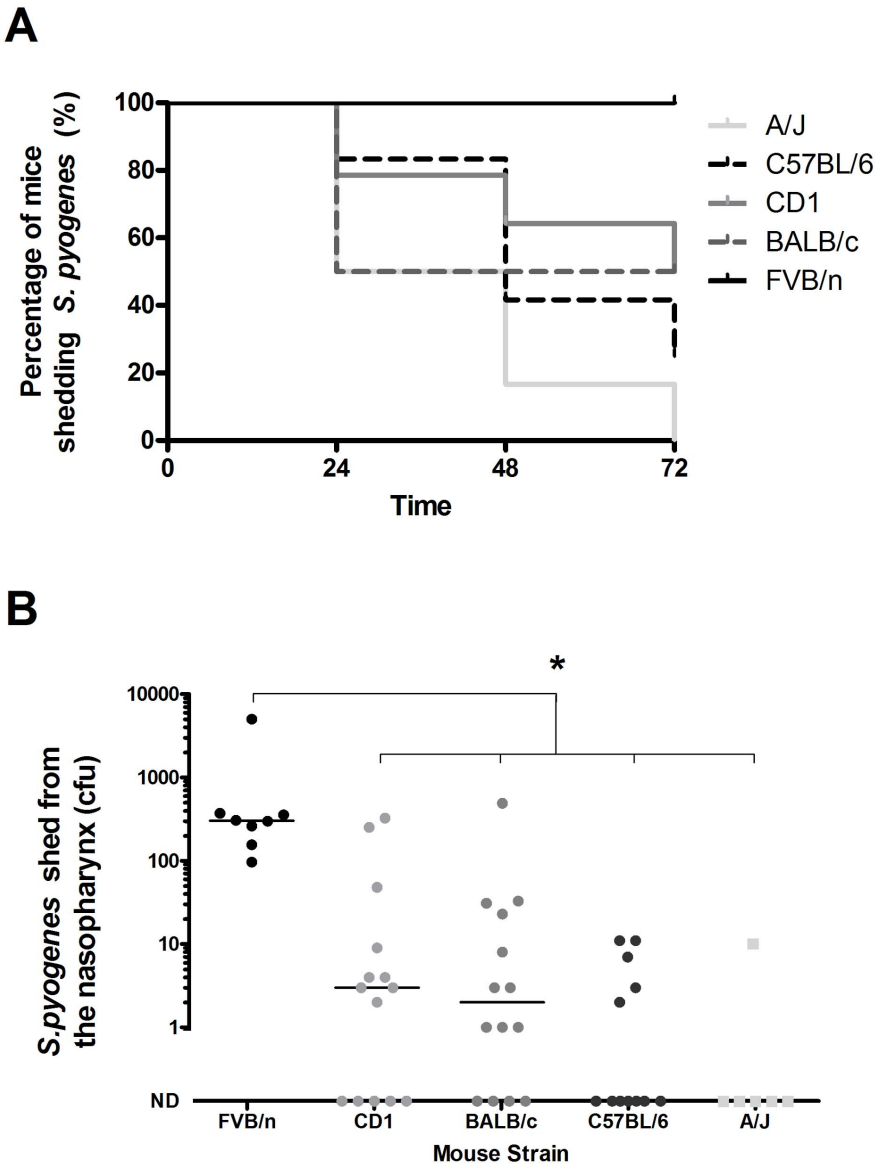


Figure 3. Comparison of nasopharyngeal shedding of *S. pyogenes* between different mouse strains. Five week old male mice of different strain backgrounds were inoculated intranasally with *emm*75 *S. pyogenes* (1.5×10^8 cfu). Duration and quantity of shedding were determined from colonies recovered from direct nasal sampling of the mouse nasopharynx. (A) Kaplan-Meier plot showing percentage of mice shedding *S. pyogenes* in each group. (B) Bacterial counts shed by FVB/n (n = 8) CD1 (n = 14), BALB/c (n = 14), C57BL/6 (n = 12) and A/J (n = 6) at 72 hours. Individual points represent individual mice. (Kruskal Wallis with Dunns Post Test $p<0.05$). Bars indicate the median, ND = no detectable bacteria.
doi:10.1371/journal.pone.0061655.g003

Nasopharyngeal Shedding as a Method to Longitudinally Monitor S. pyogenes Infection in the Upper Respiratory Tract

To select an appropriate bacterial strain for development of the model, BALB/c mice were intranasally inoculated with four clinical *S. pyogenes* strains of different *emm* genotypes. An *emm*75 pharyngitis strain was found to have shed for the longest period using direct nasal sampling (Table 2) and was used in subsequent experiments. Importantly, a significant correlation was found between the numbers of colonies recovered from nasal shedding of *S. pyogenes* and bacterial numbers from dissected and homogenised nasal tissue on the same day (Figure 2, $r^2>0.95$, n = 36). This longitudinal method of monitoring was therefore employed in subsequent experiments consistent with the principles of the 3Rs (Replacement, Refinement, and Reduction) by reducing the numbers of animals used.

Longevity of Nasopharyngeal Shedding is Greater in FVB/n Mice

To determine the most appropriate mouse strain for model development, male mice of different host backgrounds were infected intranasally with *emm*75 *S. pyogenes*, and observed longitudinally for 72 h using direct nasal sampling. Data were used to create Kaplan Meier plots to analyse the duration of shedding for each strain of mouse (Figure 3 A). FVB/n mice carried *S. pyogenes* longer and shed significantly more *S. pyogenes* on the final day of the time course than all other strains tested

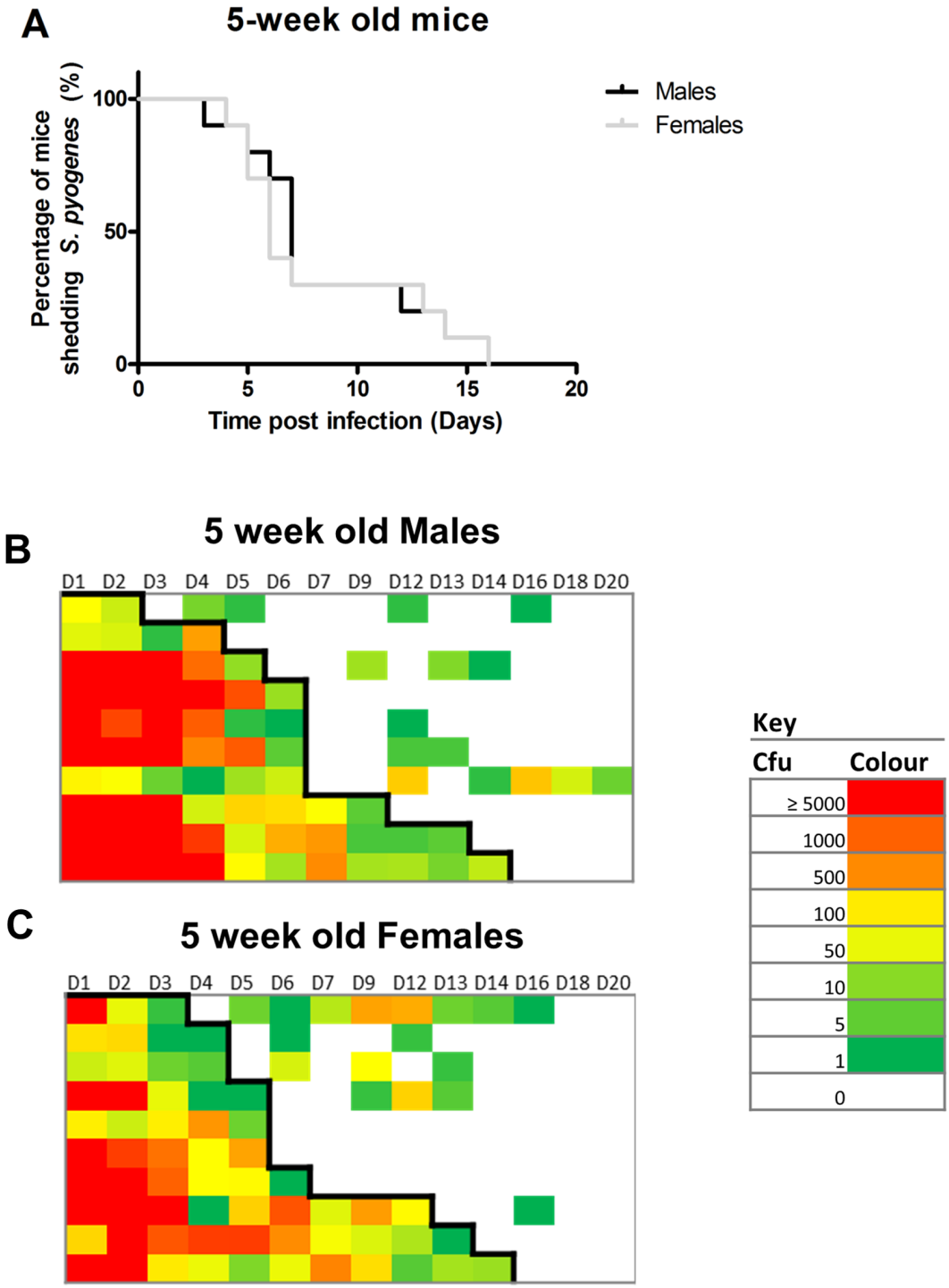


Figure 4. Sex differences in *S. pyogenes* nasopharyngeal carriage and shedding intensity in 5 week old mice. Male and female FVB/n mice 5 weeks (A, $p>0.05$ Mantel–Cox Logrank test, n = 10) of age were infected intranasally with *emm75 S. pyogenes* (1.1×10^8 cfu) and sampled non-invasively through direct nasal sampling over 21 days. Shedding intensity maps display the data from direct nasal samples throughout the time course from the male mice (B) and the female mice (C). Rows indicate individual mice throughout the time course, colours indicate the numbers of *S. pyogenes* recovered from direct nasal samples with red indicating the highest recorded levels of carriage (≥5000 cfu) and green indicates the lowest levels of carriage (1 cfu) and blank blocks indicate no recovery of *S. pyogenes*. Black line indicates survival based on the first loss of carriage.
doi:10.1371/journal.pone.0061655.g004

(Figure 3 B). FVB/n mice carried *S. pyogenes* were therefore used for all future studies.

Gender has an Effect on the Nasopharyngeal Carriage of *S. pyogenes* that is Dependent on the Age of the Mice

To determine whether gender influenced *S. pyogenes* infection of the nasopharynx, peri pubertal (n = 10 per group, 5 per cage, 5

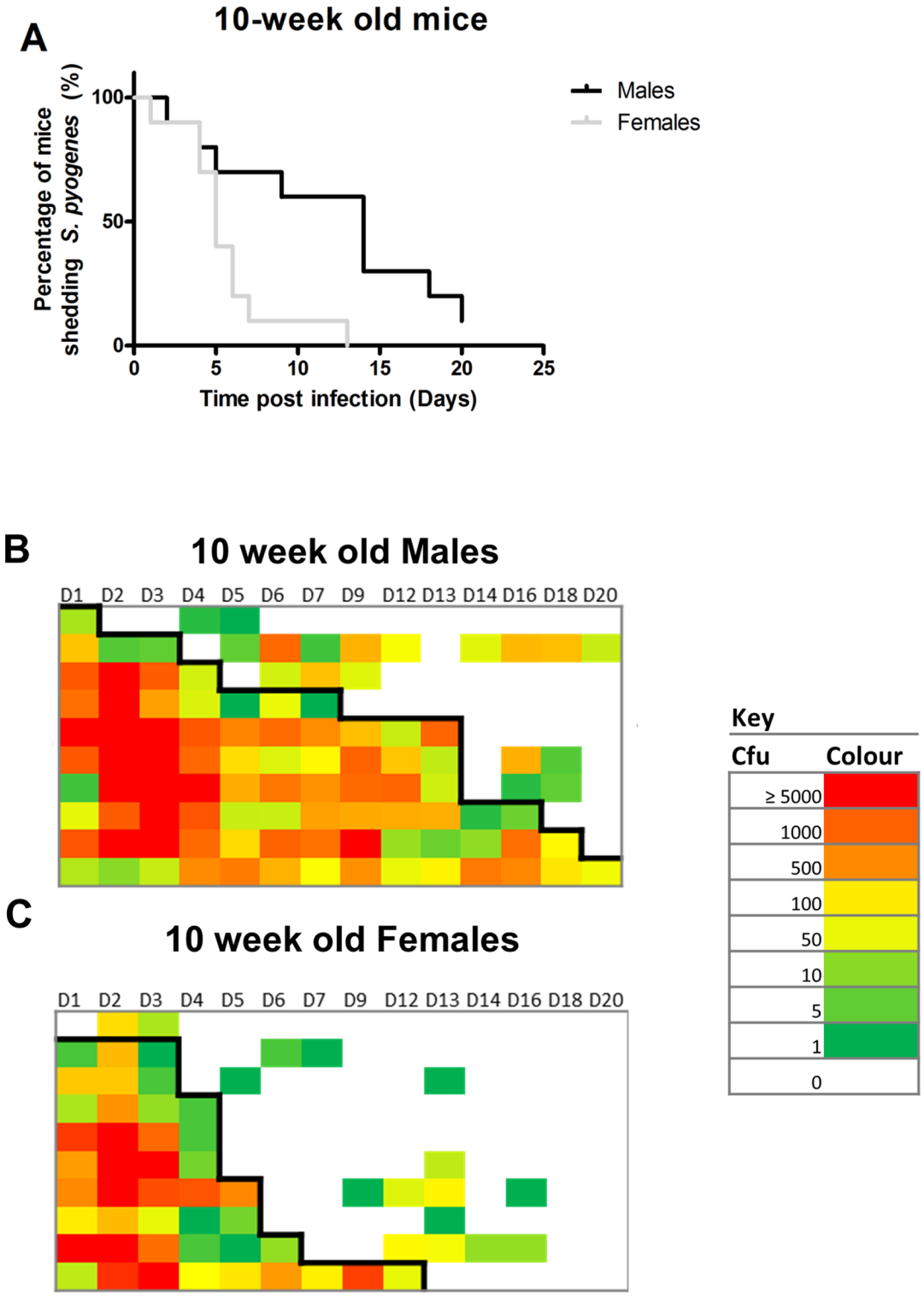


Figure 5. Sex differences in *S. pyogenes* nasopharyngeal carriage and shedding intensity in 10 week old mice. Male and female FVB/n 10 weeks (A, $p<0.05$ Mantel–Cox Logrank test, n = 10) of age were infected intranasally with *emm75 S. pyogenes* (1.1×10^8 cfu) and sampled non-invasively through direct nasal sampling over 21 days. Male mice carried *S. pyogenes* for significantly longer than the female mice in this age group. Shedding intensity maps display the data from direct nasal samples throughout the time course from the male mice (B) and the female mice (C). Rows indicate individual mice throughout the time course, colours indicate the numbers of *S. pyogenes* recovered from direct nasal samples with red indicating the highest recorded levels of carriage (≥5000 cfu) and green indicates the lowest levels of carriage (1 cfu) and blank blocks indicate no recovery of *S. pyogenes*. Black line indicates survival based on the first loss of carriage.
doi:10.1371/journal.pone.0061655.g005

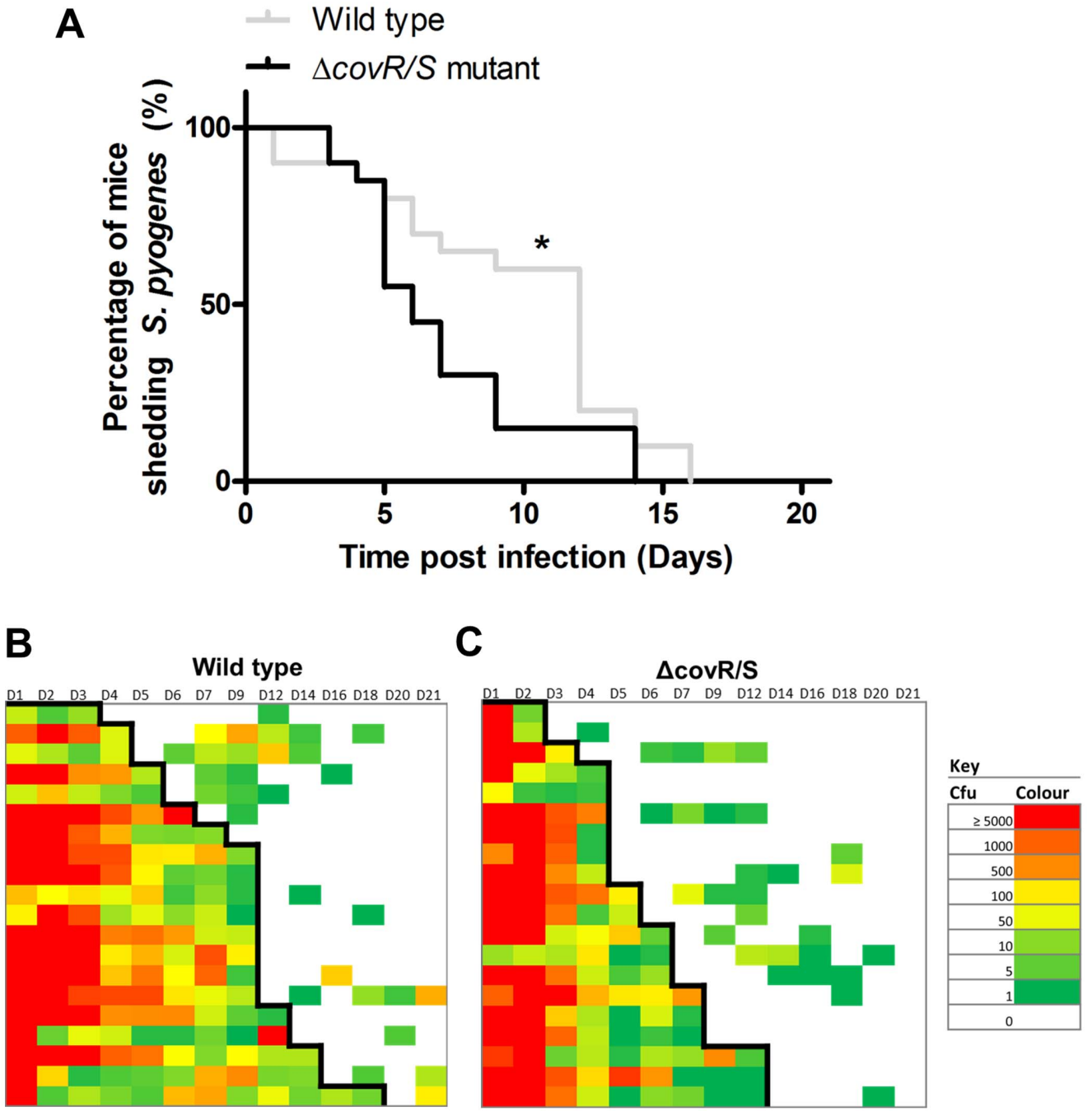


Figure 6. Nasopharyngeal infection is adversely affected by *covR/S* mutation. Five week old female FVB/n mice were inoculated intranasally with either *emm75 S. pyogenes*, or Δ*covR/S S. pyogenes*. To determine the duration of shedding, direct nasal samples were taken over a 21 day period. The wild type strain was shed over a significantly longer time period than the Δ*covR/S* strain (A, 1.5×10^8 cfu per dose, n = 20 per group, Logrank Mantel Cox $p<0.05$). Shedding intensity maps display the data from direct nasal samples throughout the time course from the groups infected with the wild type *emm*75 strain (B) and the mice infected with the Δ*covR/S* strain (C). Rows indicate individual mice throughout the time course, colours indicate the numbers of *S. pyogenes* recovered from direct nasal samples with red indicating the highest recorded levels of carriage (≥5000 cfu) and green indicates the lowest levels of carriage (1 cfu) and blank blocks indicate no recovery of *S. pyogenes*. Black line indicates survival based on the first loss of carriage.
doi:10.1371/journal.pone.0061655.g006

weeks of age) and post pubertal (n = 10 per group, 5 per cage, 10 weeks of age) male and female FVB/n mice were intranasally inoculated with *S. pyogenes*. There was no significant difference in infection duration between 5 week old males and females over a 21 day period (Figure 4, Logrank $p>0.05$), whereas 10 week old males shed *S. pyogenes* for significantly longer than 10 week old female mice (Figure 5, Logrank test $p<0.05$). However, the older males had to be housed separately to prevent intraspecific aggression and for this reason further experiments were conducted using female mice.

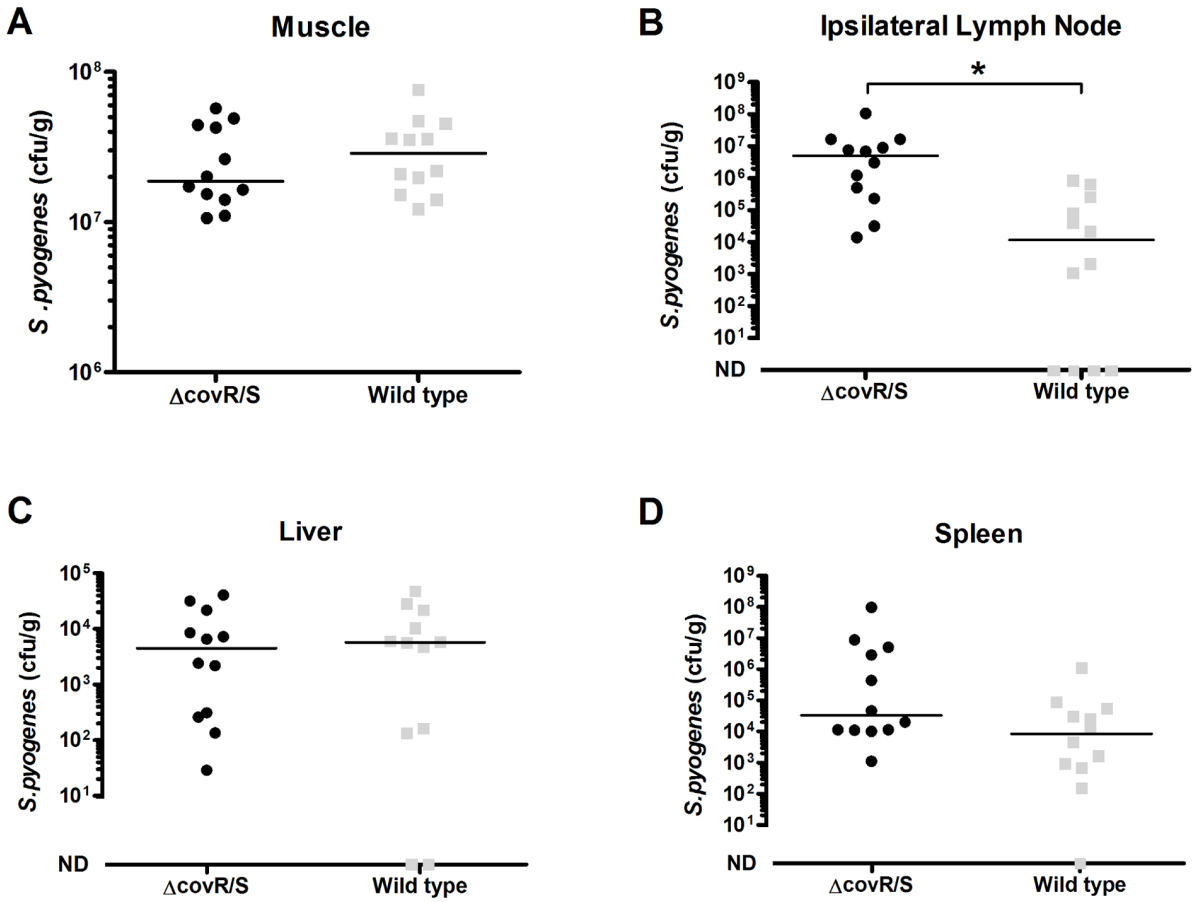


Figure 7. The effects of *covR/S* mutation on dissemination from an invasive intramuscular infection. Five week old FVB/n female mice (n = 12) were infected intramuscularly in the right thigh with either wild type *S. pyogenes* or an isogenic Δ*covR/S* strain (6×10^8 cfu per dose). After three days there was no significant difference in bacterial growth within the thigh (A, Mann Whitney U $p>0.05$), but there was a significant difference in bacterial numbers that had disseminated to the inguinal node (B, Mann Whitney U $p<0.05$). No significant difference in dissemination to the liver (C) and the spleen (D) was found between the wild type and the Δ*covR/S* strains. Median indicated by a black line.
doi:10.1371/journal.pone.0061655.g007

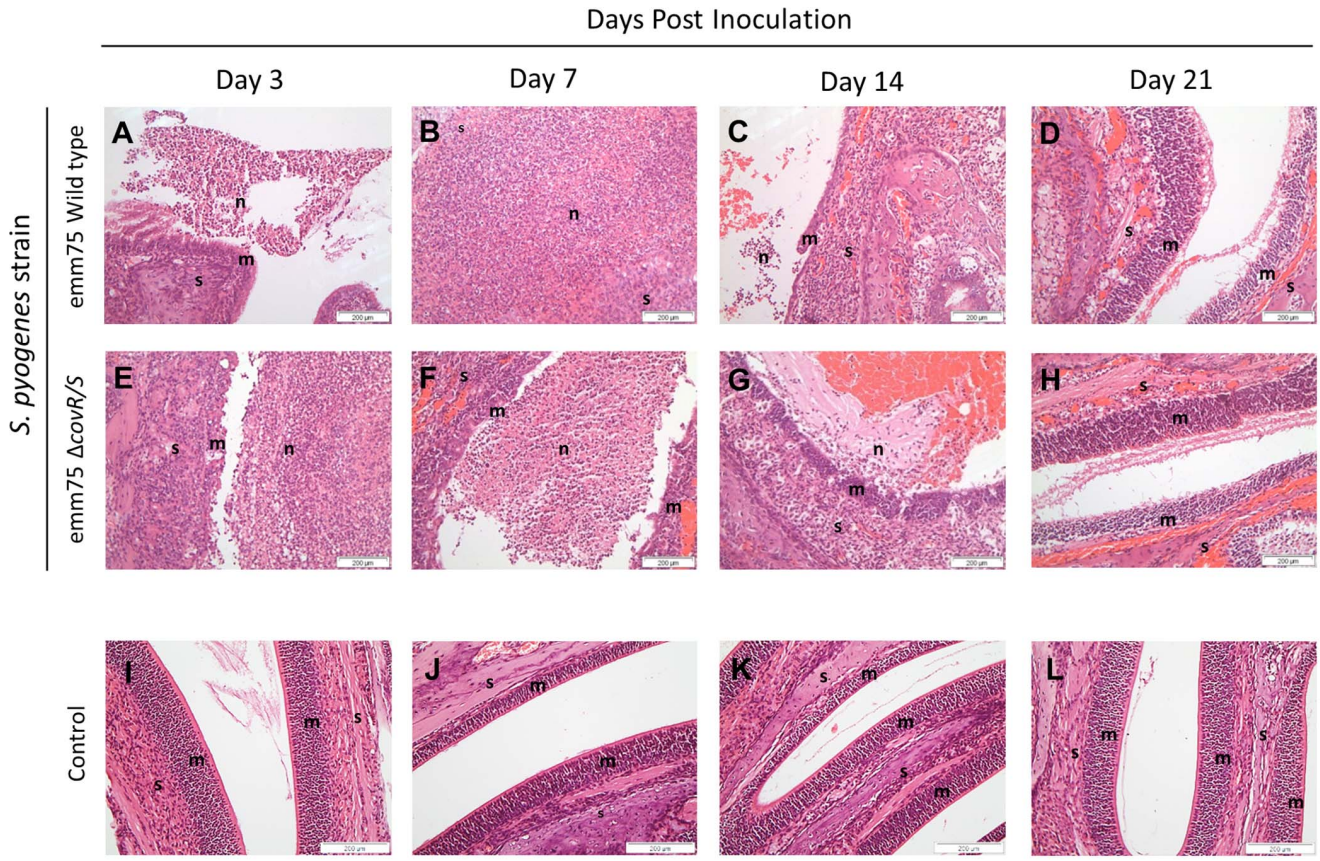
Δ*covR/S* Mutation is Detrimental to Long Term *S. pyogenes* Infection of the Nasopharynx

Two groups of FVB/n female mice (n = 20, 5 per cage) were infected intranasally with 5 µl of 10^8 cfu of *emm*75 *S. pyogenes* or an isogenic Δ*covR/S* strain and observed over 21 days. Kaplan Meier analysis of daily nasal samples demonstrated that the Δ*covR/S* strain was shed from the nasopharynx for a shorter length of time compared to its wild type counterpart. (Figure 6, Mantel Cox Logrank $p<0.05$).

We considered the possibility that the reduced longevity of infection reflected a general fitness defect in the Δ*covR/S* strain. However, following intramuscular infection of groups of mice with each strain, both the Δ*covR/S* strain and wild-type strain survived equally well within the thigh muscle (n = 12 per group, 6 per cage, Figure 7 A). Furthermore the Δ*covR/S* strain disseminated to the ipsilateral inguinal lymph node in greater numbers than the wild-type (Figure 7 B, $p<0.05$ Mann-Whitney), consistent with the predicted phenotype of a Δ*covR/S* strain. Streptococci were detected in the liver (Figure 7 C) and in the spleen (Figure 7 D), but these differences were not significant.

Intranasal Administration of *S. pyogenes* Results in a Suppurative Upper Respiratory Tract Infection that Resolves Over 21 Days

5 week old female FVB/n mice infected with *emm*75 *S. pyogenes* demonstrated inflammatory changes affecting the nasal cavity over the first week of infection (Figure 8, A–D), particularly in the caudal (ethmoturbinate) region. A moderate to marked suppurative rhinitis with complete erosion or ulceration of the nasal mucosa and neutrophilic exudate on the mucosal surface was observed. On days 3 and 7, mice occasionally demonstrated necrosis of underlying turbinate bone and extension of inflammation and infection across the cribriform plate, resulting in a localized meningoencephalitis affecting the olfactory bulbs (data not shown). However, by Day 21, the inflammatory damage to the nasal mucosa had resolved. The *S. pyogenes* Δ*covR/S* strain elicited a similar inflammatory response (Figure 8, E–H), albeit over a slightly shorter time period. Mice demonstrated mild to marked suppurative rhinitis at days 3 and 7 that resolved by day 14. Both strains of *S. pyogenes* could be recovered from cultures of the nasopharynx from mice even after the inflammation resolved (Data not shown). Semi quantitative assessment of sections from mice infected with both the wild type and Δ*covR/S emm*75 strains were undertaken in comparison with control sections from uninfected mice; this demonstrated that the observed inflamma-



M

Strain	Day 3	Day 7	Day 15	Day 21
	Histology grade			
Wildtype	++	++++	+++	+
	++++	+	+	ND
	++	+	+	+
ΔcovR/S	+	+++	-	ND
	+	++	-	+
	+++	++	++	-
Control	-	-	-	-
	-	-	-	-
	-	-	-	-

Figure 8. Histopathological analysis of the caudal nasal cavity during long term nasal infection. Photomicrographs demonstrating five week old female FVB/n mice infected with either the *emm75 S. pyogenes* (A–D) or the *emm75 ΔcovR/S* strain (E–H) (1.5×10^8 cfu per dose, n = 3 per group) were taken at days 3, 7, 14 and 21 after inoculation (Haemotoxylin & Eosin staining). **n** = Neutrophilic Exudate, **m** = Nasal mucosa, **s** = Nasal stroma. Scale bar as shown. Damage to the nasal mucosa with surface neutrophilic exudate was apparent at day 3 post inoculation with both strains (A & E). The nasal epithelia of mice in both groups were widely eroded or ulcerated by day 7 (B) than those infected with the *ΔcovR/S* strain (F). At day 14 the inflammation had begun to resolve in both strains (C & G). By day 21, mice in all groups had histologically normal mucosa (D & H). Control mice over the time course are shown in (I–L). Semi quantitative analysis of the histopathology was undertaken to determine the severity of infection and assigned a numerical designation for each time point (n = 3 mice per time point). − = No significant abnormality,+ = Mild,++ = Moderate,+++ = Marked,++++ = Severe and ND = Non diagnostic sections (M).
doi:10.1371/journal.pone.0061655.g008

tion decreased throughout the time course consistent with the lowering of the bacterial load (Figure 8 I–M).

Transmission of *S. pyogenes* within a Mouse Cage is Dependent on the Proportion of Infected Donor Mice Present

Preliminary work showed that *S. pyogenes* shed by infected mice could lead to the infection of uninfected mice in the same cage. Transmissibility of *S. pyogenes* in the nasopharynx was formally investigated through introducing infected donor mice into cages of uninfected recipient mice (n = 8 per cage). The effect of varying the ratio of donor to recipient (D:R) mice present in a cage on transmission was evaluated.

Within 4 hours of donor introduction transmission occurred to all recipients. A higher D:R ratio resulted in greater counts of *S. pyogenes* cultured from recipient mice in those cages. Recipient mice in the cage with a D:R ratio of 4:4 had significantly more bacteria in the nasopharynx compared to mice in the cage with a D:R ratio of 2:6 (Figure 9 $p<0.05$).

Δ*covR/S* Mutation is Detrimental to the Transmission of *S. pyogenes* in a Mouse Model

Mice were observed over the first three days of infection, when shedding of the wild-type and the Δ*covR/S* strain were shown to be similar, to determine whether a mutation in *covR/S* affects transmission.

Female FVB/n mice infected with either the wild-type or the Δ*covR/S* strains were introduced into cages at a D:R ratio of 3:5. After inoculation, the infected mice were separated for six hours before being introduced to the recipients, to prevent passive inoculum transfer. Direct nasal samples were taken from recipient mice over three days after the introduction of the donor mice.

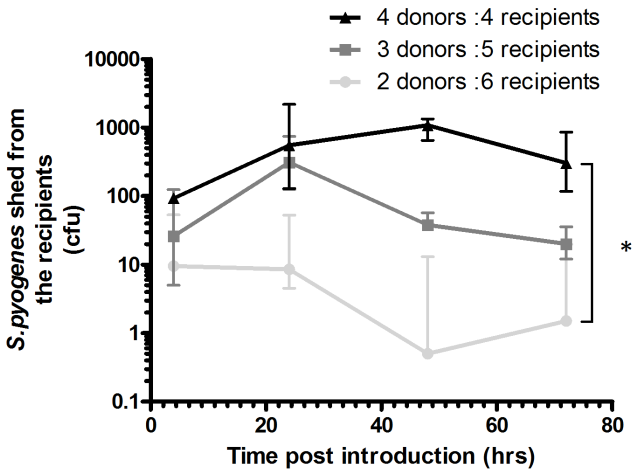


Figure 9. Density of infected carriers determines the burden of transmitted infection. Five week old female FVB/n donor mice infected intranasally with *S. pyogenes* (1.63×10^8 cfu per dose) were introduced into a cage of naïve recipient female mice. The Donor: Recipient (D:R) ratio was varied between 4:4, 3:5 and 2:6 between cages. Recipient mice were sampled at 4, 24, 48, 72 and 96 hours after the infection and introduction of the donor mice to a cage. Data show counts from direct nasal sampling from recipient mice only. Donor mice had >5000 cfu recovered at all time points (not shown). The burden of transmitted infection was significantly higher in cages with a D:R ratio of 4:4 compared with cages with a 2:4 ratio. (AUC analysis, followed by Kruskal Wallis with Dunns Post test $p<0.05$). Lines indicate the median and the interquartile range.
doi:10.1371/journal.pone.0061655.g009

Recipient mice housed with donor mice carrying wild type *S. pyogenes* acquired significantly more bacteria over the time course than the recipient mice housed with donor mice carrying the Δ*covR/S* strain (Figure 10 A, AUC analysis, with Mann Whitney U $p<0.05$).

There was no statistically significant difference in the abundance of airborne *S. pyogenes* in the cages of mice infected with the wild-type compared with the cages of mice infected with the Δ*covR/S* strain. (Figure 10 B, AUC analysis with Mann Whitney U $p>0.05$).

Discussion

To facilitate the investigation of bacterial and host factors that influence *S. pyogenes* in nasopharyngeal infection, an improved, new model of nasopharyngeal colonisation was devised, with an optimised dosing volume to avoid fulminant infections. A non-invasive method of longitudinal monitoring was developed that does not require culling of mice at multiple time points, thus reducing the numbers of animals used.

An *emm*75 strain of *S. pyogenes* was found in preliminary experiments to be carried better than other *emm* types by BALB/c mice, although previous studies have however found that the BALB/c strain is more resistant to infection than other strains [9]. A number of mouse strains were therefore tested in this study, of which the FVB/n was found to be the most susceptible to *S. pyogenes* intranasal infection. *Emm* types 1, 2, 3, 4, 6, 12, 22 and 89 were also successfully carried by FVB/n mice (data not shown), although in some cases causing a far more severe disease than the *emm*75 strain, making them unsuitable for long term infection studies.

We found that gender had an impact on susceptibility to carriage in post pubertal mice only. Data were consistent with other published work demonstrating an increase in susceptibility to infection in male mice [9,25]. However, the intraspecific aggression expressed by males of this strain made them difficult to house in groups, and thus the older individuals were housed individually. In previous studies, housing mice singly has been demonstrated to increase immune responses [26,27,28], and would theoretically increase their resistance to infection.

Histological analysis during infection revealed that nasal shedding of *S. pyogenes* was associated with on-going inflammation that subsided in the second and third weeks of infection. Previous studies have demonstrated bacterial infection of the mouse NALT [6]. However this study focussed on the site of infection in the deeper nasal passages, which demonstrated a suppurative rhinitis. Studies have shown that *S. pyogenes* distributes to the ethmoid sinuses in humans during rhinosinusitis [29,30].

The model was used to demonstrate that a functional *covR/S* is required for optimum infection and transmission from the nasopharynx. The failure of the Δ*covR/S* strain to survive in the mouse nasopharynx was not due to a consistent fitness burden, since in invasive infection, the *covR/S* strain disseminated in significantly greater numbers than the wild type bacteria to the inguinal lymph node.

During preliminary experiments, we became aware that individual mice occasionally became re-infected after clearing the initial infection. To address transmission, and the factors that may influence this, co-mingling experiments were conducted. These demonstrated that transmission occurred as early as 4 hours post introduction, and the numbers of bacteria recovered from the nares of the recipients increased as the number of infected donor mice in the cage was increased. Importantly, such transmission events may not necessarily constitute a productive infection, as *S.*

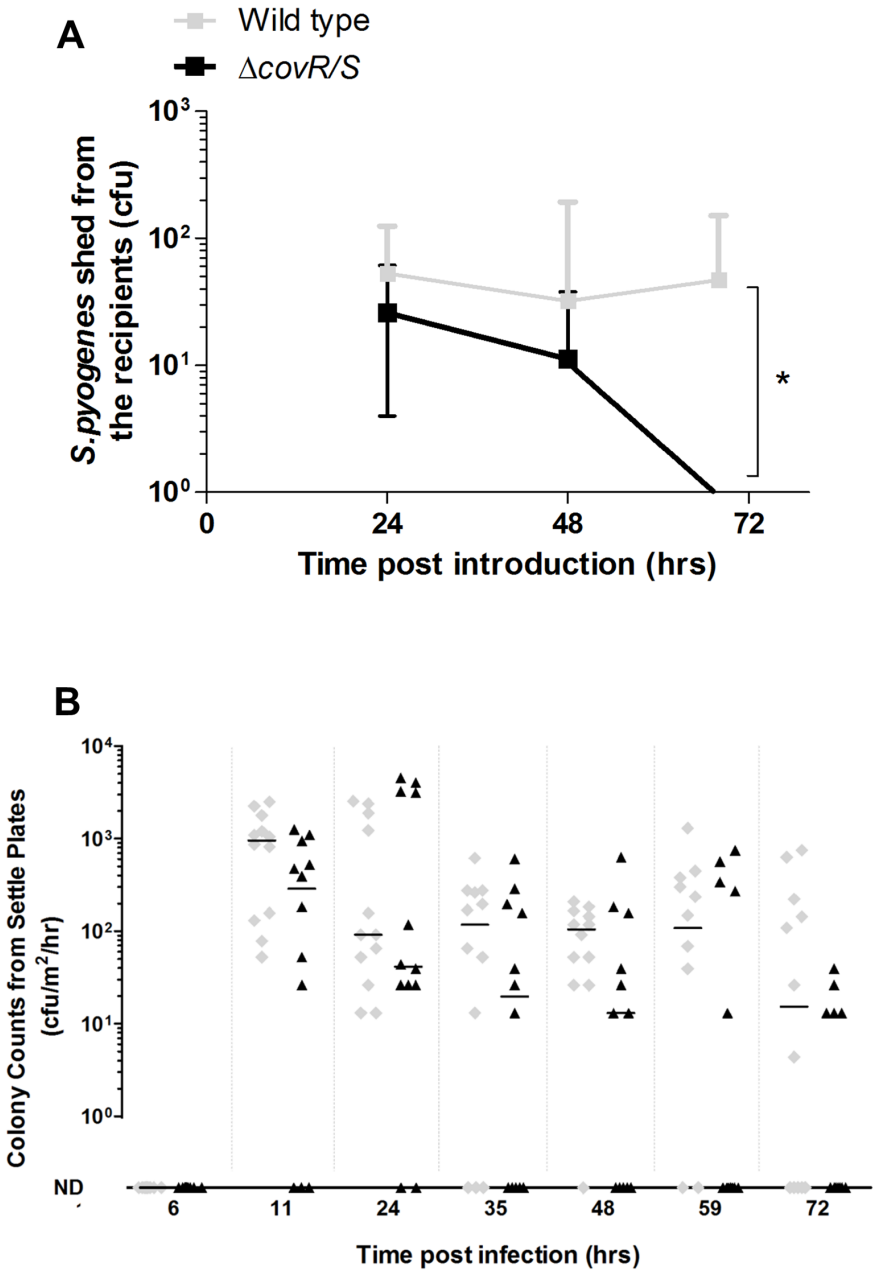


Figure 10. Transmission of *S. pyogenes* is hampered by loss of *covR/S* regulation. Naïve five week old female FVB/n recipients co-mingled at a D:R ratio of 3:5 with female FVB/n mice infected with either the *emm*75 wild type strain or it's isogenic Δ*covR/S* strain (5 $\times 10^8$ cfu per dose) and sampled after the introduction of the donor mice. Donor mice had >5000 cfu recovered from direct nasal sampling throughout the experiment. The Δ*covR/S* strain transmitted significantly less well to recipients compared to the wild type strain (A, n = 15 recipients per group, AUC analysis, followed by Mann-Whitney U test). Line indicates median, error bars indicate interquartile range. Settle plates exposed to the air in the cages revealed no significant differences in the bacteria deposited on the surface of the plates by mice infected with the strain, or the Δ*covR/S* strain (B, n = 4 plates per cage, AUC analysis followed by Mann-Whitney U test $p>0.05$) Data is shown for individual animals with medians indicated by black line.
doi:10.1371/journal.pone.0061655.g010

pyogenes did not reach the same abundance in recipient mice as observed in donor mice.

Co-mingling was then used to examine the impact of *covR/S* on transmission. Despite the fact that the infection burden (as measured by direct nasal sampling) was similar between the two donor groups in the first 72 h, recipients housed with donor mice carrying the Δ*covR/S* were demonstrated to have a shorter shedding duration than the recipient mice housed with the donors carrying the wild type strain.

Furthermore, despite some differences between the experimental groups, settle plates placed in each cage revealed no significant difference in aerosolization between the two strains. This suggests that the impairment of the *covR/S* primarily affects the survival of *S. pyogenes* in the nasopharynx after the initial transmission event has taken place.

There is thus a fitness cost conferred by *covR/S* mutation specific to the nasopharynx that may explain why such bacteria have not

become prevalent in community *S. pyogenes* pharyngitis despite being advantageous in invasive infection.

The model described represents a refinement of previous systems to study upper respiratory tract infection by *S. pyogenes*; the model is non-invasive and allows longitudinal monitoring of bacterial infection, using the same mice throughout the study. Such a model will facilitate research which might otherwise require prohibitively large numbers of animals and could be of importance in future evaluation of vaccines, antimicrobials, as well as the factors that influence transmission.

Author Contributions

Conceived and designed the experiments: FA SS. Performed the experiments: FA. Analyzed the data: FA KS. Contributed reagents/materials/analysis tools: CT SW SS. Wrote the paper: FA CT KS SW SS.

References

1. Carapetis JR, Steer AC, Mulholland EK, Weber M (2005) The global burden of group A streptococcal diseases. Lancet Infect Dis 5: 685–694.
2. Wiles S, Hanage WP, Frankel G, Robertson BD (2006) Modelling infectious disease–time to think outside the box? Nature Rev Microbiol 4: 307–312.
3. Hillenius WJ (1992) The evolution of nasal turbinates and mammalian endothermy. Paleobiology 18: 17–29.
4. Slípka J (1988) Palatine tonsils–their evolution and ontogeny. Acta Oto-Laryngol 454: 18–22.
5. Wu HY, Nguyen H, Russell MW (1997) Nasal lymphoid tissue (NALT) as a mucosal immune inductive site. Scand J Immunol 46: 506–513.
6. Park HS, Francis KP, Yu J, Cleary PP (2003) Membranous cells in nasal-associated lymphoid tissue: a portal of entry for the respiratory mucosal pathogen group A streptococcus. J Immunol 171: 2532–2537.
7. Mannam P, Jones KF, Geller BL (2004) Mucosal vaccine made from live, recombinant *Lactococcus lactis* protects mice against pharyngeal infection with *Streptococcus pyogenes*. Infect Immun 72: 3444–3450.
8. Jordan RT, Ohno S (1958) Comparative pathological changes in AKR mice following intranasal instillation of tumor cells and streptococci. Cancer Res 18: 47–50.
9. Medina E, Goldmann O, Rohde M, Lengeling A, Chhatwal GS (2001) Genetic control of susceptibility to group A streptococcal infection in mice. J Infect Dis 184: 846–852.
10. Husmann LK, Dillehay DL, Jennings VM, Scott JR (1996) *Streptococcus pyogenes* infection in mice. Microb Pathogenesis: 213–224.
11. Bronze MS, McKinsey DS, Beachey EH, Dale JB (1988) Protective immunity evoked by locally administered group A streptococcal vaccines in mice. J Immunol 141: 2767–2770.
12. Eyles JE, Spiers ID, Williamson ED, Alpar HO (2001) Tissue distribution of radioactivity following intranasal administration of radioactive microspheres. J Pharm Pharmacol 53: 601–607.
13. Sumby P, Whitney AR, Graviss EA, DeLeo FR, Musser JM (2006) Genome-Wide Analysis of Group A Streptococci Reveals a Mutation That Modulates Global Phenotype and Disease Specificity. PLoS Pathog 2: 0041–0049.
14. Graham MR, Smoot LM, Migliaccio CA, Virtaneva K, Sturdevant DE, et al. (2002) Virulence control in group A Streptococcus by a two-component gene regulatory system: global expression profiling and in vivo infection modeling. Proc Natl Ac Sci U S A 99: 13855–13860.
15. Kansal RG, Datta V, Aziz RK, Abdeltawab NF, Rowe S, et al. (2010) Dissection of the molecular basis for hypervirulence of an in vivo-selected phenotype of the widely disseminated M1T1 strain of group A Streptococcus bacteria. J Infect Dis 201: 855–865.
16. Turner CE, Kurupati P, Jones MD, Edwards RJ, Sriskandan S (2009) Emerging role of the interleukin-8 cleaving enzyme SpyCEP in clinical *Streptococcus pyogenes* infection. J Infect Dis 200: 555–563.
17. Walker MJ, Hollands A, Sanderson-Smith ML, Cole JN, Kirk JK, et al. (2007) DNase Sda1 provides selection pressure for a switch to invasive group A streptococcal infection. Nature Med 13: 981–985.
18. Engleberg NC, Heath A, Miller A, Rivera Starr C, DiRita VJ (2001) Spontaneous mutations in the CsrRS two-component regulatory system of *Streptococcus pyogenes* result in enhanced virulence in a murine model of skin and soft tissue infection. J Infect Dis 183: 1043–1054.
19. Hollands A, Pence MA, Timmer AM, Osvath SR, Turnbull L, et al. (2010) Genetic switch to hypervirulence reduces colonization phenotypes of the globally disseminated group A Streptococcus M1T1 clone. J Infect Dis 202: 11–19.
20. Treviño J, Perez N, Ramirez-Peña E, Liu Z, Shelburne SA, et al. (2009) CovS simultaneously activates and inhibits the CovR-mediated repression of distinct subsets of group A Streptococcus virulence factor-encoding genes. Infect Immun 77: 3141–3149.
21. Hook EW, Wagner RR, Lancefield RC (1960) An epizootic in Swiss mice caused by a group A streptococcus, newly designated type 50. Am J Epidemiol 72: 111–119.
22. Yung DL, McIver KS, Scott JR, Hollingshead SK (1999) Attenuated expression of the mga virulence regulon in an M serotype 50 mouse-virulent group A streptococcal strain. Infect Immun 67: 6691–6694.
23. Sriskandan S, Unnikrishnan M, Krausz T, Cohen J (1999) Molecular analysis of the role of streptococcal pyrogenic exotoxin A (SPEA) in invasive soft-tissue infection resulting from *Streptococcus pyogenes*. Mol Microb 33: 778–790.
24. Wiles S, Clare S, Harker J, Huett A, Young D, et al. (2004) Organ specificity, colonization and clearance dynamics in vivo following oral challenges with the murine pathogen *Citrobacter rodentium*. Cell Microbiol 6: 963–972.
25. Willoughby DS, Watson DW (1964) Host-parasite relationships among group A streptococci II. Influence of sex on the susceptibility of inbred mice toward streptococcal infection. J Bacteriol 87: 1457–1461.
26. Shanks N, Renton C (1994) Influence of Change From Grouped to Individual Housing on a T-Cell-Dependent Immune Response in Mice?: Antagonism by Diazepam. Pharmacol Biochem Behav 47: 497–502.
27. Grewal IS, Heilig M, Miller A, Genetics M (1997) Environmental regulation of T-cell function in mice?: group housing of males affects accessory cell function. Immunology 90: 165–168.
28. Rabin BS, Lyte M, Hamill E (1987) The influence of mouse strain and housing on the immune response. J Neuroimmunol 17: 11–16.
29. Brook I (2011) Microbiology of sinusitis. Proc Am Thorac Soc 8: 90–100.
30. Ozcan M, Unal A, Aksaray S, Yalcin F, Akdeniz T (2002) Correlation of middle meatus and ethmoid sinus microbiology in patients with chronic sinusitis. Rhinology 40: 24–27.